XXXIe Moorexkursion

in the central Jura and the Morvan Mountains

16-22 september 2007

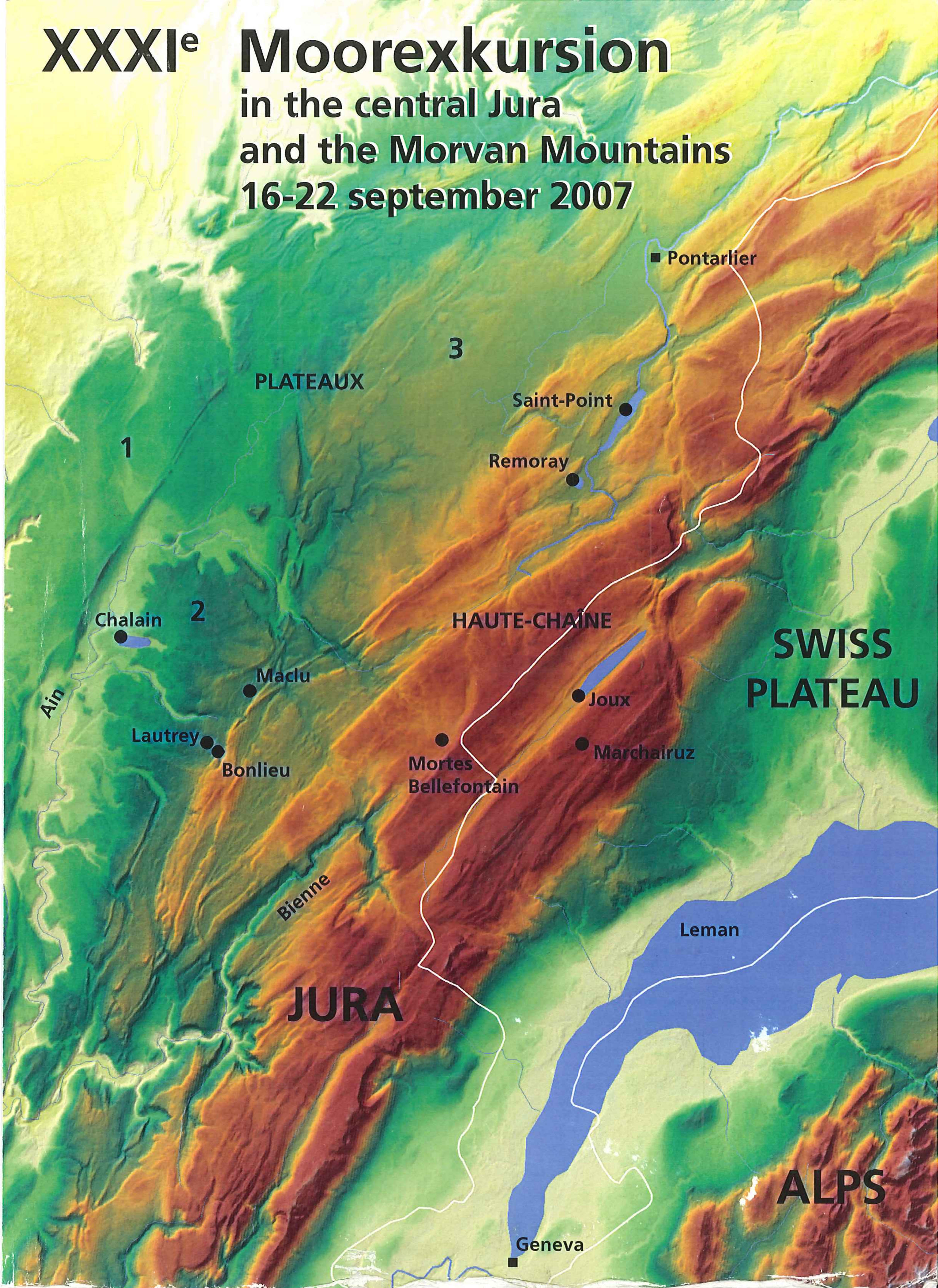

XXXIe Moor exkursion
in the central Jura and the Morvan Mountains
16-22 september 2007

Itinerary

Sunday, 16 September

Meeting point Besançon, ca 17.00 h. Welcome Party.
Overnight in Besançon city.
Meeting point: Hotel Ibis La City,

Avenue Louise 25000 Besançon
Tel: 00 33 3 81 85 11 70

Monday, 17 September

- **Marchairuz pass:**
  The Pollandcal program - Relation between vegetation cover and pollen records.
  Responsible of the site: Florence Mazier, Jacqueline van Leeuwen, Pim van der Knaap.
- **Lake of Joux:**
  Lake level fluctuations, human impact and climate oscillations during the last millennium.
  Responsible of the site: Emilie Gauthier and Michel Magny

Overnight at Bois d'Amont: Hotel Club Le Risoux, 39220 Bois d'Amont
Tel: 00 33 3 84 60 94 24

Tuesday, 18 September

- **Lake Mortes:**
  Variations in the treeline during the Lateglacial-Holocene transition in the Jura Mountains.
  Responsible of the site: Carole Bégeot.
- **Lake Saint-Point:**
  Lateglacial and Holocene environmental changes in the upper Doubs valley.
  Responsible of the site: Aurélie Leroux, Vincent Bichet and Anne-Véronique Walter-Simonnet.

Overnight at Bois d'Amont: Hotel Club Le Risoux, 39220 Bois d'Amont
Tel: 00 33 3 84 60 94 24

Wednesday, 19 September

- **Lake Lautrey:**
  A high resolution multi-proxy record of environmental and climatic changes during the Lateglacial–Holocene transition.
  Responsible of the site: Boris Vannière, Anne-Véronique Walter-Simonnet and Michel Magny.
- **Lake Bonlieu:**
  Quantitative reconstructions of climatic parameters using pollen, chironomid and lake-level data.
  Responsible of the site: Elena Ducci and Laurent Millet

Overnight at Bois d'Amont: Hotel Club Le Risoux, 39220 Bois d'Amont
Tel: 00 33 3 84 60 94 24

Thursday, 20 September

- **Lakes Maclu :**
  Holocene climate oscillations as reflected by changes in lake-levels.
  Responsible of the site: Michel Magny.
- **Lake Chalain** :
  Human impact on vegetation, climate oscillations and history of the agricultural societies during the Neolithic and Bronze Age periods.
  Responsible of the site: Emilie Gauthier, Michel Magny.

Overnight at Arbois.
Special session in a local cellar for tasting regional wines
"Franc-Comtois" menu
Hotel Les Messageries, 39600 Arbois
Tel: 00 33 3 84 66 15 45

Friday, 21 September

- **Port-des-Lamberts peat bog:**
  Vegetation history and early palaeometallurgy since the late Neolithic.
  Responsible of the site: Isabelle Jouffroy-Bapicot, Fabrice Monna, Christophe Petit .
- **Mont-Beuvray:**
  Archaeological excavations of the celtic oppidum and protohistoric open-air mines.
  Responsible of the site: Jean-Paul Guillaumet.

Overnight at Mont-Beuvray. Farewell Party with a Gallic banquet.
Centre Archéologique Européen du Mont Beuvray
Tel: 00 33 3 86 78 69 00

Saturday morning, 22 September

Return to Besançon around 11/12 h and departure. Return home.

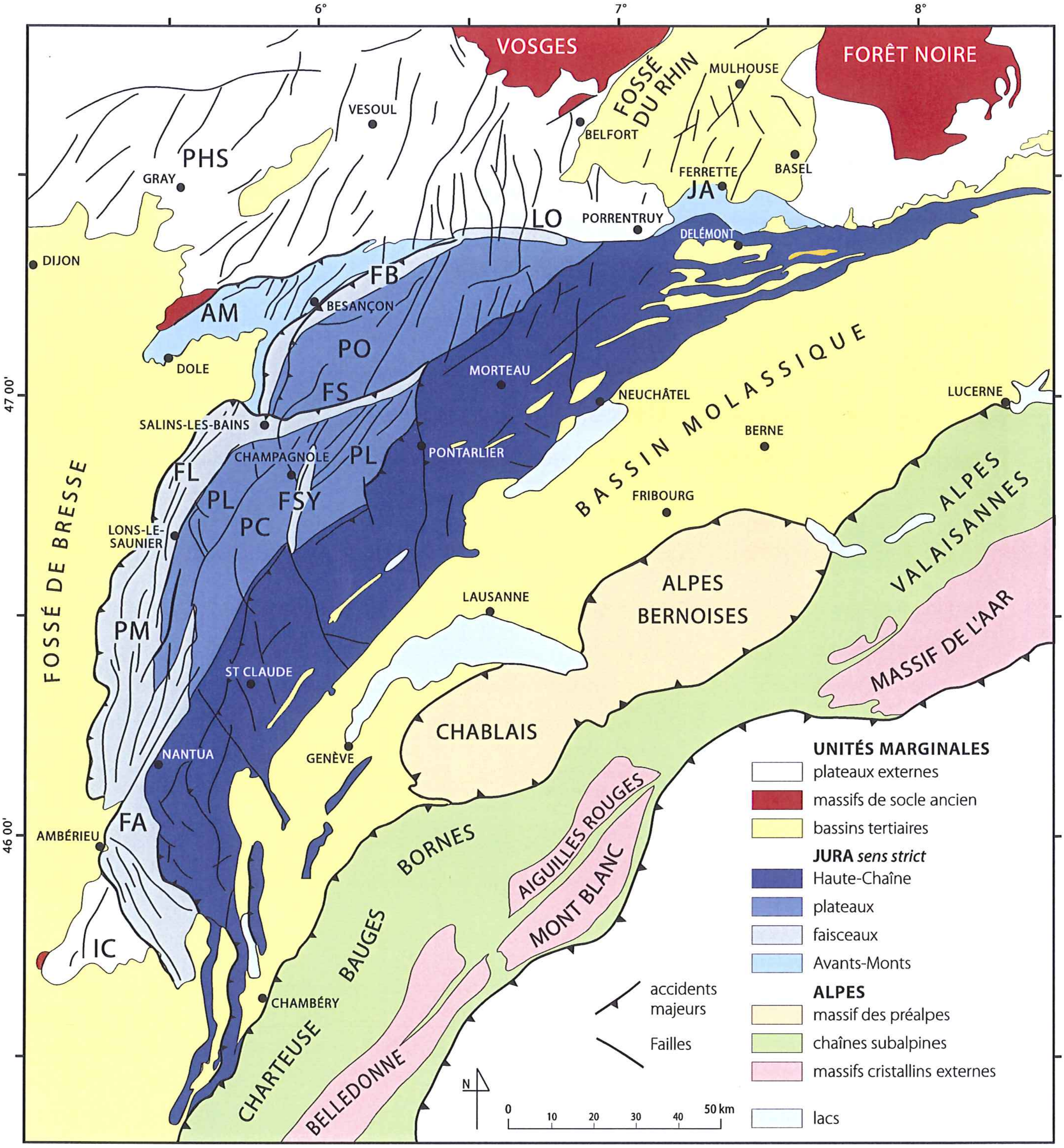

Unités et contexte structural de la Chaîne jurassienne (d'après A. Sommaruga).
Units and structural context of the Jura Chain (after A. Sommaruga).

PHS = Plateaux de Haute-Saône - IC = Ile Crémieu - AM = Avants-Monts - JA = Jura Alsacien - FA = Faisceau d'Ambérieu - Fb = Faisceau bisontin - Lo = Lomont
FL = Faisceau lédonien - PM = Petite Montagne - FS = Faisceau salinois - FSy = Faisceau de Syam - PC = Plateau de Champagnole - PL = Plateau de Levier
PL = Plateau lédonien - PO = Plateau d'Ornans.

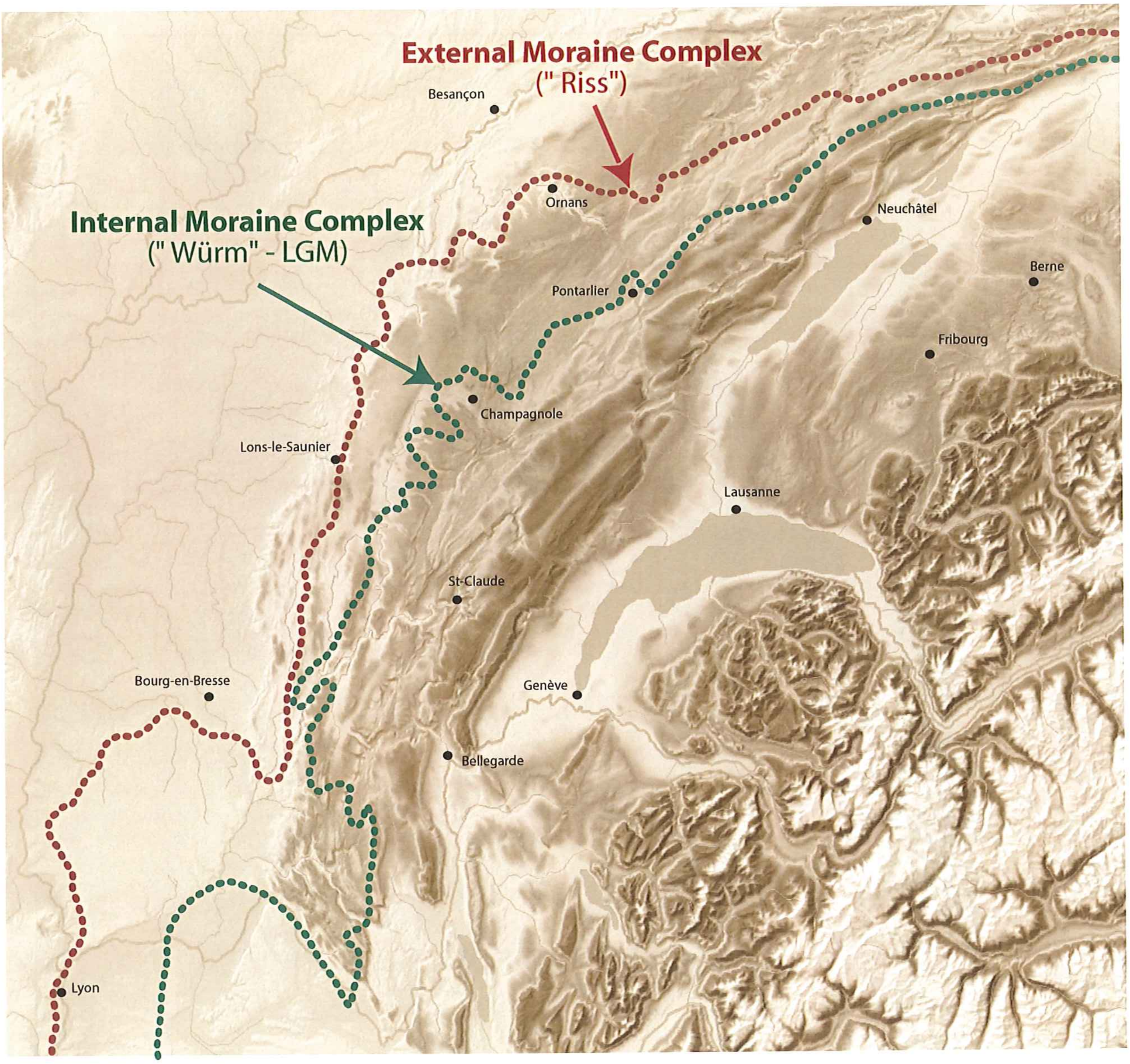
External Moraine Complex
(" Riss")
Internal Moraine Complex
(" Würm" - LGM)
Besançon
Ornans
Neuchâtel
Berne
Pontarlier
Fribourg
Champagnole
Lons-le-Saunier
Lausanne
St-Claude
Bourg-en-Bresse
Genève
Bellegarde
Lyon

CAMPY M. 2007

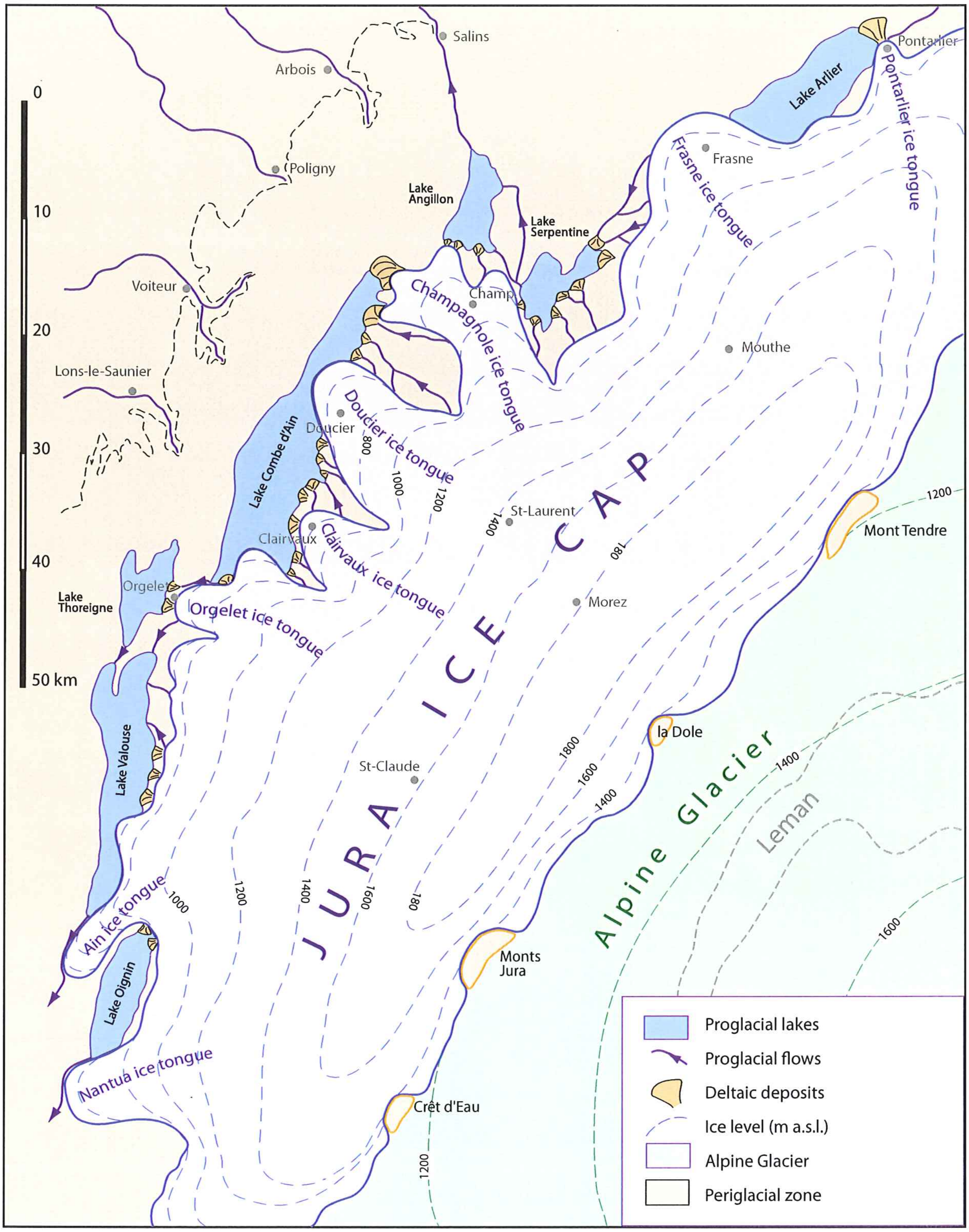
0
10
20
30
40
50 km
Salins
Arbois
Poligny
Voiteur
Lons-le-Saunier
Lake Angillon
Lake Serpentine
Lake Arlier
Pontarlier
Pontarlier ice tongue
Frasne
Frasne ice tongue
Champ.
Champagnole ice tongue
Mouthe
Doucier
Doucier ice tongue
Lake Combe d'Ain
Clairvaux
Clairvaux ice tongue
St-Laurent
Lake Thoreigne
Orgelet
Orgelet ice tongue
Morez
JURA ICE CAP
Mont Tendre
la Dole
Lake Valouse
St-Claude
Ain ice tongue
Lake Oignin
Nantua ice tongue
Monts Jura
Crêt d'Eau
Alpine Glacier
Leman
800
1000
1200
1400
1600
1800
180
Proglacial lakes
Proglacial flows
Deltaic deposits
Ice level (m a.s.l.)
Alpine Glacier
Periglacial zone

CAMPY M. 2007

Coupes transversales du Jura montrant les régions phytogéographiques et les étages de végétation.

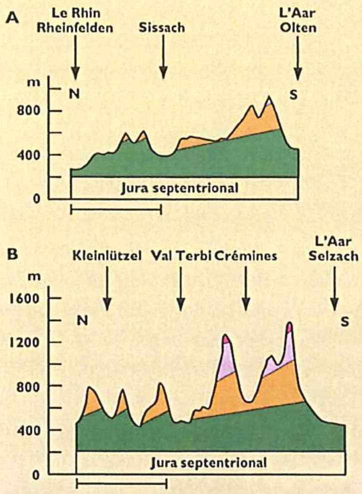

Paysage caractéristique des vallées du Jura plissé septentrional: la vallée de Moutier-Grandval.

🟥 Étage subalpin
▨ Étage montagnard supérieur
🟧 Étage montagnard inférieur
🟩 Étage collinéen

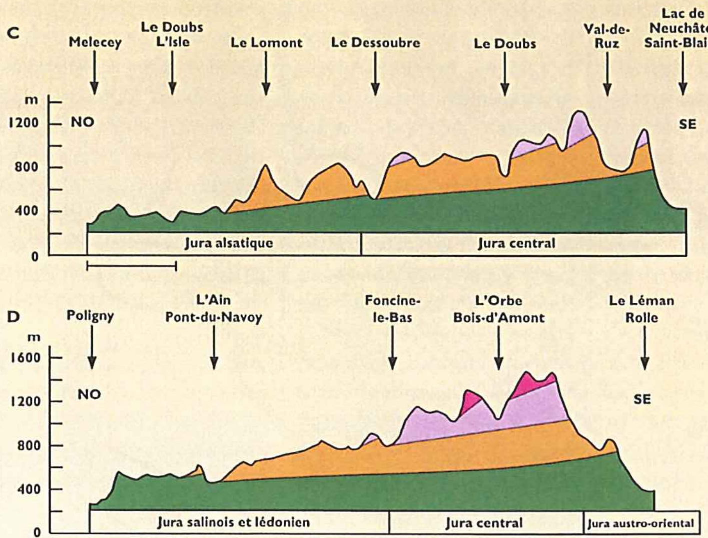

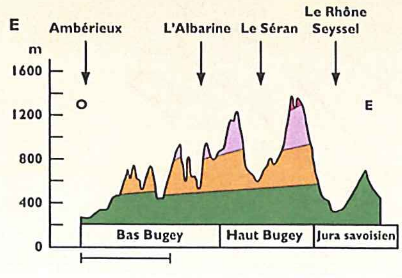

La dent du Chat, dans le Jura savoisien, surplombe le lac du Bourget.

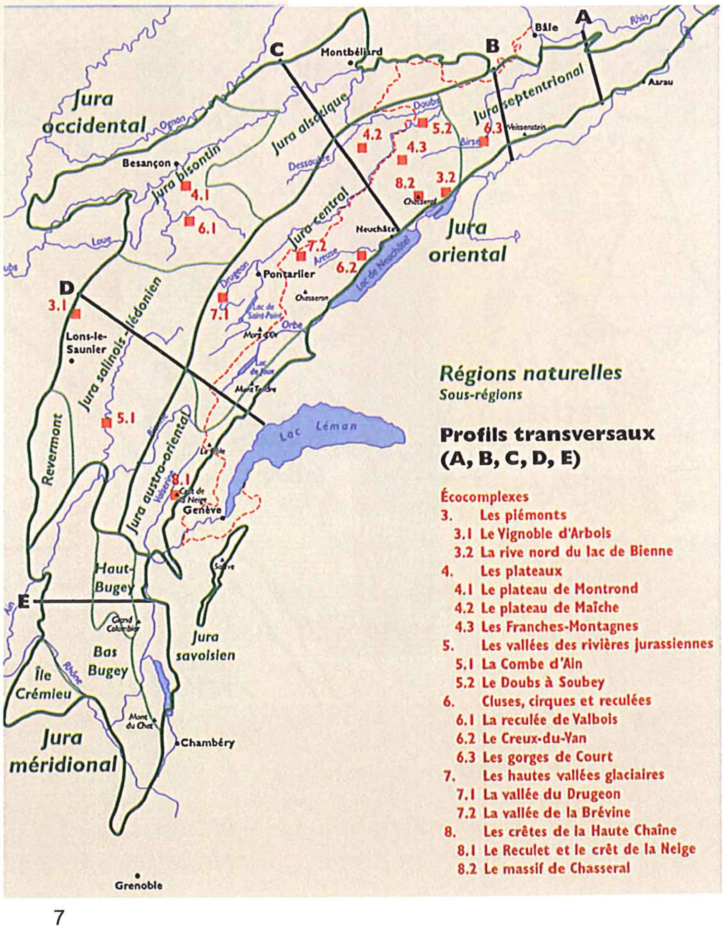

Régions naturelles
Sous-régions

Profils transversaux (A, B, C, D, E)

Écocomplexes

- 3. Les piémonts
  - 3.1 Le Vignoble d'Arbois
  - 3.2 La rive nord du lac de Bienne
- 4. Les plateaux
  - 4.1 Le plateau de Montrond
  - 4.2 Le plateau de Maîche
  - 4.3 Les Franches-Montagnes
- 5. Les vallées des rivières jurassiennes
  - 5.1 La Combe d'Ain
  - 5.2 Le Doubs à Soubey
- 6. Cluses, cirques et reculées
  - 6.1 La reculée de Valbois
  - 6.2 Le Creux-du-Van
  - 6.3 Les gorges de Court
- 7. Les hautes vallées glaciaires
  - 7.1 La vallée du Drugeon
  - 7.2 La vallée de la Brévine
- 8. Les crêtes de la Haute Chaîne
  - 8.1 Le Reculet et le crêt de la Neige
  - 8.2 Le massif de Chasseral

The Holocene 16,2 (2006) pp. 277–286

The effect of climate variability on pollen productivity, AD 1975–2000, recorded in a *Sphagnum* peat hummock

Per Sjögren,[*1] Jacqueline F.N. van Leeuwen,[1]
W.O. van der Knaap[1] and Klaas van der Borg[2]

([1]Institute of Plant Sciences, University of Bern, Altenbergrain 21, CH-3013 Bern, Switzerland; [2]Van de Graaff Laboratory, Utrecht University, Princetonplein 5, NL-3584 CC Utrecht, The Netherlands)

Received 9 May 2005; revised manuscript accepted 17 September 2005

A
HOLOCENE
RESEARCH
PAPER

Abstract: Pollen accumulation rates and pollen percentages from a *Sphagnum* peat hummock in the Jura Mountains were used to determine past pollen deposition. Post-bomb calibrated radiocarbon dates allowed estimations of annual variability in pollen productivity AD 1975–2000. Percentages of abundant taxa were modified (downweighted) to reduce the influence of plant cover, mean pollen productivity, and interdependence of the variables. Significant correlations with seasonal climatic parameters (tested with simple linear regression) were found both for pollen accumulation rates and for modified pollen percentages. Winter temperature is an important factor for pollen productivity of several tree species. The climatic effect on the modified pollen assemblage is best explained by a wet/warm to cold/dry gradient, but seasonal influence is considerable (ordination by PCA, RDA). Modified pollen percentages showed similarities in annual fluctuations between sites in the Jura Mountains, the Western Alps and the Eastern Alps.

Key words: Annual resolution, climate, pollen productivity, *Sphagnum* hummock.

Introduction

It is commonly assumed that changes in fossil pollen records are caused by changes in the surrounding vegetation (von Post, 1916). But if changes in vegetation are caused by climatic fluctuations problems might occur. Pollen productivity will change together with the climate, making it hard to estimate the response in the vegetation pattern. Many palaeoecological investigations have given results that are problematic to explain entirely with shifts in the vegetation cover, eg, when there is no detectable time-lag between a shift in climate and pollen values (Ammann *et al.*, 2000), when a very rapid increase of pollen values of a taxon occurs over a large area (Tallantire, 2002), or when pollen is absent and macrofossils are present (Kullman, 1998). Estimates of relative pollen productivity have resulted in different values (eg, Andersen, 1970; Hjelle, 1998; Broström *et al.*, 2004). The methodology has not been the same in all investigations, but the most likely explanation is that there are regional differences in pollen productivity, likely caused by different climatic settings.

The need to better understand the influence of climate on pollen productivity has increased in the past decennia as more subtle and short-lived climatic shifts come under study (eg, Tinner and Lotter, 2001; Hausmann *et al.*, 2002). Under such circumstances the importance of pollen productivity increases compared with migrations, die-backs and colonization. New methods for quantitative landscape reconstruction are also developing in which correct estimation of pollen productivity is crucial (Prentice, 1985; Sugita, 1994).

One reason why the impact of climate on pollen productivity has earned relatively little attention is that it is difficult to investigate. To directly compare pollen productivity with climatic change, a site with stable and well-documented past vegetation is needed, and few, if any, such data sets exist, mainly because of large changes in landuse during the past few centuries (Nielsen and Odgaard, 2004). And even if our current climate is changing fast it is not fast enough for the time frame of modern research projects. The aim of many investigations is to predict climatic change and/or possible effects of such a change, and in that perspective it is not an option to wait until the change has occurred. An alternative is to study modern pollen productivity in different climatic regions. Different estimations of relative pollen productivity might be compared

---

[*] Author for correspondence: (e-mail: per.sjoegren@ib.uit.no)

10.1191/0959683606hl924rp

(Broström *et al.*, 2004), but currently these investigations are few. In regions with similar vegetation but with different climate, pollen traps can be used to measure actual differences in pollen influx (Hicks *et al.*, 2001), but such investigations are time-consuming and measurements can only be achieved for one or a few taxa at the time.

The method pursued in this investigation is to study annual variability in pollen productivity compared with climatic parameters. A climatic change can be described as a changed frequency of years with certain characteristics, eg, a mean warmer climate is equivalent to an increased number of years with warmer summers, mild winters, etc. It is thus possible to use the annual variability to assess the effect of climatic change on pollen productivity. An assumption is that the reaction of a taxon to specific weather conditions for a single year is similar to the reaction to the same condition over a sustained period of time.

The most exact results are achieved by studying the direct flowering of the plants (Litschauer, 2000) or by yearly measurements of pollen influx with pollen traps (Hicks, 2001; van der Knaap *et al.*, 2001). To get even reasonably long time series with these methods a considerable amount of work and planning is needed. An alternative is to use existing lake or peat deposits as natural archives of fluctuations in pollen productivity (van der Knaap and van Leeuwen, 2003).

In this investigation a *Sphagnum* peat hummock from the Jura Mountains is used as an environmental archive. Annually constrained pollen samples, pollen accumulation rates and modified pollen percentages will be used to achieve statistical relationships with measured climatic parameters (see van der Knaap and van Leeuwen, 2003), and similarities in annual pollen deposition with two sites in the Swiss and the Austrian Alps will be shown.

Methods

Site description and fieldwork

The peat section AH1 (Amburnex Hummock 1) was cut from a *Sphagnum* hummock in a small mire in Combe des Amburnex (Les Amburnex mire, 46°32′23″ N, 6°13′54″ E, 1370 m a.s.l.) in the Swiss Jura Mountains (Figure 1). The mire is partly covered by *Picea* and the hummock grows at the edge of the forested part. The hummock was growing below *Picea* branches, which seems to be the case for all *Sphagnum* hummocks in the area. The vegetation around the mire is a mosaic of pasture and forest. *Picea* is the most abundant tree, followed by *Abies*, *Fagus* and some *Acer*.

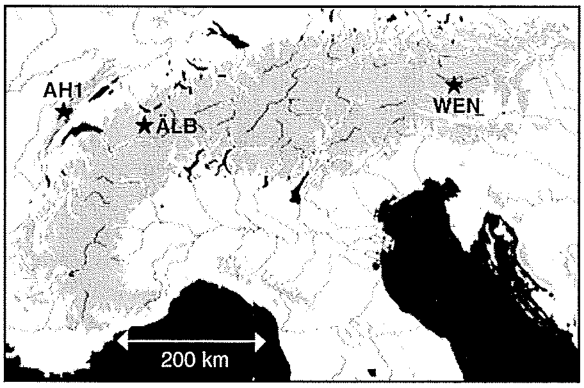

Figure 1 Overview map of localities: AH1, Les Amburnex Hummock 1 (southwest Swiss Jura Mountains); ÄLB, Älbi Flue mire (northwest Swiss Alps); WEN, Wengerkopf mire (Austrian Alps). Grey indicates areas above 1000 m altitude

Laboratory work

Subsampling was done with scissors, whereby the existing peat layering was followed. Pollen samples were prepared using the standard acetolysis method (Berglund and Ralska-Jasiewiczowa, 1986). *Lycopodium* spores were added to establish pollen concentrations (Stockmarr, 1971). For identification of pollen Moore *et al.* (1991), Punt and Blackmore (1991) and the reference collection at the University of Bern were used. Nomenclature follows ALPADABA (Alpine Palynological Data-Base, housed in Bern, Switzerland).

Radiocarbon dating and depth–age relationship

Five *Sphagnum* samples were used for radiocarbon analysis with the AMS facility of Utrecht University (Table 1). The results of the ^{14}C analysis showed elevated activities expressed as fractions modern, and were accounted for by the effects of the atomic bomb activity in the atmosphere (Nydal and Lövseth, 1983). Using the computer program CALIBomb (Reimer *et al.*, 2004; data set: Levin and Kromer, 2004) 1σ-calendar ages were retrieved. From the calendar ages we derived the depth–age relationship of AH1 (Figure 2). Age determination of the pollen samples is based on linear interpolation between the calibrated ^{14}C-dates and the time of the hummock was collected (AD 2001.8). For AH1–6 an age of AD 1997 was used, ie, the first full year within the confidence interval (> AD 1996.2). A younger age would infer decreased peat accumulation rate between 10 and 17 cm depth, which is unlikely because of the upward decrease in compaction and decomposition.

Annual resolution

In order to compare pollen data with climatic data each pollen sample is assigned to a full year. The pollen data cover the period 1976 to 2001 with 29 samples. Samples assigned to the same year are averaged. The pollen years are not exactly equivalent to calendar years, as the sampling precision is too low and natural conditions make this impossible, so a smoothing of 2–3 years compared with annually separated pollen deposition can be assumed. The growth pattern of *Sphagnum* also affects the pollen signal. Field and laboratory observations suggest that *Sphagnum* (in central European mountain regions) grows rapidly in height early in the growing season primarily by expansion of biomass accumulated the previous year. Later in the season *Sphagnum* does not grow so much in height but forms a dense surface layer that can expand in the next year. The surface of a *Sphagnum* hummock thus remains more or less the same from summer until the following spring. Thus late-flowering taxa deposit their pollen on the same surface as early-flowering taxa of the following year, so the 'pollen deposition year' runs from summer to summer. Additional time-lag must therefore be allowed for late-flowering taxa. The uppermost pollen sample (collected in the autumn 2001) will thus theoretically contain pollen from the late-flowering season AD 2000 together with the entire flowering season 2001. Together with uncertainties in the depth–age relationship this sums up to a possible deviation of 1 year of a taxon-specific pollen signal, which must be accounted for in the analysis of the data.

Modification of pollen percentage values

The six most abundant taxa in the pollen record (*Fagus*, *Picea*, *Pinus*, *Quercus*, Gramineae and *Urtica*) have been downweighted, as the high original percentage values disturb the climatic signal. The reduction factors have been calculated by dividing the mean pollen percentage value (AD 1976–2001) of *Betula* (the seventh most abundant pollen taxon) with the

Table 1 Radiocarbon analysis.

Sample	Depth (cm)	Lab code	$\delta^{13}C$ (‰)	Fraction modern pMC	1σ-calendar age	Mean
AH1–6	9.5	UtC-12572	−29.5	1.091±0.006	1996.2–2002.0	1999.1±2.0
AH1–16	17.7	UtC-11407	−28.7	1.173±0.005	1986.1–1990.2	1988.2±2.0
AH1–24	23.9	UtC-11408	−29.1	1.249±0.005	1980.7–1983.7	1982.2±1.0
AH1–30	28.4	UtC-11722	−29.4	1.462±0.006	1972.3–1972.8	1972.6±1.0
AH1–32	29.5	UtC-11409	−30.6	1.562±0.006	1968.2–1969.9	1969.1±1.0

mean pollen percentage value of the specific taxa. The original pollen percentage values of a taxon have then been multiplied with the reduction factor (Table 2) and subsequently new percentages have been calculated. With this modification the mean effective pollen sum decreases from 592 to 303. The mean pollen percentage value for the downweighted taxa after percentage recalculation is 6.1%. In the ideal case all taxa should be downweighted to the same value, because this would completely remove any differences between taxa in mean pollen productivity and plant cover. This has, however, the disadvantage that it would enhance the statistical error in taxa with low pollen counts. The removal of taxa with low pollen counts (eg, < 1% of the pollen sum) also has disadvantages, since it reduces the effective pollen sum and increases interdependence between the remaining taxa, and in addition the list of excluded taxa would depend on the taxonomic resolution of the investigation. The modification of the pollen percentages done here is a reduction of intertaxa differences in mean pollen productivity and vegetation cover, thus increasing the signal-to-noise ratio.

Comparison between sites

Two Alpine sites have been compared with AH1 (see Figure 1). ÄLB (Älbi Flue mire, 46°35′55″ N, 7°58′35″ E, 1850 m a.s.l.) is situated in the northern Alps of central Switzerland just below the forest limit (van der Knaap and van Leeuwen, 2003). The nearest trees (at 12 m distance) are *Pinus cembra,* but the general vegetation in the area is dominated by *Picea*. WEN (Wengerkopf, 47°10′40″ N, 13°52′40″, 1790 m a.s.l.) is situated in the Austrian Alps (Goslar *et al.*, 2005). *Pinus mugo* grows on the mire itself, while the surrounding forest is dominated by *Picea* with an admix of *Larix* and *Pinus cembra*.

The pollen records of ÄLB and WEN have been prepared in the same way as that of AH1 with reduction of the six most common taxa to the mean value of the seventh most common taxon (Table 2). In ÄLB the effective pollen sum decreased from 1226 to 383 and the mean modified pollen percentage of the downweighted taxa is 6.7%. In WEN the numbers are 703 to 306, and 7.2%. Taxa with a mean modified pollen percentage > 1% at all the sites have been used for comparison, and those with visible similarities among sites have been graphically displayed. Cyperaceae, *Potentilla* and *Vaccinium* are considered local plants and are therefore not included in the pollen sum or subject to downweighting.

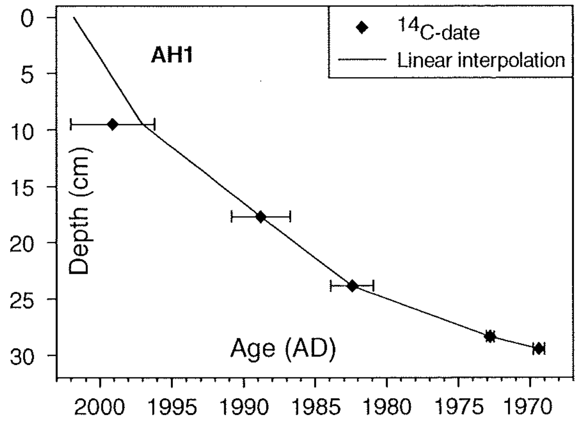

Figure 2 Depth-age relationship for AH1 (Les Amburnex Hummock 1, southwest Swiss Jura Mountains). Error bars show 1σ confidence interval. Linear interpolation used to infer the age of pollen samples is shown with line. Upper end of line is the surface (0 cm at AD 2001.8)

Climatic parameters and pollen–climate relationships

The climatic data are derived from the measurement station of Geneva (MeteoSchweiz; Begert *et al.*, 2005) *c.* 35 km south of the sampling site Amburnex (AH1). The main pollen source areas are the Jura Mountains (*Abies*, *Fagus*, *Picea*, herbs) and the Swiss plateau (deciduous trees, herbs). The absolute climatic measurements are primarily valid for the Swiss plateau, but both areas are likely affected by the same weather systems and can be expected to show similar annual variance in climatic parameters. Especially annual variations in temperature are representative for large areas (ie, Switzerland), while

Table 2 Reduction factors.

Sites and taxa	Reduction factor	Average percentage
Les Amburnex (AH1)		
Betula	1.00	3.1
Fagus	0.73	4.3
Gramineae	0.13	23.9
Picea	0.12	25.3
Pinus non-*cembra*	0.52	6.1
Quercus	0.81	3.9
Urtica	0.83	3.8
Älbi Flue (ÄLB)		
Alnus viridis	0.45	4.7
Betula	0.98	2.1
Gramineae	0.13	16.6
Picea	0.046	45.2
Pinus cembra	0.21	10.8
Pinus non-*cembra*	0.79	2.6
Urtica	1.00	2.1
Wengerkopf (WEN)		
Alnus glutinosa	1.00	3.1
Betula	0.61	5.1
Gramineae	0.42	7.5
Larix	0.35	8.8
Picea	0.097	32.2
Pinus cembra	0.28	11.0
Pinus non-*cembra*	0.30	10.5

Abundant taxa have been multiplied by a reduction factor to obtain a value similar to the seventh most abundant taxon. Average percentage refers to the average percentage value of the taxa AD 1976–2001 prior to modification.

annual precipitation anomalies might show larger spatial differences (Begert *et al.*, 2005).

Climatic parameters will not only affect the pollen productivity but also the pollen dispersal, primarily by prolonged rainfall, and wind direction and strength during the flowering season. Wind is not considered here, but as the wind pattern to some degree will vary together with temperature and precipitation it should be kept in mind.

Seasonal and annual temperature and precipitation were used as climatic parameters. Seasons are January/March (Winter), April/June (Spring), July/September (Summer), and October/December (Autumn). Results from pollen traps show that the pollen deposition of trees is affected by the weather conditions of the previous year (Hicks, 2001; van der Knaap *et al.*, 2001). Considering the uncertainties in the determination of the depth–age relationship and the characteristics of *Sphagnum* peat growth, both a 1-yr and a 2-yr time lag are used.

Statistics

Simple linear regression was used to test the correlation of single taxa with climatic parameters. Modified pollen percentages were used for further analyses of the assemblage because it is the more robust data set, and because the advantage of interdependence is limited in the methods used. Relationships within the modified pollen assemblage were tested with detrended correspondence analysis (DCA), which gave a short gradient length (0.95 SD), suggesting that a linear response model is appropriate (ter Braak and Prentice, 1988). Principal component analysis (PCA) and redundancy analysis (RDA) (ter Braak, 1987; ter Braak and Prentice, 1988) were applied to assess the internal relationships of the modified pollen assemblages and the relation between the modified pollen assemblages and climatic parameters. In PCA the grouping is done on the species composition, so the environmental variables do not affect the analysis. In RDA the ordination axes are linearly related to the climatic variables and thus show the impact of climate, but the choice of climatic variables affects the outcome. Both methods thus complement each other. *Sorbus*-type was removed from both PCA and RDA as the single strong peak would distort the analyses. The annual parameters of precipitation and temperatures were removed from the RDA to reduce autocorrelation between the climatic parameters. The statistical analyses were made with SYSTAT (Wilkinson, 1990) and CANOCO.

Results

Pollen diagrams

An unmodified pollen percentage diagram (Figure 3), a diagram of annually constrained pollen accumulation rates (Figure 4) and a diagram of annually constrained modified pollen percentages (Figure 5) are presented. Selected climatic parameters have been added for comparison. Cyperaceae, *Potentilla*-type and *Vaccinium* are not included in the pollen sum and have not been subjected to downweighting. These taxa occur on the mire itself and their pollen values are largely dependent on the plant distribution within the nearest few metres. *Picea* also occurs in the direct vicinity, but trees show less local influence on small distances (van der Knaap *et al.*, 2001), and it is included. In general as many species as feasible are included in the pollen sum (Wright and Harvey, 1963).

The unmodified pollen percentage diagram (Figure 3) does not show any clear trends, suggesting that no major changes in

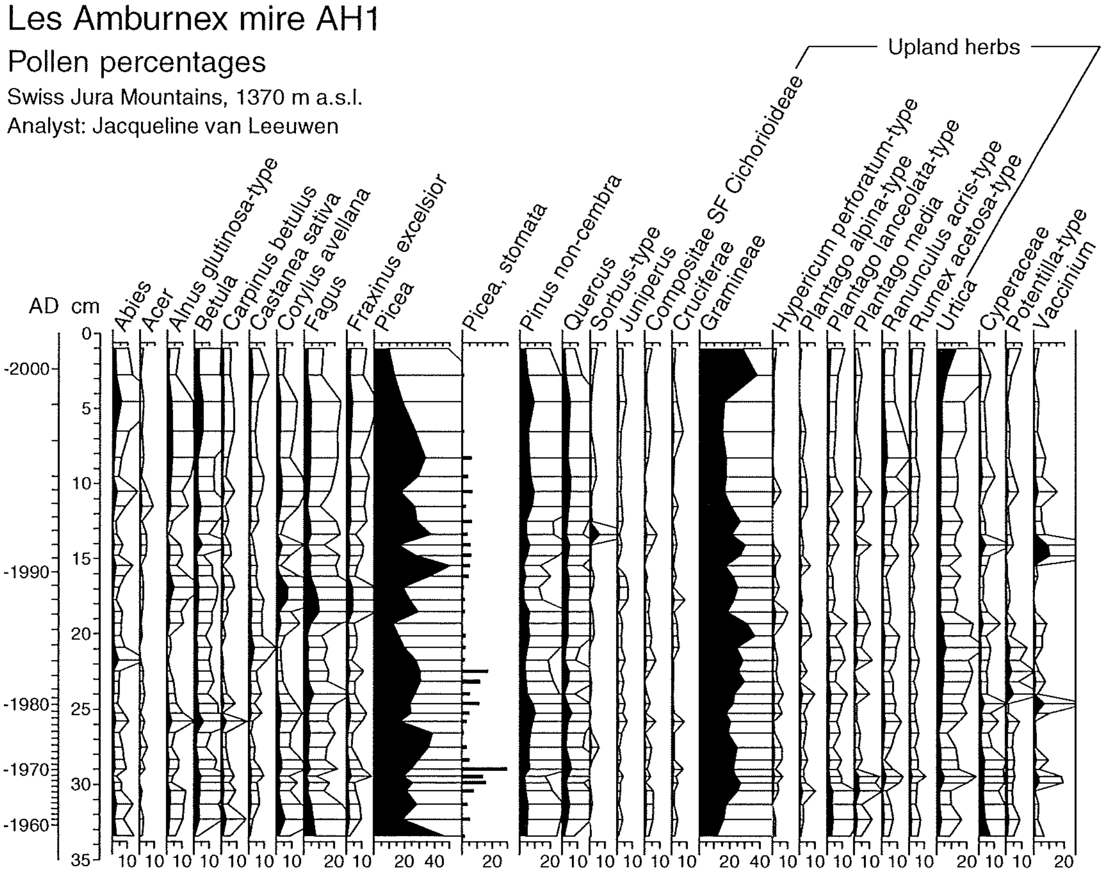

Figure 3 Pollen percentage diagram of Les Amburnex Hummock 1 (AH1). Percentages are based on the upland pollen sum. The scale (%) follows the black curve, and the white curve shows × 5 exaggeration. Bars in the white curve represent sample positions

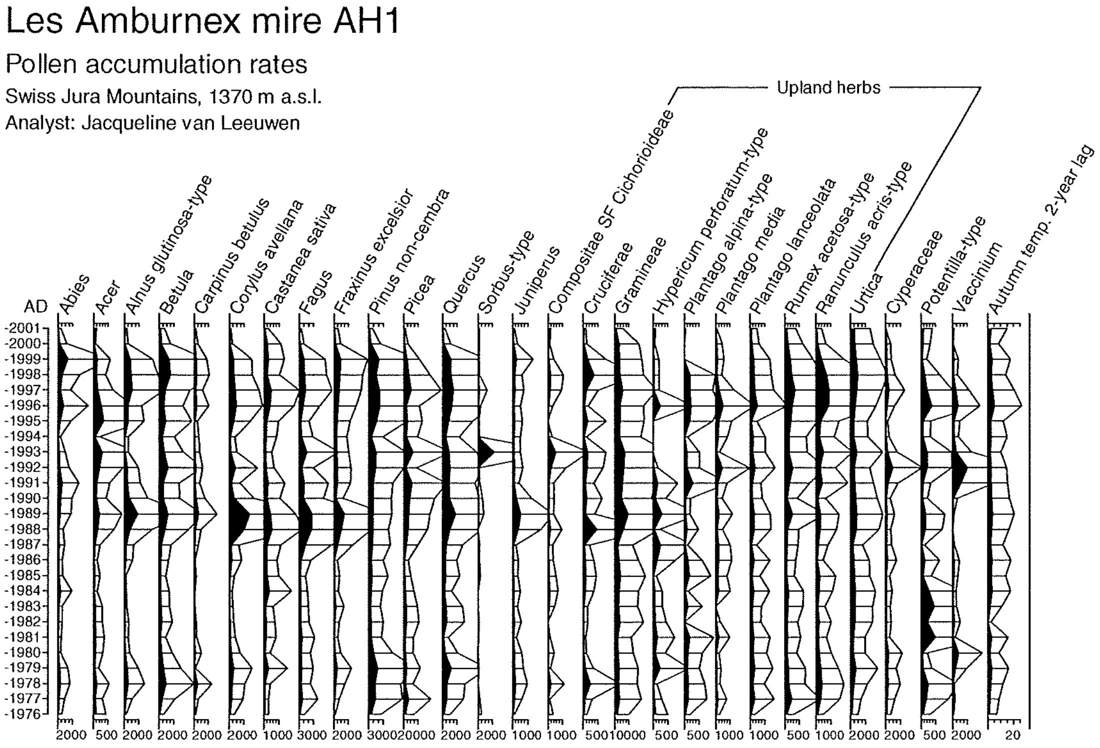

Figure 4 Pollen accumulation rates of Les Amburnex Hummock 1 (AH1). Autumn temperature has been added for comparison. Taxa with a mean modified percentage > 1% are included. The scale (grains/cm per yr) follows the black curve, and the white curve shows × 5 exaggeration. Bars in the white curve represent sample positions

the surrounding vegetation can be expected. The position of the hummock below *Picea* branches allows a ready supply of *Picea* needles. Undecomposed needles are sieved away during pollen preparation, so the frequencies of *Picea* stomata are probably more reflective of the needle decomposition rate than the deposition rate. Interestingly, increased values of *Picea*

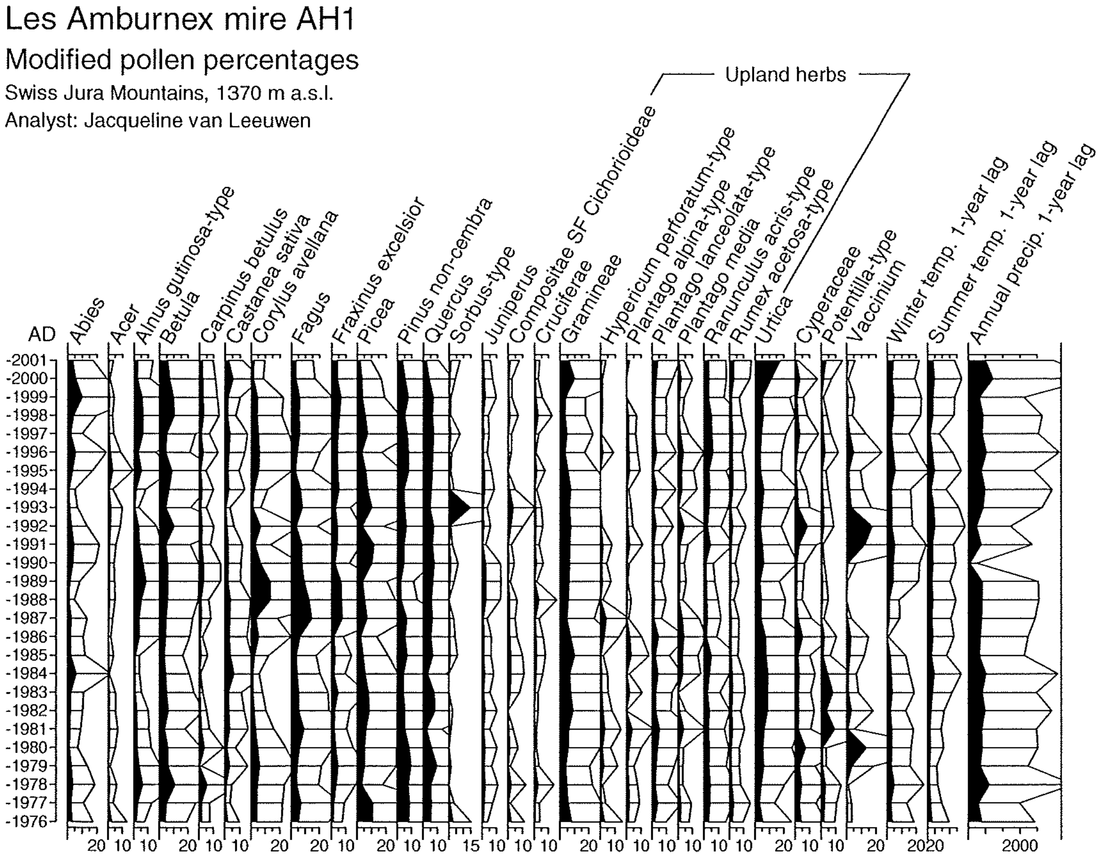

Figure 5 Modified pollen percentages of Les Amburnex Hummock 1 (AH1). The scale (%) follows the black curve, and the white curve shows × 5 exaggeration. Bars in the white curve represent sample positions. Climatic parameters have been added for comparison. The scale for summer temperature starts at 15°C, for annual precipitation at 500 mm/yr. Taxa with a mean percentage > 1% are included

stomata correspond to increased pollen values of *Vaccinium*, suggesting a common cause.

The diagram of pollen accumulation rates (Figure 4) shows low values for most taxa AD 1980–1987 and high values 1988–2000. Peaks occur 1978, 1988–1989 and 1996–1999.

The modified pollen percentage diagram (Figure 5) shows clear synchronous peaks and dips for some taxa. In 1978 there is a peak in *Alnus*, *Betula*, and Cruciferae, while *Fagus*, *Picea* and Gramineae dip. In 1987–1989 there is a peak in *Corylus*, *Fagus* and *Fraxinus*.

Comparison between sites

Several taxa show visual similarities (Figure 6) in annual fluctuations between the sites (*Betula*, *Corylus*, *Fagus*, *Fraxinus*, *Picea*, *Pinus*, *Quercus*, Cyperaceae and *Vaccinium*). Other taxa show little or no visual similarities (*Alnus glutinosa*, Gramineae, *Plantago lanceolata*-type, *Rumex acetosa*-type, *Urtica* and *Potentilla*-type). Simple linear regression analysis resulted in statistical significant correlation ($p \leq 0.05$) of *Corylus* for AH1–WEN, *Fagus* for AH1–ÄLB and *Fraxinus* for both AH1–ÄLB and AH1–WEN. *Potentilla*-type shows negative correlation for AH1–ÄLB, but this makes no ecological sense and is likely by chance. The strong correlation of *Vaccinium* for ÄLB–WEN ($P = 0.001$) might depend on the single-peak distribution of the *Vaccinium* pollen values.

Annual fluctuation in pollen deposition can be correlated between sites with different vegetation over a distance of 600 km. This suggests that climatic forcing of pollen production occurs on at least a regional scale. Trees correlate better than upland herbs.

Correlation of single taxa with climatic parameters

Annually constrained pollen accumulation rates and modified pollen percentages were tested with simple linear regression against seasonal and annual climatic parameters (Table 3). Only taxa with a mean modified percentage above 1 were tested. Pollen accumulation rates give independent measurements for each taxon but are sensitive to peat characteristics, age determination and laboratory work. Modified pollen percentages are more robust in the above senses, but the value of each taxon is relative to the pollen assemblage.

Pollen accumulation rates for many taxa give significant positive correlations with autumn temperature at a 2-yr time lag, and all other taxa respond positively. There is no ecological explanation to why all taxa should respond in the same way to autumn temperature, so the alternative explanation of short-term variations in peat growth is likely. Autumn temperature will therefore not be used to infer variance in pollen productivity from pollen accumulation rates. It should nevertheless be noted that if a climatic parameter affects several taxa in the same direction, this will be difficult to observe in the modified pollen percentages because of the interdependence of the taxa. With the exception of autumn temperatures, most of the correlations that are statistically significant in pollen accumulation rates are also significant for modified pollen percentages. The only exception is annual temperature, where significant positive correlations of *Acer*, *Plantago media*, *Ranunculus acris* and *Rumex acetosa* only occur in the pollen accumulation rate data set but not for the modified pollen percentages.

Modified pollen percentages give, in general, clearer statistical relationships with climate than pollen accumulation rates. Both pollen accumulation rates and modified pollen percentages indicate that winter temperature is an important factor for pollen productivity by several arboreal taxa (*Abies*, *Acer*, *Betula*, *Carpinus*, *Fagus* and possibly *Fraxinus*). See Table 3 for other interpretations of climate favourable for pollen productivity of individual taxa. Both pollen accumulation rates and modified pollen percentages have been considered in the interpretation.

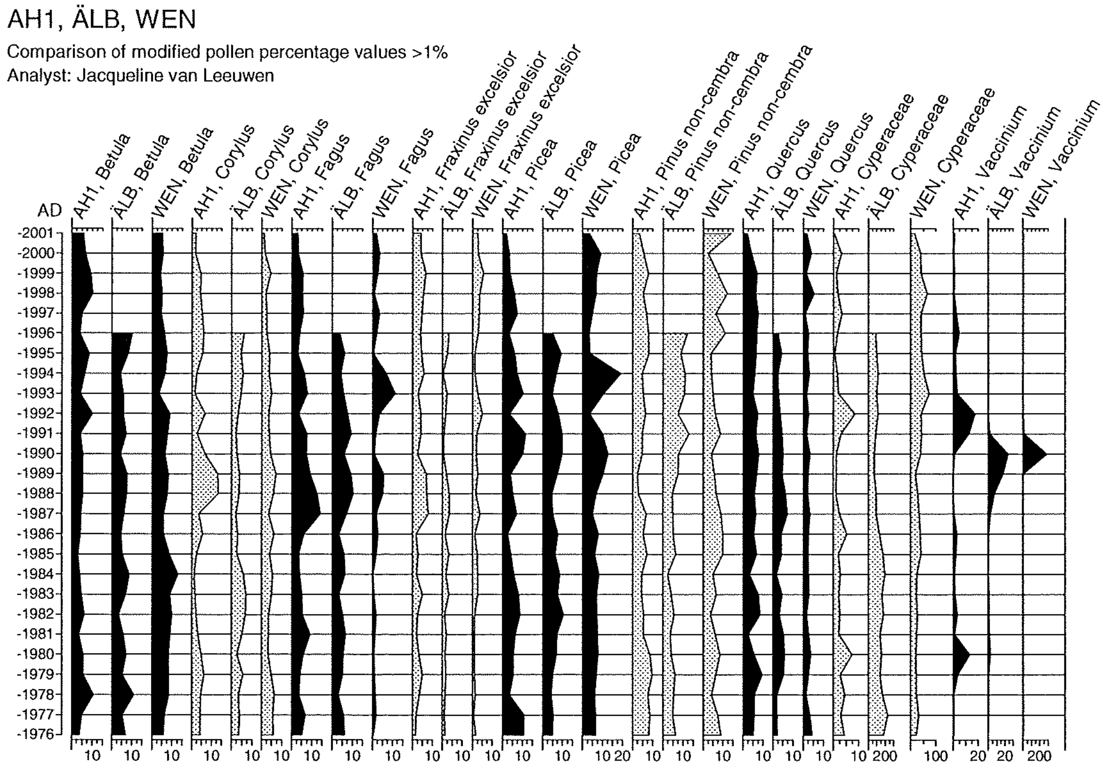

Figure 6 Comparison of modified pollen percentages between sites in Jura Mountains and Alps; see Figure 1 for sites. Taxa with modified pollen percentage values > 1% at all sites are used

Table 3 Statistically significant correlations (simple linear regression) between pollen accumulation rates or modified pollen percentages of single taxa and climatic parameters.

Taxa	Pollen accumulation rates										Modified pollen percentages										Interpretaion
	Temperature					Precipitation					Temperature					Precipitation					
	Win	Spr	Sum	Aut	Ann	Win	Spr	Sum	Aut	Ann	Win	Spr	Sum	Aut	Ann	Win	Spr	Sum	Aut	Ann	Favourable climate
Trees																					
Abies	+			(+)	(+)						+(+)	(+)			+(+)	(*n*)					Warm winter, year, spring?
Acer	+				+						+										Warm winter
Alnus				(+)										(+)							Warm autumn?
Betula	+										+	(+)									Warm winter, spring?
Carpinus	+			(+)							+										Warm winter
Castanea				(+*)													+				Wet spring?
Corylus				(+)										(+)					*n*		Warm autumn? dry autumn?
Fagus	(*n*)								(*n*)		(*n**)							(*n**)	(*n**)		Cold winter, dry autumn
Fraxinus				(+*)			(+)				(*n*)						(+*)				Cold winter? wet spring?
Picea														(*n*)		*n*				(*n*)	Cold autumn? dry?
Pinus				(+)									*n*								Cold summer?
Quercus				(+)																*n*	Dry?
Sorbus			(+)										(+)								Warm summer
Herbs																					
Cruciferae							+										+*				Wet spring
Gramineae														(*n*)							Cold autumn?
Hypericum		(*n*)		(+)		+*	*n*		(*n*)			(*n**)			*n**(*n*)	+(+)		(*n*)	*n*(*n*)		Cold spring, wet and dry
Plantago alpina												*n**									Cold spring?
P. lanceolata				(+)											*n*						Cold?
P. media				(+)	(+)																Warm?
R. acris				(+)	(+)															+	Warm? wet?
Rumex acetosa				(+)	(+)							+						+*(+)	+*		Warm? wet spring? summer?
Urtica				(+)																(+)	Wet?
Wetland																					
Cyperaceae												*n*			*n*						Cold spring? year?
Vaccinium	(+)																	*n* (*n*)			Warm winter? Dry?

+ = significant positive correlation ($p \leq 0.05$) at 1-yr time lag; *n* = significant negative correlation ($p \leq 0.05$) at 1-yr time lag; (+) and (*n*) as above but with 2-yr time lag. +* and n* mark highly significant correlations ($p \leq 0.01$). No significant correlation was found for *Juniperus*, Compositae Subfam. Cichorioideae, and *Potentilla*. Win, Winter (January/March); Spr, Spring (April/June); Sum, Summer (July/September); Aut, Autumn (October/December); Ann, Annual. Interpretation gives the clearest trends for the taxon. A question mark is added if the correlation only occurs in one of the data sets. Correlations of pollen accumulation rate with autumn temperature are not considered; see text for explanation.

Statistical analyses of the pollen assemblage and its relation to climatic parameters

The modified pollen assemblage (modified pollen percentages) has been analysed with ordination methods. In PCA the first two ordination axes explain 49% of the variance, for RDA this is 42%. The RDA ordination axes together are significant ($P = 0.004$). PCA and RDA show essentially the same pattern (Figure 7), suggesting that the applied climatic parameters explain the general pattern in the modified pollen assemblages. The first RDA axis is primarily related to summer temperature and autumn precipitation, the second RDA axis to winter, spring and autumn temperature together with summer and autumn precipitation. Some taxa are clearly grouped together: *Abies* and *Betula*; *Alnus*, *Corylus* and *Fraxinus*; Gramineae and Compositae Subfam. Cichorioideae; *Ranunculus acris*-type, *Rumex acetosa*, *Plantago lanceolata* and *Urtica*. It is likely that the taxa in a group react in a similar way to specific weather conditions.

Discussion and conclusions

Even a rather short timeseries of 26 years is sufficient to capture the relation of annual variation in climatic conditions with pollen productivity for many taxa, and the similarities in annual variation between sites far apart (600 km) suggests that pollen/climate relationships are valid on a regional scale. Still, differences in growing conditions likely affect the biotic responses to variations in climatic parameters. The results here are thus primarily valid for central European mid-altitude areas. For example, precipitation does not seem to affect pollen productivity in the northern boreal forests (Hicks, 2001), and pollen productivity of plants growing near their highest altitudinal limit is primarily affected by summer temperatures (van der Knaap and van Leeuwen, 2003). The pollen accumulation rates in the site studied here gave much better estimates of variations in pollen productivity than in earlier investigations (van der Knaap and van Leeuwen, 2003), where pollen

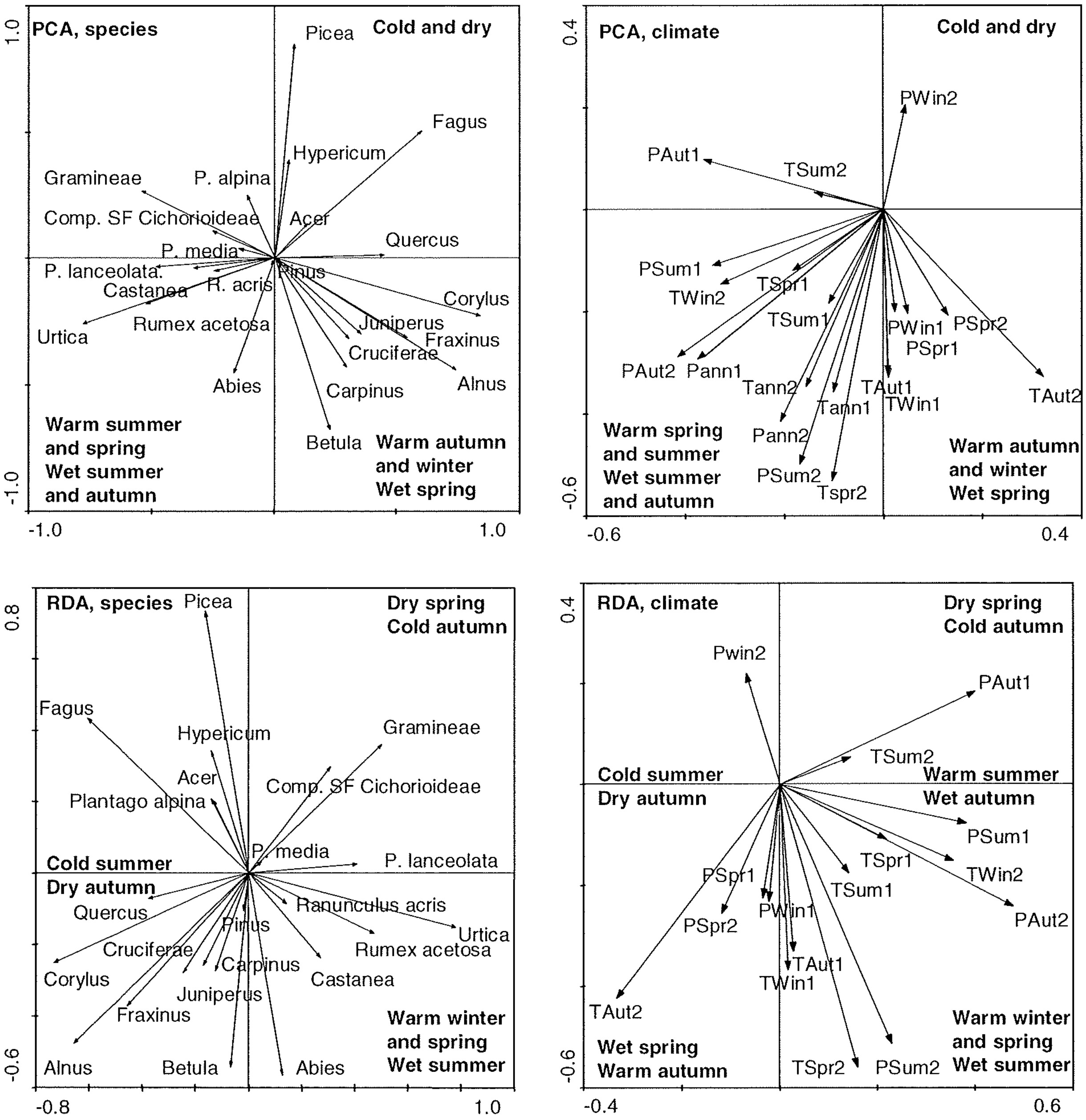

Figure 7 PCA and RDA scatter plots of modified pollen percentages (*Sorbus*-type excluded), and annual and seasonal temperature and precipitation with 1- and 2-yr time lag. Species and climatic parameters are displayed on separate plots. First ordination axis of PCA explains 30% of the variance, the first two 49%. First ordination axis of RDA explains 26% of the variance, the first two 42%. The general relationships between the climatic parameters and the modified pollen assemblage have been noted in the plots

accumulation rates (called there 'detrended pollen concentrations') were shown to be strongly affected by short-term variations in peat growth. This indicates that the sensitivity of peat growth to specific weather conditions varies between climatic settings.

The main results are shown in Table 3 and Figure 7, and the most important conclusions are discussed below.

(1) *Sphagnum* hummocks, or fast growing peat, can be dated with an accuracy of ±1 yr from 1960 onwards. This allows environmental parameters to be traced with annual resolution, but a 2–3 yr smoothing of the signal has to be allowed for.
(2) Downweighting of the most abundant pollen taxa reduces the effects of plant cover, mean pollen productivity, and interdependence of the pollen values. This increases the direct annual effect of climate on single taxa and allows comparison between sites with different surrounding vegetation.
(3) Pollen accumulation rates show climate-induced annual variations both in pollen productivity and in peat growth. Possible annual variation in peat growth can be expected if many taxa with different ecological requirements show a similar response to climatic parameters. Combined use of pollen accumulation rates and modified pollen percentages allows determination of the most important climatic parameters for the pollen productivity of a specific taxon.
(4) Similarities in annual pollen deposition can be seen in sites up to 600 km apart. Tree species show stronger similarities than herbaceous taxa, and lowland trees (*Corylus*, *Fagus* and *Fraxinus*) show the most similar pattern.
(5) The increased modified pollen percentages of *Fagus* and *Fraxinus* AD 1987–1994 that occurred in the Jura Mountains and the Alps can hardly be explained by anything other than climatic conditions. One explanation might be the rise in temperature in central Europe during the 1980s (Auer *et al.*, 2001). Several taxa show large variations in pollen deposition during the past 100 years (van der Knaap *et al.*, 2000), which is normally attributed to changes in vegetation cover or landuse. Considering the large changes in the landscape during the past century this is likely a correct assumption, but the results here suggests that it shall not be done uncritically.
(6) Winter temperature is important for the pollen productivity of many tree taxa. *Abies* and *Betula* respond positively to both winter and spring temperature; *Acer* and *Carpinus* respond positively to winter temperature; *Fagus* and possibly *Fraxinus* respond negatively to winter temperature; *Alnus* and *Corylus* respond positively to autumn temperature. The pollen productivity of many trees thus seems to be affected by climatic conditions outside the main growing season (summer). A possible explanation is that frost damage, failed hibernation or premature flowering are more critical than summer warmth. Careful studies of the physiology, phenology and ecology of specific taxa will be required to better understand the processes involved.
(7) Three major climatic gradients affect pollen productivity: summer and spring temperature (April–September) together winter and autumn precipitation (October–March); autumn and winter temperature (October–March) together with winter and spring precipitation (January–June); and temperature together with precipitation in general. The clearest climatic gradient in PCA and RDA is warm/wet to dry/cold, but the seasonal influence is considerable.

Acknowledgements

We thank Brigitta Ammann for encouragement and valuable comments, and Florencia Oberli for carrying out much of the laboratory work. Comments by Bas van Geel and an unknown referee were helpful to improve the manuscript. This paper is a contribution to the Swiss National Science Foundation (SNF) project NCCR Plant Survival; the European Union project PINE (Predicting Impact on Natural Ecotones, project EVK2-CT-2002-00136; and the NordForsk framework POLLANDCAL (Pollen/landscape calibration network). Additional support has been given by the Marie Curie Fellowship Association (MCFA) through the framework Cultural Landscapes of Europe (CULTLAND) at the University of Bergen.

References

Ammann, B., **Birks, H.J.B.**, **Brooks, S.J.**, **Eicher, U.**, **von Grafenstein, U.**, **Hofmann, W.**, **Lemdahl, G.**, **Schwander, J.**, **Tobolski, K.** and **Wick, L.** 2000: Quantification of biotic responses to rapid climatic changes around the Younger Dryas – a synthesis. *Palaeogeography, Palaeoclimatology, Palaeoecology* 159, 313–47.

Andersen, S.T. 1970: The relative pollen productivity and pollen representation of North European trees and correction factors for tree pollen spectra. *Danmarks Geologiske Undersogelse* Series II 96, 1–99.

Auer, I., **Böhm, R.** and **Schöner, W.** 2001: Austrian long-term climate 1767–2000–multiple instrumental time series from central Europe. *Österreichische Beiträge zu Meteorologie und Geophysik* 25, 1–147.

Begert, M., **Schlegel, T.** and **Kirchhofer, W.** 2005: Homogeneous temperature and precipitation series of Switzerland from 1864 to 2000. *International Journal of Climatology* 25, 65–80.

Berglund, B.E. and **Ralska-Jasiewiczowa, M.** 1986: Pollen analysis and pollen diagrams. In Berglund, B.E., editor, *Handbook of Holocene palaeoecology and palaeohydrology*. J. Wiley and Sons, 455–84.

Broström, A., **Sugita, S.** and **Gaillard, M.-J.** 2004: Pollen productivity estimates for reconstruction of past vegetation cover in the cultural landscape of Southern Sweden. *The Holocene* 14, 371–84.

Goslar, T., **van der Knaap, W.O.**, **Hicks, S.**, **Andrič, M.**, **Czernik, J.**, **Goslar, E.**, **Räsänen, S.** and **Hyötylä, H.** 2005: Radiocarbon dating of modern peat profiles: pre- and post-bomb ^{14}C variations in the construction of age–depth models. *Radiocarbon* 47, 115–34.

Hausmann, S., **Lotter, A.F.**, **van Leeuwen, J.F.N.**, **Ohlendorf, C.**, **Lemcke, G.**, **Grönlund, E.** and **Sturm, M.** 2002: Interactions of climate and land use documented in the varved sediments of Seebergsee in the Swiss Alps. *The Holocene* 12, 279–89.

Hicks, S. 2001: The use of annual arboreal pollen deposition values for delimiting tree-lines in the landscape and and exploring models of pollen dispersal. *Review of Palaeobotany and Palynology* 117, 1–29.

Hicks, S., **Tinsley, H.**, **Huusko, A.**, **Jensen, C.**, **Hättestrand, M.**, **Gerasimides, A.** and **Kvavadze, E.** 2001: Some comments on spatial variation in arboreal pollen deposition: first records from the Pollen Monitoring Programme (PMP). *Review of Palaeobotany and Palynology* 117, 183–94.

Hjelle, K.L. 1998: Herb pollen representation in surface moss samples from mown meadows and pastures in western Norway. *Vegetation History and Archaeobotany* 7, 79–96.

Kullman, L. 1998: Non-analogous tree flora in the Scandes Mountains, Sweden, during the early Holocene–macrofossil evidence of rapid geographic spread and response to palaeoclimate. *Boreas* 27, 153–61.

Levin, I. and **Kromer, B.** 2004: Post nuclear-testing – the tropospheric $^{14}CO_2$ level in mid-latitudes of the Northern Hemisphere (1959–2003). *Radiocarbon* 46, 1261–72.

Litschauer, R. 2000: Blüh- und Fruktifikationsverhalten der Waldbäume. *FBVA Berichte* 123, 45–66.

Moore, P.D., Webb, J.A. and **Collinson, M.E.** 1991: *Pollen analysis.* Blackwell.

Nielsen, A.B. and **Odgaard, B.V.** 2004: The use of historical analogues for interpreting fossil pollen records. *Vegetation History and Archaeobotany* 13, 33–43.

Nydal, R. and **Lövseth, K.** 1983: Tracing bomb ^{14}C in the atmosphere, 1962–1980. *Journal of Geophysical Research* 88, 3621–42.

Prentice, I.C. 1985: Pollen representation, source area, and basin size: towards a unified theory of pollen analysis. *Quaternary Research* 23, 76–86.

Punt, W. and **Blackmore, S.** editors 1991: *Northwest European pollen flora, VI.* Vol. VI. Reprint from *Review of Palaeobotany and Palynology* 69. Elsevier, 1–275.

Reimer, P., Brown, T. and **Reimer, R.** 2004: Post nuclear-testing ^{14}C – discussion: reporting and calibration of post-bomb ^{14}C data. *Radiocarbon* 46, 1299–304.

Stockmarr, J. 1971: Tablets with spores in absolute pollen analysis. *Pollen et Spores* 13, 615–21.

Sugita, S. 1994: Pollen representation of vegetation in Quaternary sediments: theory and method in patchy vegetation. *Journal of Ecology* 82, 881–97.

Tallantire, P.A. 2002: The early-Holocene spread of hazel (*Corylus avellana* L.) in Europe north and west of the Alps: an ecological hypothesis. *The Holocene* 12, 81–96.

ter Braak, C.J.F. 1987: Ordination. In Jongman R.H.G., ter Braak, C.J.F. and van Tongeren, O.R., editors, *Data analysis in community and landscape ecology.* Pudoc, 91–173.

ter Braak, C.J.F. and **Prentice, I.C.** 1988: A theory of gradient analysis. *Advances in Ecological Research* 18, 271–313.

Tinner, W. and **Lotter, A.F.** 2001: Central European vegetation response to abrupt climate change at 8.2ka. *Geology* 29, 551–54.

van der Knaap, W.O. and **van Leeuwen, J.F.N.** 2003: Climate/pollen relationships AD 1901–1996 in two small mires near the forest limit in the northern and central Swiss Alps. *The Holocene* 13, 809–28.

van der Knaap, W.O., van Leeuwen, J.F.N., Fankhauser, A. and **Ammann, B.** 2000: Palynostratigraphy of the last centuries in Switzerland based on 23 lake and mire deposits: chronostratigraphic pollen markers, regional patterns, and local histories. *Review of Palaeobotany and Palynology* 108, 85–142.

van der Knaap, W.O., van Leeuwen, J.F.N. and **Ammann, B.** 2001: Seven years of annual pollen influx at the forest limit in the Swiss Alps studied by pollen traps: relations to vegetation and climate. *Review of Palaeobotany and Palynology* 117, 31–52.

von Post, L. 1916: Skogsträdpollen i sydsvenska torvmosselagerföljder. In proceedings to *16. Skandinaviska Naturforskarmotet*, Kristiania (Oslo), 433–65.

Wilkinson, L. 1990: *SYSTAT and SYGRAPH: the system for graphics, v. 5.05.* SYSTAT, Inc.

Wright, H.E. and **Harvey, L.P.** 1963: The pollen sum. *Pollen et Spores* V, 445–50.

The Holocene 16,2 (2006) pp. 210–223

The development of pasture woodland in the southwest Swiss Jura Mountains over 2000 years, based on three adjacent peat profiles

Per Sjögren*

(Institute of Plant Sciences, University of Bern, Altenbergrain 21, CH-3013 Bern, Switzerland)

Received 10 January 2005; revised manuscript accepted 10 September 2005

A
HOLOCENE
RESEARCH
PAPER

Abstract: The pollen content of three adjacent peat profiles has been analysed to study the development of pasture woodland in the small valley Combe des Amburnex (1300 m a.s.l.). Chronostratigraphy based on lowland pollen assemblages and radiocarbon dates was used to correlate and date the profiles. Forest and mire grazing occurred throughout at least the past two millennia. Before the ninth century the forest consisted of about equal parts of *Abies*, *Fagus* and *Picea*. Thereafter *Picea* increased and is today strongly dominant in the area, likely an effect of selective browsing. The central part of the valley obtained its modern structure of pastures and forests in the twelfth century, and the pasture woodland in general came into existence during the seventeenth century as an effect of extensive fire activity, possibly charcoal production. In the twentieth century grass and nutrient-demanding species increased relative to other herbs.

Key words: Cultural landscape, Jura Mountains, palaeoecology, forest history, pasture woodland, pollen analysis, Switzerland, late Holocene.

Introduction

Pasture woodland is a typical landscape for the Jura Mountains at middle elevation (*c.* 900–1400 m a.s.l.). It consists of a mosaic of open pastures, wooded pastures and forests, which are kept in this state by summer grazing and forest management (Gillet and Gallandat, 1996). This type of cultural landscape was probably once widespread across Europe, but today it is present only in limited areas because of modern agriculture and forestry practices.

The park-like landscape with its solitary spruces, well trimmed by cattle, has a high aesthetic value, and is important in both biological and economic respects. The mosaic landscape in general and the wooded pastures with their mixed vegetation in particular show a high biodiversity (Gallandat *et al.*, 1995). Traditional types of land use, now in modern forms, have in the recent decennia been complemented with tourism; hiking, cross-country skiing and picnicking in the picturesque landscape are particularly popular recreation activities.

This study is part of the project National Centre of Competence in Research (NCCR) Plant Survival, in which modern and historical ecology of pasture woodland are investigated in order to improve the scientific base of the management strategies for this type of landscape. The small valley Combe des Amburnex in the high part of the Jura Mountains is used as an investigation area for several different ecological studies. The major questions are how and to what degree the modern landscape pattern and species composition are dependent on historical land-use changes and/or internal dynamics.

The contribution of this paper is to assess a detailed long-term vegetation history and development of pasture woodland within the investigation area. Special weight is given to the spatial scale in order to understand the landscape patterns, in this case differences between the central and peripheral part of the valley. The period of concern is the past 2000 years, as this is relevant for the development of today's pasture–woodland landscape, but the past 100 years are considered of special importance as this time period provides the link between palaeoecological results and ecological investigations and models of the present vegetation.

The study is based on the analysis of pollen in three peat profiles. The sites are within 1 km of each other, which enables

---

*Author for correspondence: (e-mail: per.sjoegren@ib.uit.no)

10.1191/0959683606hl921rp

assessment of local changes in the landscape structure. Different basin sizes are used to improve the spatial resolution (eg, Björkman and Sjögren, 2003; Koff and Kangur, 2003). Most mires in the area are heavily grazed so the top part of the peat is compressed or disturbed. To enable comparison between the sites under such conditions a chronostratigraphy was established on the basis of low-land pollen assemblages (non extra-local pollen) and radiocarbon dates.

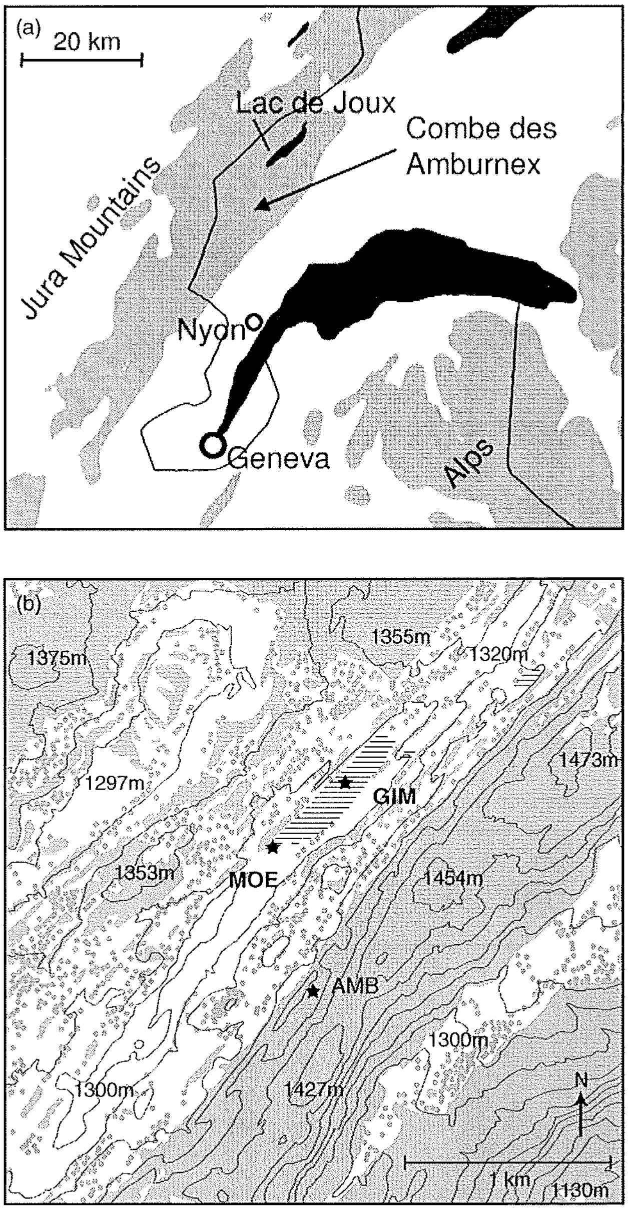

Figure 1 Overview map (a) and site map (b). a. Grey represents areas above 1000 m a.s.l. The thin line marks the border between France and Switzerland. b. Grey represents forest, small dots are single or small groups of trees, mainly *Picea*. Wetlands are marked with stripes, site locations are marked with stars. The map covers the northern part of Combe des Amburnex

Study sites and regional settings

Geographical setting

The valley Combe des Amburnex at 1300 m altitude in the Jura Mountains is separated from the Swiss lowland by one main ridge (Figure 1). The nearest larger agricultural areas are situated *c.* 5 km to the east. The dominating humid wind direction is from the south-southwest, with weak winds from the north-northeast. Mean yearly temperature is *c.* 3°C, with a mean July temperature of *c.* 11°C and a mean February temperature of *c.* −4°C. Single days may be extremely cold, and frost may occur even in summer.

Precipitation is high, *c.* 1600 mm/yr, but the water is quickly drained away in the permeable limestone bedrock and summer droughts do occur. Wetlands are common in the lower parts of the valley where depressions are sealed off with clay and fed by springs. Nearly half the area has a tree cover. The tree composition is dominated by *Picea*, while *Abies*, *Fagus* and a few *Acer* trees occur in areas protected from grazing, such as on stony ridges and in denser stands. The pastures are species-rich, and 550 vascular plant species have been listed in the valley and surrounding area (Vittoz, 1998).

The general Holocene vegetation history of the southwest Jura Mountains is well established (Wegmüller, 1966), as is the general development of the cultural landscape (Gauthier, 2004). Several palaeoecological investigations along the south-eastern edge of the mountain chain have been published (eg, Ruffaldi, 1993; Schoellammer, 1997; van der Knaap *et al.*, 2000; Mitchell *et al.*, 2001; Roos-Barraclough *et al.*, 2004), but they have little focus on the cultural landscape.

Historical setting

In 58 BC the Helvetii, who occupied all the land between the Jura Mountains and the river Rhine, burnt their own cities and villages, and set out to conquer Gaul (France). But they were defeated in the same year by the Roman commander Julius Caesar and, heavily decimated, they were forced to return to their old lands (Caesar, −51). The Romans founded Nyon (Colonia Iulia Equestris) in 45/44 BC as a colony for retired soldiers. It lies at the shore of Lake Geneva 20 km south of the investigation area, but it is unclear whether or not the colony included the slopes of the Jura Mountains (Tarpin *et al.*, 2002). Monks were active in the Jura Mountains already in the fifth century, but in the investigation area they had no major impact until the twelfth century. The Abbey du Lac de Joux was founded in AD 1126 and became important for the opening up of the Joux valley, less than 5 km northwest of the investigation area. Pastures in Combe des Amburnex were mentioned in connection with the opening of the Carthusian monastery of Oujon (near Azier, 8 km south), in AD 1146 (Mottaz, 1982). Later written sources mention pastures in Combe des Amburnex in AD 1301, then owned by the village St Oyens, 8 km southeast (Rochat, 1995). In AD 1348 the plague (Black Death) severely reduced the population in this part of Europe.

Major glass and iron production were established in the Jura Mountains in the Middle Ages (Rieben, 1957). Charcoal was produced in the area around Combe des Amburnex from at least the sixteenth century (Rochat, 1995). As glass and charcoal production increased in the eighteenth and nineteenth centuries the forests became increasingly overexploited. Charcoal production stopped first when the railroad allowed importation of cheap stone coal in the second half of the nineteenth century. Old maps show that the treeless areas in Combe des Amburnex were about 10% larger in 1892–93 than today (*Die Siegfried Karten*, Marchairuz, section XVI, 2b). In 1902 different cantonal and federal laws finally allowed organized forestry, and in the 1950s–1970s separation of forest and pastures was promoted. Since 1973 the area has been under protection as part of the 70 km^2 Parc Jurassien Vaudois and it is kept open by a combination of summer grazing and selective forestry (Gillet and Gallandat, 1996).

Material and methods

Coring sites and field work

Three adjacent profiles were used. The main pollen profile, GIM, is based on a core from the middle part of the large mire Sèche de Gimel (*c.* 12 ha) at 1300 m altitude (Figure 1b). The same site was used for palaeoecological investigations by S. Wegmüller (1966, 'Le Marais des Amburnex'). A second profile, MOE, is based on a core from the southwestern edge of the same mire. This mire is famous among botanists for the occurrence of *Saxifraga hirculus*, the only locality in Switzerland. A third core, AMB, came from a small raised bog (*c.* 0.2 ha) on the valley side at 1370 m altitude. This bog is largely overgrown by *Picea*, and a colony of badgers has settled in the southern part. Both MOE and AMB are used for water extraction and are today also fenced and protected from grazing. The short names derive from geographical places, ie, GIM for Sèche de Gimel, MOE for Le Moé and AMB for Les Amburnex.

The GIM core was obtained in 2003 with a gauge corer of 6 cm diameter. The first 0.5 m of the top drive was dug free from surrounding peat before extraction to allow an undisturbed peat recovery. For the lower part of the profile a parallel core 1.2 m distant was used, as this had a longer and undisturbed recovery for the lower drives. Total coring depth was 3.4 m. The MOE and AMB profiles was collected in 2002 as *c.* 50 cm deep monoliths.

GIM has a decomposed top layer of *c.* 40 cm, below which the peat is well preserved. MOE has a *c.* 30 cm thick top layer of well-preserved *Sphagnum*, but below that the peat is strongly decomposed. AMB has a *c.* 10 cm thick layer of well-preserved *Sphagnum* overlying decomposed peat.

Pollen analysis

The pollen samples were prepared by the acetolysis method (Faegri and Iversen, 1989): hot KOH 8 min, addition of *Lycopodium*-tablets dissolved in HCl, sieving at 0.2 mm, acetolysis 2 min, hot KOH 5 min, glycerine, mounting in glycerine and staining with fuchsine. The dissolved *Lycopodium* tablets were added first directly prior to sieving because some plant material did not settle well in HCl. Analysis was carried out at 400 × magnification. Reference material used for identification of pollen types included literature (Punt and Clarke, 1984; Moore *et al.*, 1991; Reille, 1992, 1995, 1998; Punt *et al.*, 1995; van Geel *et al.*, 2003; Beug, 2004) and the reference collection at the Institute of Plant Sciences in Bern. Nomenclature follows ALPADABA (Alpine Palynological Data-Base, housed in Bern). Approximately 500 upland pollen grains have been counted in each sample (mean pollen sum for the main diagrams is 570).

Biostratigraphy

Because of uneven peat accumulation the correlation between sites is based on biostratigraphy (Figure 2). Pollen assemblages from taxa not growing in the area (ie, extra-regional) and assumed not to have grown there in the past were used to establish the biostratigraphy. The maximum distance between the sites is 1 km, and at least 5 km exists to any substantial population of the taxa used for correlation, so the extra-regional pollen assemblages should be the same in all three sites (eg, Janssen, 1966, 1981; Jacobson and Bradshaw, 1981; Prentice, 1985). Minor differences in the extra-regional pollen assemblages among the sites are attributed to differences in local air currents, sedimentation surfaces, decomposition, sampling resolution and statistical errors resulting from low extra-regional pollen sums (mean 110). The zonation is based on distinctive features within zones and at zone transitions (increases, decreases and amplitude). Features used for correlation are either recognized in two or in three of the profiles. In addition, pollen assemblage zones (PAZ) have been determined statistically by optimal sum-of-squares partitioning (Birks and Gordon, 1985; Birks, 1986) and their significance has been tested with the broken-stick method (MacArthur, 1957; Bennett, 1996). Considering the different resolutions of the cores, the PAZ correlate well, and are in accordance with the biostratigraphical zonation.

Characteristics used for the biostratigraphical zonation are as follows:

Zone 1, high values for *Quercus*, moderate values for *Ulmus*, *Pinus* and *Fraxinus*. Appearing towards the top of the zone are *Carpinus*, *Juglans* and *Castanea*. *Artemisia* increases.

Zone 2, *Quercus* and *Pinus* decrease. *Carpinus* increases and reaches a maximum in the upper half of the zone. *Fraxinus* reaches a maximum early in the zone. *Artemisia*, *Cannabis* and *Cerealia* increase.

Zone 3, *Ulmus*, *Carpinus* and *Fraxinus* decrease. *Juglans*, *Castanea*, *Pinus*, *Cannabis*, *Secale* and *Mercurialis annua* increase.

Zone 4, *Pinus* increases and *Secale* decreases. *Cannabis* makes a dip in the lower part of the zone but recovers.

Zone 5, *Carpinus*, *Juglans* and *Castanea* decrease.

Zone 6, *Carpinus* and *Pinus* make a dip. *Juglans* and *Castanea* peak. *Fraxinus* reappears.

Zone 7, *Carpinus*, *Pinus*, *Fraxinus* and *Mercurialis annua* increase. *Cannabis* and *Secale* decrease.

Zone 8, *Juglans* and *Mercurialis annua* decrease. *Ambrosia* appears.

Zone 9, *Fraxinus* increases.

Radiocarbon dating and chronozonation

The ages of the biostratigraphic zone boundaries are determined in two steps, resulting in chronozones. In step one site-specific ages are calculated on the basis of radiocarbon dates. In step two the ages of the zone boundaries are derived from the best fit of the site-specific ages.

A total of 30 samples have been ^{14}C-dated (Table 1). Calibration of pre-bomb samples (AD < 1950) was done by OxCal (Bronk Ramsey, 1995, 2001) with the IntCal98 calibration set (Stuiver *et al.*, 1998). Calibration of post-bomb dates (AD > 1950) is based on the peak and subsequent decline in atmospheric ^{14}C following nuclear weapon tests in the early 1960s (Nydal and Lövseth, 1983). For age determinations the measurements from Vermunt (Levin *et al.*, 1994) and Schauinsland (Levin and Kromer, 1997) were used. Post-bomb dates have an accuracy of 2–3 years (Goslar *et al.*, 2005). For the site-specific depth-age models (Figure 3) linear interpolation between calibrated dates was used (Table 1).

Some dates are problematic. MOE-33cm gives a too young age, probably because of contamination with post-bomb material. Too high ^{14}C-activity is often found in peat samples between AD 1930 and 1955 (Goslar *et al.*, 2005), which is explained by integration of younger material. Some ^{14}C dates are based on the peat fraction < 0.2 mm. Even though most modern and younger material was sieved away, as shown in the test sample Amb-32cmB, the peat fraction < 0.2 mm seems to give age determinations that are between 0 and 1000 years too young. For the age determination of an important transition in AMB at 32.5 cm, peat accumulation rates were considered (derived from pollen concentration).

The chronozones follow the biostratigraphic zones (Figure 2). The ages of the chronozones have been determined by comparison of site-specific ages in the three sites (Table 2),

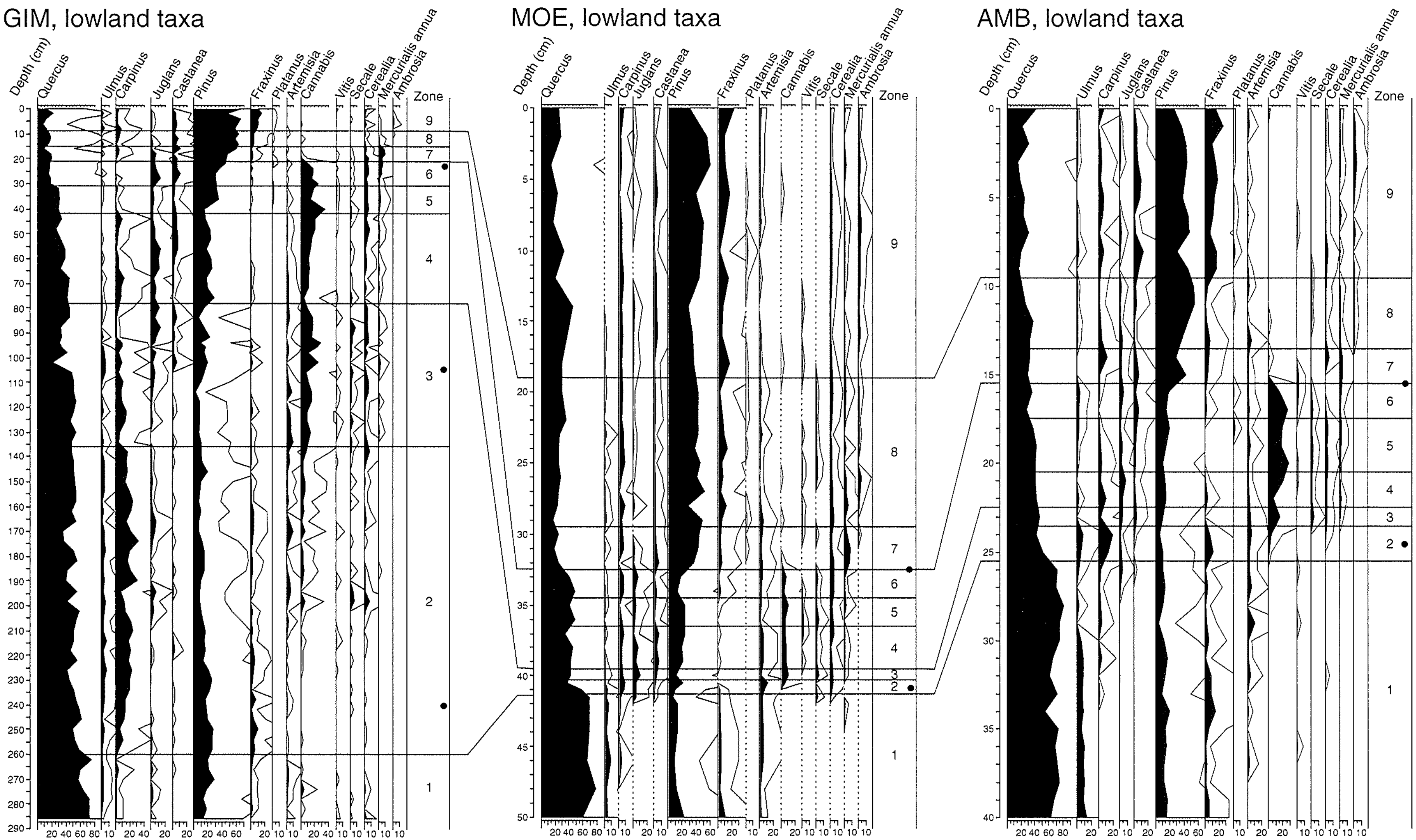

Figure 2 Pollen percentage diagrams from GIM, MOE and AMB for correlation based on the extra-regional (ie, non extra-local) pollen sum. Biostratigraphical zone boundaries are marked with lines and statistically determined PAZ boundaries are marked with solid circles. The zone boundaries drawn between the diagrams are for clarification purpose only

Table 1 Radiocarbon dates

Site	Depth	^{14}C-age (1σ)	Calibrated ^{14}C-age[a] (1σ)	Cal. age range	Date used[b]	Lab. no.	Material
GIM	5 cm	−840±30 BP	AD 1995	AD 1995	AD 1995	Poz-5968	Moss stems
GIM	10 cm	−4120±25 BP	AD 1963, 1967	AD 1963, 1967	AD 1967**	Poz-3768	Mosses, primarily stems
GIM	15 cm	150±30 BP	AD 1670–1700 (11.2%), 1720–1780 (29.4%), 1800–1820 (6.7%), 1840–1880 (7.4%), 1910–1950 (13.5%)	AD 1810±140	AD 1930**	Poz-3769	Mosses, primarily stems
GIM	30 cm	515±30 BP	AD 1407–1433	AD 1420±15	Not used*	Poz-5969	Moss stems
GIM	45 cm	315±30 BP	AD 1520–1600 (56.1%), 1620–1640 (12.1%)	AD 1580±60	AD 1580	Poz-3770	Moss parts, primarily stems
GIM	66 cm	675±35 BP	AD 1280–1310 (33.4%), 1350–1390 (34.8%)	AD 1335±55	AD 1335	Poz-5970	Moss stems
GIM	90 cm	790±30 BP	AD 1223–1232 (15.6%), 1240–1272 (52.6%)	AD 1250±25	AD 1250	Poz-3771	Moss stems, 4 Cyperaceae seeds
GIM	112 cm	875±35 BP	AD 1060–1090 (11%), 1120–1140 (8.6%), 1150–1220 (48.6%)	AD 1140±80	AD 1140	Poz-5971	15 Cyperaceae seeds
GIM	148 cm	1375±40 BP	AD 620–630 (2.6%), 635–690 (65.6%)	AD 655±35	AD 655	Poz-3772	Moss stems, 2 Cyperaceae seeds
GIM	200 cm	1780±40 BP	AD 130–150 (3.4%), 170–200 (5.1%), 210–340 (59.7%)	AD 235±95	AD 235	Poz-5972	Moss parts
GIM	250 cm	1870±40 BP	AD 80–220 (68.2%)	AD 150±70	Not used*	Poz-5974	Moss stems
GIM	270 cm	2065±30 BP	150–130 (5.0%), 120–40 (58.7%), 10–0 (4.5%) BC	75±75 BC	75 BC	Poz-8710	Moss stems, 5 Cyperaceae seeds
MOE	10 cm	−1080±35 BP	AD 1991	AD 1991	AD 1991	Poz-5981	*Sphagnum* and *Polytrichum* stems
MOE	21 cm	−2695±25 BP	AD 1963, 1974	AD 1963, 1974	AD 1974	Poz-1713	*Sphagnum*
MOE	26 cm	−3530±45 BP	AD 1963, 1969	AD 1963, 1969	AD 1963*	Poz-1714	*Sphagnum*
MOE	31 cm	−10±35 BP	*c.* AD 1950	*c.* AD 1950	AD 1950	Poz-1704	*Sphagnum*
MOE	33 cm	−15±25 BP	*c.* AD 1950	*c.* AD 1950	Not used*	Poz-3778	*Sphagnum*, 2 Cyperaceae seeds
MOE	40 cm	155±30 BP	AD 1670–1700 (11.8%), 1720–1780 (32.0%), 1790–1820 (7.4%), 1850–1860 (2.6%), 1910–1950 (14.4%)	AD 1810±140	AD 1685**	Poz-3779	*Sphagnum*, 4 *Potentilla* seeds
MOE	42 cm	2090±40 BP	170–50 (68.2%) BC	110±55 BC	110 BC***	Poz-1706	Peat fraction <0.2 mm
MOE	50 cm	3000±40 BP	1370–1360 (1.5%), 1320–1190 (55.1%), 1180–1160 (6.2%), 1150–1130 (5.3%) BC	1250±120 BC	1250 BC	Poz-5982	Moss stems
AMB	5 cm	−975±30 BP	AD 1993	AD 1993	AD 1993	Poz-5983	Moss stems
AMB	11 cm	−1660±40 BP	AD 1959, 1960, 1962, 1983	*c.* AD 1960, 1983	AD 1960	Poz-1715	*Sphagnum* stems
AMB	15 cm	45±35 BP	AD 1700–1730 (12.4%), 1810–1830 (8.9%), 1880–1920 (35.3%), 1940–1950+ (11.5%)	AD 1825±125	AD 1900*	Poz-1702	*Sphagnum*, 14 *Potentilla* seeds, 1 *Viola* seed, ¼ *Picia* needle
AMB	20 cm	155±35 BP	AD 1670–1700 (11.4%), 1720–1820 (36.0%), 1840–1880 (7.2%), 1910–1950 (13.7%)	AD 1810±140	AD 1770*	Poz-3759	Conifer bark, small carbonised *Picea* needle fragment; small (0.36 mg C)
AMB	22 cm	455±35 BP	AD 1422–1467 (68.2%)	AD 1445±25	AD 1445	Poz-1701	Carbonised *Picea* needle fragment
AMB	25 cm	1550±50 BP	AD 430–560 (68.2%)	AD 495±65	AD 495	Poz-3760	Bark; very small (0.16 mg C)
AMB	32 cm A	2110±40 BP	200–190 (2.5%), 180–50 (65.7%) BC	125±75 BC	Not used*	Poz-1703	Peat fraction <0.2 mm
AMB	32 cm B	−100±40 BP	*c.* AD 1950	*c.* AD 1950	Test sample	Poz-1716	Peat fraction >0.2 mm
AMB	40 cm	3300±40 BP	1620–1520 BC	1570±50 BC	1570 BC	Poz-5873	10 Cyperaceae seeds, ½ seed indet.; small (0.38 mg C)
AMB	53 cm	3400±35 BP	1750–1680 (50.4%), 1670–1630 (17.8%) BC	1690±60 BC	Not used*	Poz-1717	Peat fraction <0.2 mm

[a] Underlined age-intervals are used for the depth–age models.
[b] 'Date used' are used for the site-specific depth–age models.
*Determination of the date used for the depth–age model is based primarily on within-profile stratigraphy.
**Determination of the date used for the depth–age model is based primarily on correlation between profiles.
***Possibly too young.

weighted according to the temporal resolution of the pollen diagram and the distance between dates. GIM is considered the most suitable in the Roman period and the Middle Ages (AD 1–1650), AMB in Modern Time (AD 1650–1900), and MOE in the late twentieth century (AD 1950–2000). The accuracy of the zone ages is approximately ±50 yr, and ±10 yr

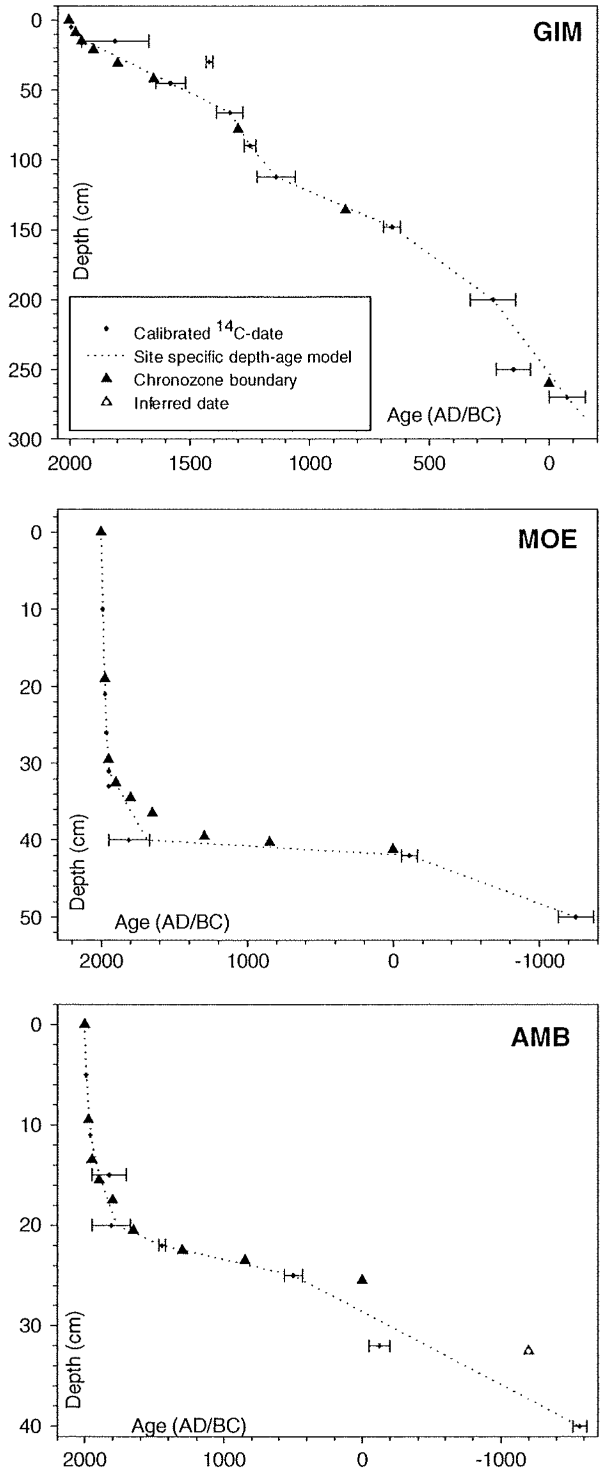

Figure 3 Calibrated ^{14}C-dates (1σ), site-specific depth–age models and chronozone boundaries for GIM, MOE and AMB. For AMB an indirect age determination is inferred from expected peat accumulation rate (based on pollen concentration). See text for details

in the twentieth century. Ages throughout the paper are based on the chronozones.

In MOE the site-specific depth–age model deviates considerably in some parts from the chronozone age. This might be due to partial mixing of the peat, which brought down younger material, and therefore also the pollen stratigraphy might be disturbed, and caution should be taken with the interpretation. Also the site-specific depth–age model for AMB shows in the lower part deviations from the chronozone ages. This is likely caused by the low and uneven peat accumulation that results in very low resolution. There are no signs that peat material is missing, but this cannot be ruled out, considering the high degree of decomposition and compaction.

The trends of some pollen-types in Switzerland during the last millennium are rather well established (van der Knaap *et al.*, 2000), and the same trends can be identified in the correlation diagrams. Comparison (Table 3) shows that the consistency is good, which confirms that the chronozones are fairly correct for the comparable time period.

Pollen source area

The pollen load (the pollen deposited in a place) can be divided into different components depending on mode of transport and area of origin, often expressed as the distances from the site (Tauber, 1965; Janssen, 1966). Prentice (1985) suggested the following components (distance from edge of basin): local, 0–20 m; extra-local, 20 m–2 km; regional, 2–200 km; and extra-regional, > 200 km. This terminology will be used in the present investigation, but some clarification is needed. The local pollen includes fen, bog and wetland plants that grow on or in direct connection with the mires studied. Most of these pollen types can be identified by the preferred habitat of the plant and/or its spiky appearance in the pollen diagram. This component is, as usual, excluded from the pollen sum. The extra-local pollen load is here equalled with the component that derives from the relevant source area of pollen (RSAP), which is defined as the limit beyond which pollen does not sense the spatial patterns of vegetation (Sugita, 1994). Simulated RSAP for moss polsters ($r = 0$ m) in the area is 700–800 m (Florence Mazier, personal communication, 2005), so the RSAP for the sites should be similar or somewhat larger depending on the basin sizes. The regional pollen component is here considered to be from the Jura Mountains above *c.* 1000 m, and the extra-regional component is thus the pollen that derives from outside that area. Most of the trees that are common above 1000 m also occur at lower altitude, but it can be assumed that the strongest pollen signal arrives from within the region. As an example, Tauber (1965) estimated that in a forest composed of species with light pollen grains *c.* 75% of all pollen would come from within 5 km, and for species with heavier pollen grains the percentage would be even higher.

In the pollen diagrams the taxa are grouped according to their modern distribution: highland taxa are regional taxa (excluding *Pinus*), lowland taxa are extra-regional taxa (excluding highland taxa), and wetland taxa are taxa growing on or in close association with the wetlands. *Pinus* is excluded from the highland taxa because it does not occur extra-locally and only in scattered populations in the region as a whole. *Alnus*, *Corylus*, *Betula* and *Fraxinus* do not grow in the area today and are thus treated as lowland species, but according to the climate they might well have grown locally in earlier times. Complicating factors for interpreting pasture woodland is that grazing may reduce the pollen productivity for herbs (Hjelle, 1998), while free-standing and well-exposed trees might have an increased pollen production (Aaby, 1988). As GIM comes from the middle part of the largest mire it can be assumed that it has a stronger regional pollen signal than MOE and AMB (eg, Janssen, 1966; Jacobson and Bradshaw, 1981).

Results and interpretation

The pollen data are presented in diagrams (Figures 4–6), and the main trends are described in the text below. In MOE partial mixing of the peat (and therefore the pollen) may have

Table 2 Intercept dates for site-specific depth–age models and biostratigraphical zone boundaries

Chrono-zone	Lower boundary depth			Lower boundary intercept age			Lower boundary age	
	GIM	MOE	AMB	GIM	MOE	AMB	Date	Interval
ZONE 9	9 cm	19 cm	9.5 cm	AD 1973	**AD 1977**	AD 1968	**AD 1975**	AD 1970–1980
ZONE 8	15 cm	29.5 cm	13.5 cm	AD 1930	**AD 1954**	AD 1923	**AD 1950**	AD 1930–1955
ZONE 7	21 cm	32.5 cm	15.5 cm	AD 1880	AD 1905	**AD 1887**	**AD 1900**	AD 1880–1910
ZONE 6	31 cm	34.5 cm	17.5 cm	AD 1745	AD 1847	**AD 1835**	**AD 1800**	AD 1750–1850
ZONE 5	42 cm	36.5 cm	20.5 cm	**AD 1615**	AD 1788	**AD 1689**	**AD 1650**	AD 1600–1700
ZONE 4	78 cm	39.5 cm	22.5 cm	**AD 1293**	AD 1729	**AD 1287**	**AD 1300**	AD 1250–1350
ZONE 3	136 cm	40.25 cm	23.5 cm	**AD 817**	AD 1461	AD 970	**AD 850**	AD 800–1000
ZONE 2	260 cm	41.25 cm	25.5 cm	**25 BC**	AD 563	AD 426	**AD 1**	AD 50–50 BC

Bold face refers to the more reliable dates used for age determination of the chronozones. Time interval refers to the range within which it is highly probable that the real age occurs.

occurred at 32.5–40.25 cm depth (zones 2–6). Changes in the pollen values of *Abies*, *Fagus*, *Picea* and *Acer* are assumed to be mainly of extra-local origin. However, *Fagus* thrives on the lower slopes and in the lowland, ie, extra-regionally, so some caution should be taken with the interpretation of this taxon. High values of *Alnus*, *Corylus* and *Betula* in the lower part of the diagrams might partly be of local and extra-local origin, although strong fluctuations of these taxa in the Swiss lowlands make any interpretation uncertain (Ammann *et al.*, 1996; van der Knaap and Ammann, 1997). In fact AMB correlates rather well with the lowland locality Lobsigensee, *c.*100 km northeast (Ammann, 1989), which suggests that the extra-regional pollen component may be considerable. With some hesitation *Alnus*, *Corylus* and *Betula* will be treated as locally present in the lower parts of the profiles. Correction factors are used to estimate forest composition. Correction factors are: *Pinus*, *Betula*, *Quercus*, *Alnus* 1:4; *Carpinus* 1:3; *Ulmus*, *Picea* 1:2; *Fagus*, *Abies* 1:1; *Tilia*, *Fraxinus*, (*Acer*) 1:0.5 (Andersen, 1970). Characteristic features in the pollen diagrams are described and commented on below. After a general assessment of the development (based on the best represented sites) site-specific characteristics are presented.

Chronozone 1, > 1600–1 BC; closed forest with some human impact

The highland tree pollen assemblages show that the forest had approximately equal parts of *Abies*, *Fagus* and *Picea*, and some *Acer*, *Alnus*, *Betula* and *Corylus* might have occurred locally at the mire edge or scattered in the forest. In the early part of the period (> 1200 BC) there are no indications of local human impact. The few pollen grains from *Plantago lanceolata* and other apophytes might derive from the lowland or be part of the natural vegetation. During the first centuries BC the presence of indicators for heavy grazing (eg, *Plantago media* and *Plantago montana*) at all three sites show that open pastures are present. MOE: an increase in herb and grass pollen occurs in the last sample, but this cannot be dated exactly because of the low temporal resolution in this part of the profile. AMB: A local pollen assemblage dominated by Cyperaceae is succeeded around 1200 BC by dominance of fern spores. In the latter part of the period (1200–1 BC) there is an increase in herb and grass pollen that a peaks in the first centuries BC.

Table 3 Comparison of biostratigraphic events (dates based on the chronozones) and the relevant biostratigraphy of Switzerland (van der Knaap *et al.*, 2000)

Taxa	Trend	Combe des Amburnex	Switzerland
Ambrosia	1st grain	AD 1950	AD 1950
Mercurialis annua	Last maximum	AD 1925	AD 1950
Mercurialis annua	3rd increase	AD 1900	AD 1920
Mercurialis annua	2nd increase	AD 1850	AD 1820–1880
Mercurialis annua	1st increase	(AD 850)	AD 1770–1990
Cannabis sativa	Last decline	AD 1900	AD 1900
Cannabis sativa	Last maximum	AD 1825	AD 1850
Cannabis sativa	3rd increase	AD 1650	AD 1700
Cannabis sativa	2nd increase	AD 1550	AD 1500
Cannabis sativa	1st increase	AD 850	AD 1000

Chronozone 2, AD 1–850; closed forest with mire and forest grazing

Higher values of tree pollen indicate that the forest became more closed in the first centuries AD (AD 1–250). Pollen from *Alnus*, *Corylus* and *Betula* increased initially and then declined, suggesting a succession with pioneers. A short open phase AD 250–350 was followed by a new forest-regeneration phase AD 350–550, which shows a similar pattern of succession as the previous regeneration phase. After this the landscape slowly began to open up again (AD 550–850). Higher amounts of microscopic charcoal appeared AD 800, suggesting anthropogenic opening up of the surrounding landscape. GIM: peaks in local pollen types such as Rubiaceae, *Rumex acetosa*-type and Cruciferae, together with the presence of a wide array of NAP suggest local grazing and nearby pastures throughout the chronozone. MOE: the peat is very compressed and a hiatus might be present. Many indicators of heavy grazing, such as *Plantago media* and *Plantago montana* pollen, together with very high NAP values and the occurrence of *Podospora* spores (a dung fungus on cow pats), indicate that this part of the mire and the immediate surroundings were grazed. At the start of the period a high peak in *Urtica* pollen suggests a local disturbance and/or nutrient enrichment (eg, a nearby pathway, waterhole or cottage), at some time during the chronozone. AMB: in contrast to MOE there are no clear signs of human impact during this period, suggesting limited use of peripheral areas.

Chronozone 3, AD 850–1300; grazed forest and open pastures

A decrease of *Abies* and *Fagus* pollen and an increase in *Picea* pollen indicate that the forest became more dominated by *Picea*, which at this time probably constituted more than 50% of the forest cover. Lower pollen values for *Alnus*, *Corylus* and *Betula* suggest a reduction in these taxa. GIM: the amount of open pastureland, as reflected in the NAP, *Plantago lanceolata* and Poaceae pollen, is rather constant during most of the period (AD 850–1150) but expands in the latter

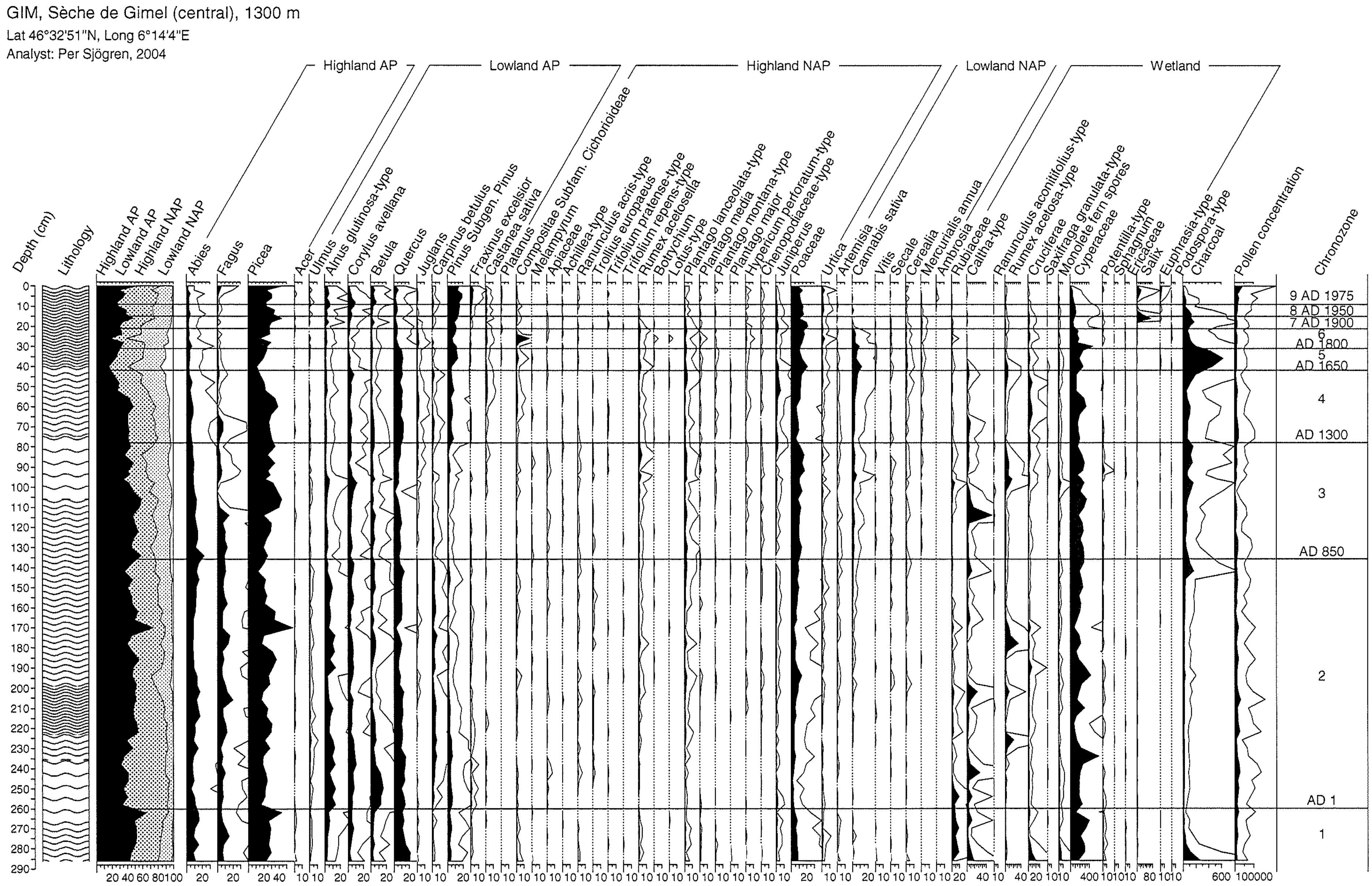

Figure 4 Pollen diagram for GIM in the middle part of Le Marais de Sèche de Gimel. The non-local (non-wetland) sum of pollen and spores has been used for percentage calculation. Some wetland (local) taxa in GIM are in MOE and AMB classified as highland taxa. Unfilled curves show × 5 exaggeration. Note that wetland and some non-pollen curves differ in scale. The lithology shows the degree of decomposition by increasingly close line spacing: 1, undecomposed peat; 2, peat; 3, decomposed peat; 4, strongly decomposed peat

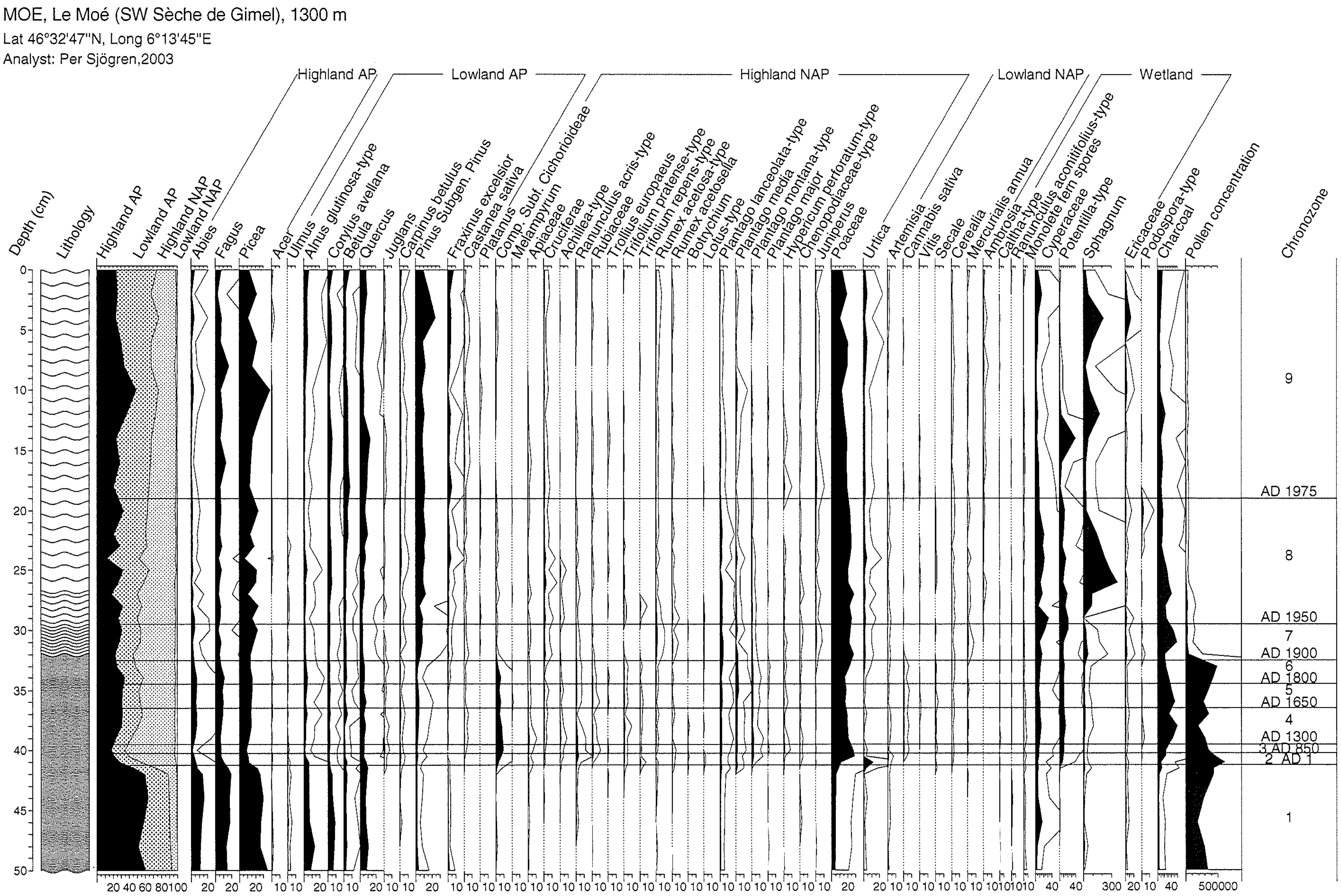

Figure 5 Pollen diagram for MOE in the southwestern part of Le Marais de Sèche de Gimel. See Figure 4 caption for explanation

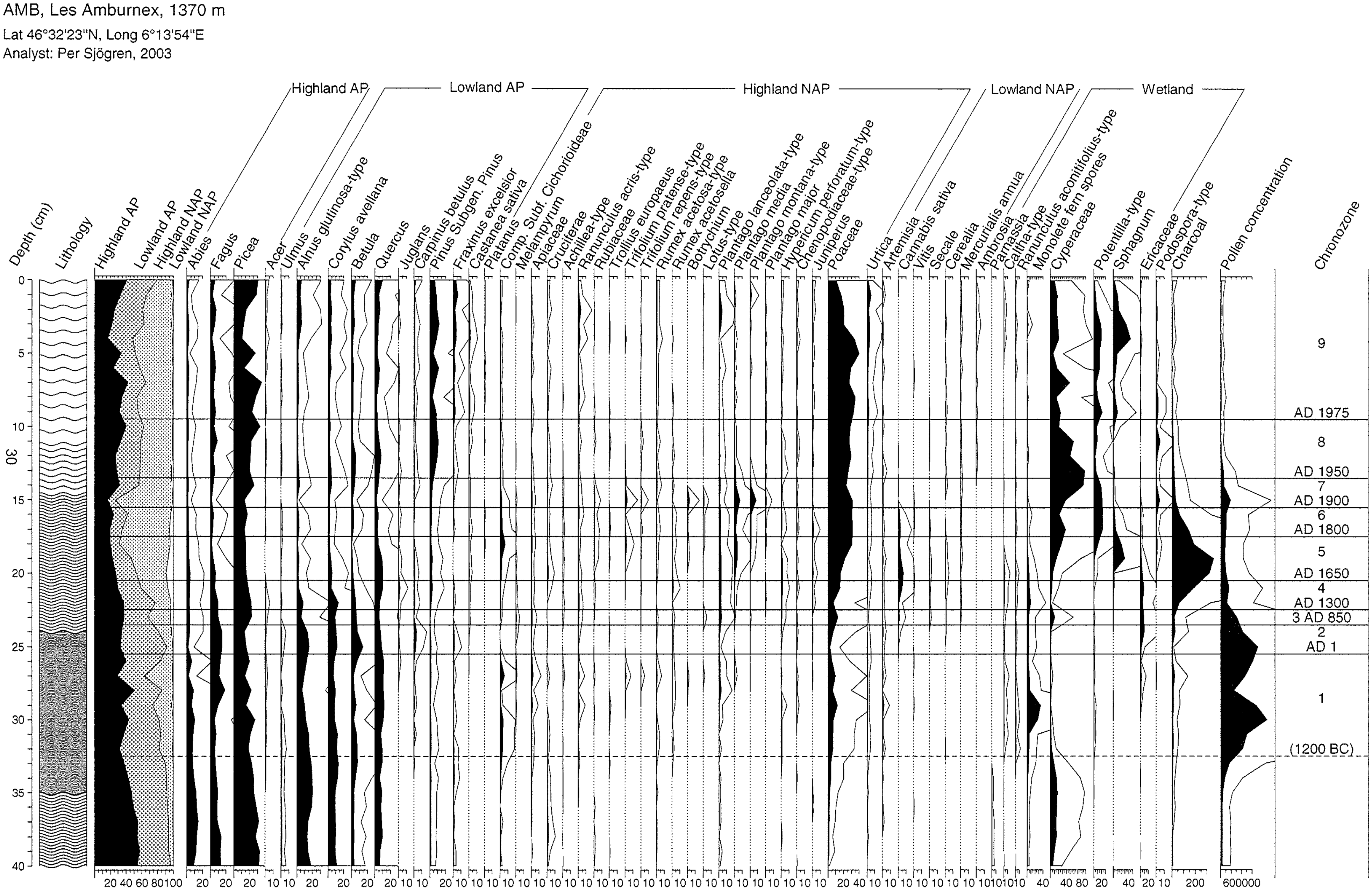

Figure 6 Pollen diagram for AMB, Les Amburnex mire. See Figure 4 caption for explanation

half (AD 1150–1300), and the central parts of the valley probably became as open as today.

Chronozone 4, AD 1300–1650; grazed forest and open pastures

The earlier part (AD 1300–1500) is marked by higher values of tree pollen. In the younger part (AD 1500–1650) there is a decline in *Fagus* and *Picea* pollen, with a corresponding increase in NAP. GIM: the early increase in tree pollen mainly comes from *Quercus* and *Pinus*, which do not grow in the vicinity, and the decrease in NAP is primarily caused by well-dispersed pollen types such as *Plantago lanceolata*, Poaceae and *Juniperus*. Other NAP types are little or not affected at all. It thus seems that the central part of the valley was little affected by this regeneration phase. AMB: in contrast with GIM the increase in tree pollen in the early part of the zone primarily comes from *Alnus* and *Corylus*, trees that may have grown locally. In the younger part (AD 1500–1650) there is a decline in *Alnus*, *Corylus* and *Betula* pollen, suggesting a local reopening of the area around the site.

Chronozone 5–6, AD 1650–1800, AD 1800–1900; pasture woodland

Microscopic charcoal particles indicate major fire activity in the area, and a general openness comparable with today was probably reached in the eighteenth century. The largest lasting expansion of pastureland during this period seems to be in the peripheral areas, possibly because most useful land in the central part already had been turned into pastures. The more frequent occurrence of *Podospora* spores suggests an increased number of cattle. GIM: The zone starts with a peak in Poaceae and a dip in the *Picea* pollen frequencies. This may be the result of forest clearing. Otherwise the Poaceae and herb pollen content suggests that the grazing pressure and the extent of the surrounding pastures are similar to that of the end of chronozone 4. Locally the pollen values indicate that *Caltha* more or less disappeared while Cyperaceae increased, suggesting tussock formation. AMB: the Poaceae value doubles during the chronozone, and there is an increase in many herb pollen types, including indicators for heavy grazing. The values for *Fagus* decline, and the pollen assemblages suggest that any remaining stands of *Alnus*, *Corylus* and *Betula* finally were cleared away. Locally *Sphagnum* spores increases and peaks in AD 1700, followed by an increase in Cyperaceae and *Potentilla* pollen. The presence of *Podospora* spores suggests local cattle grazing.

Chronozones 7–9, AD 1900–1950, 1950–1975, 1975–2000; improved pasture woodland

The maximum openness and grazing pressure occur around AD 1900. During the twentieth century pollen values decline for most herbs except *Urtica*, and Poaceae pollen values remain high, which suggests increased nutrient levels. From here on an increase in lowland pollen from *Alnus*, *Corylus*, *Betula*, *Pinus* and *Fraxinus* occurs and suppresses the local and extra-local pollen signals. GIM: pollen and spore values of Cruciferae, ferns and Cyperaceae decrease after 1950, while peaks occur in *Salix* and *Euphrasia*-type pollen. MOE: pollen and spore values of Cyperaceae, *Potentilla* and *Podospora* decrease after AD 1975, suggesting a shift in local land use. AMB: a very high grazing pressure around AD 1900 is indicated with peaks in *Trifolium repens*, *Plantago media*, *Plantago montana*, *Plantago major*, *Botrychium* and *Lotus*. There is also a peak in *Podospora* spores, which suggests local grazing.

Discussion

Landscape development

After the open phase in the first centuries BC the following forest-regeneration phases can be detected: AD 1–250, AD 350–550, AD 1300–1500 and AD 1925–2000. Pasture-expansion phases are AD 250–350, AD 800–1300 and AD 1500–1900. Phases with maximum openness are AD 1200–1300 and AD 1700–1900.

During the early Middle Ages increasingly large areas in the central part of the valley were cleared, and in the thirteenth century the central part was probably as open as today. The general opening of the landscape occurred in the seventeenth and eighteenth centuries, and now a pasture-woodland landscape similar to present day came into existence. This opening is closely related to fire activity, and the most reasonable explanation for the landscape development is that the forest was cut down and burnt for charcoal. An increased number of husbandry animals, most likely cattle, hampered forest regeneration. From AD 1925 a minor regeneration of the forest can be seen. This correlates well with the approximately 10% reduction of open land since the end of the nineteenth century shown by the Siegfried-map (*Die Siegfried Karten*, Marchairuz, section XVI, 2b, 1892–93). It is primarily wooded pastures and grazed forests that become denser, while open pastures are little affected.

Forest composition and regeneration

An estimation of the natural forest composition at the end of the first millennium BC would be approximately 30% each of *Abies*, *Fagus* and *Picea*, 5% scattered *Acer* and 5% of *Alnus*, *Corylus* and *Betula*. The low pollen productivity of *Acer* makes it hard to estimate its cover, but it has at least been present during the time period studied here. For *Alnus*, *Corylus* and *Betula* variations between the sites suggest local differences, and thereby local presence. *Picea* started to increase relative to *Abies* and *Fagus* in the ninth century, an increase that continued to AD 1950. In the thirteenth century it had increased to around 50% of the forest composition, and in the nineteenth century to 60%. *Picea* is relatively little browsed, and increased grazing pressure in the surrounding forests likely favoured it compared with other trees. The wooded pastures of today consist nearly entirely of *Picea*, and considering the increasing *Picea* dominance in the forest composition this vegetation type might have started to occur in the ninth century, and was most likely common in the twelfth century. Woodland pastures also started to occur across Europe at approximately the same time, ie, in the Middle Ages starting at the eighth century (Behre, 1988). *Alnus*, *Corylus* and *Betula* decreased from the ninth century and disappeared completely from the area in the seventeenth century. In the twentieth century *Picea* and *Fagus* expanded.

The opening of the landscape is shown to be a rather slow process, while forest regrowth is fast. This is to be expected considering the labour needed to clear a forest and the suitable increase in livestock that must follow to keep the area open, while reforestation can occur over large areas simply through neglect. Forest regrowth typically starts with an increase in *Alnus*, *Corylus* and *Betula*, followed 100–200 years later by an increase in *Abies*, *Fagus* and *Picea*.

Pastures and herb composition

Pastureland in the last two millennia was generally nutrient-poor and well grazed (indicated by *Plantago media*, *Plantago montana*, *Botrychium* and *Lotus*), but areas with weaker grazing pressure, more nutrient-rich and/or in a state of regeneration were also present (indicated by Apiaceae, *Trollius*, *Rumex obtusifolius* and *Urtica*). The surrounding forest was grazed and rather open (indicated by *Melampyrum*). Poaceae was common throughout and became even more dominating after AD 1900. During the twentieth century Poaceae pollen increased from *c.* one-half to two-thirds portion of NAP. Together with the increase in Poaceae an increase in *Urtica* suggests a nutrient enrichment of the area, probably as an effect of twentieth-century manuring.

Local mire development

Local development at the three localities is different and each is described separately.

GIM: the presence of Rubiaceae, *Rumex acetosa* and Cruciferae suggest that local grazing occurred throughout the past 2000 years. Increased peat-accumulation rates around the thirteenth century are likely an effect of a rise in the water-table following deforestation in the twelfth century. The local vegetation changed around AD 1700; *Caltha*, *Rumex acetosa* and Cruciferae decreased while Cyperaceae increased. These changes are associated with a more frequent occurrence of *Podospora* spores and increased fire activity, which suggest an increased number of cattle and a general deforestation. This general deforestation probably had a limited effect on the groundwater table as the central part of the valley was deforested already in the Middle Ages. Increased grazing pressure, especially trampling by heavy cattle, would have had a negative impact on the peat accumulation rate and might have caused tussock formation. It is also possible that the mire was ditched and drained, perhaps to improve grazing conditions. Ditches exists today but are partly overgrown and the drainage capacity is limited. Some major changes in the local vegetation also occurred around AD 1975. Cruciferae and Cyperaceae decreased while *Euphrasia* and *Salix* increased. The absence of earlier high values for *Euphrasia* and *Salix* suggest that they are invading the mire.

MOE: a marked increase in *Potentilla* occurred during the centuries around the birth of Christ and *Sphagnum* started to occur more regularly. These changes are associated with increased openness and grazing pressure, including the presence of *Podospora* spores. A strong peak in *Urtica* pollen coincides with the local changes in vegetation. This peak occurs before the presence of *Cannabis* pollen, making any dates younger than the eighth century unlikely. Herb and grass pollen are, at this point, rather low, which suggest that the changes are limited to the mire and local surroundings. *Urtica* thrives on disturbed and nutrient-rich soils, and the peak might have been caused by a nearby pathway or waterhole, perhaps in connection with forest grazing. MOE shows very high NAP values from shortly after this time and onwards, and this part of Sèche the Gimel was likely transformed into pastureland in the Middle Ages or even earlier. The peat at MOE shows very strong decomposition and partly mixing of the peat (AD 1–1900), which also suggests a very heavy local grazing pressure. From AD 1950 onwards the peat-accumulation rate increases rapidly, likely an effect of decreased grazing pressure (the area is today fenced and protected from grazing).

AMB: around 1200 BC (estimated age 1400–1000 BC) the local vegetation changed from Cyperaceae fen, including *Parnassia*, to one dominated by ferns. This change coincided with a marked increase in pollen concentration (increased peat decomposition) that perhaps reflects a lowering of the water-table. The period 1550–1150 BC is characterized by high lake levels in the Jura Mountains (Magny, 2004), and the end of this period coincides with the estimated date for the local vegetation change in AMB. On the other hand, a new phase of high lake-levels started at 800 BC, without any reversal in vegetation and decomposition rate in AMB. The pollen record shows weak increases in Poaceae and several herbs, including Compositae subfam. Cichorioideae, *Rumex acetosa*, *Rumex acetosella*, *Caltha* and *Ranunculus aconitifolius*, suggesting the development of a wet meadow or pasture (Behre, 1981). The local changes in mire vegetation coincided with a local opening of the forest, and human impact (forest grazing) is the most probably cause. Around AD 1700 there is a marked increase in pollen and spores from Cyperaceae, *Potentilla*-type and *Sphagnum*, while *Caltha*, *Ranunculus aconitifolius*-type, monolete ferns and Ericaceae decrease. Peak values in charcoal and increasing values of NAP suggest deforestation, and increased values of *Podospora* dung-spores and pollen from *Plantago media* and *Plantago montana*-type indicates a higher grazing pressure. The peat accumulation rate increases at the same time. Deforestation (higher water-table) and increased grazing pressure is likely responsible for the changes in the local vegetation, which is similar to the changes that occurred in MOE earlier.

Lowland vegetation

The percentage of *Quercus* pollen decreased during the first centuries AD and then rose again in the nineteenth century. *Carpinus* pollen frequencies reached their highest values AD 1–850. The *Carpinus* curve is consistent with that in the lowland (Rachoud-Schneider, 1998), but increased a few hundred years earlier than in many other parts of the Jura Mountains (eg, Wegmüller, 1966; van der Knaap *et al.*, 2000; Mitchell *et al.*, 2001; Gauthier, 2002). Around AD 850 a clear increase in *Cannabis sativa* pollen occurred. The highest values occurred AD 1650–1900, after which it declined sharply. Around AD 1300 the amount of *Pinus* pollen increases. This is likely related to the forest-regeneration phase that started at the same time. The percentage of *Pinus* pollen did not decrease after the landscape was opened up again, implying that either different parts of the landscape were deforested or that *Pinus*, after its initial establishment, was able to compete with existing trees or establish in earlier uncolonized areas.

During the twentieth century an increase in *Alnus*, *Corylus*, *Betula*, *Pinus*, *Fraxinus* and *Castanea* pollen occurred. This is probably due to the general reforestation after abandonment in the twentieth century. In some cases, especially for *Fraxinus* and *Castanea*, it may be because pollarding stopped, which would increase pollen production from existing trees.

Regional and historical context

Wegmüller (1966) studied four other sites by pollen analysis along the eastern edge of the Jura Mountains (Le Couchant at 1400 m, Creux du Croue at 1360 m, La Pile at 1220 m, La Maréchaude at 1590 m). All those sites recorded an opening in the first centuries BC, while the peat from the past 2000 years was missing or very compressed. This suggests that the peat development at those sites was similar to that at MOE and AMB. Pollen analysis of a sediment core from the large lake Lac du Joux *c.* 10 km north of the investigation area showed the same general pattern in expansion and regeneration phases (Wegmüller, 1966). A peat core from the Praz-Rodet bog (Mitchell *et al.*, 2001), 5 km to the northwest, shows some differences, but the main features can be recognized. For the Jura Mountains as a whole the two general forest-regeneration phases in the time period of concern are *c.* AD 250–600 and *c.* AD 1350–1500 (Gauthier, 2004). These correlate with the locally recorded forest-regeneration phases at AD 350–550 and AD 1300–1500. The late-Holocene vegetation history in the lowland north of Lake Geneva is not well recorded, as the top part of most peat deposits has been damaged by human activities (Gaillard, 1984). However, the vegetation history recorded in Lake Geneva itself (Rachoud-Schneider, 1998) shows that the main trends are similar between the lowland and Combe des Amburnex.

The forest-regeneration phase AD 1–250 was less pronounced in the Joux valley (Wegmüller, 1966; Mitchell *et al.*, 2001) and very minor in the lowland (Rachoud-Schneider, 1998), which suggests an abandonment of more peripheral areas in the early Roman Period. This regeneration phase started at more or less the same time as the migration of the Helvetii. For the rest of the history the general development in Combe des Amburnex is similar to that of the surrounding areas, suggesting that the valley was well integrated in the economic system. A transhumance system similar to that of today probably developed towards the end of the first millennium AD. The major difference compared with the lowland is the much larger impact of forestry in the high Jura Mountains during Modern Time, which together with summer grazing finally created the pasture woodland we see today.

Acknowledgements

I thank Brigitta Ammann, Pim van der Knaap, Jacqueline van Leeuwen, Leif Björkman, Marie-José Gaillard, Kari Loe Hjelle, Florencia Oberli and Herbert Wright for help, advice and/or interesting discussions. This research was funded by the Swiss National Science Foundation (SNF), with additional funding from Nordisk Forskerutdanningsakademi (NorFA) through the POLLANDCAL network, and from the European Union through the Marie Curie Fellowship Association (MCFA) programme Cultural Landscapes of Europe (CULTLAND).

References

Aaby, B. 1988: The cultural landscape as reflected in percentage and influx pollen diagrams from two Danish ombrotrophic mires. In Birks, H.J.B., Birks, H.H., Kaland, P. and Moe, D., editors, *The cultural landscape – past, present and future.* Cambridge University Press, 209–28.

Ammann, B. 1989: Late-Quaternary palynology at Lobsigensee – regional vegetation history and local lake development. *Dissertationes Botanicae* 137, 1–157.

Ammann, B., Gaillard, M.-J. and **Lotter, A.F.** 1996: Switzerland. In Berglund, B.E., Birks, H.J.B., Ralska-Jasiewiczowa, M. and Wright, H.E., editors, *Palaeoecological events during the last 15000 years: regional syntheses of palaeoecological studies of lakes and mires in Europe.* J. Wiley & Sons, 647–66.

Andersen, S.T. 1970: The relative pollen productivity and pollen representation of North European trees and correction factors for tree pollen spectra. *Danmarks Geologiske Undersogelse* Serie. II 96, 1–99.

Behre, K.-E. 1981: The interpretation of anthropogenic indicators in pollen diagrams. *Pollen et Spores* 23, 225–45.

—— 1988: The role of man in European vegetation history. In Huntley, B. and Webb, T., III, editors, *Vegetation history.* Kluwer, 633–72.

Bennett, K.D. 1996: Determination of the number of zones in a biostratigraphical sequence. *New Phytologist* 132, 155–70.

Beug, H.-J. 2004: *Leitfaden der Pollenbestimmung für Mitteleuropa und angrenzende Gebiete.* Verlag Dr. Friedrich Pfeil.

Birks, H.J.B. 1986: Numerical zonation, comparison and correlation of Quaternary pollen-stratigraphical data. In Berglund, B.E., editor, *Handbook of Holocene palaeoecology and palaeohydrology.* J. Wiley & Sons, 743–74.

Birks, H.J.B. and **Gordon, A.D.** 1985: *Numerical methods in Quaternary pollen analysis.* Academic Press Inc. (London) Ltd.

Björkman, L. and **Sjögren, P.** 2003: Long-term history of land-use and vegetation at Ire, an agriculturally marginal area in Blekinge, south Sweden. *Vegetation History and Archaeobotany* 12, 61–74.

Bronk Ramsey, C. 1995: Radiocarbon calibration and analysis of stratigaphy: the OxCal program. *Radiocarbon* 37, 425–30.

—— 2001: Development of the radiocarbon program OxCal. *Radiocarbon* 43, 355–63.

Caesar, C.J. 51 BC: De Bello Gallico. In Warrington, J., editor, *Caesar's war commentaries.* 1953, J. M. Dent & Sons Ltd, 1–184.

Faegri, K. and **Iversen, J.** 1989: *Textbook of pollen analysis.* J. Wiley & Sons.

Gaillard, M.-J. 1984: Étude palynologique de l'Évolution Tardi- et Postglaciaire de la Végétation du Moyen-Pays Romand (Suisse). *Dissertationes Botanicae* 77, 1–322.

Gallandat, J.D., Gillet, F., Havlicek, E. and **Perrenoud, A.** 1995: A multiscalar dynamical approach to pastoral values and biodiversity in wooded pastures. In *Mountain grassland, biodiversity and agricultural value.* Food and Agriculture Organisation Regional Office for Europe Technical Series 39, 76–81.

Gauthier, É. 2002: Évolution des activités agropastorales du Haut Jura (France) au cours des trois derniers millénaires. *Quaternaire* 13, 137–47.

—— 2004: Forêts et Agriculteurs du Jura les quatre derniers millénaires. *Environnement, sociétés et archéologie* 6, 1–197.

Gillet, F. and **Gallandat, J.D.** 1996: Wooded pastures of the Jura mountains. In Étienne, M., editor, *Western European silvopastoral systems.* INRA Editions, Science Update series, 37–53.

Goslar, T., van der Knaap, W.O., Hicks, S., Andrič, M., Czernik, J., Goslar, E., Räsänen, S. and **Hyötylä, H.** 2005: Radiocarbon dating of modern peat profiles: pre- and post-bomb ^{14}C variations in the construction of age–depth models. *Radiocarbon* 47, 115–34.

Hjelle, K.L. 1998: Herb pollen representation in surface moss samples from mown meadows and pastures in western Norway. *Vegetation History and Archaeobotany* 7, 79–96.

Jacobson, G.L. and **Bradshaw, R.H.W.** 1981: The selection of sites for paleovegetational studies. *Quaternary Research* 16, 80–96.

Janssen, C.R. 1966: Recent pollen spectra from the deciduous and coniferous-deciduous forests of northeasten Minnesota: a study in pollen dispersal. *Ecology* 47, 805–25.

—— 1981: On the reconstruction of past vegetation by pollenanalysis. *Botany* 84, 197–210.

Koff, T. and **Kangur, M.** 2003: Vegetation history in northern Estonia during the Holocene based on pollen diagrams from small kettlehole and lake sediments. In Tonkov, S., editor, *Aspects of palynology and palaeoecology.* Pensoft, 113–26.

Levin, I. and **Kromer, B.** 1997: *$^{14}CO_2$ records from Schauinsland.* Carbon Dioxide Information Analysis Center, Oak Ridge National Laboratory, U.S. Department of Energy.

Levin, I., Kromer, B., Schonch-Fisher, H., Bruns, M., Münnich, M., Berdau, D., Vogel, J.C. and **Münnich, K.O.** 1994: *$^{14}CO_2$ record from Vermunt.* Carbon Dioxide Information Analysis Center, Oak Ridge National Laboratory, U.S. Department of Energy.

MacArthur, R.H. 1957: On the relative abundance of bird species. *Proceedings of the National Academy of Science, USA* 43, 293–95.

Magny, M. 2004: Holocene climate variability as reflected by mid-European lake-level fluctuations and its probable impact on prehistoric human settlements. *Quaternary International* 113, 65–79.

Mitchell, E.A.D., van der Knaap, W.O., van Leeuwen, J.F.N., Buttler, A., Warner, B.G. and **Gobat, J.-M.** 2001: The palaeoecological history of the Praz-Rodet bog (Swiss Jura) based on pollen, plant macrofossils and testate amoebae (Protozoa). *The Holocene* 11, 65–80.

Moore, P.D., Webb, J.A. and **Collinson, M.E.** 1991: *Pollen analysis.* Blackwell Scientific Publications.

Mottaz, E. 1982: *Dictionnaire historique, géographique et statistique du Canton de Vaud.* Slatkine.

Nydal, R. and **Lövseth, K.** 1983: Tracing bomb ^{14}C in the atmosphere, 1962–1980. *Journal of Geophysical Research* 88, 3621–42.

Prentice, I.C. 1985: Pollen representation, source area, and basin size: towards a unified theory of pollen analysis. *Quaternary Research* 23, 76–86.

Punt, W. and **Clarke, G.C.S.**, editors 1984: *Northwest European pollen flora, IV.* Elsevier.

Punt, W., Blackmore, S. and **Hoen, P.P.**, editors 1995: *Northwest European pollen flora, VII.* Elsevier.

Rachoud-Schneider, A.-M. 1998: Le Léman palynologique depuis le dernier âge glaciaire. *Actes du colloque pluridisciplinaire* Nyon, 431–50.

Reille, M. 1992: *Pollen et spores d'Europe et d'Afrique du Nord.* Laboratoire de Botanique historique et Palynologie.

—— 1995: *Pollen et spores d'Europe et d'Afrique du Nord – Supplement 1.* Laboratoire de Botanique historique et Palynologie.

—— 1998: *Pollen et spores d'Europe et d'Afrique du Nord – Supplement 2.* Laboratoire de Botanique historique et Palynologie.

Rieben, E. 1957: La forêt et l'économie pastorale dans le Jura. Thèse de l'École Polytechnique Fédérale, Zürich.

Rochat, A. 1995: Notes et études diverses sur la commune du lieu, ses églises, ses cloches, mais surtout ses forêts. *Editions le Pèlerin* 43, 1–95.

Roos-Barraclough, F., van der Knaap, W.O., van Leeuwen, J.F.N. and **Shotyk, W.** 2004: A Late Glacial and Holocene record of climate change and possible modern anthropogenic influences from a Swiss humification profile. *The Holocene* 14, 7–19.

Ruffaldi, P. 1993: *Histoire de la végétation du Jura Méridional depuis le retrait du glacier Würmien à partir des analyses palynologiques du lac de Cerin (Ain, France).* Université de Franche-Comté.

Schoellammer, P. 1997: *Recherche des signatures paléoclimatiques dans les remplissages lacustres fini- et postwürmiens du Locle (Neuchâtel, Suisse) et d'Ilay (Jura, France) a partir des analyses palynologiques, minéralogiques et géochimiques.* Université de Neuchâtel.

Stuiver, M., Reimer, P.J., Bard, E., Beck, J.W., Burr, G.S., Hughen, K.A., Kromer, B., McCormac, G., van der Plicht, J. and **Spurk, M.** 1998: Intcal98 radiocarbon age calibration, 24000–0 cal BP. *Radiocarbon* 40, 1041–83.

Sugita, S. 1994: Pollen representation of vegetation in Quaternary sediments: theory and method in patchy vegetation. *Journal of Ecology* 82, 881–97.

Tarpin, M., Favrod, J. and **Hirt, A.** 2002: Die geschichtliche Entwicklung. In Flutsch, L., Niffeler, U. and Rossi, F., editors, *SPM – Die Schweiz vom Paläolithikum bis zum frühen Mittelalter.* Gesellschaft für Ur- und Frühgeschichte.

Tauber, H. 1965: *Differential pollen dispersion and the interpretation of pollen diagrams.* C.A. Reitzels Forlag.

van der Knaap, W.O. and **Ammann, B.** 1997: Depth–age relationship of 25 well-dated Swiss Holocene pollen sequences archived in the Alpine Palynological Data-Base. *Revue de Paléobiologie* 16, 433–80.

van der Knaap, W.O., van Leeuwen, J.F.N., Fankhauser, A. and **Ammann, B.** 2000: Palynostratigraphy of the last centuries in Switzerland based on 23 lake and mire deposits: chronostratigraphic pollen markers, regional patterns, and local histories. *Review of Palaeobotany and Palynology* 108, 85–142.

van Geel, B., Buurman, J., Brinkkemper, O., Schelvis, J., Aptroot, A., van Reenen, G. and **Hakbijl, T.** 2003: Environmental reconstruction of a Roman Period settlement site in Uitgeest (The Netherlands), with special reference to coprophilous fungi. *Journal of Archaeological Science* 30, 873–83.

Vittoz, P. 1998: *Flore et végétation du Parc jurassien vaudois: typologie, écologie et dynamique des milieux.* Université de Lausanne.

Wegmüller, S. 1966: Über die spät- und postglaziale Vegetationsgeschichte des südwestlichen Juras. *Beiträge zur Geobotanischen Landesaufnahme der Schweiz* 48, 1–143.

The origins of woodland pasture landscape, ecosystem and species diversity of the Jura mountains

Florence Mazier
Department of Biology and Environmental Science, University of Kalmar, Sweden

The functioning of the majority of modern global ecosystems is in part contingent on a significant history of human impact, demanding that integrated strategies for preservation, conservation or sustainable management of ecosystems incorporate an understanding of long term responses to climate and human activities (Dearing, 2000; Oldfield et al., 2000). Land-use/land-cover changes in the past have impact on both biodiversity and climate change. More accurate and objective methods for quantitative reconstruction of vegetation are necessary for these purposes and could be done using fossil pollen records from large and small sites (lakes and/or peat stratigraphies)

A) LANDSCAPE RECONSTRUCTION – THEORY

The development and validation of new research strategies and models (Anderson *et al.*, 2006; Broström *et al.*, 2004; 2005; Hellman *et al.*, in press; Sugita, 2007a, 2007b; Sugita *et al.*, 1999) allows quantitative reconstructions of past vegetation with a precision that was not possible with the traditional interpretation tools, and give the opportunity to test hypotheses that couldn't be tested earlier (European program POLLANDCAL – POLlen LANDscape CALibration). Today, the Landscape Reconstruction Algorithm LRA (Fig. 1) (Sugita, 2007a, 2007b) is the soundest approach to achieve quantitative vegetation reconstructions at the regional and local scales. The LRA is an entirely novel method. It relies on the demonstration that large sites (lakes or bogs) provide pollen assemblages that do not vary significantly between sites within a region and, therefore, represent regional vegetation, while small sites (10^2 km^2) provide pollen assemblages that differ between sites and, thus, represent local vegetation (Sugita, 1994, 2007a, 2007b). Using appropriate models (REVEALS and LOVE models, (Sugita, 2007a, 2007b) and pollen assemblages from a combination of large and small sites, it is possible to reconstruct quantitatively land-cover/vegetation units (in % cover) on both large (10^4 - 10^5 km^2) and small (2-20 km^2) spatial scales.

A crucial factor in obtaining regional and local vegetation reconstructions are accurate pollen productivity estimates (PPE) and dispersal ability of the taxa characteristic for the actual landscape.

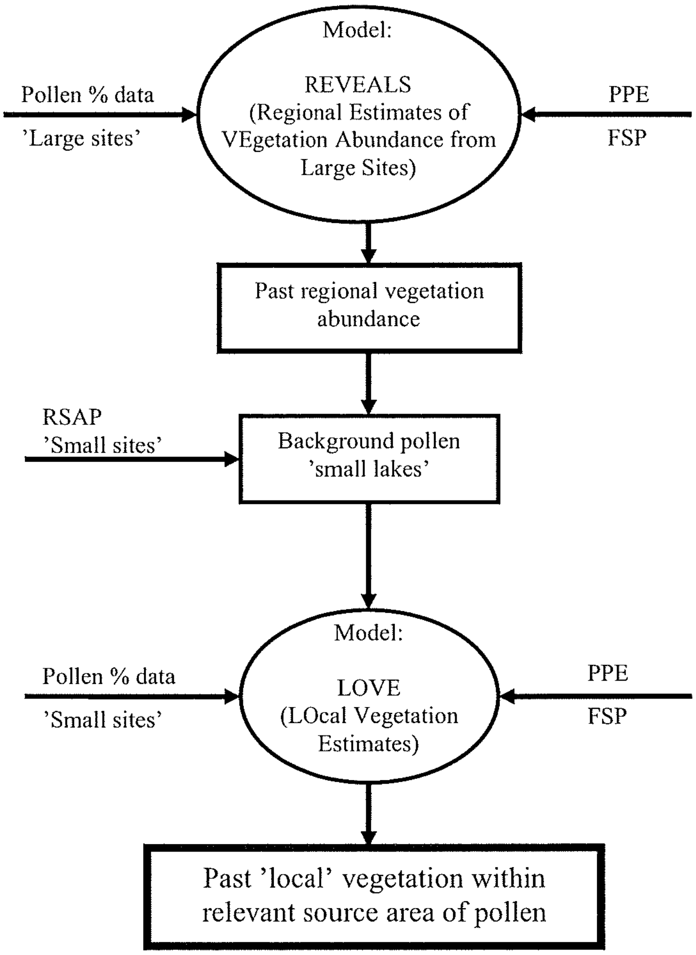

Fig.1. The Landscape Reconstruction Algorithm approach for quantitative reconstruction of past regional and local vegetation (modified from Sugita, 2007a and b; Hellman, 2005). Input parameters for the REVEALS and LOVE models are PPEs (pollen productivity estimates) and FSPs (fall speeds of pollen).

B) POLLEN PRODUCTIVITY AND DISPERSAL

Pollen productivity (PPE) and dispersal (such as fall speed - FSP) are two majors factors that control the pollen representation of surrounding vegetation in pollen records from a basin of given size such as a lake, bog or forest hollow (Prentice, 1985).PPE can be calculated from modern pollen and vegetation data using ERV (extended R-value)-models (Parsons and Prentice, 1981; Prentice and Parsons, 1983; Sugita, 1994).

Twenty sites were randomly distributed in the Jura mountains ("Parc Jurassien Vaudois") and the central points of the sites are at least 400 m apart. The sites include grassland and wooded pasture, but are mainly located in coniferous and mixed forests. Moss polsters were collected in a radius of 0.5 m. The vegetation was surveyed in 1 m wide concentric rings out to 1500 m from the pollen sample area, combining detailed field survey data (scale 0-10m for herbs and trees and 10m-100m for trees) and digital vegetation maps (scale 10-100m for herbs and 100-1500m for herbs and trees).

Pollen productivity estimates for 11 plant taxa characteristic for pasture woodland landscape in Jura Mountains have been obtained based on pollen and vegetation data (Mazier, 2006). *Abies*, *Picea*, Rubiaceae and *Trollius europaeus* have higher pollen productivity relative to Poaceae, whereas *Fagus*, *Plantago media* and *Potentilla*-type produce rather the same quantity and *Acer*, Cyperaceae, and *Plantago montana*-type have lower pollen productivity.

The relevant source area of pollen for mosspolsters in this specific semi-open region is c. 300m as inferred from empirical pollen and vegetation data.

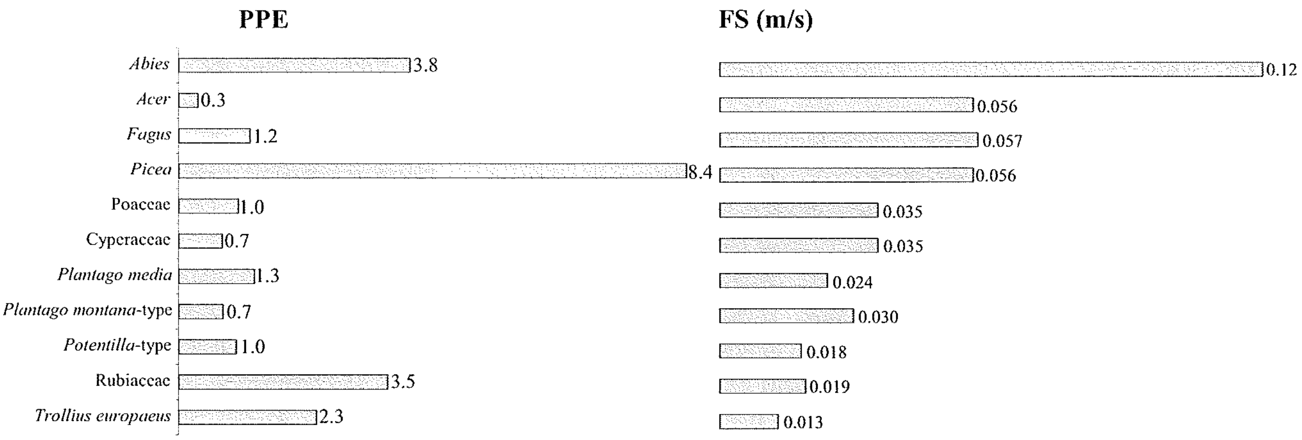

Fig 2: Pollen productivity estimates (PPE) and Fall speed (FS) were calculated for 11 key taxa (4 trees and 7 herbs taxa). PPE are expressed relative to the reference taxon Poaceae.

These results will be a useful contribution to the development of robust tools for the quantitative reconstruction of vegetation composition, abundance and structure in a mountainous landscape in central Europe using the Landscape Algorithm approach.

C) NEXT STEP - Simulate hypothetical landscapes for the last millennia and selected time periods

Next step will be to quantify the background pollen from large lakes (Lake Joux and Saint Point) for the last entire millennia and selected time periods and to estimate regional plant abundance.

The results will be used in the Landscape reconstruction algorithm to estimate regional and local vegetation abundance from fossil pollen samples of several small (P. Sjögren's data (2005; 2006)) and large sites (E. Gauthier's data) from the Jura mountains.

The final goal will be to produce historical landscape patterns in the Jura Mountains both for regional and local scale. Combining vegetation dynamics models with environmental features, such as climate, topography, soil, ecology will certainly add insights into the changes in the pollen-vegetation relationships and could provide plausible scenarios of land-cover/land-use changes in the past (Fig. 3.).

With the fossil pollen record, simulated hypothetical landscapes can be produced. Using ERV models, pollen assemblage can be simulated and compared with the real one. It is possible that different landscapes give the same pollen signal. The hypothetical landscape must always be evaluated from ecological soundness, and several fossil cores closely spaced can reduce the number of possible landscapes (in the Marchairuz three closely spaced (<1 km) cores are present).

Such approach may aim to assess the processes which control or induce pasture woodland and to suggest management strategies to the conservation of the landscape.

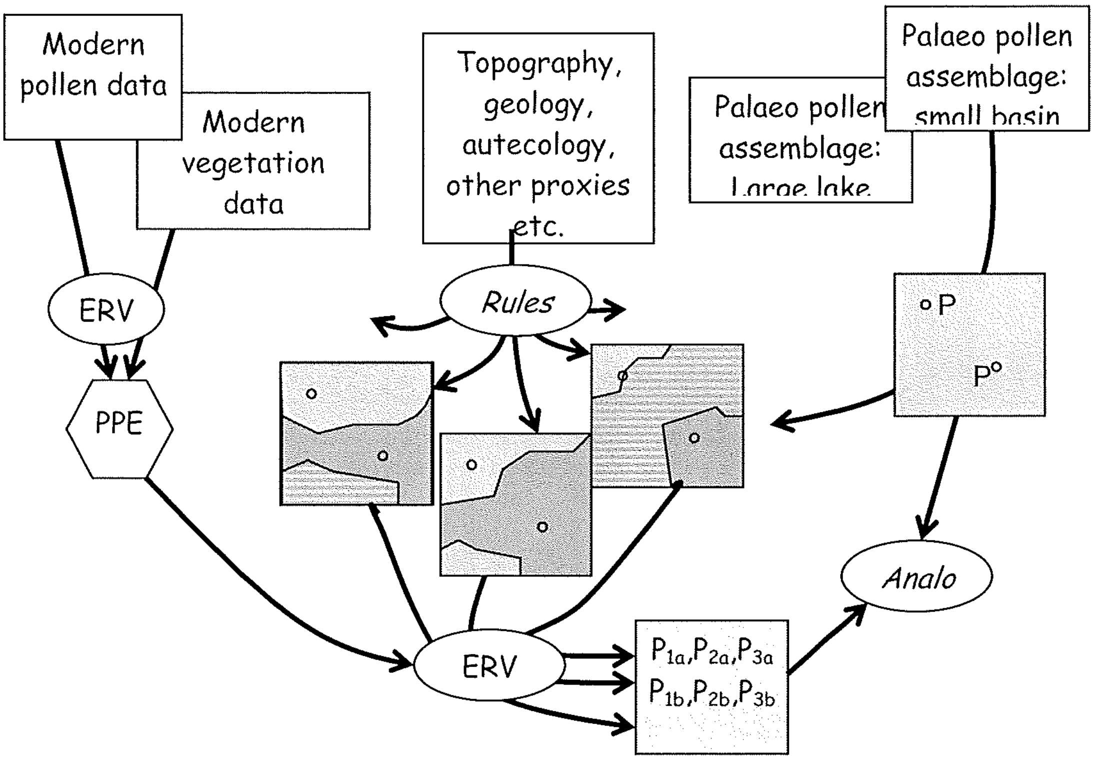

Fig 3: Multiple Landscape scenarios from Bunting (HITE/POLLANDCAL congress - 2005)

REFERENCES

Anderson, J., Bugmann, H., Dearing, J.A. and Gaillard, M.-J., 2006. Linking palaeoenvironmental data and models to understand the past and to predict the future. Trends in Ecology & Evolution, 21(12): 696-704.

Broström, A., Sugita, S. and Gaillard, M.-J., 2004. Pollen productivity estimates for the reconstruction of past vegetation cover in the cultural landscape of southern Sweden. The Holocene, 14(3): 368-381.

Broström, A., Sugita, S., Gaillard, M.-J. and Pilesjo, P., 2005. Estimating the spatial scale of pollen dispersal in the cultural landscape of southern Sweden. The Holocene, 15(2): 252-262.

Dearing, J.A., 2000. Non-linear reponses and surprises. PAGES Newsletter, 8(3): 10.

Hellman, S., Gaillard, M.-J., Broström, A. and Sugita, S., in press. The REVEALS model, a new tool to estimate past regional plant abundance from pollen data in large lakes - validation in southern sweden. Journal of Quaternary Science.

Mazier, F., 2006. Modélisation de la relation entre pluie pollinique actuelle, végétation et pratiques pastorales en moyenne montagne (Pyrenees et Jura). Application pour l'interprétation des données polliniques fossiles, Université de Franche-Comté / Université de Neuchâtel, Besançon, 228 pp.

Oldfield, F., Dearing, J.A., Gaillard, M.-J. and Bugmann, H., 2000. Ecosystem processes and human dimensions - the scope and future of HITE (Human Impact on Terrestrial Ecosystems). PAGES Newsletter, 8(3): 21-23.

Prentice, I.C., 1985. Pollen representation, source area, and basin size: Toward a unified theory of pollen analysis. Quaternary research, 23: 76-86.

Sjögren, P., 2005. Palaeoecological investigatons of pasture woodland in Combe des Amburnex, Swiss Jura Mountains. Thèse Thesis, Institut für Planzenwissenschaften, Bern, 85 pp.

Sjögren, P., 2006. The development of pasture woodland in the southwest Swiss Jura Mountains over 2000 years, based on three adjacent peat profiles. The Holocene, 16: 210-223.

Sugita, S., 1994. Pollen representation of vegetation in quaternary sediments: theory and method in patchy vegetation. Journal of Ecology, 82: 881-897.

Sugita, S., 2007a. Theory of quantitative reconstruction of vegetation II: all you need is LOVE. The Holocene, 17(2): 243-257.

Sugita, S., 2007b. Theory of quantitative reconstruction of vegetation. I: Pollen from large lakes REVEALS regional vegetation composition. The Holocene, 17(2): 229-241.

Sugita, S., Gaillard, M.-J. and Broström, A., 1999. Landscape openness and pollen records: a simulation approach. The Holocene, 9: 409-421

The Holocene 16,1 (2006) pp. 91–103

Modern pollen assemblages from grazed vegetation in the western Pyrenees, France: a numerical tool for more precise reconstruction of past cultural landscapes

Florence Mazier,[1*] Didier Galop,[1] Cécile Brun[1] and Alexandre Buttler[1,2]

([1]Laboratoire de Chrono-Ecologie, UMR 6565 CNRS, Université de Franche-Comté, 16 route de Gray, F-25030 Besançon Cedex, France; [2]Laboratoire des Systèmes écologiques – ECOS, Ecole polytechnique fédérale de Lausanne (EPFL) et Institut fédéral de recherches WSL, Antenne romande, Case postale 96, CH-1015 Lausanne, Switzerland)

Received 11 May 2005; revised manuscript accepted 27 July 2005

A
HOLOCENE
RESEARCH
PAPER

Abstract: Modern pollen assemblages from grazed vegetation in the Pyrenees Mountains (France) were studied with the aim of providing a calibrated model for reconstructing past pastoral activities. The modern analogues were selected to cover the major gradients of grazing pressure and degree of openness. The vegetation was surveyed by means of the synusial integrated method, assessing the structure and the patchiness of the pastoral phytoceonoses. A correlative model (Redundancy analysis) was devised relating 61 modern pollen spectra with 37 explanatory vegetation and land-use variables. It was shown that wooded, open grazed and nitrophilous sites are clearly separated from one another and that the model can be simplified using three relevant vegetation types as explanatory variables: dry heathland, semi-open oak forest and overgrazed community, respectively related to gradients of openness, soil richness and grazing pressure. When reconstructing past pastoral activities with fossil pollen spectra, it is important to consider scale-dependent influences of plant species. Low frequencies of well-dispersed taxa such as *Artemisia*, Chenopodiaceae, *Plantago lanceolata* and *Plantago major/media* must be interpreted with care since they reflect more regional, rather than local, input into the pastoral landscape. In contrast, the simultaneous occurrence of Asteroideae, Cichorioideae, *Cirsium*-type, *Galium*-type, Ranunculaceae, *Stellaria*-type and *Potentilla*-type pollen is clearly related to grazing on a local scale. Calculation of Davis indices also shows that Cichorioideae, *Galium*-type and *Potentilla*-type indicate the very local presence of the corresponding plants. These pastoral plant indicators may have a limited geographical validity, ie, mountainous regions with crystalline bedrock, which may indeed also provide the framework for the application to fossil spectra of the modern pollen/vegetation/land-use models presented here.

Key words: Integrated synusial approach, modern pollen, vegetation history, land use, pastoral indicators, scale, numerical analyses, western Pyrenees, France.

Introduction

The reliability of pollen analysis as a tool for the reconstruction of past vegetation depends on good calibration between present pollen deposition and vegetation, and on the precise understanding of how current species composition is reflected in pollen assemblages. In attempting to evaluate not only human presence but also the nature, extent and duration of human activity, it is important to be able to recognize which specific plant community or individual taxon is representative of a certain type of land use such as cultivation, pasturing, trampling and human settlement or mowing.

The interpretation of anthropogenic activity in pollen diagrams relies on several complementary approaches. The most common approach is the 'indicator species' approach, which uses the ecological characteristics of different species,

*Author for correspondence: (e-mail: florence.mazier@univ-fcomte.fr)

10.1191/0959683606hl908rp

especially those favoured by human activity and today found mainly in human-induced vegetation types (Behre, 1981; Vorren, 1986; Hicks, 1988). Another interpretation tool is the 'comparative approach': comparisons of modern and fossil pollen spectra using all taxa, therefore a community-based approach (Wright, 1967). A wide range of communities/pollen assemblages is needed to increase our understanding of past landscapes and past land-use changes. In northern Europe, modern pollen assemblages and related vegetation, as well as land-use data, have been used to provide a basis for numerical comparisons (Berglund and Ralska-Jasiewiczowa, 1986; Berglund *et al.*, 1986; Gaillard *et al.*, 1992, 1994; Hicks and Birks, 1996; Hjelle, 1999a; Räsänen, 2001). These studies identified pollen assemblages and taxa indicators of various human-induced vegetation types. Despite these valuable contributions to the interpretation of pollen diagrams, the pollen/vegetation/land-use relationships found in northern Europe are not necessarily applicable in other areas, such as the mountainous regions of Mediterranean Europe (Galop, 1998; Galop *et al.*, 2003; Court-Picon, 2005). Many pollen diagrams from the western Pyrenees Mountains have been produced recently (Galop, 1998; Galop *et al.*, 2003), but no reconstruction of past vegetation or landscape units by means of comparisons of modern and fossil pollen spectra has been attempted so far.

Therefore, the objectives of the present study in the Pyrenees Mountains were:

- to investigate pollen representation of trees and herbs in modern pollen assemblages from characteristic vegetation types;
- to assess the major gradients in modern pollen assemblages and relate these to measured environmental variables;
- to test whether different vegetation types with their specific vegetation structure, as described by the integrated synusial approach, can be used efficiently to express the vegetation/pollen relationship;
- to establish whether various degrees of openness and grazing pressure produce significantly distinct modern pollen spectra, and to identify pollen taxa characteristics of pastoral activities.

The comparative approach requires a search for modern analogues of past landscapes and vegetation communities. Owing to the elevation and the steep slopes, grazing seems to have always been the main land-use practice in the Iraty Mountains of the Basque Country. Today, farmers maintain traditional land-use practices based on transhumance from the valley to the summer pastures. The main activity is sheep raising for milk and cheese. This production system necessitates, for each shepherd and his flock, small enclosures for gathering the herd, a milking corridor, a hut for cheese production and specific patches in summer pastures. It also calls for extensive and intensive pastures, some with forested areas and some treeless.

The modern analogues used for establishing the pollen/land-use relationship should present, as far as possible, ecological conditions similar to those prevailing in the past (Gaillard *et al.*, 1992). Moss polsters are commonly used as surface samples for local modern pollen deposition (Gaillard *et al.*, 1992; Hicks and Birks, 1996; Hjelle, 1998). They are assumed to record an average of several years of pollen deposition (Bradshaw, 1981; Heim, 1970), which is recommended since previous investigations have shown annual variation in pollen productivity (Hicks, 2001; Hicks *et al.*, 2001; van der Knaap *et al.*, 2001; Räsänen *et al.*, 2004). Moreover, the modern pollen assemblage should be a good analogue of a fossil pollen assemblage, which usually covers more than one year of pollen deposition. However, contradictory views exist as to the timespan of pollen deposition covered by mosses (Cundill, 1991; Räsänen *et al.*, 2004).

Methods

Study area and sampling design

The data presented in this study were collected within the interdisciplinary research programme 'Palaeo-environment and dynamics of human activities in the Pyrenees Mountains' (Galop *et al.*, 2004). A field site for the programme was selected in the Iraty Mountains in the Basque Country (western part of the Pyrenees chain in southern France) and lies between 700 and 1500 m a.s.l. The silicate bedrock and acidic soils present there induce abundant peat deposits in small basins.

The landscape is hilly and characterized by a mosaic of vegetation types variously affected by pastoral activity. On sloping grounds the vegetation is dominated by heather moorland of *Calluna vulgaris*, *Erica* sp., *Molinia coerulea* and patches of *Ulex europaeus* and *Pteridium aquilinum*, still used for animal litter. Some slopes, especially the steepest ones, are dominated by deciduous forest patches of beach and oak. Intensive grazed pastures are prevalent on the smooth mountain crests.

Our investigations focused on a small watershed centred on the topogenic Sourzay's peat bog with the aim of investigating modern pollen/vegetation and pollen/land-use relationships in a mosaic pasture–woodland landscape, and to use these relationships in the interpretation of fossil pollen records from the same area. The modern analogues were selected near the fossil sequence to assess the effect of the vegetation structure on the pollen record. For collection of the modern pollen and related vegetation data, a preferential design was selected with stratification based on degree of landscape openness and current land use along four axes across the watershed and centred on the fossil pollen record site (Figure 1). Thus, the major relevant vegetation communities and gradients of grazing pressure, from open to forested areas, were covered. The transects were chosen so as to exclude as much as possible any areas disturbed by thalwegs, streams and human activities other than pastoral ones. Some relevant vegetation types such as grazed oak forests or enclosures were absent from the study site. The modern analogue data set was therefore completed outside the watershed.

Field method

Vegetation data

A set of 71 vegetation relevés from various forest types (oak, beech), heath and wet vegetation communities was collected from both grazed and ungrazed areas during the summer of 2001. Vegetation analysis was undertaken according to the integrated synusial approach (Gillet *et al.*, 1991, 2002; Gillet and Gallandat, 1996), which is a method based on the Braun-Blanquet approach (Braun-Blanquet, 1964), but allows better structural description and characterization of plant communities in their landscape context (Figure 2). This method aims at:

- describing complex vegetation structures, taking into account both horizontal and vertical heterogeneity;
- emphasizing functional and dynamic links between various constituent elements among several spatio-temporal organization levels.

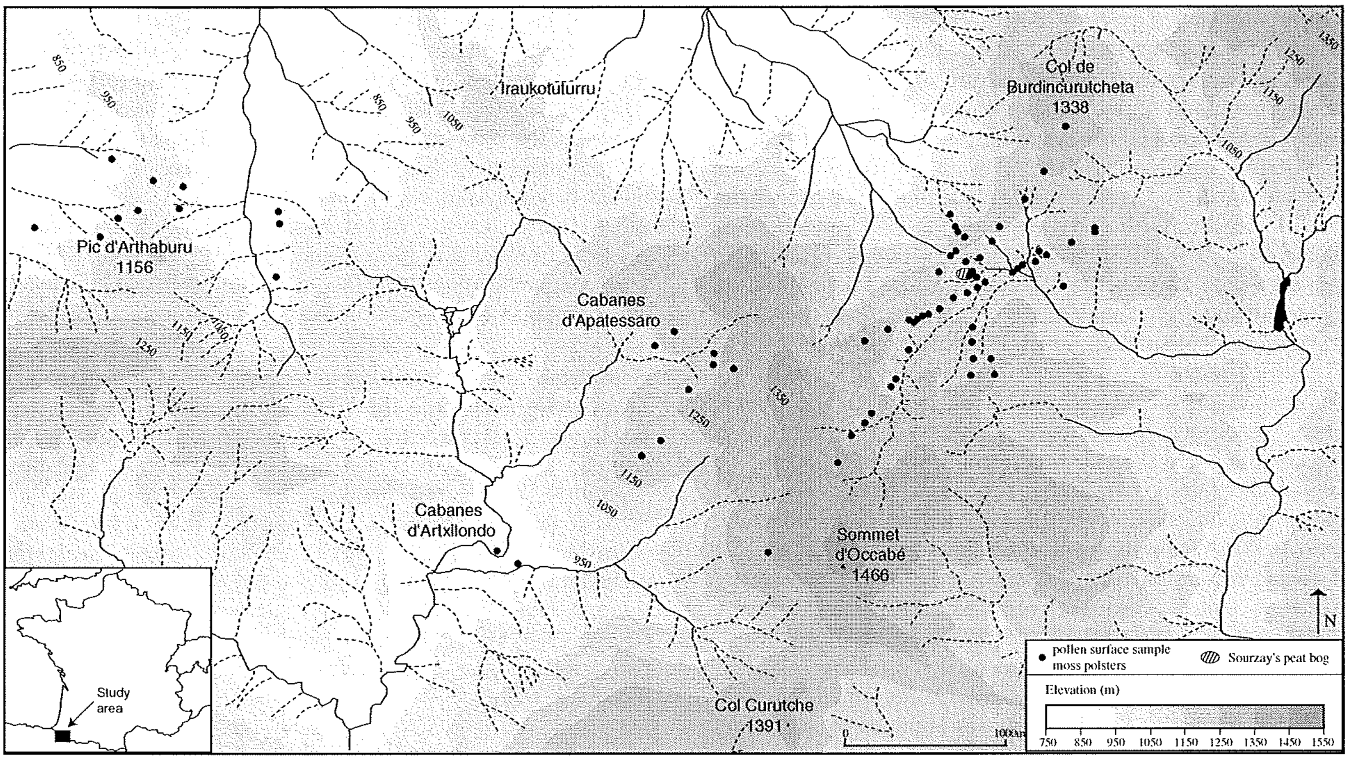

Figure 1 The study area in southern France and the Iraty mountains of the Pays Basque. Location of the 71 modern analogues (solid circles) where pollen samples (moss polsters) and related vegetation data were collected. In the vicinity of the fossil pollen sequence (Sourzay's peat bog), the modern analogues are located along four transects with a stratification based on the degree of grazing and openness

Only two levels were considered in this study, those of the synusia and the phytocoenosis. The synusia is an elementary one-layered concrete vegetation unit (patch) directly linked to uniform environmental conditions. Thus, every synusia is a floristically, physiognomically and ecologically homogeneous vegetation unit. In the field, several vegetation stands were divided vertically and horizontally into synusiae, each therefore undergoing sampling for a floristic relevé. The synusial relevé furnishes a semi-quantitative description, according to Braun-Blanquet (1964), of the species occurring in the sample patch. Synusiae are organized in space and in time within phytocoenosis, as elements of a mosaic or a zoning of stratal communities (Gillet and Gallandat, 1996). Thus, a phytocoenosis is a complex of synusiae (herb, shrub and tree synusiae), functionally strongly linked in both space (mosaics, stratification) and time. A phytocoenotic relevé also furnishes a semi-quantitative description of the synusiae observed in a concrete phytocoenosis. The investigated sites presented homogeneous vegetation (floristically and structurally) on a minimal surface of 100 m^2 (not necessarily a square), which was the surveyed surface for each phytocoenosis. Vascular plant nomenclature follows Tutin *et al.* (1964–1980).

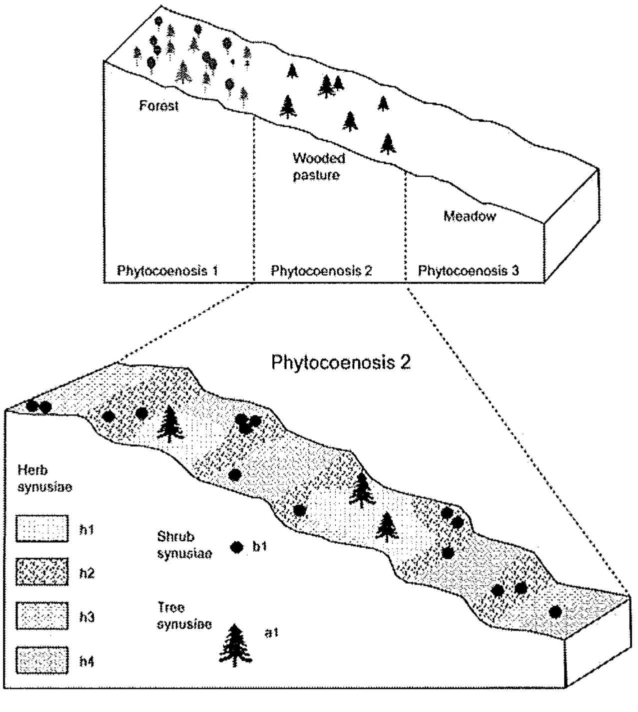

Figure 2 Schematic representation of the two integration levels used for vegetation description, according to the integrated synusial method (adapted from Gillet and Gallandat, 1996)

Sampling of moss polsters

In the present study, moss polster samples were taken down to but not including the soil, and collected at the end of the flowering season, September 2001 (Räsänen *et al.*, 2004). Moss species vary from site to site, but whenever possible species producing dense life forms were chosen (Boyd, 1986). For the wet sites, *Sphagnum* sp. was the only available species and the upper green part (the first 4 cm) was collected.

For each phytocoenosis, and on the entire surface of the vegetation relevé, ten mosses were sampled and mixed together into one sample per site (Gaillard *et al.*, 1992).

Environmental variables

The sampling sites were classified into categories according to the degree of grazing, dunging and trampling pressure, assessed as the proportion of the surveyed surface showing signs of recent cattle activity. On an ordinal scale, classes ranged from 0 to 3 as follows: (0) no pressure, (1) pressure $<5\%$ of the surface, (2) pressure between 5 and 50% of the surface, (3) pressure $>50\%$ of the surface. Livestock type (absence/presence nominal variable) was also taken into account, designated as sheep, horse, cow or pig, since livestock in this region was not mixed for all 71 sites. The altitude, slope (quantitative variables), aspect, nature of bedrock (absence/presence nominal variable) were measured or identified for each phytocoenosis. The aspect was transformed into a quantitative variable based on a trigonometric measure for both the north and east scales (eg, for the N-NE aspect the measure on the north scale was sin 67.5 = 0.92 and on east scale cos 67.5 = 0.38). In order to investigate how variation in the pollen data might be explained by the main gradients in the vegetation data, phytocoenosis typology was used, providing explanatory qualitative variables. Each plant community, 13 in all, was expressed as a presence/absence nominal variable.

For each phytocoenosis, mean soil depth (ten measures taken, randomly spread over the surveyed surface) was measured and soil samples were taken from the top 10 cm of soil, which corresponded to the A horizon, homogenized and pooled into one sample per surveyed surface (Gaillard *et al.*, 1992, 1997). A subsample was then air dried. The fraction (%) of coarse material (> 2 mm) was determined by the sieving procedure. The fresh sample was used for pH (KCl) and pH (H_2O) measurements. Organic matter (%), derived from the ash content, and total N (%) were analysed. These classical methods followed standard procedures (Anderson and Ingram, 1993). The water-holding capacity was obtained by saturating the soil sample over 96 hours, removing the excess water by filtration and oven drying the sample. The potential water content (% of dry soil) was obtained by the weight difference between saturated and dry soil.

Altogether, 37 explanatory variables were recorded and divided into five general categories: edaphic, geologic, geomorphologic, land use and vegetation variable types.

Laboratory methods

Moss samples were treated according to standard procedures (Faegri and Iversen, 1989) by boiling in 10% NaOH for 45 min, sieving, treating with 40% HF (to digest fine silica), $ZnCl_2$ (to eliminate clay material), and acetolysis (one part H_2SO_4 and nine parts acetic anhydride, heated in water bath for 8 min). Samples were mounted in glycerol, and pollen were identified to the most precise taxonomic level possible, using pollen keys (Faegri and Iversen, 1989; Moore *et al.*, 1991; Reille, 1992).

As the focus of this study is the effect of the vegetation structure on the pollen assemblages, pollen from trees, dwarf-shrubs and herbs were thus included in the analysis. A minimum of 400 pollen grains was counted per sample, and a total of 113 pollen and spore taxa were recorded. Moreover, as one of the main goals was to investigate the plant–pollen relationships on a local scale, some taxa were excluded from the pollen sum. Only pollen taxa of plants potentially present in the flora of the region were included in the analysis. For example, pollen of *Olea* was excluded and considered exogenous as it comes from cultivated areas in Spain, far from the study area. The calculation sum, used to obtain percentages of the pollen taxa in numerical analyses, excludes exogenous and aquatic taxa as well as fern spores. In all, 28 taxa were excluded. Thus, the modern pollen data set consists of 71 samples and 85 pollen taxa.

Data analysis

Vegetation typology

The vegetation was described through examination of 71 phytocoenotic relevés and 256 synusial relevés among these phytocoenoses. Synusial typology was first carried out based on the comparison and classification of the synusial relevés using floristic-statistical tools to identify syntaxa (typological units of this organization level). These tools combine step by step various applications such as ordinations and clustering using different options of the package MULVA-5 (Wildi and Orloci, 1996). The analytical procedure was performed separately on the data of each layer, herb, shrub and tree. The optimal number of groups of relevés and species was determined by comparing the results of the various classifications using criteria such as concentration analysis and contingency coefficient provided in the package. The phytocoenotic relevés were compared using the same numerical tools and classified into coenotaxa (typological units of this organization level).

Association and representation indices

In order to understand the pollen–plant relationships at the taxonomic level used for pollen analysis, plant taxa were grouped according to pollen morphological types. For the vegetation, the species list was first derived from all the synusial relevés included in each phytocoenotic relevé. Taxa occurring only as plants or only in the pollen assemblages were excluded from the calculation of the Davis indices of association (A), under-representation (U) and over-representation (O) (Davis, 1984; Hjelle, 1997; Bunting, 2003). These indices are based on presence–absence data of the taxon list and are defined as follows:

$$A = B_0(P_0 + P_1 + B_0)^{-1}$$

$$U = P_1(P_1 + B_0)^{-1}$$

$$O = P_0(P_0 + B_0)^{-1}$$

Where B_0 is number of samples in which both the pollen type and its associated plant are present, P_0 is number of samples in which the pollen type is present in the surface sample but not the plant taxa and P_1 is number of samples in which the pollen type is not present in the surface sample but the plant taxa is present in the vegetation.

Ordination by principal component analysis (PCA) was used to display the relationship between the calculated indices (A, U, O as descriptors) and the pollen taxa (objects). PCA used a covariance matrix with the eigenvectors adjusted by variance. The taxa were then classified into groups using agglomerative hierarchical clustering with proportional-link linkage, and a connection of 0.7. Euclidian distance was used. PCA and cluster analysis were implemented respectively by the CANOCO program for Windows 4.0 (Leps and Smilauer, 2003; Ter Braak and Smilauer, 1998) and Progiciel R (Casgrain and Legendre, 2001).

Pollen/vegetation/environment relationships

Direct gradient analyses were considered appropriate for exploration and testing patterns of modern pollen variation in relation to environmental and anthropogenic explanatory variables. The fitting model depends on whether the pollen taxa respond roughly linearly to gradients (linear response), or perform best around some environmental optima (unimodal response) (Ter Braak and Smilauer, 1998). Preliminary Detrended Canonical Correspondence Analysis (DCCA) showed that this data set has a gradient length of 1.309 standard deviation units of species turnover (SD). This implied that linear-based methods of data analysis such as Redundancy Analysis (RDA) were suitable in this case (Ter Braak and Prentice, 1988).

RDA attempts to explain pollen taxa responses by ordination axes that are constrained to be linear combinations of the 37 explanatory variables available, including the 13 coenotaxa (vegetation communities). Thirteen pollen taxa present only once in the 71 pollen assemblages were omitted. The pollen percentage data was log-transformed [ln $(ay+c)$ with $a=1$ and $c=1$) and double-centred. Forward selection and Monte Carlo test with 999 unrestricted permutations were run to check statistical significance and to select the best explanatory variables for further analysis. The permutation tests were later applied to the canonical axes.

First, the investigated matrix contained the pollen data set and 37 independent variables from 71 modern analogues. In preliminary RDA, pollen assemblages from enclosures and wetland communities were clearly separated from the remaining sites, but were also clearly different from fossil spectra (included passively) (Mazier, Galop, Cugny, Buttler, Legaz and Rendu, unpublished data, 2005). These sites contained some characteristic taxa in large proportion and their assemblages were quite different from the other plots, causing a long gradient in the ordinations, which resulted in a poor separation of the other samples. Ten sites and consequently two explanatory variables were therefore omitted for further RDA, resulting in the use of 61 sites, 73 pollen taxa and 35 environmental variables, of which 13 were retained for their significance, the others being passively presented in the ordination diagrams (or given as covariable).

Three main predictor variables, three vegetation groups, which had the best correlation with the first three ordination axes, were used for more precise analyses. In order to define the weight of each taxon for these three nominal variables, partial RDA was performed separately on each one. The species scores on the first canonical axis of each analysis were then considered descriptors in a new ordination using Principal Component Analysis (PCA). PCA used a covariance matrix with the eigenvectors adjusted to the square root of their variance, divided by the standard deviation (symmetric scaling $\sqrt{\lambda_h}/s_i$).

All ordination analyses were implemented by the CANOCO program for Windows 4.0 (Ter Braak and Smilauer, 1998) and diagrams constructed by Progiciel R (Casgrain and Legendre, 2001) and refined by Illustrator 10.

Results

Phytocoenosis typology

The numerical analysis of the 256 synusial relevés resulted in 21 syntaxa (cluster group): 4 within trees, 3 within shrubs and 14 within the herb layer (Table 1 presents the species composition for the herb syntaxa). The comparison and the classification of the 71 phytocoenotic relevés made it possible to identify 13 coenotaxa (Table 2) divided into two main groups: anthropogenic (4) and 'natural' communities (9). These plant communities can be ordered along a gradient of anthropogenic influence and degree of openness. Here, we describe only the three main coenotaxa, which are found as significant explanatory variables in the redundancy analysis.

Coenotaxon No. 2 occurs mainly on small areas and reflects a community type composed of two herb syntaxa. The syntaxon **H4** (*Rumex acetosella–Galium saxatile*) is correlated with intense livestock activity inducing areas of urination and defecation, as well as bare soil areas. The vegetation of the patch presents a short and sparse canopy dominated by *Rumex acetosella* and *Galium saxatile*. The other syntaxon **H3** (*Trifolium repens–Poa annua*) reflects grazed dense vegetation. This short grass patch is dominated by grazed-area species such as *Poa annua*, *Trifolium repens*, *Stellaria media* ssp. *media* and *Cerastium fontanum* ssp. *fontanum*. Coenotaxon No. 2 depends directly on the daily routine of the livestock, mainly sheep, and presents a high pastoral value. This overgrazed community is often found on mountain crests.

Coenotaxon No. 7 describes large areas of dry mountain-slope heathland, composed of seven syntaxa. The principal syntaxa are **H9** (*Ulex europaeus–Calluna vulgaris*), **H5** (*Potentilla erecta–Agrostis curtisii*) and **H14** (*Pteridium aquilinum–Agrostis curtisii*). This high-altitude community presents heathland species, with a dominance of *Agrostis curtisii*, *Potentilla erecta*, *Danthonia decumbens*, *Deschampsia flexuosa*, *Vaccinium myrtillus*, *Calluna vulgaris*, *Ulex europaeus*, *Erica vagans*, *Erica cinerea*, *Erica tetralix* and *Pteridium aquilinum*. Its species composition is closely related to coenotaxon No. 6, which includes **H8** in addition (*Calluna vulgaris–Vaccinum myrtillus*), and results from colonization by *Ulex europaeus* and *Pteridium aquilinum*, induced through a decrease in grazing pressure.

Coenotaxon No. 12 corresponds to open oak forest with a low and sparse canopy. This community includes three herb syntaxa (**H5**, **H9** and **H6** (*Vaccinium myrtillus–Deschampsia flexuosa*)), one shrub (**B21**) and two tree syntaxa (patches of oak trees alone (**A17**), and mixed beech and oak (**A16**)). The herb vegetation is dominated by *Agrostis curtisii*, *Potentilla erecta*, *Calluna vulgaris*, *Ulex europaeus*, *Deschampsia flexuosa* and *Vaccinium myrtillus*. This coenotaxon corresponds to poor soils on slopes outside the Sourzay watershed.

Association and representation indices

Only 32 taxa were found both as plants and as pollen in one or more phytocoenoses. The relationships between the different taxa and the calculated indices are summarized in the PCA scatter plot (Figure 3). The first axis explains 55.9% of the index variation, and is strongly related to the presence of both pollen and corresponding plants (eg, Poaceae, Cyperaceae). It separates strongly associated taxa, plants and pollen present in over 65% of the samples (*Galium*-type and *Potentilla*-type), from unassociated taxa occurring infrequently in the vegetation and pollen rain (eg, Rosaceae, *Rumex obtusifolius*). The second axis captures 40.1% of the variation and differentiates over-represented taxa, most often found only as pollen (eg, *Abies*, *Quercus* tot, *Urtica dioica*, Brassicaceae and *Plantago lanceolata*), from under-represented taxa often found only as plants (eg, *Sorbus*, *Polygala*, *Erica tetralix*).

Good agreement is found in the results of the two methods, ordination and classification, with strongly associated taxa of group 5 and associated taxa of group 3 on the right-hand side of the first axis. Group 1 clearly indicates over-represented taxa on the positive side of the second axis. Group 2 is centred and represents weakly associated types with low A values and relatively high U and O values. Group 4 constitutes a mixed group with unassociated, under-represented and weakly associated types. Table 3 summarizes the calculated indices for selected taxa in this study and also in previous ones, based on the classification of Bunting (2003).

Pollen/vegetation/environment relationships

Redundancy analysis (RDA) was used to describe the major gradients in the modern pollen assemblages and to relate these patterns to the environmental and anthropogenic variables. This correlative model also tests whether different degrees of openness and grazing pressure produce statistically distinct modern pollen spectra.

Among the 37 explanatory variables, 14 contribute significantly to the correlative model, using forward selection and Monte Carlo permutation tests ($P \leq 0.05$, 999 permutations). Pudding rock, mainly represented in some places of our study area, was found significant. This variable was considered to be a covariable as we did not want to interpret its effect. Therefore, a

Table 1 Synthetic presentation of the herb synusial elementary syntaxa (SyE) of the Iraty Mountains pastoral landscape

Syntaxon no.	**1**	**2**	**3**	**4**	**5**	**6**	**7**	**8**	**9**	**10**	**11**	**12**	**13**	**14**
Number of synusial relevés	4	5	5	18	50	32	6	9	21	8	6	5	6	11
Urtica dioica	V:2	r:+												
Cirsium eriophorum	IV:2	r:2			r:+									
Cirsium palustre	V:2										r:+	r:1		
Cirsium vulgare	IV:2										r:1			
Rumex obtusifolius ssp. *obtusifolius*		V:1		r:1										
Taraxacum officinale		V:1	r:+	r:+	r:+						r:r			
Ranunculus repens		V:2												
Achillea millefolium ssp. *millefolium*		IV:1												
Cynosurus cristatus		IV:2												
Lolium perenne	r:+	IV:2	r:+											
Holcus lanatus		III:2												
Capsella bursa-pastoris		III:+												
Plantago lanceolata		III:1	r:+	r:1										
Stellaria media ssp. *media*	r:1	V:2	V:1	II:2	r:+		r:1							
Cerastium fontanum ssp. *fontanum*	r:+	V:1	V:2	IV:2	r:+	r:2								
Trifolium repens	r:+	V:2	III:2	III:2		r:1		r:2			II:2			
Poa annua		V:2	V:3	III:2	r:+	I:2	II:2							
Rumex acetosella		II:+		V:2	r:2	I:2		r:3						
Danthonia decumbens			r:+	I:1	V:2				r:1	II:1	II:2	r:+		r:+
Galium saxatile		r:1	r:1	V:2	V:2	IV:2	IV:2	r:3	r:2	II:2	r:2			
Agrostis curtisii				III:2	V:2	III:2	III:1		r:3			r:+	r:1	II:3
Potentilla erecta			II:+	IV:1	V:2	II:1			r:1	V:2	V:2			
Carex flacca				II:1	V:2	IV:2	II:2	r:2	I:1	r:1	IV:1			
Deschampsia flexuosa			r:1	I:1	II:1	V:3	V:2	r:2	r:2		r:2	IV:1	II:1	II:2
Fagus sylvatica H.					r:+	III:1	II:2		r:+		r:r		r:3	
Vaccinium myrtillus				I:+	II:2	IV:2	IV:2	V:3	III:1		r:+			
Oxalis acetosella							V:3							
Calluna vulgaris					II:+	I:1		V:3	V:2	IV:2	IV:1			r:5
Ulex europaeus					r:+				V:3					
Erica vagans					I:1	r:2		r:+	V:2					
Erica cinerea			r:+		r:1			r:+	IV:2					
Erica tetralix					I:1			III:2	V:2	V:2	IV:2			
Molinia caerulea ssp. *caerulea*					III:2				r:2	V:2	IV:2	IV:2		
Viola palustris ssp. *palustris*											V:2			
Parnassia palustris										r:2	V:2			
Narthecium ossifragum					r:+					II:2	IV:2			
Juncus acutiflorus											II:1	V:3		
Eriophorum angustifolium										IV:2	II:2	IV:2		
Carex echinata										IV:2	III:1	III:2		
Carum verticillatum				I:+	I:+					III:+	V:1	II:2		
Wahlenbergia hederacea					r:1					II:1	III:2			
Juncus effusus	III:2		II:+			r:+	r:2			r:1	II:+	III:2	V:5	II:3
Agrostis capillaris	III:2	V:2	V:2	V:2	III:2	V:2	III:2	II:1		II:2	III:1	IV:2	III:1	II:2
Pteridium aquilinum			II:+	r:+	I:1	II:2			r:1				r:3	V:4

Names are given according to the main featuring species (grey bars). Each elementary syntaxon is described by a specific list of species (differential species in grey). Only the differential species are listed Relative frequency (RF) classes are indicated for each species in each syntaxon; r: species represented in less than 10% of the relevés or in a single relevé; I: 10% ≤ RF ≤ 20%; II: 20% ≤ RF ≤ 40%; III: 40% < RF ≤ 60%; IV: 60% < RF ≤ 80%; V: RF > 80. Mean abundance-dominance values are also indicated according to the Braun-Blanquet scale. The syntaxa are: H1, *Urtica dioica–Cirsium palustre*; H2, *Rumex obtusifolius–Poa annua*; H3, *Trifolium repens–Poa annua*; H4, *Rumex acetosella–Galium saxatile*; H5, *Potentilla erecta–Agrostis curtisii*; H6, *Vaccinium myrtillus–Deschampsia flexuosa*; H7, *Oxalis acetosella–Deschampsia fexuosa*; H8, *Calluna vulgaris–Vaccinium myrtillus*; H9, *Ulex europaeus–Calluna vulgaris*; H10, *Molinia coerulea–Erica tetralix*; H11, *Viola palustris–Parnassia palustris*; H12, *Juncus acutiflorus–Eriophorum angustifolium*; H13, *Juncus effusus–Agrostis capillaris*; H14, *Pteridium aquilinum–Agrostis curtisii.*

partial RDA ordination diagram of 61 pollen assemblages and 13 explanatory variables such as vegetation units and other environmental variables was performed (Figure 4).

Axis 1 shows a clear gradient from open land to forest vegetation types. It contrasts open land such as CoE No. 7, usually treeless dry heathland, with wooded sites, such as more or less open beech forest. CoE No. 7 and the North are respectively correlated, negatively ($r = -0.42$), and positively ($r = 0.47$), to axis 1. Indeed, beech forests, represented by CoE No.9, 10 and 11 included as passive variables, are generally found on northern slopes. Axis 2 appears to represent a soil richness gradient, and is positively linked with loss on ignition and total N ($r = 0.40$ and 0.36, respectively), whereas the vegetation type CoE No. 12, oak forest on poor soils, presents a negative correlation ($r = -0.37$). Thus, axis 2 contrasts the nitrophilous features of an overtrampled community (CoE No. 3) with oak forest. Axis 3 better expresses a grazing pressure gradient with sites intensively grazed and trampled on the positive side on the axis. CoE No. 2, an overgrazed community, is strongly linked with axis 3 ($r = 0.50$) and correlated to

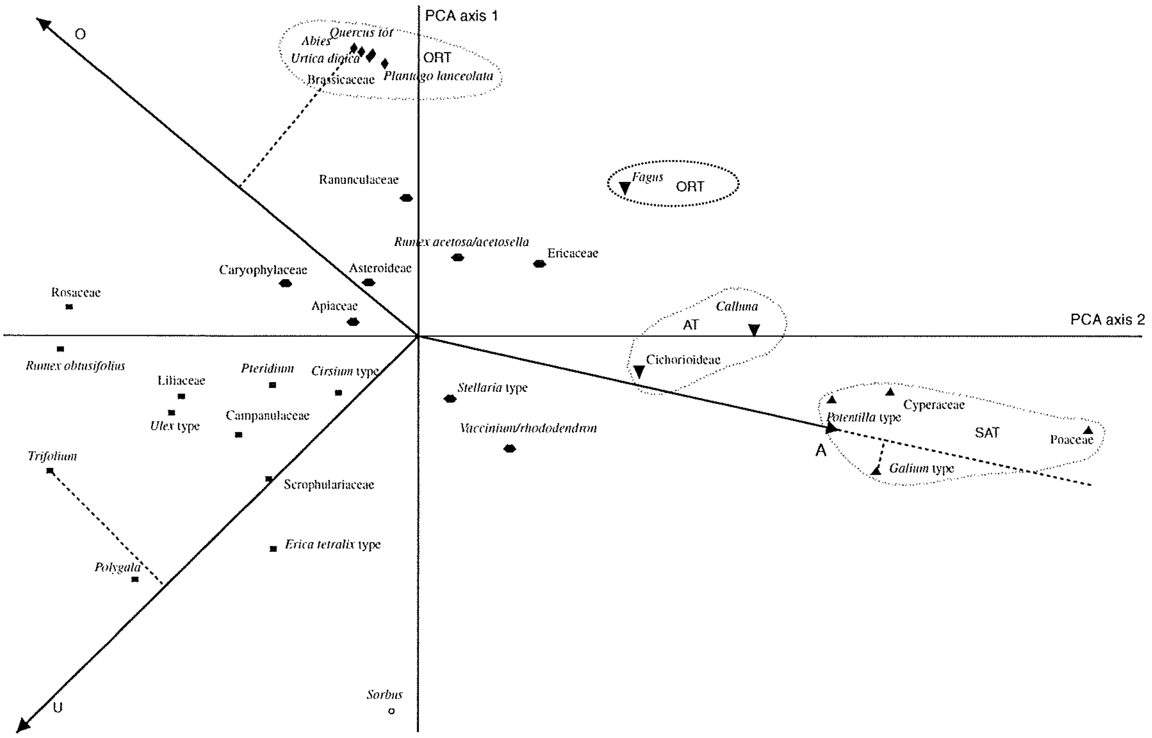

Figure 3 Principal Component Analysis (PCA) using Davis's indices of association (A), under-representation (U) and over-representation (O) (Davis, 1984). Groups according to the clustering are indicated with different symbols: 1, ◆; 2, ●; 3, ▼; 4, ■; 5, ▲. The eigenvalues of the first three principal component axes are 0.135 (55.9%), 0.099 (40.9%) and 0.008 (3.2%), respectively

Ranunculaceae are over-represented in Bunting's data set and weakly represented in this study, while the *Trifolium*-type is associated in Hjelle (1998) and weakly associated in this study.

The dissimilarities between the three data sets might be explained by differences in environmental factors between regions, such as climate, edaphic conditions and land use (Broström *et al.*, 2004). Grazing influence on flowering and pollen production of grasses is well documented (Groenman-van Waateringe, 1993; Hjelle, 1998), thus it may be that Poaceae produce less pollen in anthropogenic coenotaxa. Another explanation may be the differences in pollen production for species included in large taxonomic groups such as Poaceae, Apiaceae and Ranunculaceae (Broström, 2004). A further reason may be the differences in sampling design and in method used for vegetation inventories (Bunting and Hjelle, unpublished data, 2004).

Broström *et al.* (2004) calculated relative pollen productivity estimates (PPEs) for 11 herb taxa related to *Poaceae* (used as reference taxon) and compared PPEs for herbs (Broström *et al.*'s study) and trees (data set of Sugita *et al.*, 1999). She showed that most herb taxa have higher PPEs than *Poaceae*, for example *Calluna vulgaris*, *Rumex acetosa*-type and *Plantago lanceolata*. It is outlined in many studies that the presence of *Plantago lanceolata* in fossil pollen assemblages should be interpreted with caution, especially in pastoral areas on crystalline substrate, such as in our case. This taxon is characterized by long-distance transport and may originate from a wider landscape, for example, from valley floors in our case. Cichorioideae and Cyperaceae have lower PPEs, whereas *Potentilla*-type and Rubiaceae (*Galium*-type) have relatively higher PPEs than *Poaceae* (Broström *et al.*, 2004). We obtained similar results, showing that these taxa can be considered good local indicators and are important in inferring past land uses from local pollen diagrams. Broström *et al.* (2004) also showed that most of the common tree taxa such as *Pinus*, *Quercus* and *Fagus* produce six to eight times as much pollen per unit area as Poaceae. This emphasizes the underestimation of past open land from fossil records when translating the AP/NAP ratio into open areas (Sugita *et al.*, 1999). The overestimation of *Pinus* is well known (Heim, 1970; Broström *et al.*, 1998, 2004). Pine is considered a high pollen producer and a long-distance disperser, which implies a significant regional input. This explains the important proportion of pine recorded in all the 71 surface samples, *Pinus* presents high proportion in beech forest and in fern fallow with dense canopy of *Pteridium aquilinum* (Mazier *et al.*, unpublished data, 2005). *Pteridium aquilinum* forms a closed canopy at four sites grouped into the CoE No. 8 community, dominated by *Pteridium aquilinum* and *Agrostis curtisi*. It is surprising that *Pteridium* spores were not found in the pollen samples from these four sites, whereas it occurred in high proportion in one site of CoE No. 9 (more than 20%), just before a small mountain dominated by this species. This may be due to preferential spore dispersal in relation to prevailing winds. The interpretation of *Pteridium* occurrence in pollen diagrams should be interpreted with caution (Tinsley, 2001).

We must keep in mind that, because of annual variability in pollen productivity, the use of moss polsters could be critical when studying pollen–vegetation relationships, and identifying pollen indicators of plant communities. Interannual variation in pollen productivity is well documented, at least for tree taxa, and has been shown to be related to climatic variability (Hicks, 2001; B. Odgaard, personal communication, 2004). Moreover, the exact number of deposition years in a moss polster is not known and differs from 1 to 10 years according to the authors (Heim, 1970; Bradshaw, 1981; Cundill, 1991; Räsänen *et al.*, 2004). Räsänen *et al.* (2004) suggest that pollen assemblages in the green part of moss polsters represent more than one but less than two years of pollen deposition.

Correlative model of pollen/vegetation/environment relationships

We focused on the pollen/plant/environment relationships as explored by Redundancy Analysis (a detailed presentation of

Table 3 Indices of association and representation from three different studies (this study; Bunting, 2003; and Hjelle, 1997) based on the classification of Bunting (2003)

Pollen taxon	A	U	O	Bunting (2003)	Hjelle (1997)
Unassociated types (UT)					
Anagallis	0.00	1.00	1.00		
Centaurea jacea/nigra	0.00	1.00	1.00		
Fabaceae	0.00	1.00	1.00	UT	
Ilex	0.00	1.00	1.00		
Labiatae	0.00	1.00	1.00		
Lotus-type	0.00	1.00	1.00		WAT
Parnassia-type	0.00	1.00	1.00		
Plantago major/media	0.00	1.00	1.00	no plant	WAT
Strongly associated types (SAT)					
Poaceae	0.96	0.01	0.03	SAT	SAT
Cyperaceae	0.73	0.10	0.20	AT	
Galium-type	0.72	0.22	0.10	Rubiaceae ORT	AT
Potentilla-type	0.67	0.16	0.23	SAT	AT
Associated types (AT)					
Calluna	0.58	0.12	0.38	SAT	ORT
Comp. SF Cichorioideae	0.48	0.27	0.41		SAT
Over-represented types (ORT)					
Abies	0.04	0.00	0.96		
Urtica dioica	0.05	0.00	0.95	no plant	no plant
Plantago lanceolata	0.06	0.00	0.94	ORT	SAT
Brassicaceae	0.06	0.00	0.94	no plant	WAT
Quercus tot.	0.08	0.00	0.92		
Fagus	0.38	0.00	0.62		
Under-represented types (URT)					
Sorbus	0.11	0.89	0.00		
Weakly associated types (WAT)					
Polygala	0.03	0.97	0.50	no pollen	URT
Trifolium	0.06	0.93	0.80		SAT (*Trifolium repens* type)
Erica tetralix-type	0.16	0.82	0.44		SAT
Rumex obtusifolius	0.05	0.75	0.95	ORT (*Rumex*)	no plant
Scrophulariaceae	0.19	0.74	0.57		
Ulex-type	0.14	0.74	0.77		
Campanulaceae	0.18	0.71	0.67		AT
Liliaceae	0.14	0.71	0.78	no plant	
Rosaceae	0.02	0.67	0.98		
Pteridium	0.20	0.61	0.71	WAT	WAT
Cirsium-type	0.25	0.56	0.64	WAT	WAT
Vaccinium/Rhododendron	0.38	0.49	0.41	SAT (*Vaccinium* type)	WAT (*Vaccinium* type)
Stellaria-type	0.33	0.47	0.53		
Apiaceae	0.23	0.44	0.71	ORT	SAT
Caryophyllaceae	0.16	0.44	0.81	no plant	
Comp. SF Asteroideae	0.23	0.37	0.74		AT (*Achillea* type)
Rumex acetosa/acetosella	0.28	0.25	0.69	ORT (*Rumex*)	SAT
Ranunculaceae	0.20	0.20	0.79	ORT (*Ranunculus acris* type)	SAT (*Ranuculus acris* type)
Ericaceae	0.35	0.19	0.61		

Indices of association (A), over-representation (O) and under-representation (U) for taxa present in both plant and pollen data sets. Strongly associated types: $A > 65\%$; Associated types: $50\% < A < 65\%$; Over-represented types: low A values, high O values and $U = 0$; Weakly associated types: low A values and relatively high values for both U and O; Unassociated types: $A = 0$ and high O and U values.

the pollen-diagram will be published elsewhere; Mazier *et al.*, unpublished data, 2005).

Advantage of a synusial approach for studying vegetation

The significant explanatory variables of the canonical axes were edaphic conditions (total N, loss on ignition, pH), geomorphology (aspect North, linked to forested sites), plant communities (CoE No. 2, 3, 4, 6, 7, 8 and 12) and land use (grazing, trampling). The results show that the vegetation units under consideration, which better reflect vegetation structure than a classical relevé, can be used efficiently to explain the major environmental gradients in pollen data. Dry heathland, semi-open oak forest and overgrazed community best reflect the gradients of landscape openness, soil richness and grazing pressure, respectively. RDA axis 1 separates open land from beech sites (both lightly grazed) that are contrasted mainly on the basis of Poaceae and *Fagus*. Poaceae is mainly represented in the CoE No. 7 community, a dry heathland corresponding to an early succession stage of the *Ulex europaeus* invasion. Broström *et al.* (1998) demonstrated that Poaceae may be representative of all types of open land. However, this study shows a difference in the proportion of Poaceae within vegetation types induced by human activity, since this taxon decreases in both the overgrazed CoE No. 3 and No. 2

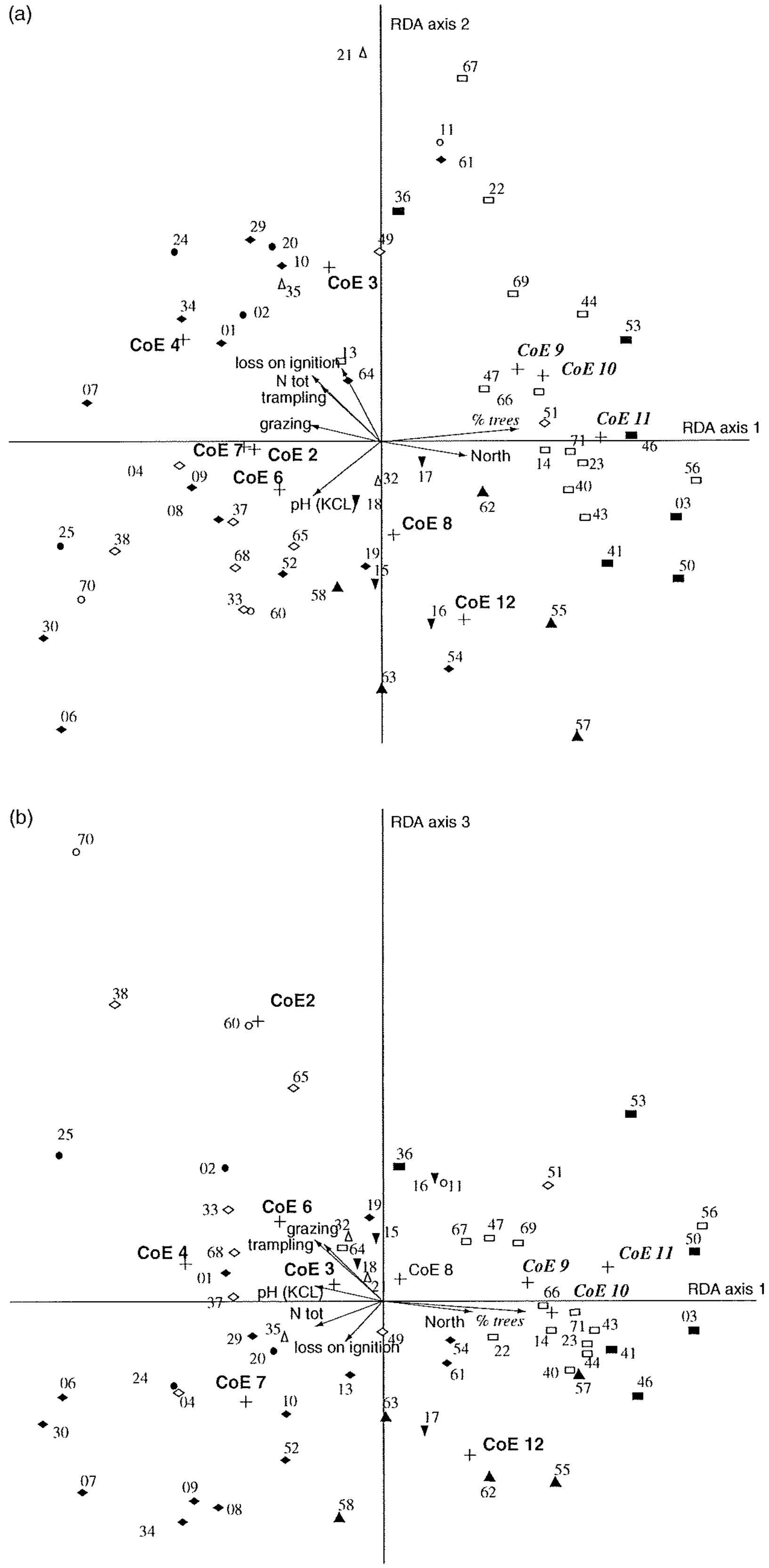

Figure 4 Redundancy analysis (RDA) of the modern pollen assemblages, using 13 explanatory variables (nominal variables are given with their centroïds (crosses) and quantitative variables with arrows), four passive variables (italic) and 61 pollen samples (points). The three first axes explain respectively 17.9, 6.2 and 5.4% of the total variation in the modern pollen data, and are all significant ($P < 0.001$ after 999 permutations). The vegetation types, ie, elementary Coenotaxa (CoE) are: ○, CoE2; △, CoE3; ●, CoE4; ◇, CoE6; ◆, CoE7; ▼, CoE8; □, CoE9/10; ■, CoE11; ▲, CoE12. (a) Sites scores and environmental variables on RDA axes 1 and 2. (b) Site scores and environmental variables on RDA axes 1 and 3

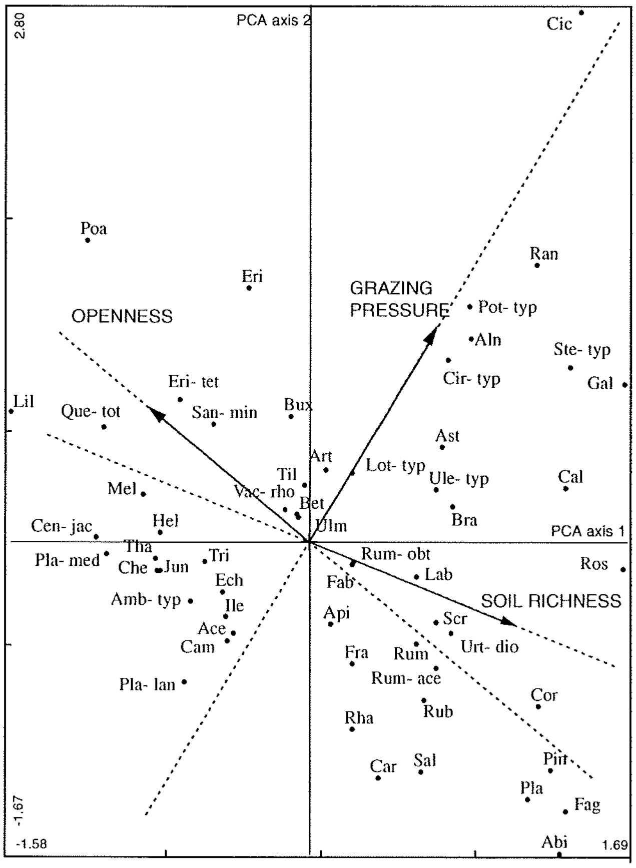

Figure 5 Principal Component Analysis (PCA) using the scores of a separate RDA with coenotaxa CoE No. 7 (dry heahland), indicative of vegetation openness, CoE No. 12 (semi-open oak forest), indicative of low soil richness, and CoE No. 2 (overgrazed community), indicative of high grazing pressure. Axis 1 and 2 represent 85% of the total variance. Abbreviations: Abi, *Abies*; Ace, *Acer*; Aln, *Alnus*; Amb-typ, *Ambrosia*-type; Api, Apiaceae; Art, *Artemisia*; Ast, Asteroideae; Bet, *Betula*; Bra, Brassicaceae; Bux, *Buxus*; Cal, *Calluna*; Cam, Campanulaceae; Car, Caryophyllaceae; Cen-jac, *Centaurea jacea*; Che, Chenopodiceae; Cic, Cichoriodeae; Cir-typ, *Cirsium*-type; Cor, *Corylus*; Ech, *Echium*; Eri, Ericaceae; Eri-tet, *Erica tetralix*; Fab, Fabaceae; Fag, *Fagus*; Fra, *Fraxinus*; Gal, *Galium*-type; Hel, *Helianthemum*;, Ile, *Ilex*; Jun, *Juncus*; Lab, Labiateae; Lil, Liliaceae; Lot-typ, *Lotus* type; Mel, *Melampyrum*; Poa, Poaceae; Pla, *Plantago*; Pla-lan, *Plantago lanceolata*; Pla-med, *Plantago major/media*; Pin, *Pinus*; Que-tot, *Quercus total*; Pot-typ, *Potentilla* type; Ran, Ranunculaceae; Rha, *Rhamnus*; Rub, Rubiaceae; Rum, *Rumex*; Rum-ace, *Rumex acetosa/acetosella*; Rum-obt, *Rumex obtusifolius*; Ros, Rosaceae; Sal, *Salix*; San-min, *Sanguisorba minor*; Scr, Scrophulariaceae; Ste-typ, *Stellaria* type; Til, *Tilia*; Ulex-typ, *Ulex* type; Ulm, *Ulmus*; Urt-dio, *Urtica dioica*; Vac-rho, *Vaccinium/Rhododendron*

communities. Nevertheless, the proportion of Poaceae is not the same in CoE No. 2, an overgrazed pasture and CoE No. 4, grazed wet vegetation. The integrated synusial approach provides some explanation for these dissimilarities between pastoral communities. Poaceae was mainly recorded in CoE No. 4 and 7, and indeed this may be explained by the presence of patches of *Juncus effusus* (CoE No. 4) and *Ulex europaeus* (CoE No. 7), both of which protect herbs from grazing, thus allowing the flowering of the grasses. Alternatively, another factor might be the animals' preference for some species. This seems to be verified for *Poa annua*, the main species in CoE No. 2 that has a higher pastoral value and a higher appetency as compared with *Agrostis curtisi*. Another explanation might be the differences in pollen productivity of the various species included in this large taxonomic group. High grazing pressure induces a specific community, such as CoE No. 2, which presents patches of syntaxon **H4** (*Rumex acetosella–Galium saxatile*) on nearly bare soils, and syntaxon **H3** (*Trifolium repens–Poa annua*) in densely grazed micro-sites. This coenotaxon seems to be the most reliable analogue for intensive pastoral activity. On the other hand, CoE No. 7 can be used as an analogue for extensive pastures and CoE No. 9, 10 or 11 for deciduous, mainly beech, forest. CoE No. 6 provides a situation of transition between extensive and intensive pastures. CoE No. 3 and 4 are more related with the soil richness, which may derive from grazing pressure.

Pollen indicators of pastoral activities

In the PCA analysis based on the three vegetation predictors CoE No. 7, 12 and 2, Cichorioideae, Ranunculaceae, *Stellaria*-type, *Cirsium*-type, *Galium*-type, Asteroideae and, to a lesser extent, *Potentilla*-type are strictly related to grazing pressure. Similar results were obtained in northern Europe (Hicks, 1988; Gaillard *et al.*, 1992, 1994; Hjelle, 1998, 1999a,b; Räsänen, 2001). It was found that Cichorioideae (Hjelle, 1999a), *Cirsium*-type (Hjelle, 1998), *Galium*-type (Gaillard *et al.*, 1992), *Potentilla*-type (Gaillard *et al.*, 1992; Hjelle, 1999a), and Ranunculaceae (Hjelle, 1999a) were characteristic of grazing. In this study *Plantago lanceolata*, Chenopodiaceae and *Plantago major/media*, the last two taxa being absent from the vegetation, are more common in sites on aspects N and NW and occur mainly in lightly grazed wooded sites. Their presence is related to the prevailing wind, which brings pollen from a wider landscape. Gaillard *et al.* (1992) showed that *Plantago lanceolata* is a mowing indicator in southern Sweden. According to Hicks and Birks (1996), Chenopodiaceae and *Rumex acetosa/acetosella* are related to human settlements. This may apply in our case for *Rumex acetosa/acetosella*, since this taxon was present in tracks and/or in the ploughed soils of CoE No. 3, but generally it was recorded sporadically in modern pollen assemblages and therefore cannot be a good pastoral indicator. In our case, the presence of the taxa Chenopodiaceae, *Plantago lanceolata* and *Artemisia* implies regional input.

Urtica dioica is related to soil richness (total N and loss on ignition) and does not constitute a strict pastoral indicator (Gaillard *et al.*, 1992), at least when low values are recorded (Mazier *et al.*, unpublished data, 2005). It is found in surface samples from enclosures, but the plant often grows outside, where dung has accumulated near stone walls.

Conclusion

(1) The correlative model, RDA of 61 modern pollen spectra and 35 external variables, shows that wooded, opened, grazed and nitrophilous sites are clearly separated from each other. The relevant variables are vegetation types CoE No. 7 (dry heathland), CoE No. 12 (semi-open oak forest) and CoE No. 2 (overgrazed community). These vegetation units are clearly related to degree of openness, soil richness and grazing pressure, respectively. Therefore, the synusial integrated approach does provide a robust method for assessing vegetation structure and links between different patches (herbs, shrubs and trees), and also for relating modern pollen assemblages to environmental conditions.

(2) The present study implies that, when reconstructing past pastoral activity, it is important to identify the scale of the landscape in question. In our case, *Artemisia*, Chenopodiaceae, *Plantago lanceolata*, and *Plantago major/media* indicate regional human activity, and are not characteristic

Table 2 Synthetic presentation of the elementary coenotaxa that constitute the Iraty mountains pastoral landscape

Coenotaxon no.	1	2	3	4	5	6	7	8	9	10	11	12	13
Number of phytocoenotic relevés	3	3	3	4	6	9	15	4	6	7	6	4	1
H2 *Rumex obtusifolius–Poa annua*	V:4												
H1 *Urtica dioica–Cirsium palustre*	V:3												
H3 *Trifolium repens–Poa annua*		V:3							r:2				
H4 *Rumex acetosella–Galium saxatile*		V:4	V:4	V:2			r:4						
H13 *Juncus effusus–Agrostis capillaris*		r:4		V:4							r:4		
H11 *Viola palustris–Parnassia palustris*					V:3								
H12 *Juncus acutiflorus–Eriophorum angustifolium*					V:4								
H10 *Molinia coerulea–Erica tetralix*					IV:2								
H8 *Calluna vulgaris–Vaccinium myrtillus*				r:4		II:4	r:4	III:4	r:2	r:3			
H5 *Potentilla erecta–Agrostis curtisii*						V:4	V:3			r:2		IV:3	
H9 *Ulex europaeus–Calluna vulgaris*							V:3					V:3	
H14 *Pteridium aquilinum–Agrostis curtisii*			r:5	r:3		r:2	I:4	V:4					
H6 *Vaccinium myrtillus–Deschampsia flexuosa*						r:3	r:4	V:2	V:2	V:2	r:1	III:2	V:2
A15 *Fagus sylvatica*									V:4	V:3	V:3		
B19 *Fagus sylvatica*										V:2	IV:3		
H7 *Oxalis acetosella–Deschampsia flexuosa*											V:2		
A16 *Quercus robur–Fagus sylvatica*						r:2						III:2	
A17 *Quercus robur*												III:2	
B21 *Quercus robur–Fagus sylvatica*							r:1					r:3	
B20 *Fagus sylvatica–Abies alba*													V:3
A18 *Fagus sylvatica–Abies alba*													V:4

Each coenotaxon (CoE) is described by a list of syntaxa, numbered according to Table 1 for the herb layers (H: 1–14); the tree (A: 15–18) and shrub (B: 19–21) syntaxa are not presented in detail (see explanation in Table 1). The dominant SyE are listed (grey bars). The coenotaxa are: CoE 1, cattle enclosure; CoE 2, overgrazed lawn; CoE 3, overtrampled lawn; CoE 4, grazed wet vegetation; CoE 5, mire vegetation; CoE 6, heathland; CoE 7, encroached heathland; CoE 8, fern fallow; CoE 9, open beech forest; CoE 10, semi-open beech forest; CoE 11, dense beech forest; CoE 12, semi-open oak forest; CoE 13, isolated site.

pastoral activities (grazing and trampling). On the negative side of axis 3, sites from CoE No.7 and 12 are related to low grazing pressure.

The investigated vegetation types represent the major relevant gradients in the modern pollen data. The first three axes respectively correspond to CoE No. 7 (dry heathland), CoE No. 12 (semi-open oak forest) and CoE No.2 (overgrazed community). These vegetation units are clearly related to the degree of openness, soil richness and grazing pressure, respectively. Therefore, in an attempt to identify indicator taxa for each of these three ecological trends, these coenotaxa were used individually as main predictors in partial RDA. The resulting species scores were further considered variables in a principal component analysis (PCA). In the ordination diagram (Figure 5), Ericaceae, *Erica tetralix*, *Sanguisorba minor*, associated to Poaceae, are positively linked with the degree of openness. As expected, *Fagus* and *Pinus* are related to forested sites. *Abies* and *Plantago* sp. are also correlated to forested sites and soil richness (more obvious on the plots of axes 1 and 3). The taxon *Potentilla* type occurs mainly in wet conditions with Apiaceae. Other data show that *Potentilla*-type and Apiaceae are mainly found in the peatbogs (Mazier *et al.*, unpublished data, 2005).

Cichorioideae, Ranunculaceae, *Stellaria*-type, *Cirsium*-type, *Galium*-type and Asteroideae, are connected with the grazing pressure, whereas Chenopodiaceae, *Plantago lanceolata* and *Plantago major/media* are negatively correlated to grazing pressure.

Urtica dioica, *Rumex*, Scrophulariaceae and Rubiaceae are associated with soil richness. Several taxa are found close to the axes origin, such as *Rumex obtusifolius*, *Artemisia*, *Betula*, *Vaccinium-Rhododendron*, *Lotus*-type and Fabaceae. This suggests that these pollen taxa have little relationship to the measured variables represented by the three selected coenotaxa. Indeed, they are commonly recorded in low abundance in most of the sites, and thus are not characteristic of the investigated vegetation types.

Discussion

Herb and tree pollen representation

The indices of Davis A, O and U provide some basic information on the general pollen–vegetation relationships of the mosaic vegetation of the Iraty Mountains, such as heathland, pastoral vegetation, and oak and beech forest. Table 3 presents the results of previous studies, in particular of Bunting (2003) and Hjelle (1997) who give indices for main taxa from Scottish and Norwegian heath communities, respectively. *Potentilla*-type and Poaceae are strongly associated, and *Cirsium*-type, *Pteridium aquilinum* are weakly associated for the three data sets. *Plantago major/media* has been found unassociated and *Plantago lanceolata* over-represented in both the Pyrenees and Scottish data sets. These comparisons indicate that these indices can be applied widely to different regions and also to different habitats.

Several taxa commonly used as anthropogenic indicator taxa, which were lightly or not at all investigated in the local vegetation communities, are recorded at low values in a very high proportion (60–90%) of the surface samples, such as *Artemisia*, Chenopodiaceae and *Plantago lanceolata* (the latter observed three times in the 71 vegetation relevés). This suggests that sporadic, low percentages of these taxa in palaeorecords need not necessarily be indicative of local pastoral activity, but may originate from long-distance transport.

Some discrepancies were observed between these three data sets, ie, *Calluna vulgaris* which is strongly associated in Bunting (2003) and associated in the Iraty data set (this study), and the *Vaccinium*-type which is strongly associated in Scotland and weakly associated in this study. Apiaceae, *Rumex*, of specific land use, whereas the simultaneous presence, in pollen assemblages, of Asteroideae, Cichoriodeae, *Cirsium*-type, *Galium-type*, Ranunculaceae, *Stellaria*-type and *Potentilla*-type is clearly associated with grazing on a local scale. Calculation of Davis indices also shows that Cichorioideae, *Galium*-type and *Potentilla*-type indicate very local presence of the corresponding plants. However, such pastoral indicators might be valid only for crystalline bedrock, and for this mountainous region.

(3) The final aim of our project is to achieve a more precise reconstruction of the cultural landscape in this mountainous area on a local scale, comparing the modern pollen assemblages to local fossil pollen assemblages from a small bog (Galop *et al.*, 2003; Mazier *et al.*, unpublished data, 2005). Thanks to the interdisciplinary research programme 'Palaeoenvironment and dynamics of human activities in the Pyrenees Mountains' this site is now also well documented in microfossil, historical and archaeological data. All these data sets will be used to validate the results of the comparative approach.

Acknowledgements

This study was possible thanks to the help of a number of people to whom we are very grateful: Didier Galop for pollen analysis, Cécile Brun for her precious assistance and encouragement during fieldwork, Pascal Vittoz and François Gillet for their advice on the integrated synusial approach and vegetation analysis, Jean-Daniel Tissot for computer programming, Anne Vignot for her permanent encouragement and Isabelle Jouffroy for guidance in the use of the End-note software. Christine Rendu and her archaeological staff, Onesime Prudhom and Bertrand Lagoguet, provided cheerful fieldwork. Thanks are due to Kari Hjelle for advice and corrections on the Davis Indices and to John Olsen for his improvement of the English text. The manuscript was improved thanks to the helpful comments and suggestions from the two referees, Sheila Hicks and Marie-José Gaillard. This investigation is a contribution to the project of the collective research program 'Paléoenvironnement et dynamiques de l'anthropisation en montagne basque' (Ministry of Culture and SRA Aquitaine), and the ATIP-CNRS 'Paléoenvironnement et Archéologie pastorale'.

References

Anderson, J.M. and **Ingram, J.S.I.** 1993: *Tropical soil biology and fertility. A handbook of methods.* 2nd edition. CAB International.

Behre, K.E. 1981: The interpretation of anthropogenic indicators in pollen diagrams. *Pollen et Spores* 23, 225–45.

Berglund, B.E. and **Ralska-Jasiewiczowa, M.** 1986: Pollen analysis and pollen diagrams. In Berglund, B.E., editor, *Handbook of Holocene palaeoecology and palaeohydrology.* John Wiley & Sons Ltd, 155–484.

Berglund, B.E., Persson, T., Emanuelsson, U. and **Persson, S.** 1986: Pollen/vegetation relationships in grazed and mowed plant communities of South Sweden. In Behre, K.-E., editor, *Anthropogenic indicators in pollen diagrams.* Balkema, 37–51.

Boyd, W.E. 1986: The role of mosses in modern pollen analysis: the influence of moss morphology on pollen entrapment. *Pollen et spores* XXVIII, 243–56.

Bradshaw, R.H.W. 1981: Modern pollen representation factors for woods in South-West England. *Journal of Ecology* 69, 45–70.

Braun-Blanquet, J. 1964: *Pflanzensoziologie. Grundzüge der Vegetationskunde.* Springer, 865.

Broström, A., Gaillard, M.-J., Ihse, M. and **Odgaard, B.** 1998: Pollen–landscape relationships in modern analogues of ancient cultural landscapes in southern Sweden – a first step towards quantification of vegetation openness in the past. *Vegetation History & Archaeobotany* 7, 189–201.

Broström, A., Sugita, S. and **Gaillard, M.-J.** 2004: Pollen productivity estimates for the reconstruction of past vegetation cover in the cultural landscape of southern Sweden. *The Holocene* 14, 368–81.

Bunting, M.J. 2003: Pollen–vegetation relationships in non-arboreal moorland taxa. *Review of Palaeobotany and Palynology* 125, 285–98.

Casgrain, P. and **Legendre, P.** 2001: *The R package for multivariate and spatial analysis version 4.0 (development release 6) user's manual.* Université de Montréal, 134.

Court-Picon, M., Buttler, A. and **de Beaulieu, J.-L.** 2005: Modern pollen–vegetation relationship in the Champsaur valley (French Alps) and their potential in the interpretation of fossil pollen records of past cultural landscapes. *Review of Palaeobotany and Palynology* 135, 13.

Cundill, P.R. 1991: Comparisons of moss polster and pollen trap data: a pilot study. *Grana* 30, 301–308.

Davis, O.K., 1984: Pollen frequencies reflect vegetation patterns in a Great Basin (USA) mountain range. *Review of Palaeobotany and Palynology* 40, 295–315.

Faegri, K. and **Iversen, J.** 1989: *Textbook of pollen analysis.* John Wiley, 328, pp.

Gaillard, M.-J., Birks, H.J.B., Emanuelsson, U. and **Berglund, B.E.** 1992: Modern pollen/land-use relationships as an aid in the reconstruction of past land-uses and cultural landscapes: an example from south Sweden. *Vegetation History and Archaeobotany* 1, 3–17.

Gaillard, M.-J., Birks H.J.B., Emmanuelson, U., Karlson, S., Lageras, P. and **Olausson, D.** 1994: Application of modern pollen/land-use relationships to the interpretation of pollen diagrams – reconstruction of land-use history in south Sweden, 3000–0. *Review of Palaeobotany and Palynology* 82, 47–73.

Gaillard, M.-J., Birks, H.J.B., Karlsson, S. and **Lagerås, P.** 1997: Quantitative reconstruction of past land-use and soil conditions using the modern analogue approach – a case study in southern Sweden. *PACT* 50, 431–42.

Galop, D. 1998: *La forêt, l'homme et le troupeau dans les Pyrénées. 6000 ans d'histoire de l'environnement entre Garonne et Méditerranée. Contribution palynologique.* GEODE – Laboratoire d'écologie terrestre – Framespa, 285 pp.

Galop, D., Mazier, F., Lopez-Saez, J.-A. and **Vannière, B.** 2003: Palynologie et histoire des activités humaines en milieu montagnard. Bilan provisoire des recherches et nouvelles orientations méthodologiques sur le versant nord des Pyrénées. *Archéologie du midi médiéval* 21, 159–70.

Galop, D., Rendu, C., Barcet, H., Buttler, A., Campnajo, P., Cugny, C., Gauthie, E., Legaz, A., Lopez-Saez, JA., Mazier, F., Metailié, J.P., Dominique, S. and **Vanníere, B.** 2004: Paléoenvironenment et archéologie pastorale. Propositions méthodologiques pour une approche intégree des modalités du l'anthropisation en haute montagne pyrénéenne du Néolithique à l'actuel. Besançon: UMR 6565 CNRS-Université de Franche-Cormté, 70 pp, unpublished.

Gillet, F. and **Gallandat, J.-D.** 1996: Integrated synusial phytosociology: some notes on a new, multiscalar approach to vegetation analysis. *Journal of Vegetation Science* 7, 13–18.

Gillet, F., De Foucault, B. and **Julve, P.** 1991: La phytosociologie synusiale intégrée: objets et concepts. *Candollea* 46, 315–40.

Gillet, F., Besson, O. and **Gobat, J.-M.** 2002: PATUMOD: a compartment model of vegetation dynamics in wooded pastures. *Ecological Modelling* 147, 267–90.

Groenman-van Waateringe, W. 1993: The effect of grazing on the pollen production of grasses. *Vegetation History and Archaeobotany* 2, 157–62.

Heim, J. 1970: Les relations entre les spectres polliniques récents et la végétation actuelle en europe occidentale. Doctoral Thesis, Université de Louvain, 179 pp.

Hicks, S. 1988: The representation of different farming practices in pollen diagrams from northern Finland. In Birks, H.H., Birks, H.J.B., Kaland, P. and Dagfinn, M., editors, *The cultural landscape – past, present and future.* Cambridge University Press, 189–207.

Hicks, S. 2001: The use of annual arboreal pollen deposition values for delimiting tree-lines in the landscape and exploring models of pollen dispersal. *Review of Palaeobotany and Palynology* 117, 1–29.

Hicks, S. and **Birks, H.J.B.** 1996: Numerical analysis of modern and fossil pollen spectra as a tool for elucidating the nature of fine-scale human activities in boreal areas. *Vegetation History and Archaeobotany* 5, 257–72.

Hicks, S., Tinsley, H., Huusko, A., Jensen, C., Hattestrand, M., Gerasimides, A. and **Kvavadze, E.** 2001: Some comments on spatial variation in arboreal pollen deposition: first records from the Pollen Monitoring Programme (PMP). *Review of Palaeobotany and Palynology* 117, 183–94.

Hjelle, K.L. 1997: Relationships between pollen and plants in human-influenced vegetation types using presence-absence data in Western Norway. *Review of Palaeobotany and Palynology* 99, 1–16.

—— 1998: Herb pollen representation in surface moss samples from mown meadows and pastures in Western Norway. *Vegetation History and Archaeobotany* 7, 79–96.

—— 1999a: Modern pollen assemblages from mown and grazed vegetation types in western Norway. *Review of Palaeobotany and Palynology* 107, 55–81.

—— 1999b: Use of modern pollen samples and estimated pollen representation factors as aids in the interpretation of cultural activity in local pollen diagrams. *Norwegian Archaeological Review* 32, 19–39.

Leps, J. and **Smilauer, P.** 2003: *Multivariate analysis of ecological data using CANOCO.* Cambridge University Press, 282, pp.

Moore, P.D., Webb, J.A. and **Collinson, M.E.** 1991: *Pollen analysis.* Blackwell Science, 216 pp.

Räsänen, S. 2001: Tracing and interpreting fine-scale human impact in northern Fennoscandia with the aid of modern pollen analogues. *Vegetation History and Archaeobotany* 10, 211–18.

Räsänen, S., Hicks, S. and **Odgaard, B.V.** 2004: Pollen deposition in mosses and in a modified 'Tauber trap' from Hailuoto, Finland: what exactly do the mosses record? *Review of Palaeobotany and Palynology* 129, 103–16.

Reille, M. 1992: *Pollen et spores d'Europe et d'Afrique du Nord.* Laboratoire de Botanique Historique et Palynologie, 535 pp.

Sugita, S., Gaillard M.-J. and **Broström, A.** 1999: Landscape openness and pollen records: a simulation approach. *The Holocene* 9, 409–21.

Ter Braak, C.J.F. and **Prentice, C.I.** 1988: A theory of gradient analysis. *Advances in Ecological Research* 18, 271–317.

Ter Braak, C.J.F. and **Smilauer, P.** 1998: *CANOCO Reference manual. User's Guide to Canoco for Windows. Software for canonical community ordination (version 4).* Centre for Biometry Wageningen, 352 pp.

Tinsley, H. 2001: Modern pollen deposition in traps on a transect across an anthropogenic tree-line on Exmoor, southwest England: a note summarising the first three years of data. *Review of Palaeobotany and Palynology* 117, 153–58.

Tutin, T.G., Heywood, V.H., Burges, N.A., Valentine, D.H., Walters, S.M., Webb, D.A. and with the assistance of **Ball, P.W.a.C., A. O.** 1964–1980: *Flora Europea.* Cambridge University Press.

van der Knaap, W.O., van Leeuwen, J.F.N. and **Ammann, B.** 2001: Seven years of annual pollen influx at the forest limit in the Swiss Alps studied by pollen traps: relations to vegetation and climate. *Review of Palaeobotany and Palynology* 117, 31–52.

Vorren, K.-D. 1986: The impact of early agriculture on the vegetation of Northern Norway. A discussion of anthropogenic indicators in biostratigraphical data. In Behre, K.-E. editor, *Anthropogenic indicators in pollen diagrams*, Balkema, 1–18.

Wildi, O. and **Orloci, L.** 1996: *Numerical exploration of community patterns.* Amsterdam: SPB Academic Publishing, 171 pp.

Wright, H.E.J. 1967: The use of surface samples in quaternary pollen analysis. *Review of Palaeobotany and Palynology* 2, 321–30.

Palaeohydrological changes and human impact history over the last millennium recorded at Lake Joux in the Jura Mountains (Switzerland)

M. Magny[1, 2], E. Gauthier[1], B. Vannière[1], O. Peyron[1]

Abstract

On the basis of sediment and pollen analyses of a radiocarbon-dated sediment sequence from Lake Joux in the Swiss Jura Mountains (west-central Europe), this paper presents a high-resolution record of lake-level and vegetation changes for the last millennium. The lake-level record makes it possible to determine that lowstands of the water table dominated at ca AD 1200-1400, and from 1720 onward, with interruptions by short-lived rise events at ca AD 1340 and 1840. Highstands prevailed at ca AD 1100, and around AD 1450, 1550, and 1700. The comparison of the Joux lake-level record with a solar irradiance record based on cosmogenic nuclides supports the hypothesis of a major solar forcing of climate variations in west-central Europe over the last millennium.

Finally, despite the severe climatic conditions which prevail in the Joux Valley, the human impact history at Lake Joux over the last millennium seems to reflect political choices and economic context more than climatic changes.

Site

Lake Joux (46° 36' 51"N, 6° 15' E) is a 9 km-long narrow and over-deepened basin of glacial origin. The present water depth reaches 33.5 m and the lake area is 8.67 km^2. It is located at an altitude of 1006 m a.s.l. in the summit zone of the Swiss Jura Mountains (Fig. 1). The surrounding mountains culminate at ca 1300-1600 m a.s.l. The catchment area of the lake covers ca 211 km^2. The substratum is mainly composed of Upper Jurassic and Tertiary limestones.

The main inlet of the lake is the Orbe River which drains a long Neocomian synclinal trough (Fig. 1). Lake Joux, like Lake Brenet located just downstream at 1005,5 m a.s.l., has not surficial outlet; the exsurgence of both lakes is formed by several karstic caves on their north-western shores, and the waters of both lakes resurge at the Orbe spring near Vallorbe, at ca 800 m a.s.l., after a 3 km-long underground course (Fig. 1). During heavy rainfalls, the karstic caves which usually form the lake outlet may work as inlets to the lake. Thus, before its artificial regulation in the early 20th century and the use of lake water for hydro-electricity, Lake Joux was characterised by large seasonal fluctuations of its water table most often due to automn rains and spring snow-melting. The maximal and minimal levels observed were respectively 1011 m in 1883 and 1004.9 m in 1865, while over the period 1847-1901 the mean highstand

and lowstand were respectively 1008.7 and 1006.2 m (Bosset, 1962; Perrin, 1904). Minimal levels resulted from summer droughts or winter frost periods.

The Joux Valley is characterised by a severe semi-continental climate. Over the period 1897-1930, the mean annual precipitation attains ca 1500 mm, with observed minimum at 851 mm in 1921 and maximum at 1990 mm in 1930. The mean annual temperature is 5.3°C, in the coldest month -3.9°C and in the warmest month 13.8°C. The annual variations in temperature may show a wide amplitude as illutrated by year 1888 with -41°C in January and 28.8°C in August. Over the period 1897-1930, the lake surface was frozen during a mean annual period of 78 days (Aubert, 1932).

The Gallic word 'Joux' (equivalent to the word 'Jura') literally means 'forest of firs and spruces'. At present, the lower montane belt (800-1100 m a.s.l.) is dominated by *Abies* and *Picea* accompanied by *Fagus*, *Fraxinus* and *Quercus*, while *Pinus uncinata* and *Betula* develop on humid areas. Above 1100 m, *Picea abies* dominates. The highest zones (ca 1600 m a.s.l.) are occupied by grasslands due to (1) anthropogenic deforestation for grazing activities and/or (2) severe climatic conditions (Wegmüller, 1966; Gauthier, 2004).

Previous pollen studies by Wegmülller (1966) from a sediment core taken at ca 15-18 m water depth and ca 150 m from the north-eastern extremity of Lake Joux have given evidence of the first anthropogenic deforestations during the Neolithic and Protohistoric times, while a continuous human impact on vegetation appears since the Roman period. Documentary sources relate the foundation of a monastery in the 5th century at Le Lieu (Fig. 1). This first establishment disappeared in AD 610 and was followed by the foundation of an abbey in AD 1126 at L'Abbaye (Fig. 1). Historical data suggest that the 15th century corresponded to an expansion of settlement in the elevated areas of the Swiss Jura, where the 16th and 17th centuries appear to have been a period of relative prosperity marked by a growing population and based on agriculture and grazing activities (Daumas and Tissot, 2004). Being in Switzerland, the valley of Joux remained untouched by the disturbances and damages due to the wars of religion that affected the neighbouring French Jura region in Modern times, particularly during the 17th century. The 18th century coincided with the development of industrial activities. Thus, at the end of the 18th century, four glassworks were established on the shores of Lake Joux. The growing need for charcoal due to the expansion of the glass industry during the 18th and 19th centuries was a threat to the preservation of forests (Wegmüller, 1966). On the map of Cassini established in the 18th century, Lake Joux was named « Lac des Charbonnières ». In addition, close to the Joux Valley, the city of Vallorbe (Fig. 1) was a centre of iron production which also involved a significant consumption of wood in blast-furnaces. In the late 19th century, grazing activities became more predominant than cultivation, while regional industry focused on high-technology activities such as the clock and watch making industry.

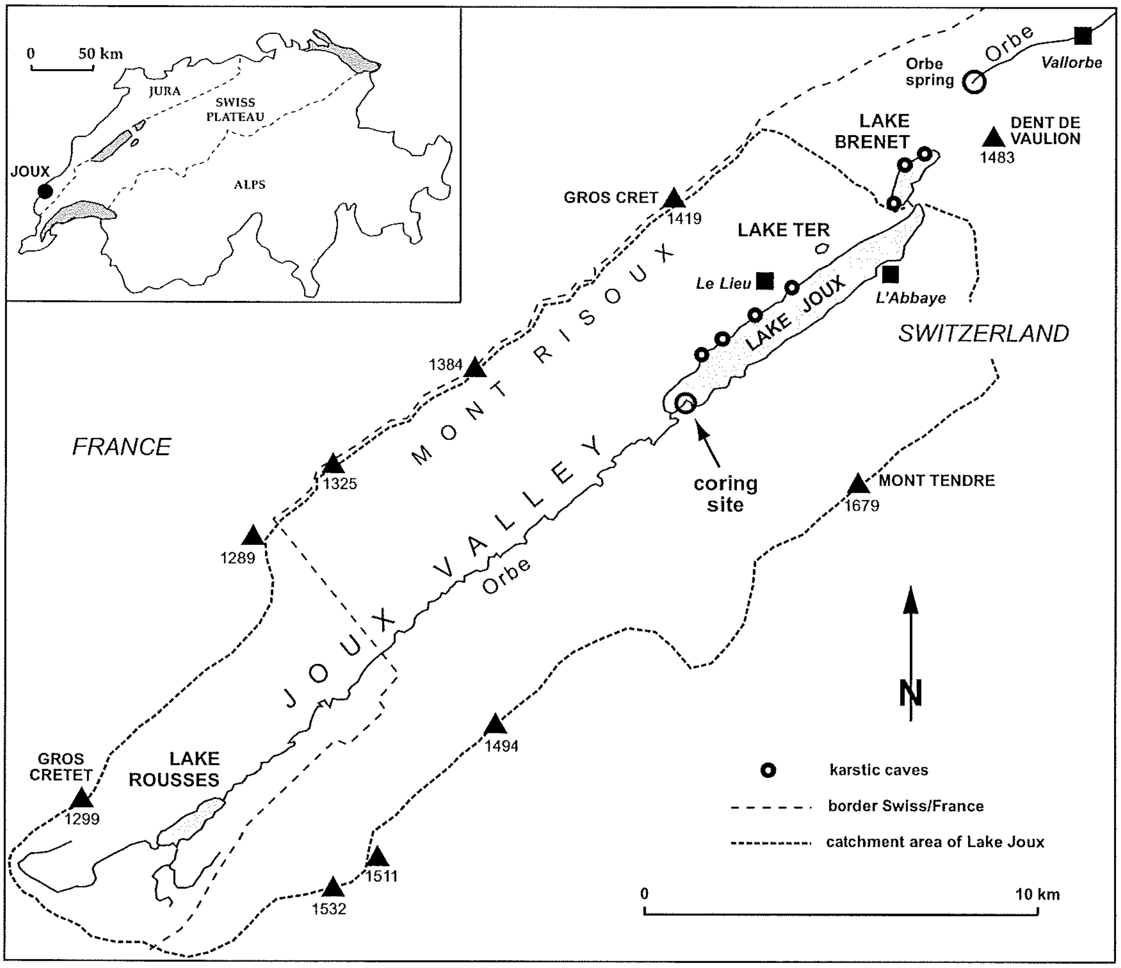
0
50 km
JURA
SWISS PLATEAU
ALPS
JOUX
Orbe
Vallorbe
Orbe spring
LAKE BRENET
DENT DE VAULION
1483
GROS CRET
1419
LAKE TER
Le Lieu
L'Abbaye
LAKE JOUX
SWITZERLAND
MONT RISOUX
1384
FRANCE
1325
1289
coring site
MONT TENDRE
1679
JOUX VALLEY
Orbe
N
GROS CRETET
1299
LAKE ROUSSES
1494
1511
1532
karstic caves
border Swiss/France
catchment area of Lake Joux
0
10 km

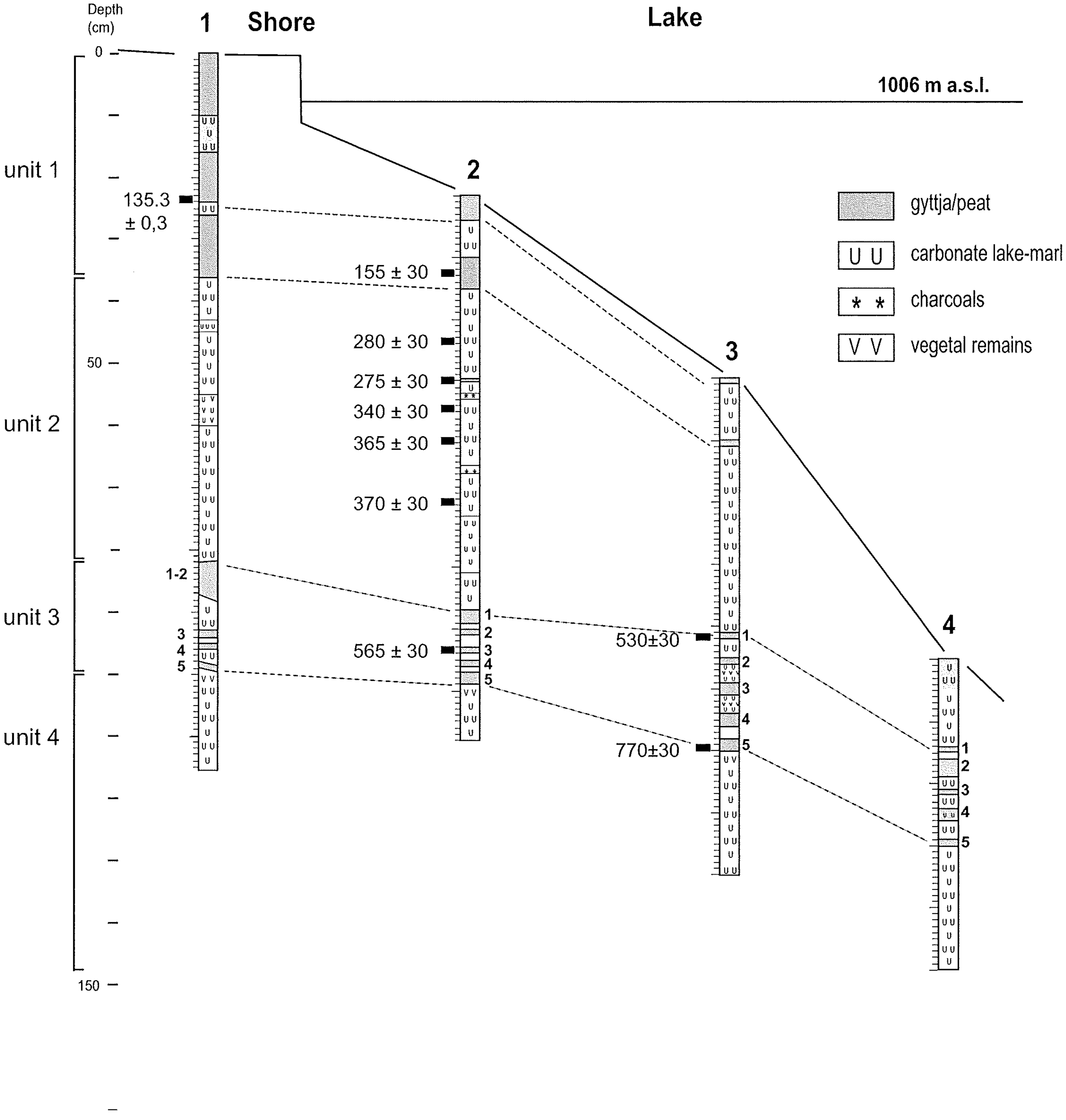
Depth (cm)
0
50
150
unit 1
unit 2
unit 3
unit 4
1
Shore
Lake
1006 m a.s.l.
2
3
4
135.3 ± 0,3
155 ± 30
280 ± 30
275 ± 30
340 ± 30
365 ± 30
370 ± 30
565 ± 30
530±30
770±30
1-2
3
4
5
1
2
3
4
5
gyttja/peat
U U carbonate lake-marl
* * charcoals
V V vegetal remains

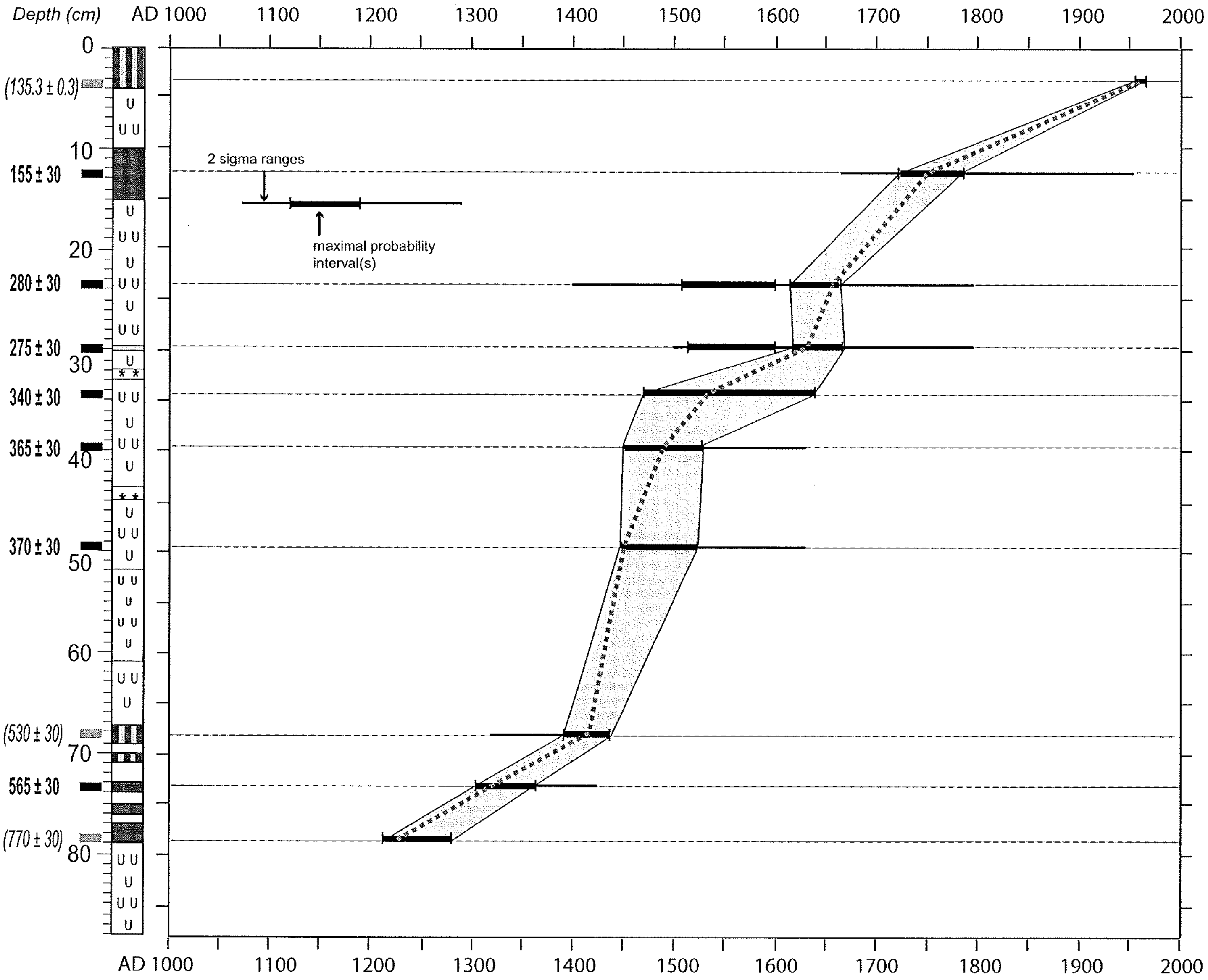
Depth (cm)
AD 1000
1100
1200
1300
1400
1500
1600
1700
1800
1900
2000
0
10
20
30
40
50
60
70
80
(135.3 ± 0.3)
155 ± 30
280 ± 30
275 ± 30
340 ± 30
365 ± 30
370 ± 30
(530 ± 30)
565 ± 30
(770 ± 30)
2 sigma ranges
maximal probability interval(s)

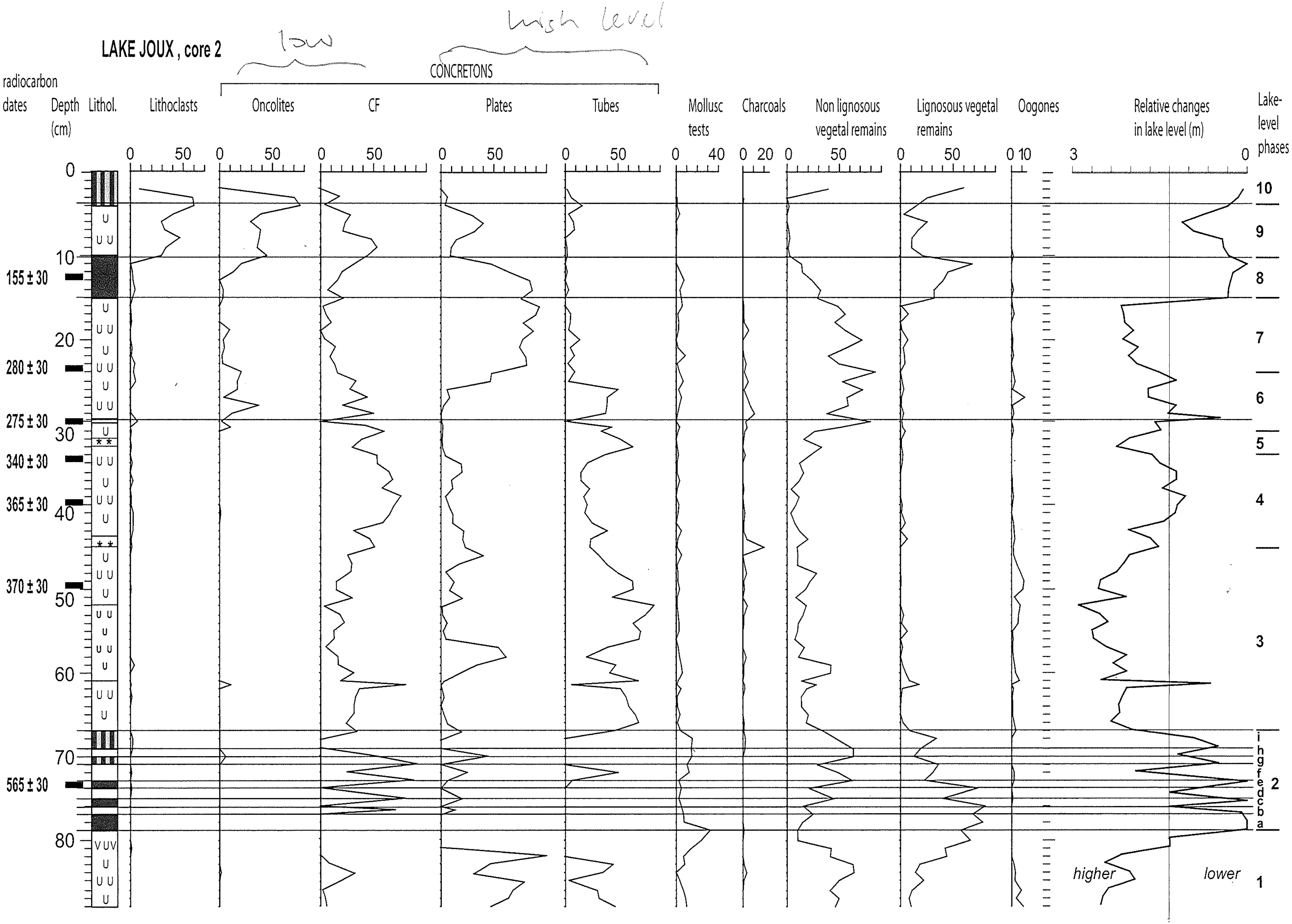
low
high level
LAKE JOUX , core 2
CONCRETONS
radiocarbon dates
Depth (cm)
Lithol.
Lithoclasts
Oncolites
CF
Plates
Tubes
Mollusc tests
Charcoals
Non lignosous vegetal remains
Lignosous vegetal remains
Oogones
Relative changes in lake level (m)
Lake-level phases
0
50
40
20
10
3
0
10
20
30
40
50
60
70
80
155 ± 30
280 ± 30
275 ± 30
340 ± 30
365 ± 30
370 ± 30
565 ± 30
higher
lower
10
9
8
7
6
5
4
3
i
h
g
f
e
d
c
b
a
2
1

Emile Gauthier

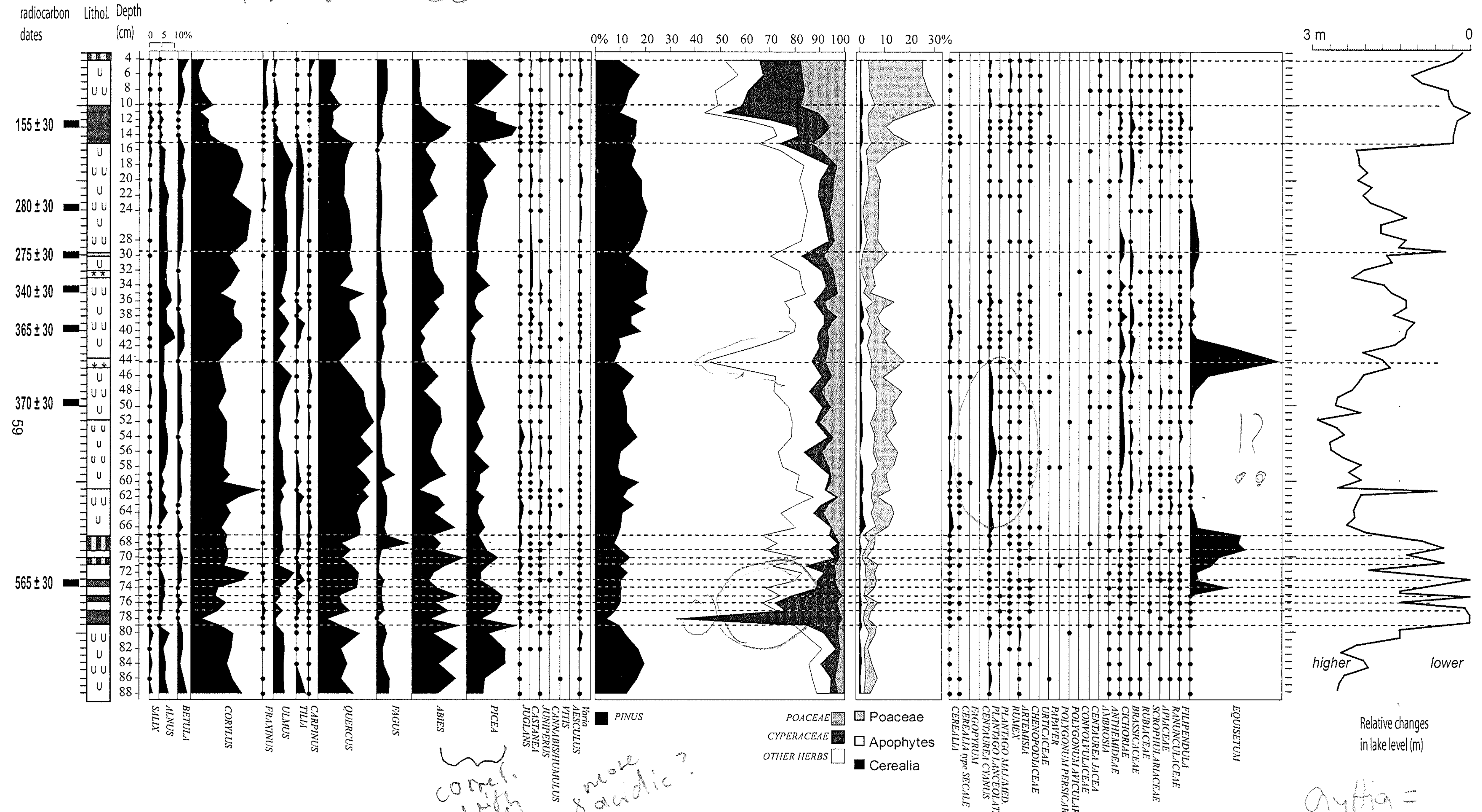

correl. with gyttja -> more acidic?

gyttja = low

Little Ice Age: cold/humid
Medieval warm: warm/dry

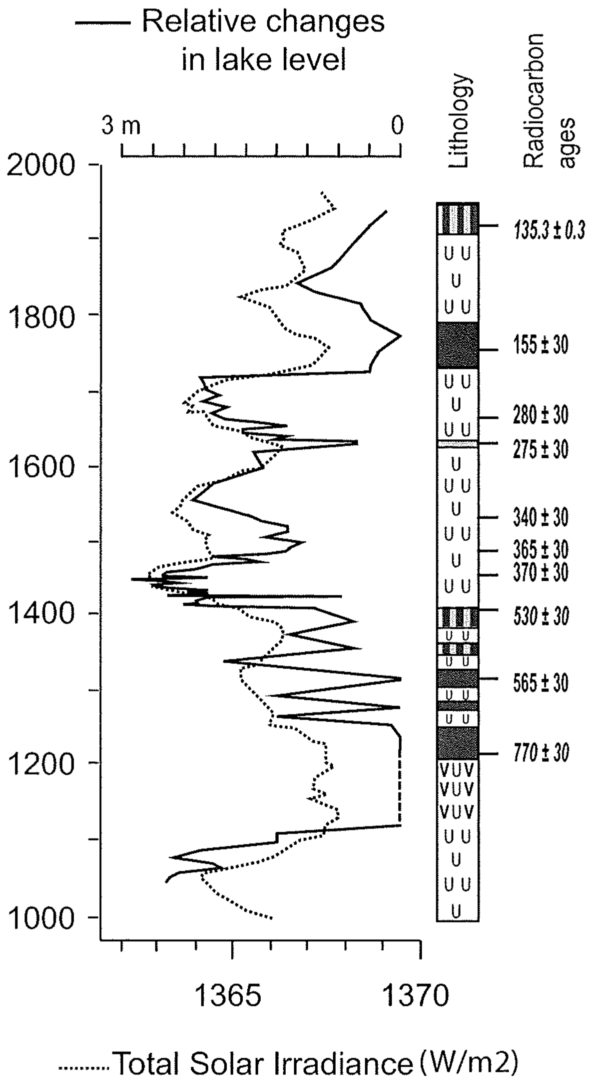
Relative changes in lake level
3 m
0
Lithology
Radiocarbon ages
2000
1800
1600
1400
1200
1000
135.3 ± 0.3
155 ± 30
280 ± 30
275 ± 30
340 ± 30
365 ± 30
370 ± 30
530 ± 30
565 ± 30
770 ± 30
1365
1370
Total Solar Irradiance (W/m2)

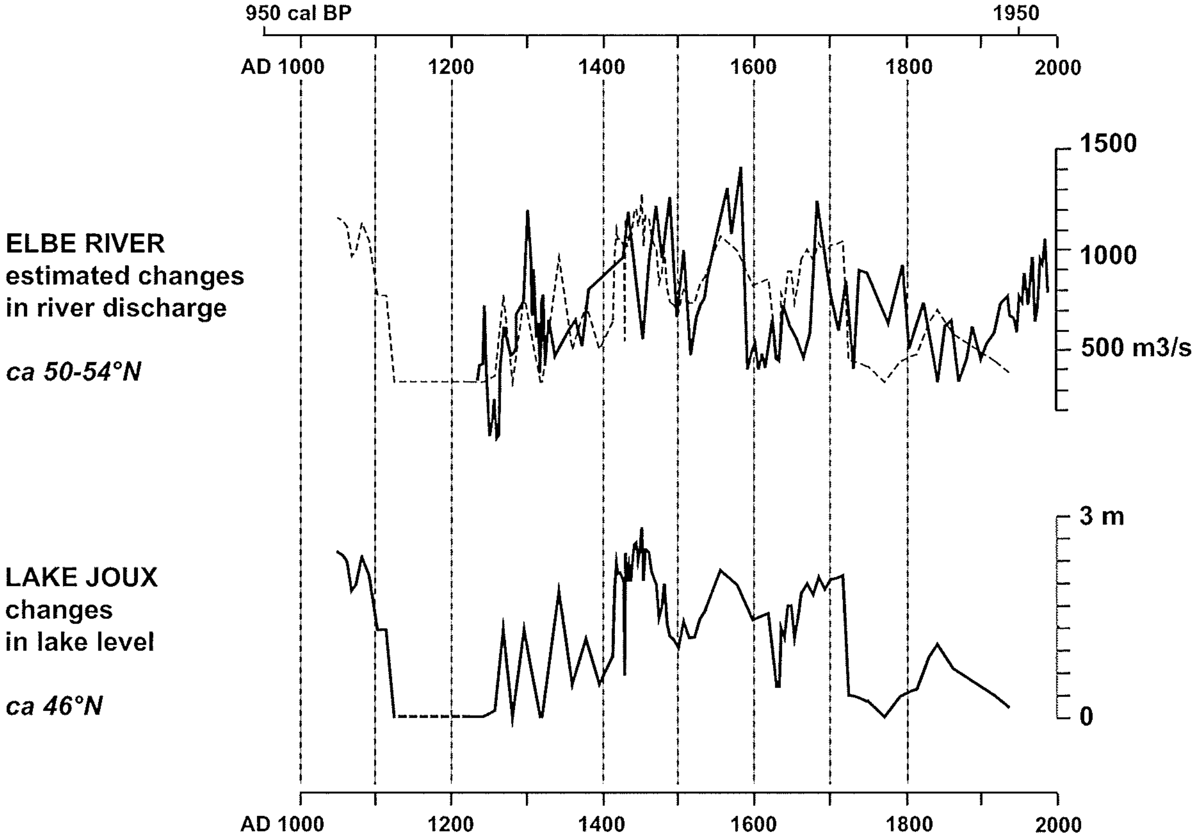
950 cal BP
1950
AD 1000
1200
1400
1600
1800
2000
ELBE RIVER
estimated changes
in river discharge
ca 50-54°N
1500
1000
500 m3/s
LAKE JOUX
changes
in lake level
ca 46°N
3 m
0
AD 1000
1200
1400
1600
1800
2000

Thuesday 18 september

Lakes Mortes and Bellefontaine
Lake Saint-Point
Lake Remoray

The “lac de Bellefontaine” (1093 asl) lies in the anticlinal valley of “les mortes” between the Mont Risoux (1419 m asl) on the west and the “Mont noir” on the east. 2 meters of a morainic deposit separate the “lac des mortes” from the “lac de Bellefontaine”. Lakes ‘water flows northward through an outlet and joins a sinkhole to the west.

The “lac de Bellefontaine” and the “lac des mortes” have a maximum depth of 6.2 m and 7.5 m, respectively. During the deglaciation the persistence of ice cap in the Bienne valley maintains lasting the area under glacial influence.

A study based upon high resolution pollen- and plant macrofossil analyses along an altitudinal transect including the lake of Bellefontaine aims to reconstruct lateglacial vegetation patterns (altitudinal distribution of arborean cover) and the impact of climate :

During the Bølling, Betula woodland was established up to 800 m a.s.l. whereas Juniperus communities were reached 1000-1100 m asl. The Older Dryas was characterized by a decline of shrubby vegetation to lower altitudes. pine forests were migrated progressively into the massif up to 1200 m a.s.l. during the Allerød. Subsequently, the treeline retreated abruptly in response to the Younger Dryas deterioration . Thus, open landscape with scattered trees was extended over a big part of the massif (at least above 800 m a.s.l.). The widespread expansion of mixed Pinus-Betula forests on highest altitudes occurred at the beginning of the Holocene.

High resolution pollen records show a great irregularity of pollen curves. Those of heliophilous shrubs show a decline in the middle part of the Bølling, around 12400 BP. This event can be correlated with the «Intra Bølling Cold Phase» recognised from ice and marine cores. During the Allerød, the predominance of *Pinus* is repeatedly interrupted by rises in *Betula* and heliophilous herbaceous. One of these phases appears just before the LST (Laacher See Tephra) and corresponds to the Gerzensee oscillation.

High NAP percentages of the Younger Dryas are interrupted by a temporary increase in arborean pollen percentages. This phase could be caused by a relative climatic improvement suggested by a slight positive oscillation from continental isotopic records.

Preboreal oscillation (PBO) is recorded by a rise in Betula and a decrease of Pinus.

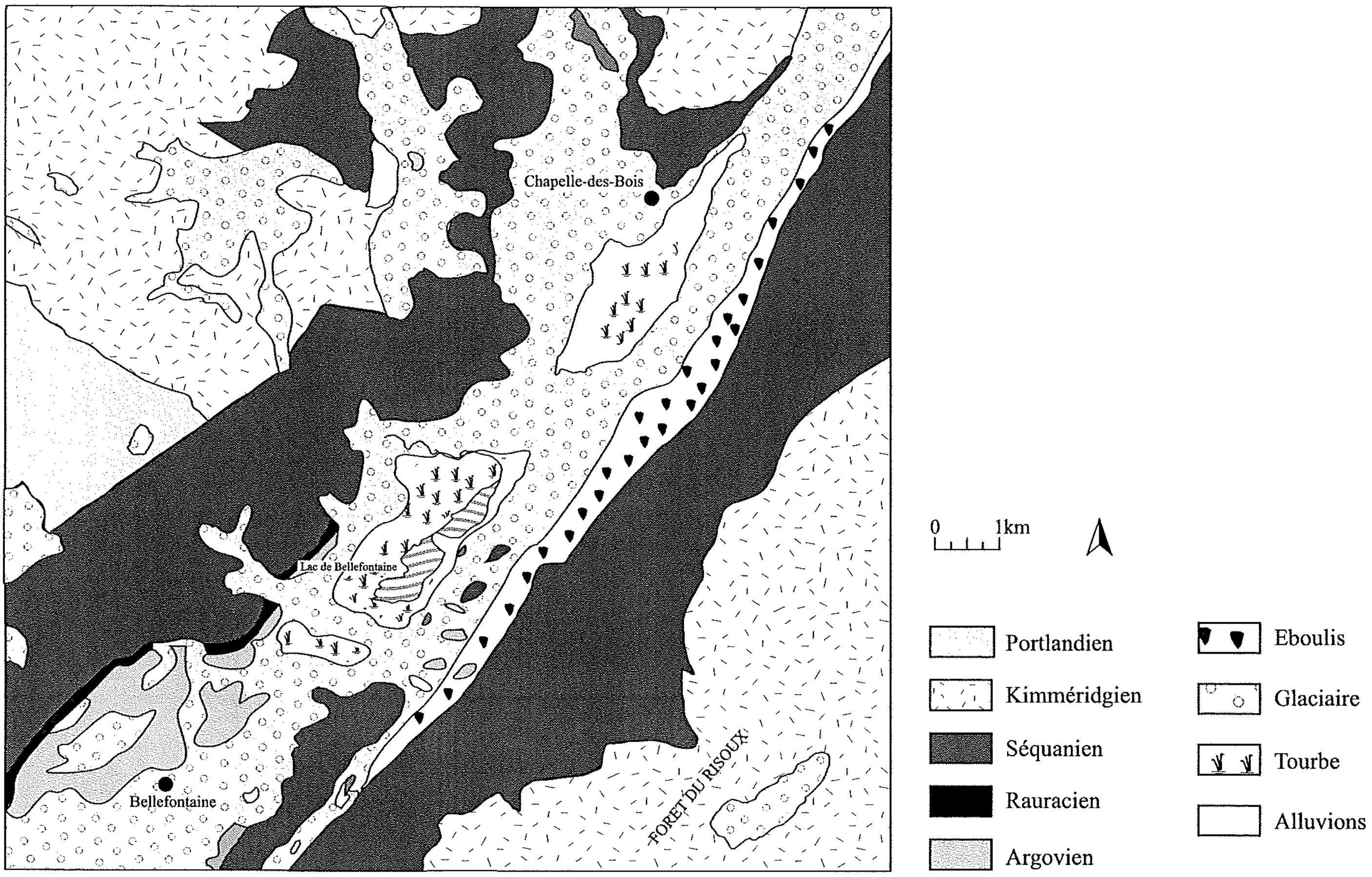
Chapelle-des-Bois
Lac de Bellefontaine
Bellefontaine
FORET DU RISOUX
0 1km
Portlandien
Kimméridgien
Séquanien
Rauracien
Argovien
Eboulis
Glaciaire
Tourbe
Alluvions

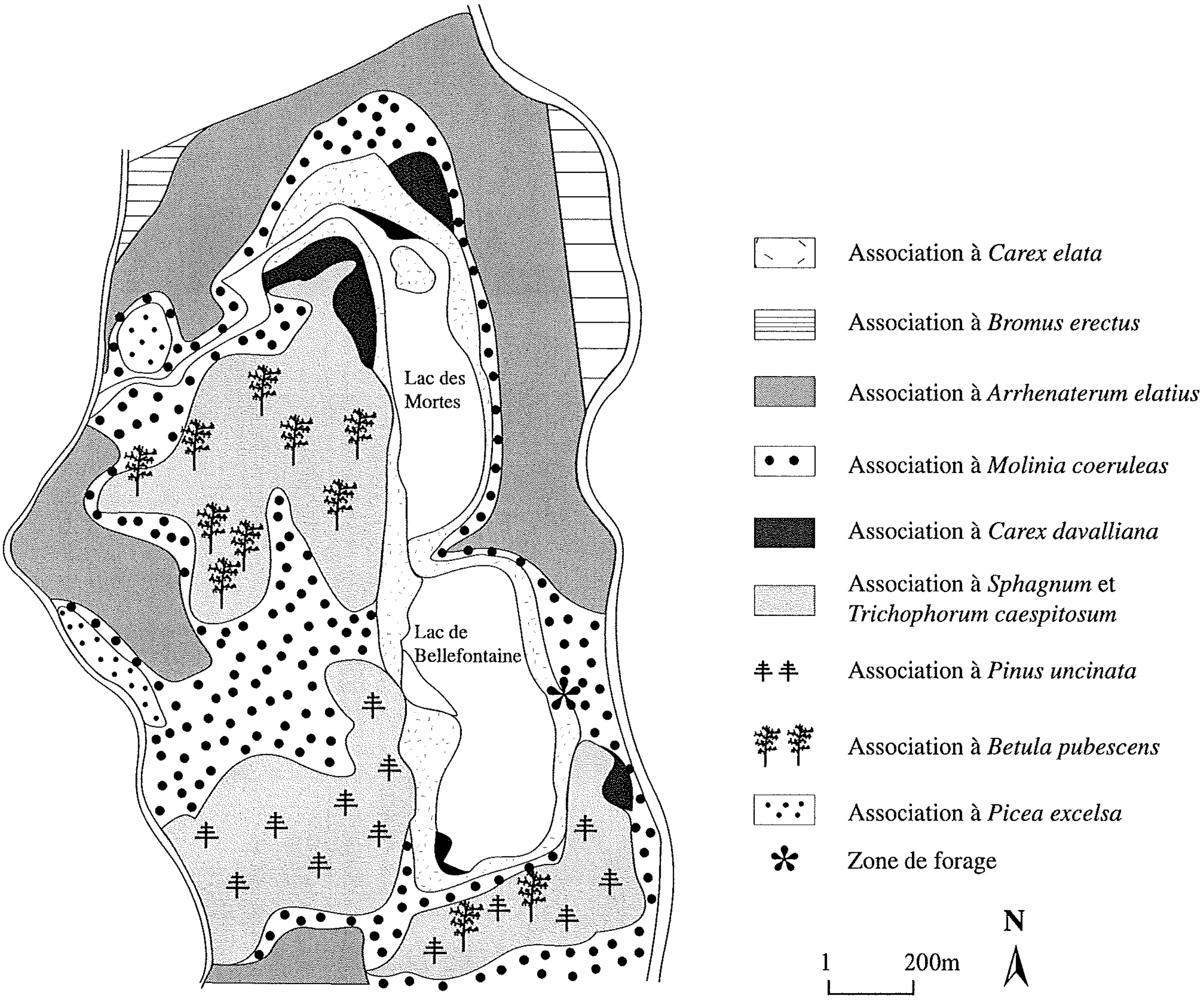
Lac des Mortes
Lac de Bellefontaine
Association à *Carex elata*
Association à *Bromus erectus*
Association à *Arrhenaterum elatius*
Association à *Molinia coeruleas*
Association à *Carex davalliana*
Association à *Sphagnum* et *Trichophorum caespitosum*
Association à *Pinus uncinata*
Association à *Betula pubescens*
Association à *Picea excelsa*
Zone de forage
N
1 200m

Analyses : C. Bégeot

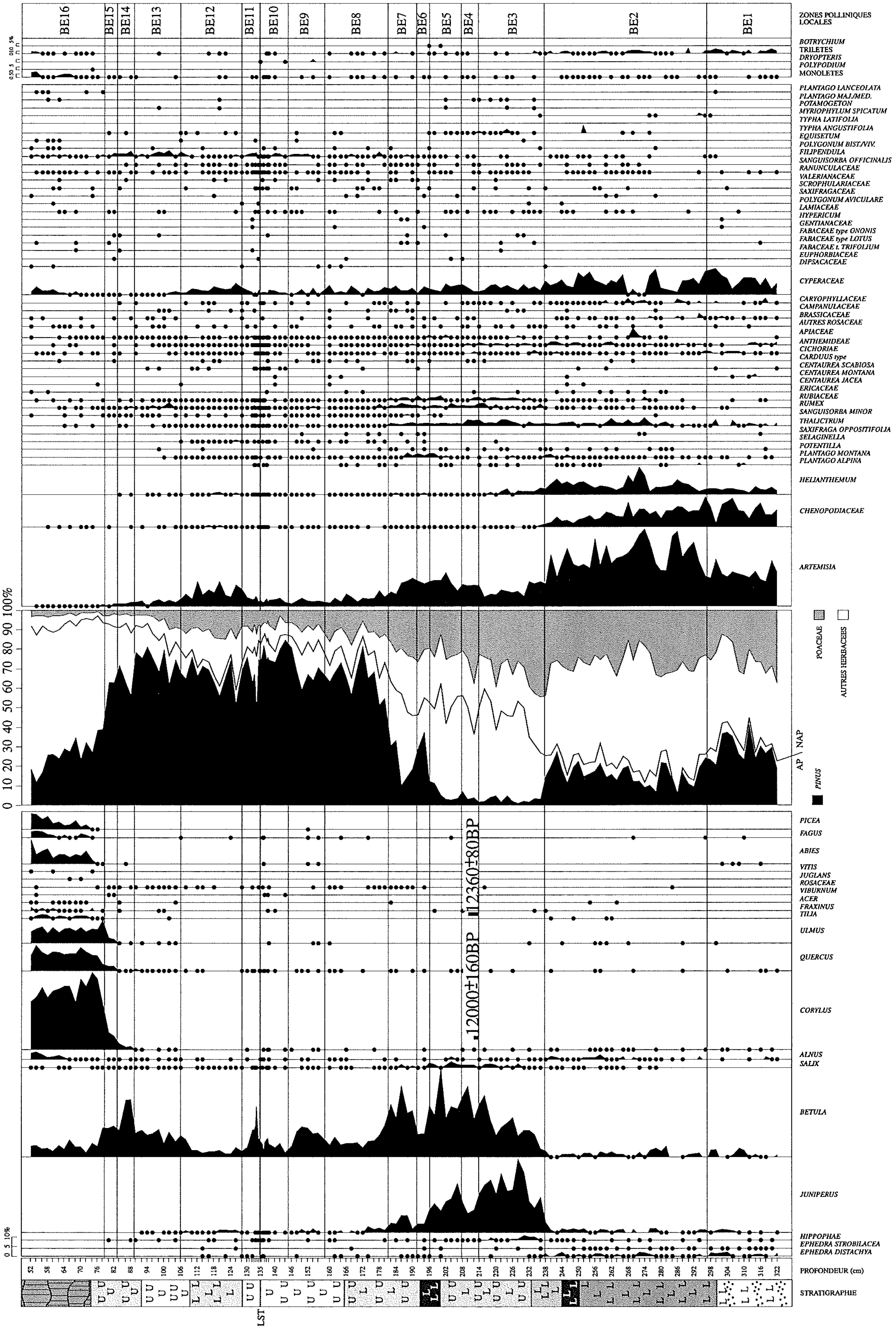

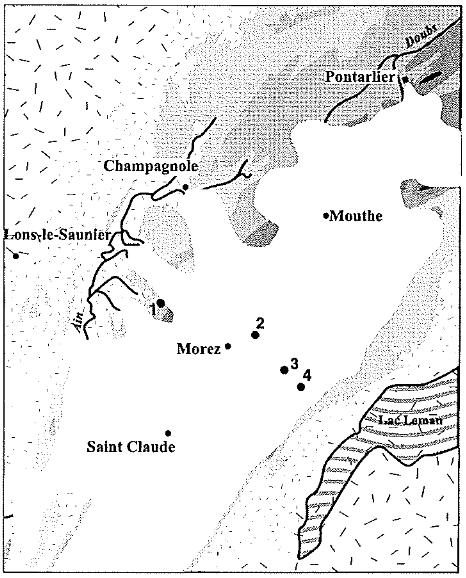

Première phase

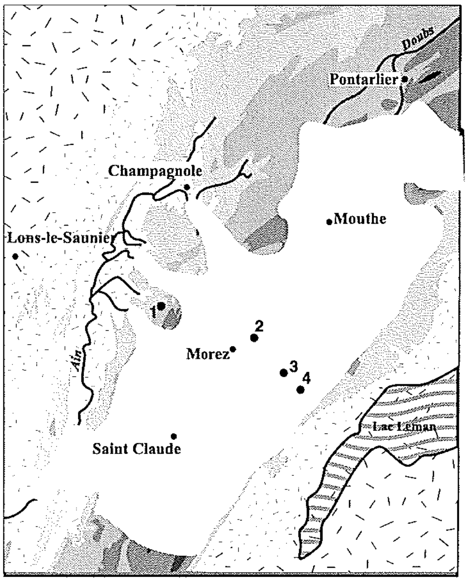

Deuxième phase

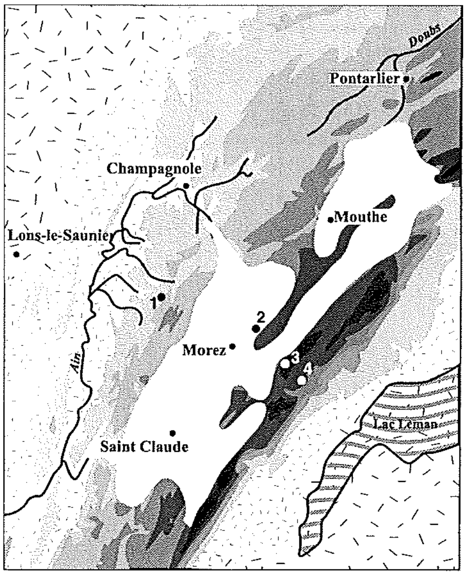

Troisième phase

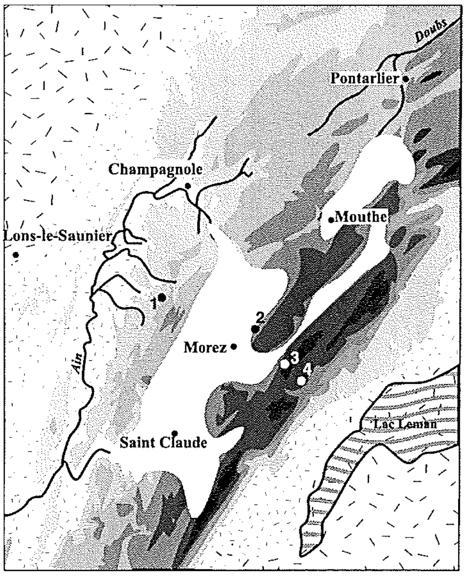

Quatrième phase

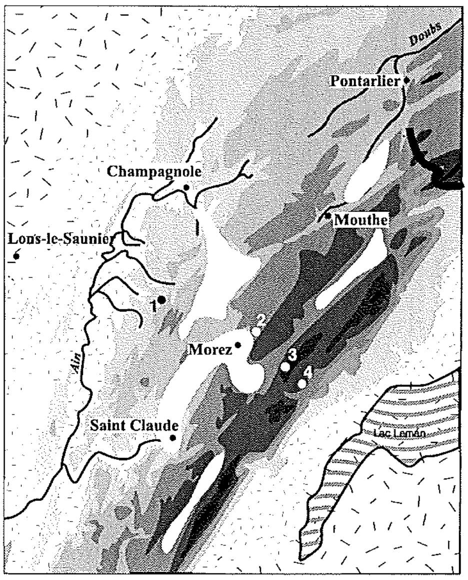

Cinquième phase

Localisation des sites étudiés
- •1 Lautrey
- •2 Bellefontaine
- •3 Creux du croue
- •4 Mont Roux

☐ Glacier jurassien

N

0 10 Km

Altitudes

▨	inf. 400 m	▨	1000-1200 m
▨	400-600 m	▨	1200-1400 m
▨	600-800 m	▨	1400-1600 m
▨	800-1000 m	■	sup.1600 m

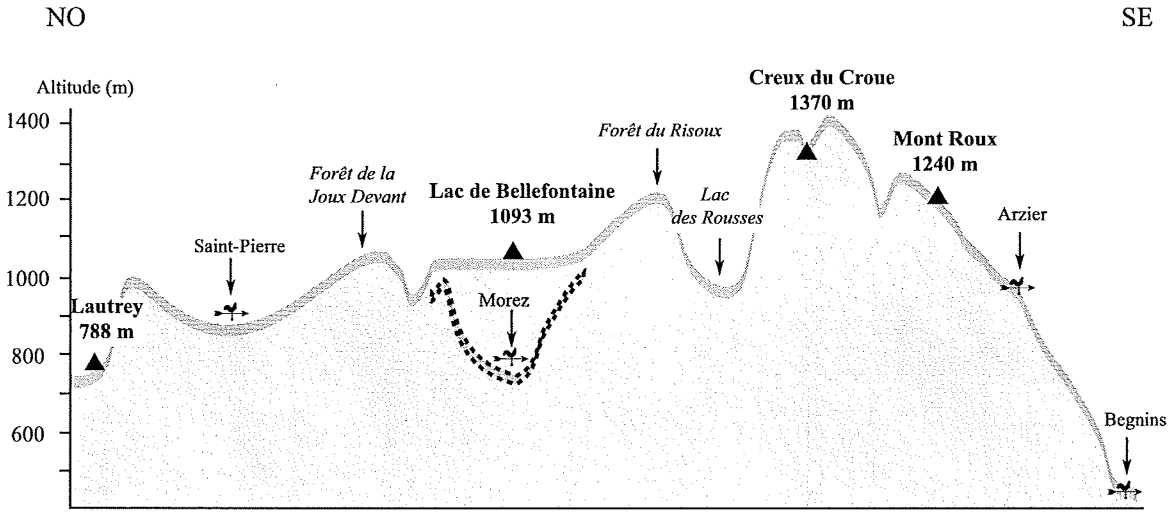
NO
SE
Altitude (m)
1400
1200
1000
800
600
Lautrey
788 m
Saint-Pierre
Forêt de la Joux Devant
Lac de Bellefontaine
1093 m
Morez
Forêt du Risoux
Lac des Rousses
Creux du Croue
1370 m
Mont Roux
1240 m
Arzier
Begnins

reconstructed Tree line variations during the Lateglacial compared
to the climatic evolution (O18 from the GRIP Ice core and T annual reconstructed from the jurassian pollen spectra)

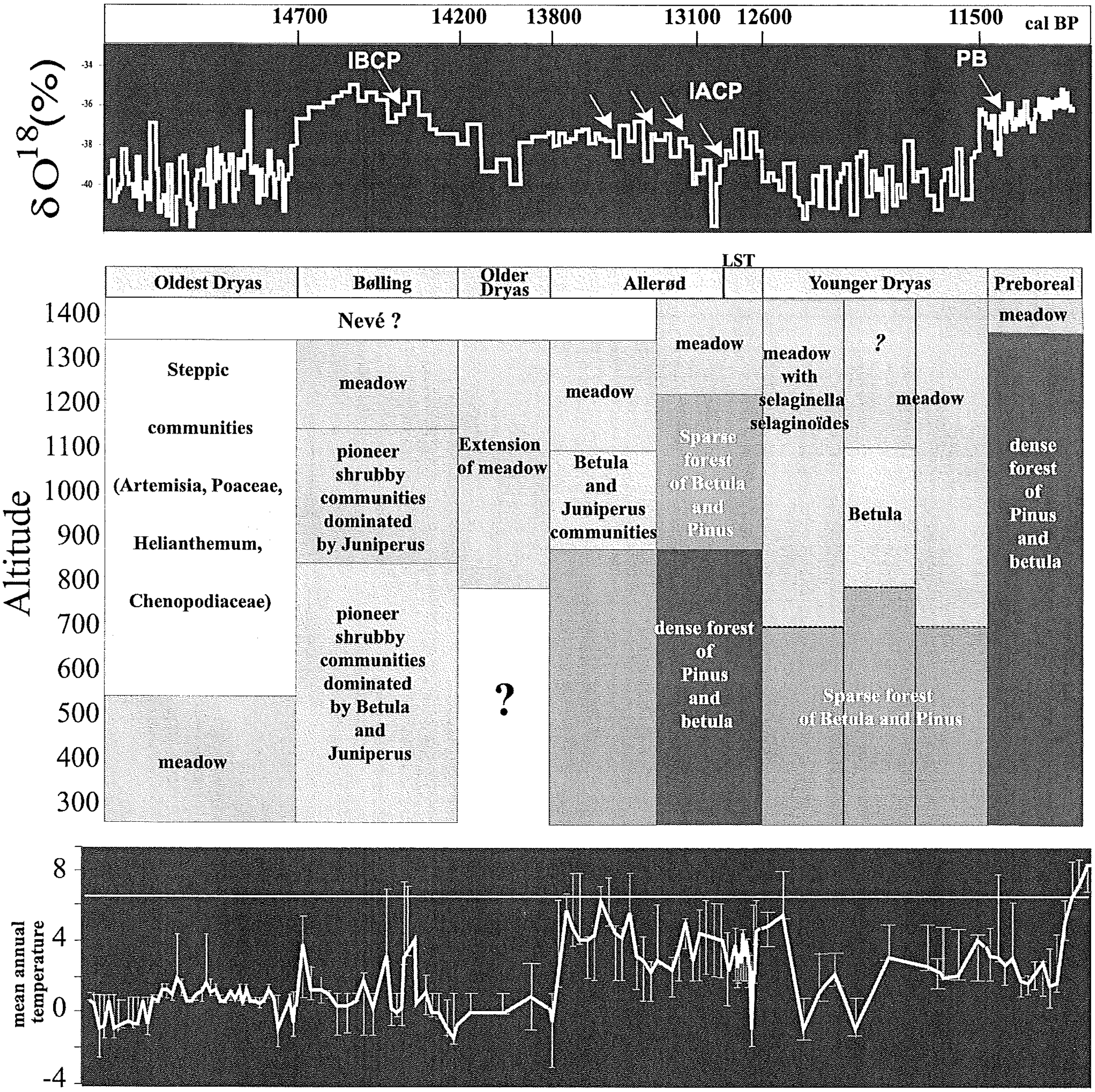

curve of climatic recontruction inferred from pollen data using the best analogue method The abrupt warming at the beginning of the Bølling anf of the Preboreal not appears clearly. This feature, currently observed in palaeoclimatic reconstructions based on pollen data, is generally imputed to the lack of modern analogues.

Lake Saint Point: a high resolution multiparameters analyse of the late glacial-holocene sequence

A.Leroux[1&2], V.Bichet[1], M.Magny[2], A-V.Walter-Simonnet[1], H.Richard[2], A. Baltzer[3]

Université de Franche-Comté, EA 2642 Géosciences, 16 rte de Gray, F-25030 Besançon
[2] Université de Franche-Comté, UMR 6565 Chrono-Ecologie, 16 rte de Gray, F-25030
Université de Normandie, UMR CNRS 6143 "Morphodynamique continentale et côtière", 24 rue des Tilleuls, 14000 Caen

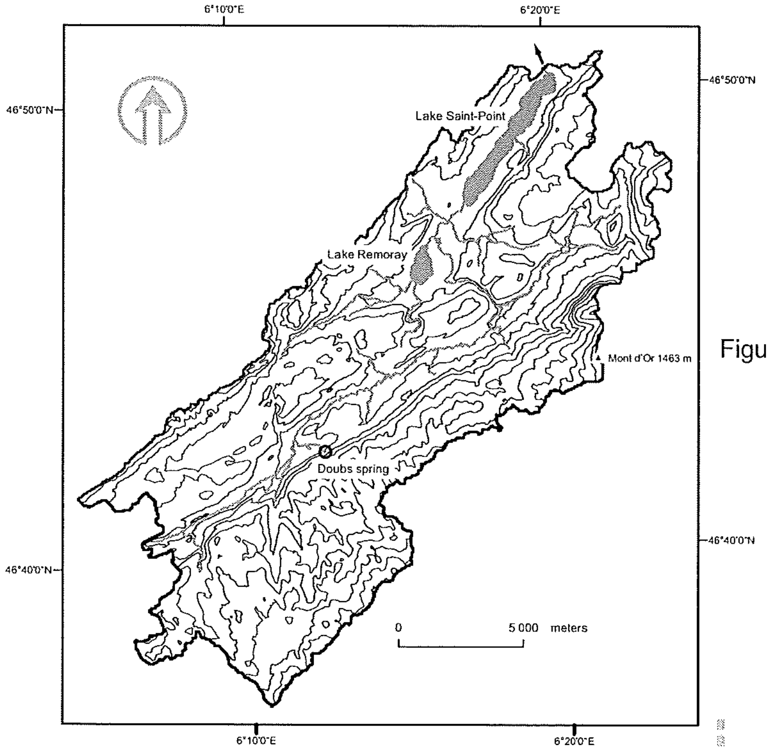

Figure 1:The lake Saint Point watershed (247km²).

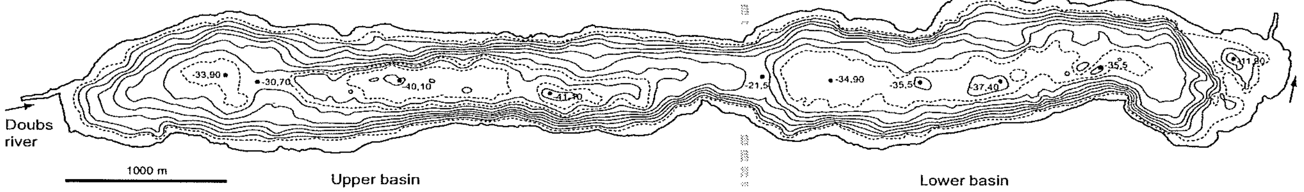

Figure 2: Lake Saint Point bathymetric map.

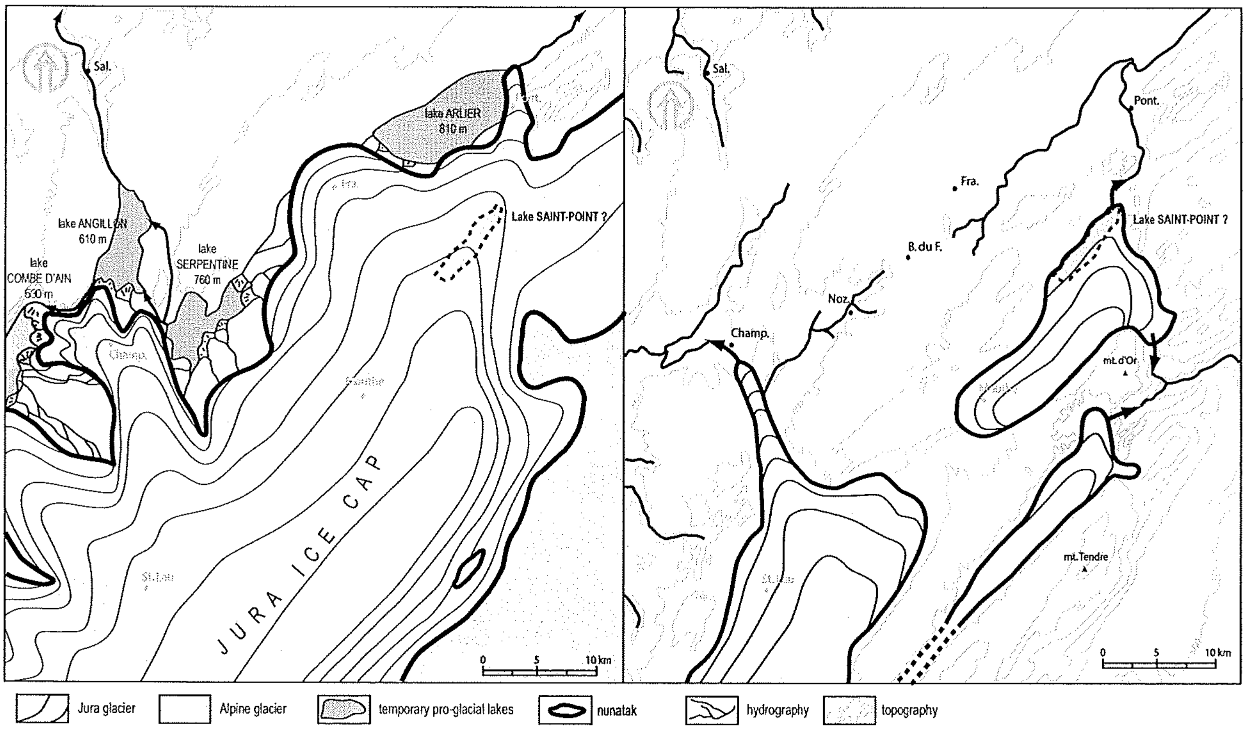

Figure 3: Location of Saint-Point Lake during LGM (around 22 ky cal. BP) and LGM ice cap retreat (around 18 ky cal. BP) - after CAMPY, 1982 modified.

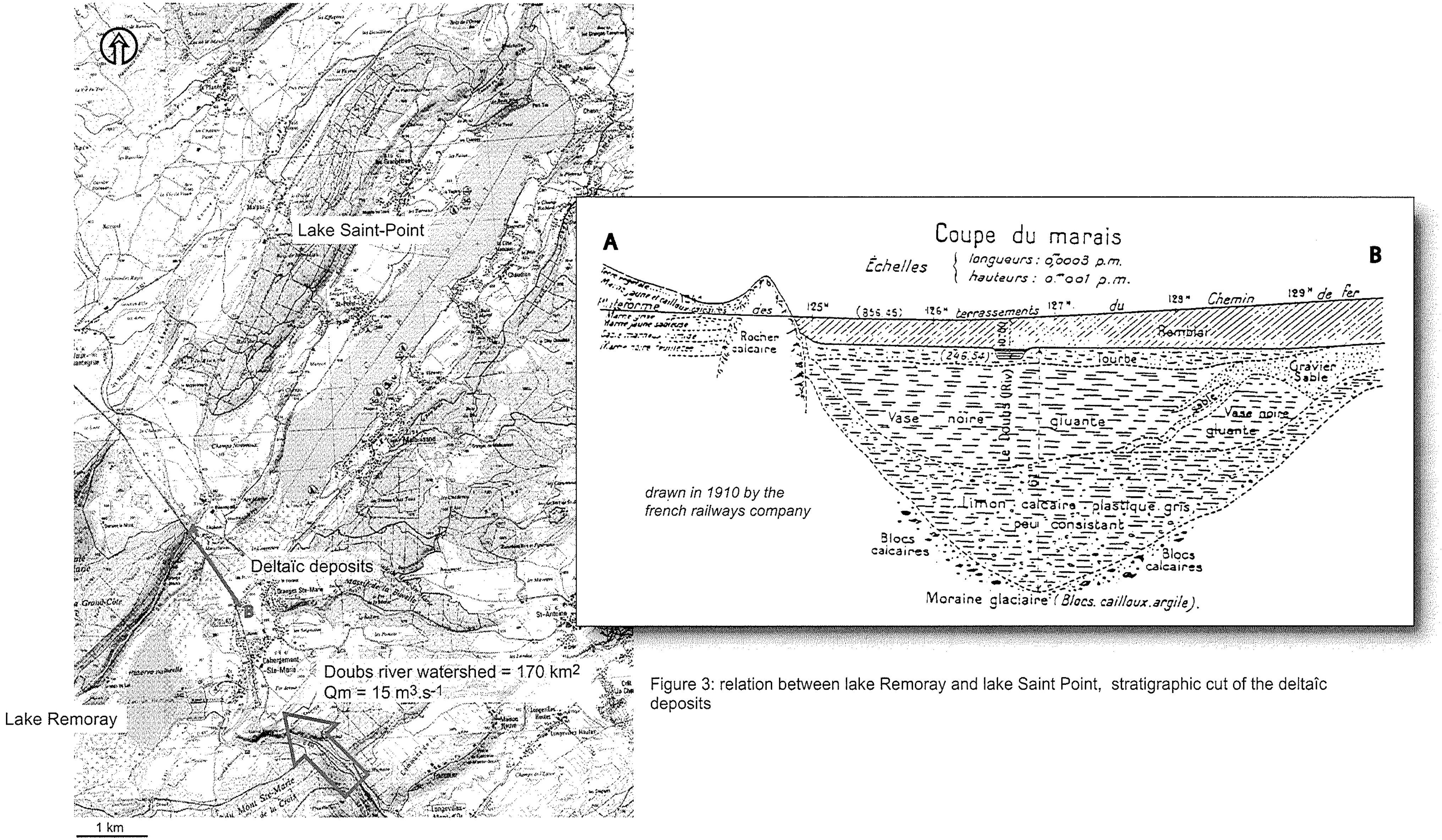

drawn in 1910 by the french railways company

Figure 3: relation between lake Remoray and lake Saint Point, stratigraphic cut of the deltaîc deposits

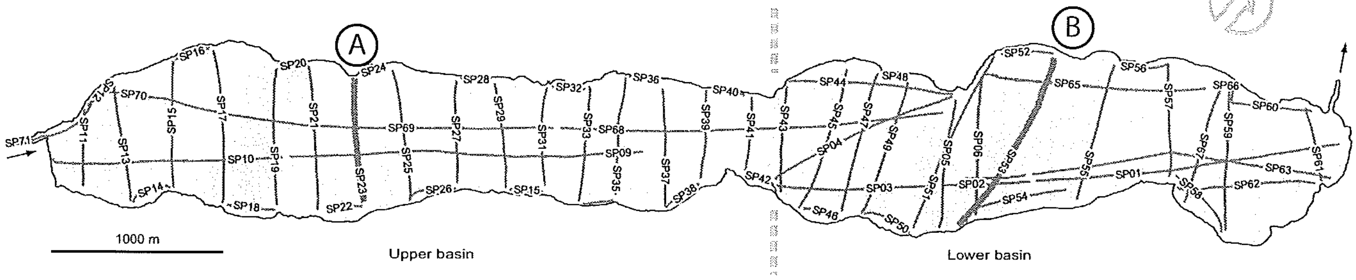

Figure 5: Sismic line location

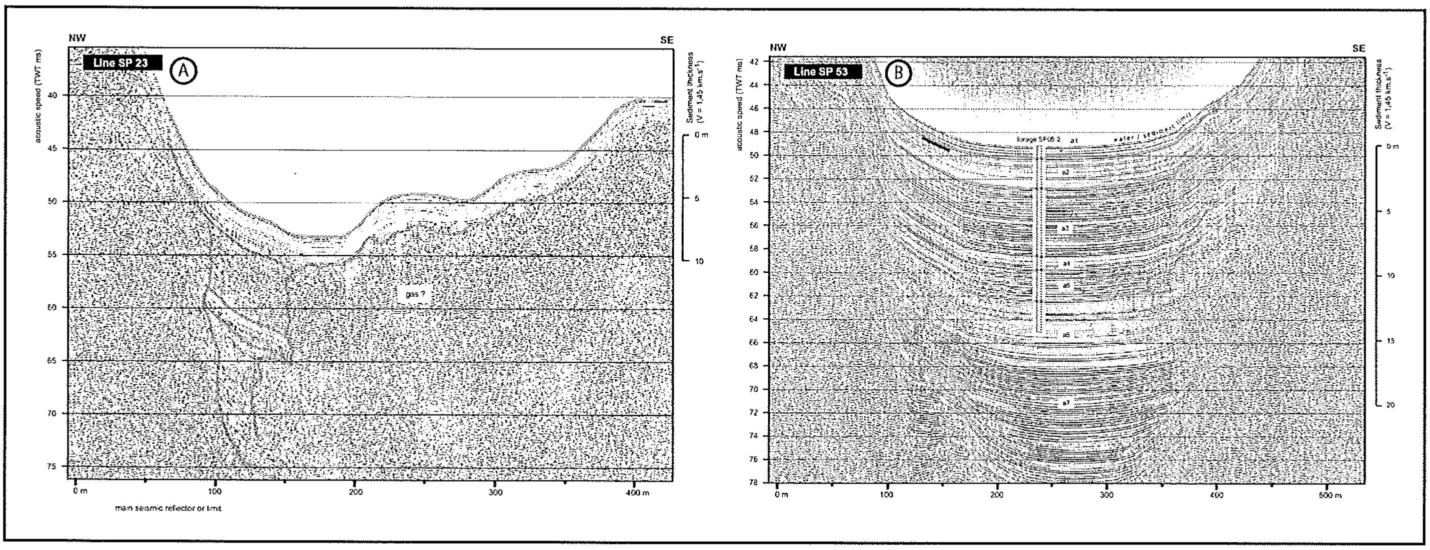

Figure 6: example of two sismic profiles obtained in the basin (resolution: 25cm)

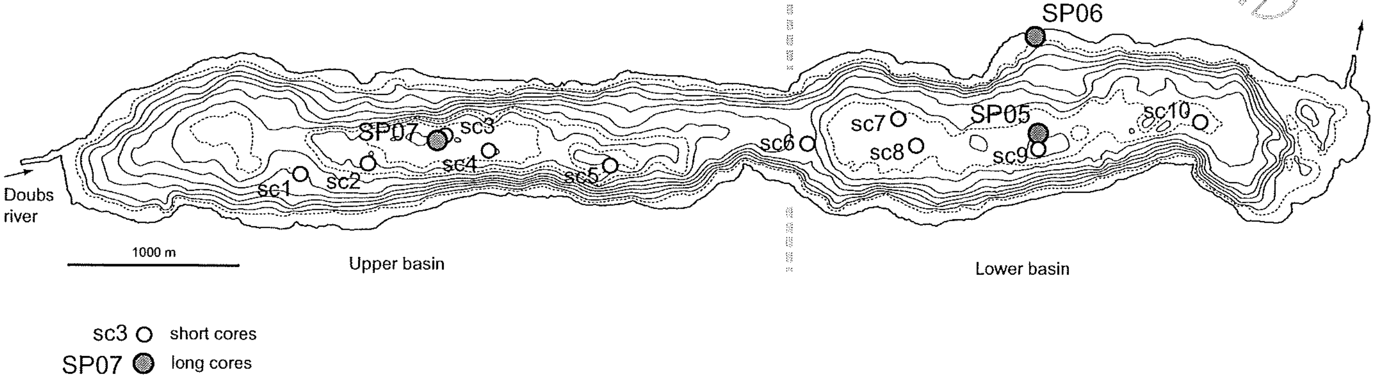

Figure7: Location of the different cores in the lake, (length of the long cores: SP05,12.5m- SP07,12 m and SP06, 6.5m)

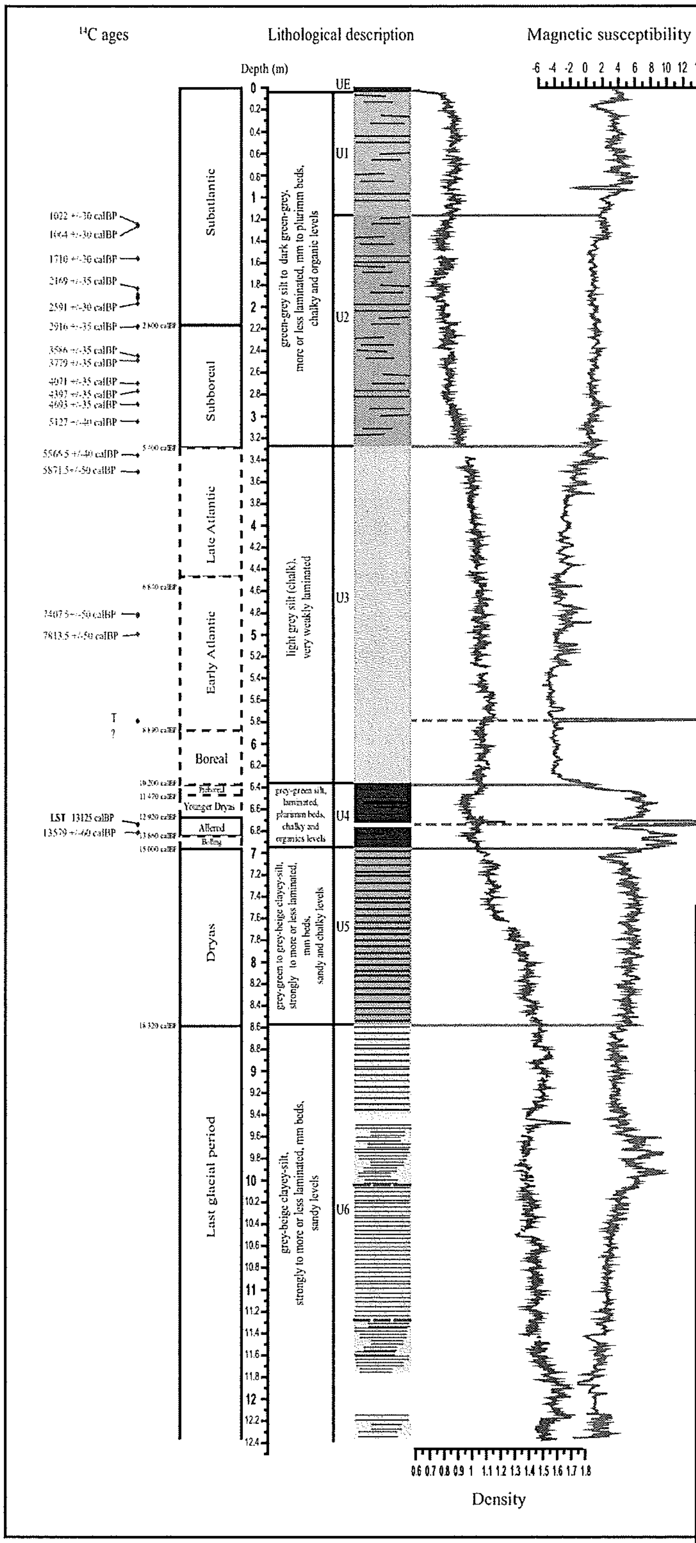

Figure 9: SP05 (lower basin) lithological description compared to physical parameters logging by Geotek. The density and the magnetic susceptibility were measured in continue.

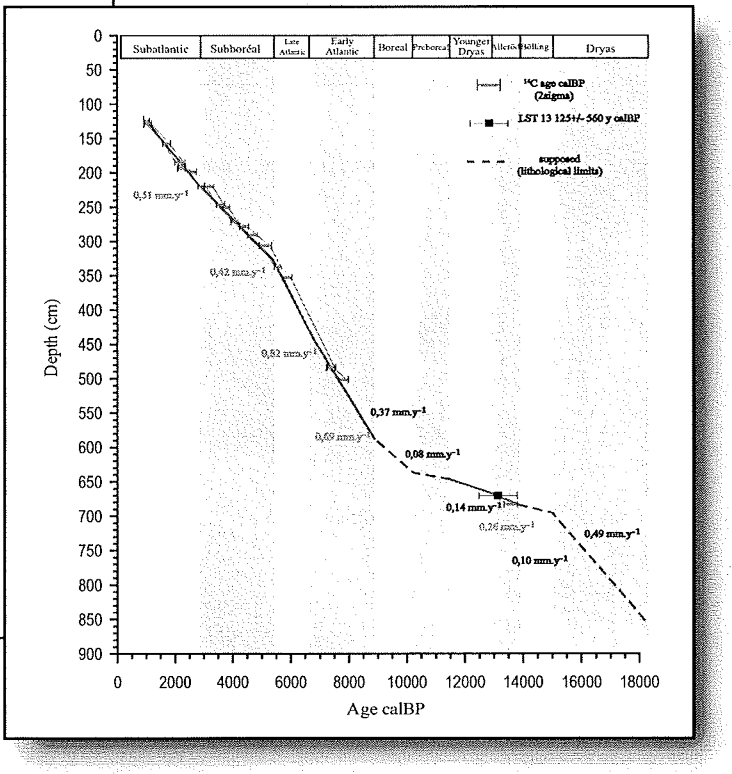

Figure 10: age-depth model established by 23 ^{14}C datations on leaves and the identification of Laacher See tephra (LST).

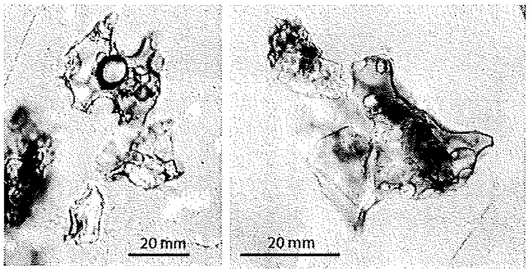

Figure 11: Volcanic shards from Laacher See tephra

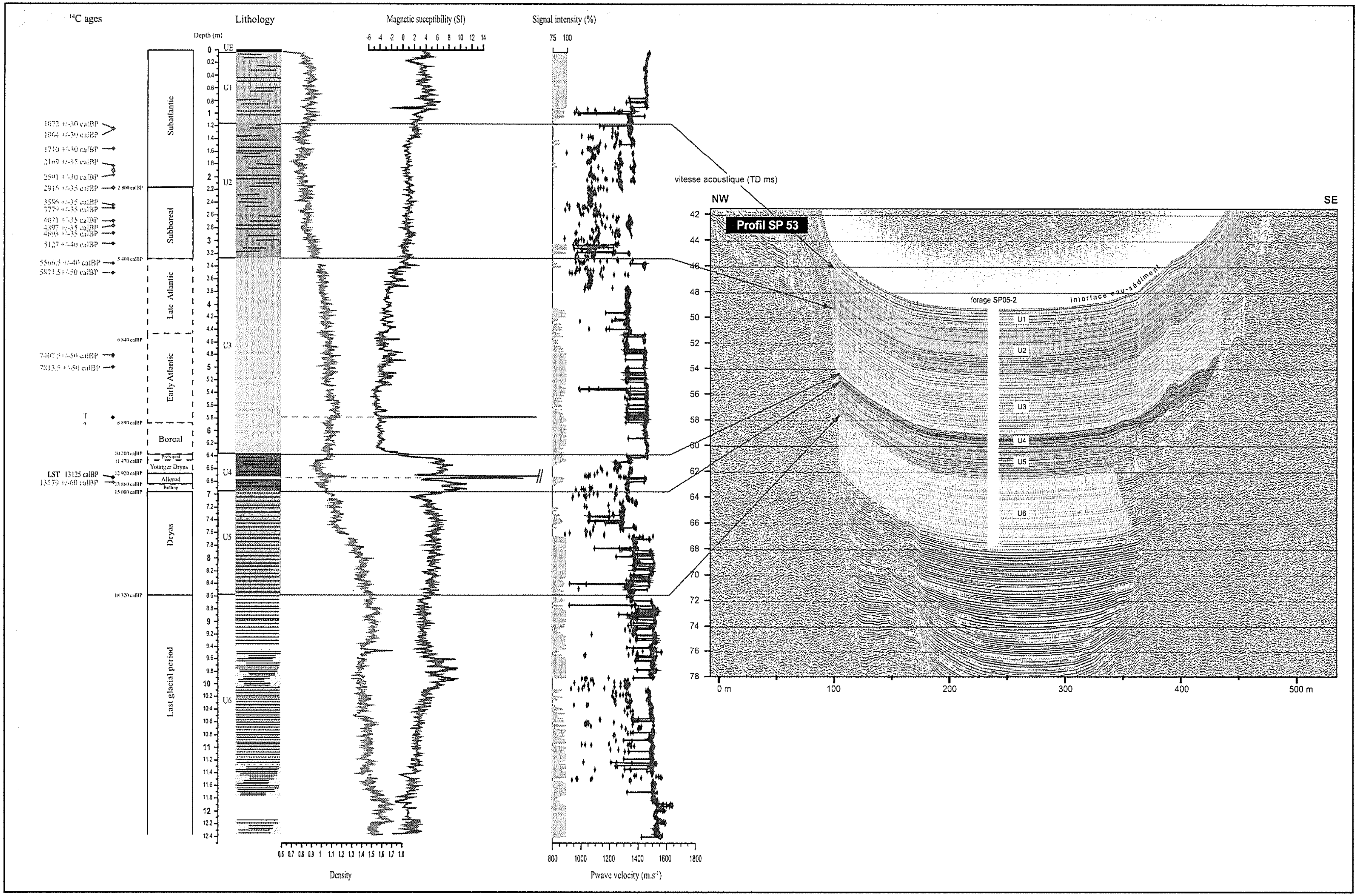

Figure 11: SP05 physical paramaters measured by Geotek and location of the sedimentological units on sismic profile by Pwave speed interpretation.

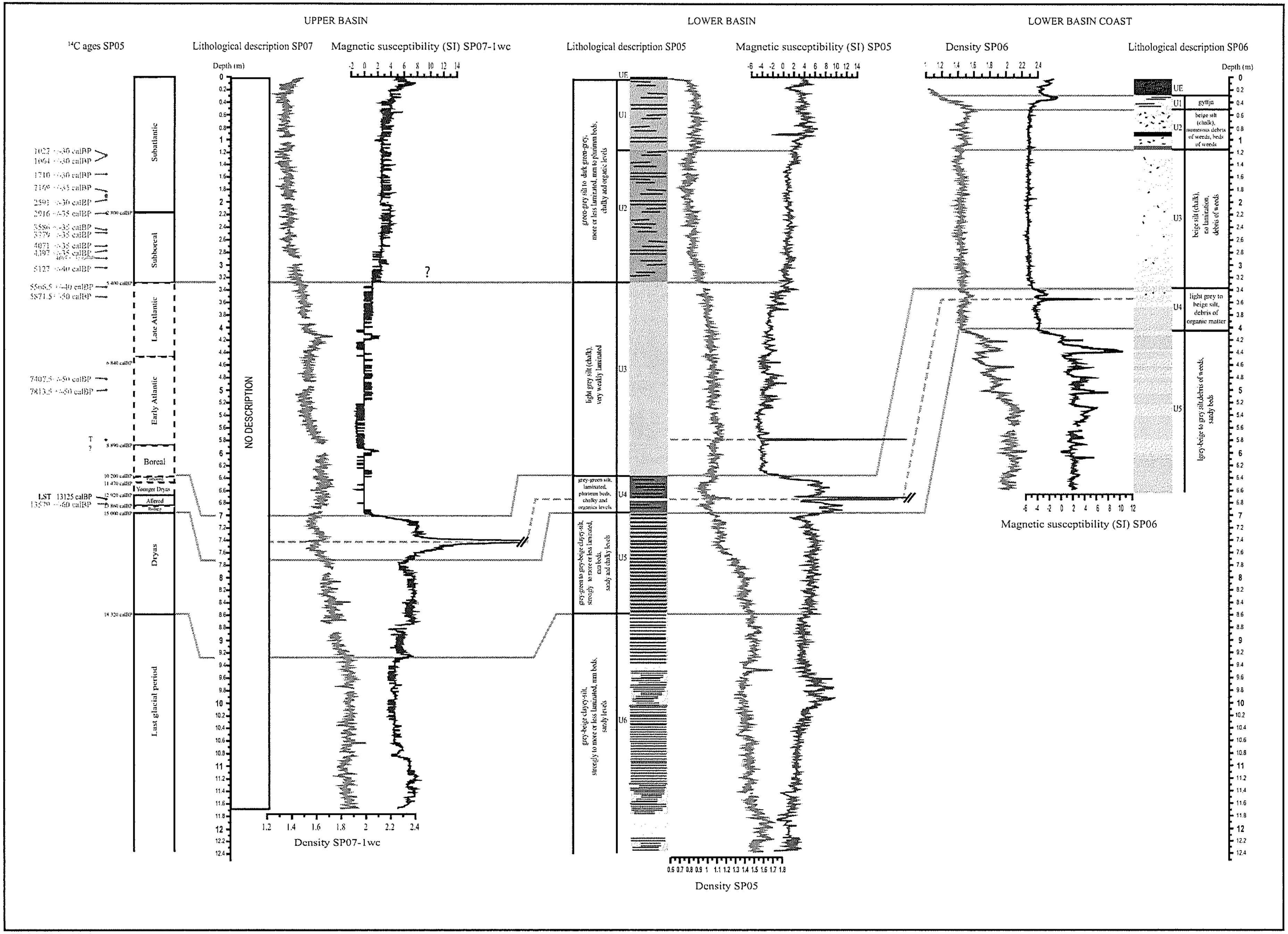

Figure 12: Correlation between SP05, SP06 and SP07 sequences based on a comparison of density and magnetic susceptibility records .

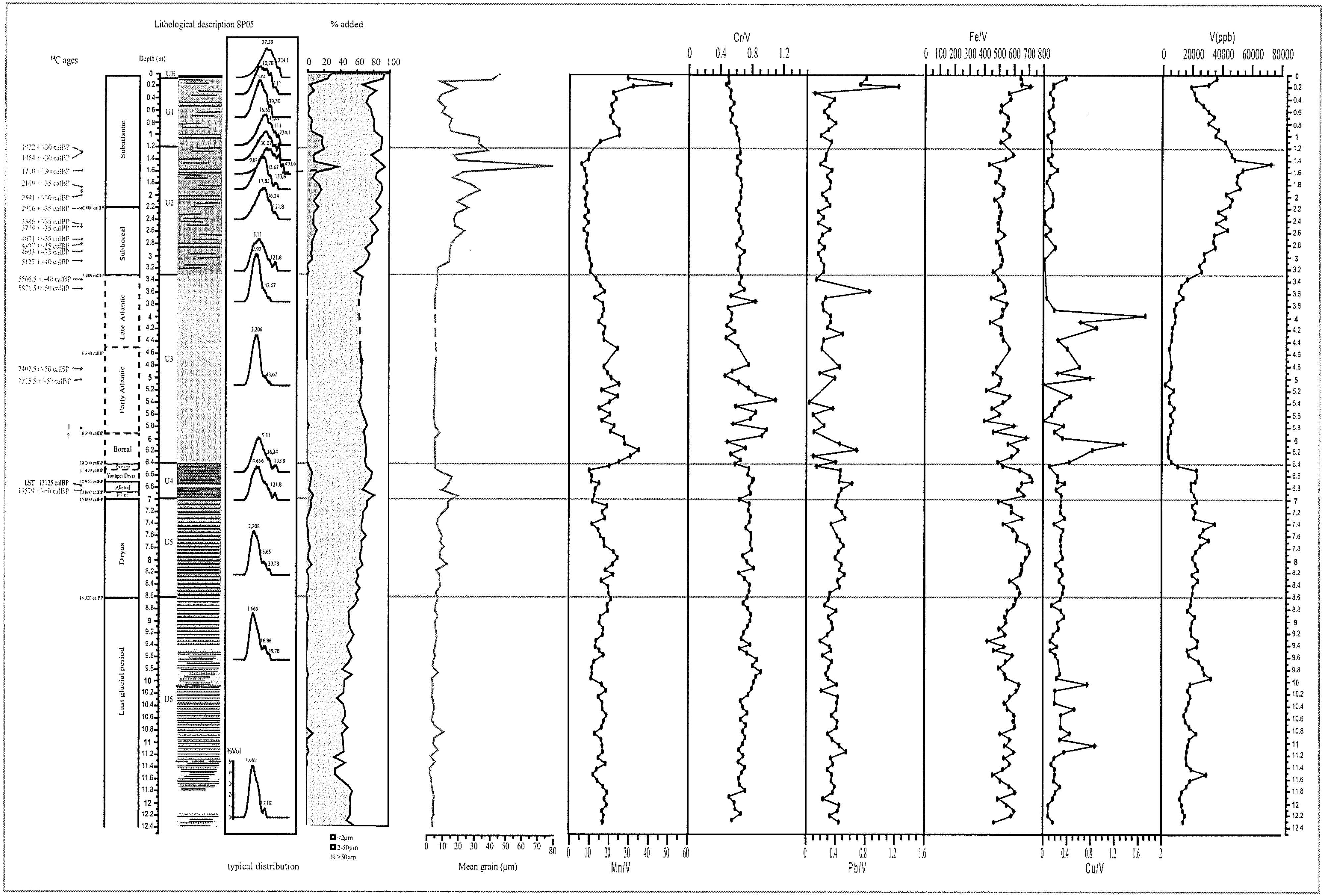

Figure 13: SP05 granulometry (total fraction) and traces elements concentration results. The core was sampled every 10cm.

Wednesday 19 september

Lake Lautrey

ELSEVIER

Quaternary Science Reviews ∎ (∎∎∎∎) ∎∎∎–∎∎∎

QSR

Environmental and climatic changes in the Jura mountains (eastern France) during the Lateglacial–Holocene transition: A multi-proxy record from Lake Lautrey

Michel Magny[a,*], Gerard Aalbersberg[b], Carole Bégeot[a], Pascale Benoit-Ruffaldi[a], Gilles Bossuet[a], Jean-Robert Disnar[c], Oliver Heiri[d], Fatima Laggoun-Defarge[c], Florence Mazier[a], Laurent Millet[a], Odile Peyron[a], Boris Vannière[a], Anne-Véronique Walter-Simonnet[a]

[a]*UMR 6565-CNRS, Faculty of Sciences, 16 route de Gray, 25 030 Besançon, France*
[b]*Faculty of Earth and Life Sciences, Vrije Universiteit Amsterdam, De Boelelaan 1085, 1081 HV Amsterdam, The Netherlands*
[c]*ISTO UMR 6113-CNRS, University of Orleans, Bâtiment Geosciences, BP 6759, Rue de St Amand, 45067 ORLEANS Cedex 2, France*
[d]*Utrecht University, Palaeoecology, Laboratory of Palaeobotany and Palynology, Budapestlaan 4, 3584 CD Utrecht, The Netherlands*

Received 13 July 2004; accepted 17 February 2005

Abstract

This paper presents a multi-proxy reconstruction of the climatic and environmental changes during the Last Glacial–Interglacial transition as recorded by a sediment sequence from Lake Lautrey (Jura, eastern France). This reconstruction is based on analysis of pollen, chironomid, organic matter, oxygen-isotope, mineralogical, magnetic susceptibility and inferred lake-level data at a high temporal resolution. The chronology is derived using AMS radiocarbon dates, the position of the Laacher See Tephra (LST), and of correlation between the Lautrey and GRIP oxygen-isotope records. This data set reveals a detailed sequence of environmental changes in the Jura mountains from Greenland Stadial 2a to the early Holocene. Biotic and abiotic indicators allow the recognition of major abrupt changes associated with the GS-2a/GI-1e, GI-1a/GS-1 and GS-1/Preboreal transitions, and other minor fluctuations related to the cold events GI-1d, GI-1b and the Preboreal oscillation (PBO). They also suggest additional cooling spells at ca 14,550 and 14,350 cal yr BP (Intra-Bølling Cold Periods), at ca 13,500 and ca 12,700 cal yr BP just before the GS-1 onset, and at ca 11,350 cal yr BP just before the PBO, as well as an intriguing brief warming episode within GS-1 at ca 12,080 cal yr BP. Summer temperature increased by ca 5 °C at the start of GI-1e, and by 1.5–3 °C at the Holocene onset, while it decreased by ca 3–4 °C at the beginning of GS-1. Major changes in local hydrology and in seasonality appear to be also associated with the GS-2a/GI-1e, GI-1a/GS-1 and GS-1/Preboreal transitions. Pollen and abiotic indicators suggest a greater sensitivity of the vegetation cover to climatic oscillations during the first part of the Lateglacial Interstadial than during the second part (after ca 13,700 cal yr BP), when a closed forest had been restored in this area. By contrast, the restoration of forest cover took less than 300 yr after the end of GS-1. At the beginning of GI-1e and GS-1, no lag occurs (within the sampling resolution of 20–50 yr) in the responses of aquatic (chironomids) and terrestrial (pollen) ecosystems, while, at the onset of the Holocene, the response of the vegetation appears slightly delayed in comparison with that of the chironomid community. Finally, the recognition of two successive tephra layers, which were deposited just before the LST at ca 12,950 cal yr BP and which originated from Le Puy de la Nugère (Massif Central, France), provides an additional tephrochronological tool for correlation between Lateglacial European sequences.

1. Introduction

Since the Last Glacial–Interglacial transition was marked by rapid and pronounced climatic oscillations

---

*Corresponding author. Tel.: 33 (0)3 81 66 62 65;
fax: 33 (0)3 81 66 65 68.
E-mail address: michel.magny@univ-fcomte.fr (M. Magny).

0277-3791/$ - see front matter © 2005 Elsevier Ltd. All rights reserved.
doi:10.1016/j.quascirev.2005.02.005

associated with successive climatic steps during general deglaciation (Lowe, 1994; Björck et al., 1996; Clark et al., 2001), many investigations have focused on this period. Stimulated by the high-resolution records obtained from the Greenland ice-cores (Johnsen et al., 1992), increasing efforts are now being undertaken to quantify Lateglacial climatic changes and to improve the temporal resolution and chronology of multi-proxy continental records. In particular, it is crucial to obtain better correlations between terrestrial, marine and ice-sheet records and to improve our understanding of the responses of terrestrial environments to rapid climatic changes (Björck et al., 1998; Brauer et al., 1999; Ammann et al., 2000; Birks and Wright, 2000; Walker et al., 2003).

As a contribution to such efforts, this paper presents the results of a multidisciplinary study undertaken at Lake Lautrey in the Jura mountains. The investigation is part of a project funded by the program ECLIPSE (Past Environments and Climates) of the French CNRS to establish and compare high-resolution records between west-central Europe and the north-western Mediterranean region. Using an integrated approach, based on a range of biotic and abiotic indicators (pollen, chironomids, organic matter (OM), oxygen-isotopes, mineralogy, magnetic susceptibility (MS), lake-level fluctuations), the aim is to establish a multi-proxy record of environmental and climatic changes from GS-2a to the early Holocene. Major climatic changes during this period have been quantified using chironomid, pollen and lake-level data.

2. The site

2.1. Location

Lake Lautrey (46°35′14″N; 5°51′50″E) is located at 788 m above sea level (a.s.l.) in the Jura mountains (eastern France) (Fig. 1). It is a small residual lake ($75 \times 40\,m^2$, $1900\,m^2$) surrounded by mires as a result of overgrowing processes. Its catchment area covers ca $2\,km^2$, and is underlain by Jurassic and Cretaceous limestones with outcrops of dolomite. It is characterised by hills culminating at ca 830 m covered by *Abies* and *Fagus* forest. The mean temperature is −1 °C in the coldest month and 16 °C in the warmest month, with annual precipitation reaching ca 1500 mm. The lake is fed by small streams and runoff from the catchment area. After a short surface course, its outlet descends into a karstic cavity to flow underground.

Systematic lithostratigraphic investigations based on a grid of 37 cores with sampling points every 50 m (Fig. 2) have shown that, during the Lateglacial period, the lake size was ca $500 \times 200\,m^2$ with a maximum water depth of 12 m (Bossuet et al., 1997, 2000). This first

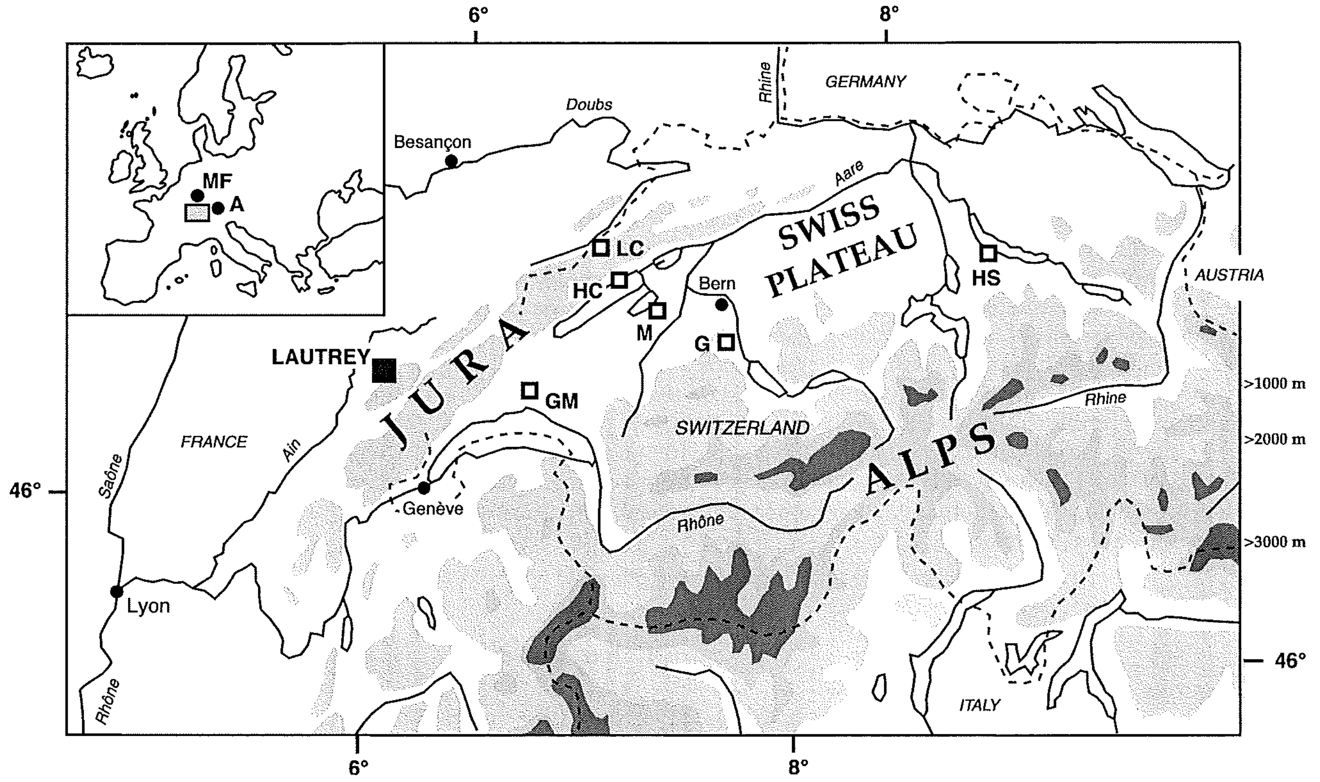

Fig. 1. Location of Lake Lautrey in west-central Europe. G, Gerzensee; GM, Grand-Marais; HC, Hauterive-Champréveyres (Lake Neuchâtel); HS, Horgen-Scheller (Zürichsee); LC, Lake Le Locle; M, Montilier (Lake Morat). Insert: A, Ammersee; MF, Merfelder Maar.

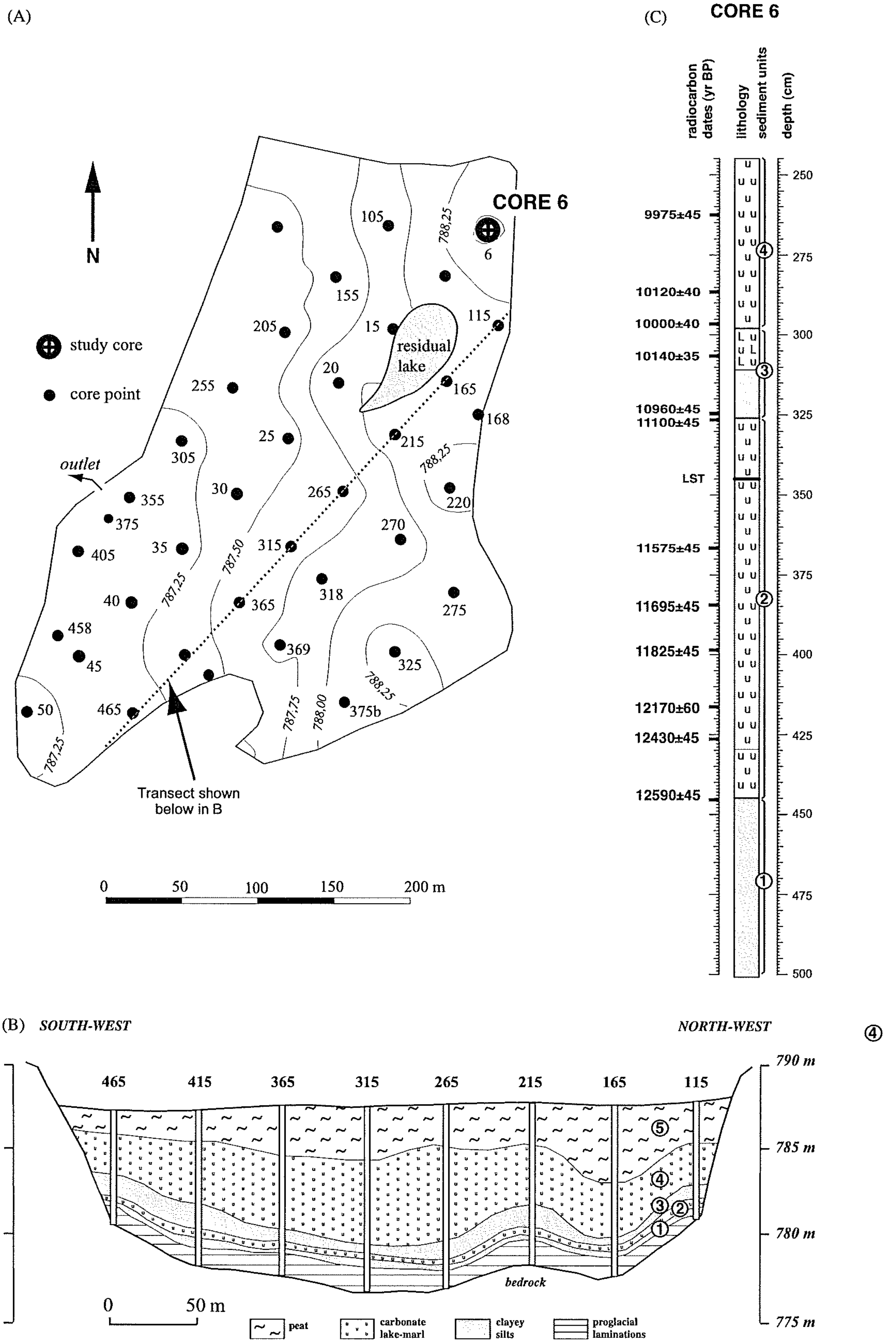

Fig. 2. (A) Map of the Lautrey mire showing the surface altimetry (m a.s.l.) and the location of the coring points for the site exploration. (B) Axial cross section from point 115 to point 465, i.e. through the deepest parts of the lacustrine basin (Bossuet et al., 2000). (C) Sediment profile of Lautrey core 6 used for this study, with an indication of the position of LST and samples for radiocarbon dating.

exploration coupled with pollen stratigraphy has also revealed an infilling sediment sequence (Fig. 2) which is typical for this region, with (1) late Pleniglacial clayey silts at the base, (2) biogenic carbonate lake-marl in the middle sector (Lateglacial Interstadial and Holocene), the deposition of which was interrupted by the accumulation of clayey silts during the Younger Dryas event (GS-1), and (3) organic sediments (gyttja and peat) at the top (final overgrowing step). Furthermore, the Laacher See Tephra (LST) was observed in the upper part of the Lateglacial Interstadial (GI-1) deposits (Bossuet et al., 1997; Vanniere et al., 2004).

2.2. *Stratigraphy*

Point 6 in the north-eastern part of the lacustrine basin (Fig. 2) was chosen for the multidisciplinary study presented here, as a best compromise meeting the various requirements of the different proxy investigations involved in the project. Two overlapping twin cores were taken with a Russian peat corer of 10 cm diameter and 100 cm length. The stratigraphy was as follows (Fig. 2):

- *Sediment unit 1 (500–445 cm)*: Clayey silts, dark-grey in colour.
- *Sediment unit 2 (445–326 cm)*: Clayey biogenic carbonate lake-marl, yellow-green in colour from 445 to 430 cm, and silty biogenic carbonate lake-marl, yellow-beige in colour from 430 to 326 cm with the LST at 345 cm.
- *Sediment unit 3 (326–298 cm)*: Clayey silts grey in colour from 325 to 311 cm, and alternating layers of grey clayey silts and yellow-beige biogenic lake-marl from 311 to 298 cm.
- *Sediment unit 4 (298–229 cm)*: Yellow-beige authigenic lake marl.
- *Sediment unit 5 (229–0 cm)*: Gyttja and peat.

Lithostratigraphic correlations, previous pollen studies and the position of the LST (Bossuet et al., 1997) indicate that sediments units 1, 2, 3 and 4 correspond to the Oldest Dryas, Bølling–Allerød, Younger Dryas and Preboreal biozones (Ammann and Lotter, 1989), respectively.

2.3. *Sampling and analytical strategy*

After measurement of the volume MS at 0.5 cm intervals, contiguous samples were taken at 1 cm intervals in the Oldest Dryas, Bølling–Allerød and Preboreal sections. Samples were removed at 0.5 cm intervals from the Younger Dryas section due to a generally weaker sedimentation rate during the Younger Dryas event as observed in previous regional studies (Bégeot, 2000). To allow an integrated approach, every sample was cut into seven portions for pollen, chironomid, lake-level, mineralogy, grain-size, isotope and OM analyses.

3. Chronology

The chronology of the Lautrey core 6 sediment sequence is based on the following evidence:

- Twelve AMS radiocarbon dates from terrestrial plant macrofossils (Table 1 and Fig. 2C). The ^{14}C ages have been calibrated using IntCal 4.3 (Stuiver et al., 1998). The radiocarbon ages obtained appear consistent with the regional Lateglacial pollen zones defined by de Beaulieu et al. (1994) and Bégeot (2000) for the Jura mountains.
- The 1 mm thick ash layer of LST was identified at 345 cm depth in core 6. On the basis of petrographic and SEM observations, the mineral composition of this tephra layer has been extensively published elsewhere (Bossuet et al., 1997; Vanniere et al., 2004).

Table 1
AMS radiocarbon dates obtained from core 6 of Lake Lautrey

Depth (cm)	Radiocarbon age (yr BP)	Calibrated age (2σ) (cal yr BP)	Laboratory number (Vienne)	Material
262	9975±45	11,904–11,130	VERA-1717	Wood fragments
286	10,120±40	12,269–11,358	VERA-1722	Wood fragments
296	10,000±40	11,918–11,257	VERA-1716	Wood fragments
305	10,140±35	12,282–11,442	VERA-1715	Wood fragments
324	10,960±45	13,154–12,657	VERA-1724	Wood fragments
326	11,100±45	14,191–12,683	VERA-1725	Wood fragments
366	11,575±45	13,836–13,317	VERA-1726	Wood fragments
384	11,695±45	15,092–13,442	VERA-1727	Wood fragments
398	11,825±45	15,205–13,587	VERA-1728	Wood fragments
416	12,170±60	15,400–13,836	POZ-4496	Wood fragments
426	12,430±45	15,517–14,139	VERA-1729	Wood fragments
445	12,590±45	15,592–14,223	VERA-1730	Wood fragments

It has been radiocarbon dated to 11,063±12 ^{14}C yr BP (Friedrich et al., 1999). Ammann et al. (2000) suggested an age of 12,836 cal yr BP based on correlation between the Gerzensee and GRIP oxygen-isotope records, and Brauer et al. (1999) estimated an age of 12,880 cal yr BP from varve counts in the Meerfelder Maar (Germany).

4. Pollen analysis

4.1. Laboratory methods

Samples were analysed at 1 or 2 cm intervals and treated by standard methods, including HCl, HF, NaOH and acetolysis. The pollen preservation was good and concentrations (calculated using a volumetric method; Cour, 1974) were always sufficient to count over 500 pollen grains per slide. Pollen percentages are based on the pollen sum of arboreal (AP) and non-arboreal (NAP) pollen grains, excluding spores.

4.2. The pollen record

Figs. 3 and 4 show percentage and concentration data for selected principal taxa. The major changes in these diagrams led to the definition of six local pollen assemblage zones (LPAZ) as follows.

Taken as a whole, LPAZ-1 (500–445 cm) is dominated by high percentages of herbaceous taxa, mainly *Artemisia*, Poaceae and other heliophilous taxa, such as Chenopodiaceae and *Helianthemum* as well as Cyperaceae. Generally speaking, pollen concentrations remain low. The relatively high percentages of *Pinus* (ca 25%) are interpreted as due to long-distance transport. These data indicate an open herbaceous landscape and can be correlated with the Oldest Dryas pollen zone (de Beaulieu et al., 1994).

Within LAPZ-1, subzone LPAZ-1b (480–454.5 cm) can be distinguished from LPAZ-1a (500–480 cm) on the basis of an increase in the percentage values of *Helianthemum* and in concentrations of herbaceous taxa. *Pinus* also shows a slight increase in the percentages but its concentrations values remain low. This general picture suggests a possible local expansion of the grassland vegetation, particularly at the upper part of subzone LPAZ-1b where the concentration values of herb taxa rapidly increase. These features are reinforced in subzone LPAZ-1c (450–445 cm) with *Helianthemum* values peaking at 12%.

LPAZ-2a (*Betula–Juniperus* zone, 444.5–436.5 cm) is marked at its beginning by a strong increase in percentages and concentrations of juniper typical of the onset of the Bølling pollen zone (de Beaulieu et al., 1994). The development of a shrub vegetation is also indicated by the presence of *Salix* and *Hippophaë* which reach maxima. Just after the first rapid expansion of *Juniperus*, *Betula* shows a conspicuous short maximum in percentage and concentration data before decreasing abruptly.

LPAZ-2b (*Betula* zone, 436.5–420.5 cm) is characterised by the establishment of a birch woodland as indicated by high percentages and concentrations of *Betula*, while *Juniperus* retreats (second part of the Bølling pollen zone). The diagrams also show a moderate fall in percentages of *Betula* (at around level 428 cm) concomitant with higher values of *Artemisia* and herbs. This may reflect a short regressive phase in vegetation development during this period, which previously has been recognised in most of pollen diagrams obtained from sites in the Jura mountains (Bégeot, 2000). During LPAZ-2c (420.5–406.5 cm), a marked regressive phase is registered by two successive decreases in *Betula* percentages and concentrations. The first was associated with an increase in grasses at the beginning of the subzone and a re-expansion of juniper, and the second with a decrease in AP concentrations. The relative decline of birch woodland appears to have favoured a simultaneous development of *Pinus*. This regressive phase at the transition between the Bølling and Allerød pollen zones is assigned to the Older Dryas pollen zone (Lotter et al., 1992; de Beaulieu et al., 1994).

LPAZ-3 (420.5–245 cm) is identified by the dominance of *Pinus*. It is correlated with the Allerød, Younger Dryas and Preboreal pollen zones and is divided into seven subzones. LPAZ-3a shows a rapid rise and domination of *Pinus* percentages indicating the regional extension of pine forests. LPAZ-3b marks two successive interruptions of this expansion with declines of *Pinus* percentages and concentrations concomitant with a 5% increase in *Artemisia* percentages while juniper reaches 3% (regressive phases). LPAZ-3c displays a considerable dominance of *Pinus* in the percentage diagram. After a continuing expansion of the pine forests until 356.5 cm depth, a strong reduction in pollen concentrations can be observed, in particular at levels 354.5 and 346.5–342.5 cm. During LPAZ-3d, the *Pinus* dominance is affected by a regression well marked in sample 328.5 cm by a strong reduction of *Pinus* percentages and concentrations, while *Betula* and *Artemisia* percentages increase.

After a partial recovery in terms of percentages and concentrations, all the evidence points to a marked long-lasting regression of the vegetation during LPAZ-3e (325.75–296.5 cm). A rise in NAP percentages, mainly *Artemisia*, Chenopodiaceae, *Helianthemum*, Poaceae and Cyperaceae, associated with a strong decrease in AP concentrations, indicates a reduction of the pine-birch forests and an expansion of open habitats and can be correlated with the Younger Dryas pollen zone (de Beaulieu et al., 1994). Before the abrupt decrease in

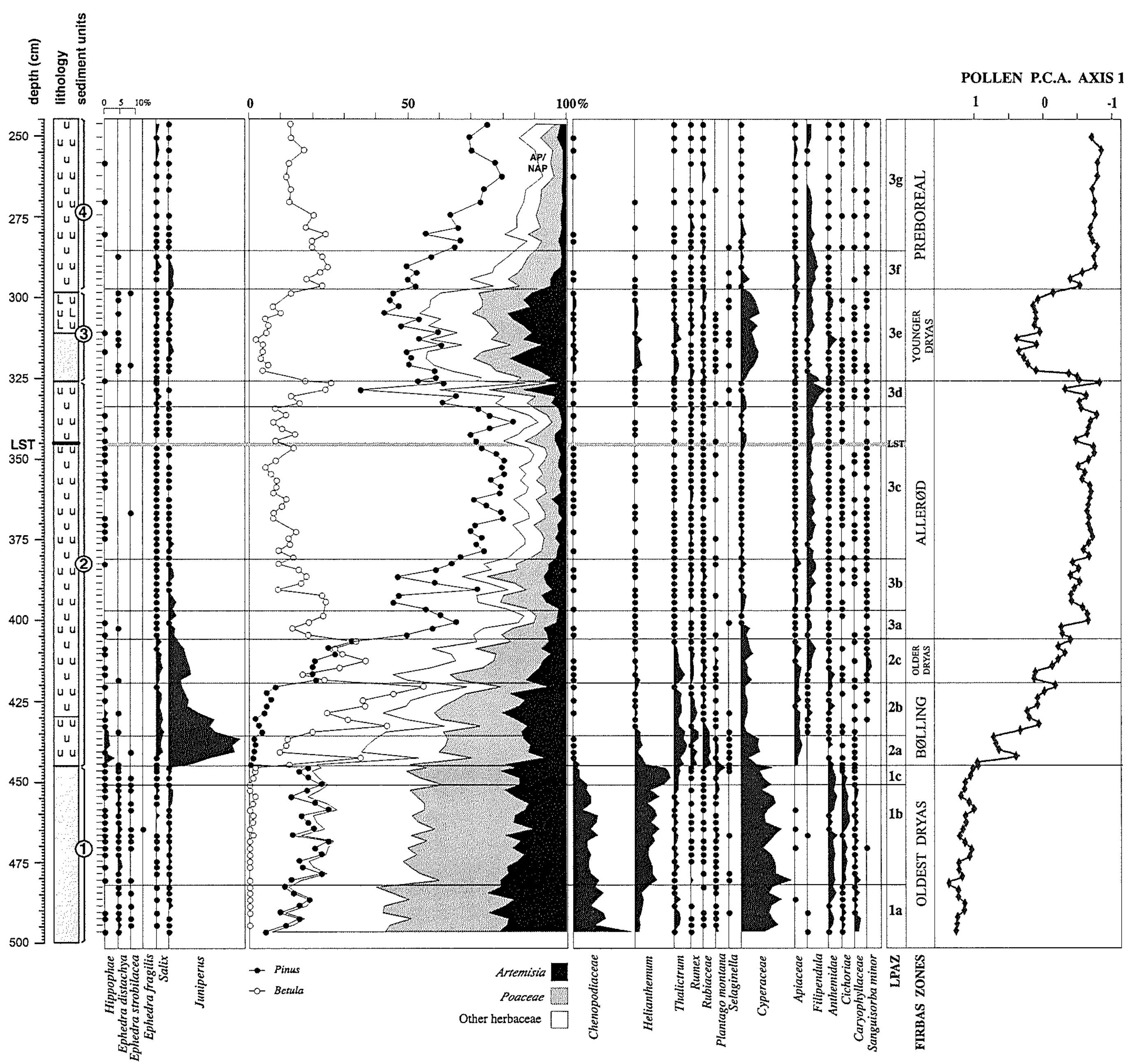

Fig. 3. Percentage pollen diagram from Lautrey core 6 (main taxa only shown). Analysis: P. Ruffaldi. Pollen PCA axis 1: see explanations in Section 12.2.

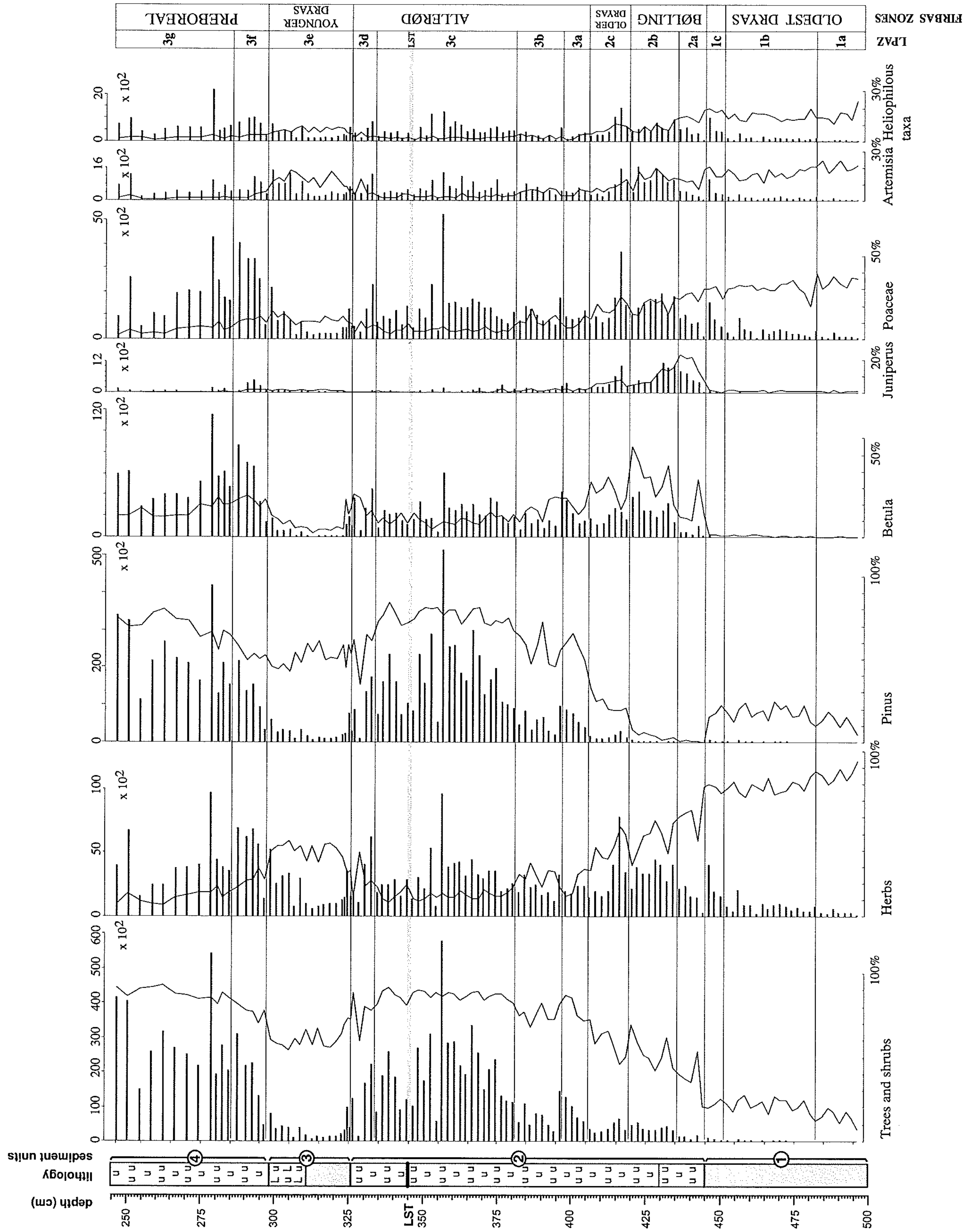

Fig. 4. Concentration pollen diagram from Lautrey core 6 (histograms). The curves present the percentage values from Fig. 3. Analysis: P. Ruffaldi.

NAP percentages at the end of LPAZ-3e, the AP and NAP pollen concentrations show a progressive increase during the upper part of this biozone.

LPAZ-3f (296.5–250 cm) is marked by a rapid re-expansion of the pine-birch woodland at the Younger Dryas/Preboreal transition. The percentage diagram indicates an increase in *Betula*, *Pinus*, *Juniperus* and *Salix* while Poaceae, *Artemisia*, Cyperaceae and most other heliophilous taxa decrease. The AP (and to a lesser extent, NAP) concentrations increase rapidly. During LPAZ-3g, the pine forests became more dense whereas *Betula*, *Juniperus* and *Salix* as well as NAP concentrations decline.

5. Chironomid analysis

The chironomid stratigraphy established from Lautrey core 6 for the Last Glacial–Interglacial transition has already been presented and discussed in previous papers (Millet et al., 2003; Heiri and Millet, 2005). For this study, the original chironomid record has been extended by 13 additional samples to extend the record for the Preboreal (Fig. 5).

5.1. *Laboratory methods*

Samples for chironomid analysis were taken at 0.5 cm interval within the Younger Dryas pollen zone, while the sampling interval was increased to 2 cm for the rest of the sediment core. Chironomid head capsules were extracted from the sediment following the procedure described by Hofmann (1986). The amount of treated sediment per sample was adjusted to obtain about 100 head capsules as recommended by Heiri and Lotter (2001) and Larocque (2001). Identification of chironomid head capsules according to Hofmann (1971) and Wiederholm (1983) was performed, in most cases, at genus or species group level. The relative abundances of taxa were calculated for each sample from a sum of total chironomids to construct a percentage diagram.

5.2. *The chironomid record*

Seven chironomid assemblage zones (CAZs) have been distinguished. Palaeoecological interpretations were inferred from modern environmental preferences of taxa characterising the biozones.

In CAZ-1, the low taxa richness indicates strongly constraining environmental conditions. The zone is dominated by *Stictochironomus* associated with *Abiskomyia*, *Parakiefferiella triquetra*, *Heterotrissocladius*, *Paracladius*, *Monodiamesa* and *Protanypus*. These taxa are characteristic of oligo- to mesotrophic lakes in Saether's typology (1979) and are often found in well-oxygenated water (Quinlan and Smol, 2001).

The definition of zone CAZ-2 was mainly based on the dominance of *Corynocera ambigua*. The modern distribution and ecology of *C. ambigua* indicates that the species prefers water with large hydrophyte beds and high production of benthic diatoms (Brodersen and Lindegaard, 1999). The appearance of *Chironomus* and the higher relative abundance of *Procladius* suggest a slightly higher organic accumulation in the sediment probably associated with a decrease of oxygen concentrations.

During CAZ-3, *C. ambigua* declines, whereas the relative abundance of *Chironomus* and taxa richness sharply increase. CAZ-3 is only composed of two samples and must be considered a transitional zone between CAZ-2 and CAZ-4.

The onset of CAZ-4 corresponds to a strong change in the chironomid community. *C. ambigua* and all oxyphilous taxa characteristic for CAZ-1 and CAZ-2 disappear from the assemblages. The general characteristics of the zone are its high taxa richness and the high relative abundance of taxa, such as *Chironomus*, *Dicrotendipes*, *Polypedilum* and *Cladopelma*, often found in anoxic lakes. The higher taxonomic richness suggests a general improvement of environmental conditions allowing the development of a more diversified aquatic biota.

During CAZ-5, *C. ambigua*, one of the most characteristic taxa of the next zone CAZ-6, appears in the assemblages. *Tribelos* shows a sharp peak, but the ecology of this taxon is still poorly known. Hence, it is difficult to interpret this zone in terms of environmental conditions. Like CAZ-3, this very short-lived zone is considered a transitional phase.

Zone CAZ-6 displays an important change in the chironomid community. In general, there is a large re-expansion of *C. ambigua* (which had been absent since the end of zone CAZ-2), an increase in the relative abundance of *Microtendipes*, *Paratanytarsus* and *Tanytarsus lugens*, and the re-appearance of *Stictochironomus* and *Micropsectra*. The presence of *Microspectra*, *Stictochironomus* and *T. lugens* suggests an improvement of oxygen conditions, while the decrease in percentage of *Chironomus* and *Polypedilum* marks a reduction in organic accumulation. The relative abundance of *C. ambigua*, *Microtendipes* and *T. lugens* shows a downward trend in contrast with that of *Parakiefferiella bathophila*-type, *Ablabesmyia*, *Tribelos* and *Corynoneura*. This may indicate a progressive increase in pelagic production during the zone.

In zone CAZ-7, the assemblages are dominated by taxa living in muddy sediment (e.g. *Chironomus*) and able to survive long periods of anoxic conditions. The high relative abundance of *Glyptotendipes* suggests an expansion of aquatic vegetation.

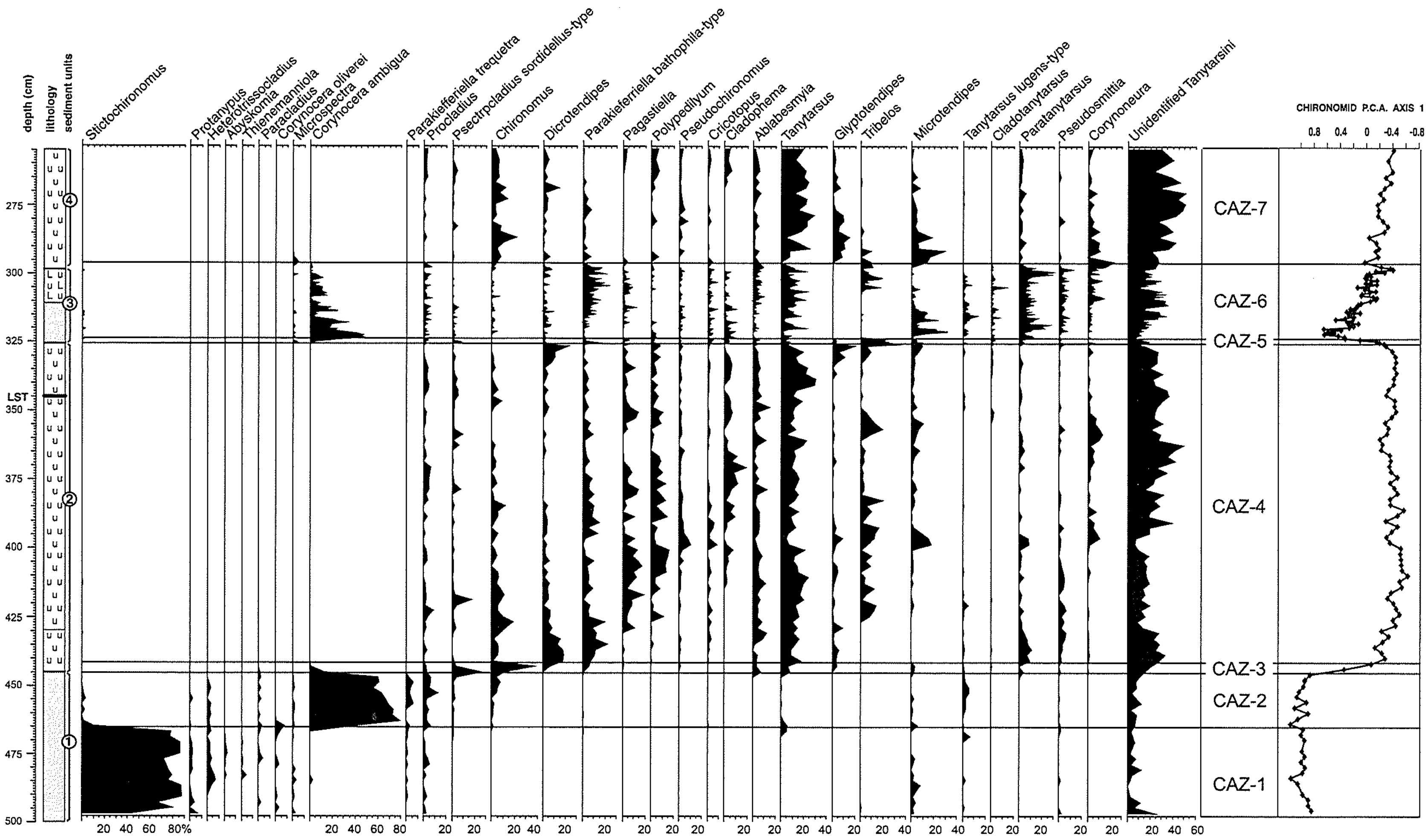

Fig. 5. Chironomid diagram from Lautrey core 6 (analysis: L. Millet). Chironomid PCA axis 1: see explanations in Section 12.2.

6. Organic matter analysis

Several studies have demonstrated that OM preserved in lake sediments can provide information on regional environmental changes (Bertrand et al., 1992; Meyers and Lallier-Vergès, 1999; Bourdon et al., 2000). In a lake sediment sequence, OM originates from three major sources: (1) planktonic and benthic algae which may represent an important fraction of the total organic content in eutrophic waters, (2) submerged or emergent vascular plants which colonise the lake margins or the whole water-body during lowstands, and (3) terrestrial plant remains and soil OM removed by weathering from the catchment area.

6.1. Methods

Seventy-eight samples were taken from the core 6 for OM analysis with a focus on the phases of major climatic and environmental changes. Total organic carbon (TOC) content (wt% of dry sediment) was determined by Rock-Eval® pyrolysis with a model 6 device (Vinci Technologies; Espitalié et al., 1985). The analyses were carried out on 100 mg of crushed samples under standard conditions. Total N and C contents (wt%) were obtained with a LECO CNS 2000 Analyser. The C/N ratio is related to both the origin and the degree of degradation of total OM (Disnar et al., 2003).

The petrographic study (palynofacies) involves a microscopic examination of total OM, in transmitted and reflected light, after acid hydrolysis of carbonates and silicates. Taking into account the chromatic and textural aspects of particles (Sifeddine et al., 1998), the analysis aims at identifying and quantifying the organic compounds (relative percentages of surface particle area), and at establishing the ratio between allochthonous and autochthonous components. Terrestrial OM (TOM) includes particles weathered from the catchment and/or windblown grains, while lacustrine OM (LOM) consists of particles derived from aquatic plants and phytoplankton.

6.2. The organic matter record

TOC values fluctuate between 0.6% and 6.5% throughout the studied sequence (but which are mostly between 1.5% and 3%) and permit the distinction of four zones (Fig. 6). Increasing TOC values may reflect (1) an increase in the algal production, (2) a lake-level lowering and a correlative reinforcement of OM (derived) from marsh plants, and/or (3) larger inputs from the catchment (soils and plants). In all cases, the increase in OM sedimentation is expected to induce a decrease in dissolved oxygen and hence a better OM preservation. Thus, the C/N ratio (i.e. TOC/total N) which varies from 2.3 to 34.7 suggests important changes in the OM origin as well as in sedimentary conditions. Accordingly, high TOC and C/N ratio values like those recorded in OMZ 2c and 2e (Fig. 6) document increased inputs from rather well preserved vascular plant debris. In contrast, rather low C/N ratio values (usually between 4 and 10) such as those found in OMZ-3 can be taken as indicative of relatively higher importance of algal-derived OM. For the rest, most of the C/N values ranging between 10 and 15 suggest a mixed contribution from algae and vascular plants.

These general trends are supported by an estimate of the relative proportions of the TOC due to LOM and TOM (respectively; Fig. 6) based on TOC values and the relative proportions of organic debris from the lacustrine and terrestrial sources determined in the palynofacies assemblages. TOM mostly follows TOC; this suggests a dominant terrestrial origin of the OM inputs all along the sedimentary record, except for OMZ-1 (Oldest Dryas pollen zone) and OMZ-3 (Younger Dryas pollen zone) where lacustrine inputs might have been predominant. The predominance of TOM in the studied section indicates that the OM sedimentation principally reflects the development of soils and vegetation on the paludal belt and in the catchment area.

7. Mineralogy and grain-size analysis

7.1. Methods

Samples for mineralogy and grain-size analysis were taken at 2 cm intervals from 250 to 497 cm depth. The grain size was measured by sieving. The bulk mineral composition was determined by X-ray diffraction, using an X'Pert Philips diffractometer with a cobalt anticathode. The diffractometer settings were 5 s per step from 3° to 72° 2θ for a bulk characterisation of non-oriented powdered samples (Holtzappfel, 1985). Given that samples reflect variable degrees of mineral mixing, the area of the major peak of each mineral was measured on the diffractograms. The semi-quantitative mineral composition was expressed as a percentage (Moore and Reynolds, 1997; Amorosi et al., 2002). The Rcm ratio indicates the variations in the occurrence of clay minerals in the sediment (Rcm = [(sum of peak areas of the clay minerals) × 100]/[sum of the peak areas of all minerals]). The relative occurrence of illite, kaolinite and chlorite was estimated by comparing with the principal peak of the dominant mineral (quartz or calcite) on the diffractograms.

In addition, further mineralogical observations were carried out on samples characterised by MS peaks (see Section 8) at levels 345, 348.5 and 352.5 cm, which were assumed to contain ash layers. These samples were

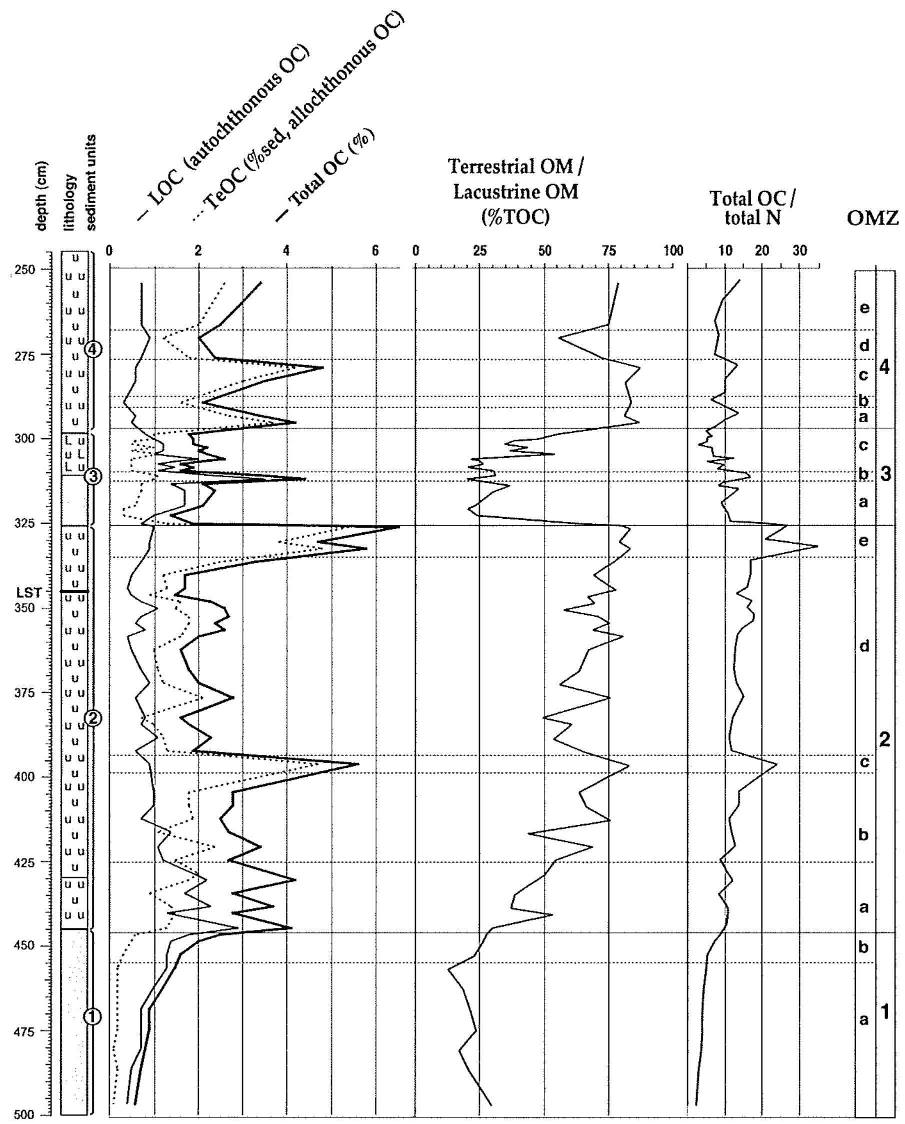

Fig. 6. Organic matter record from Lautrey core 6. TOM, terrestrial organic matter; TOC, total organic carbon; LOM, organic matter of lacustrine-autochthonous origin (in percentage of organic particle surface area in the palynofacies); LOC, organic carbon of autochthonous origin (in percentage of TOC following the equation: LOC = [TOC/100] × LOM); TeOC, organic carbon of allochthonous origin; OMZ, organic matter zones (analysis: B. Vannière).

divided into three subsamples and etched by HCl 0.5 N for carbonate dissolution and filtered. The insoluble residue was air-dried. The first and the second subsamples were observed, respectively, under a photonic microscope after setting in epoxy resin and polishing, and under a scanning electron microscope (Jeol 5600 with X-EDS Fondis-99 microanalysis). The third subsample was analysed by X-ray diffraction for the detemination of magmatic and neoformed minerals. These samples were prepared following the procedure of Kubler (1987). Each powdered residue was analysed using a SCINTAG XRD 2000 diffractometer running between 2° and 65° 2θ at 45 kV and 40 mA using Cu Kα radiation and a scan speed of 1°/min.

7.2. The mineralogy and grain-size records

Quartz and calcite are the main minerals with feldspars (mainly plagioclase) and clay minerals (illite, kaolinite, chlorite and rare smectites) as accessory minerals. Dolomite, jadeite (pyroxene) and sanidine (K-feldspar) are observed occasionally. Five zones (MZ) have been distinguished as follows (Fig. 7).

MZ-1 (500–445 cm) is characterised by (1) the predominance of quartz and the presence of feldspars, (2) low values of calcite, and (3) an important amount of clay minerals. Quartz appears as silty grains with wind abrasion marks, which suggest long-distance transport. Given the quasi-absence of biogenic calcite, the MZ-1

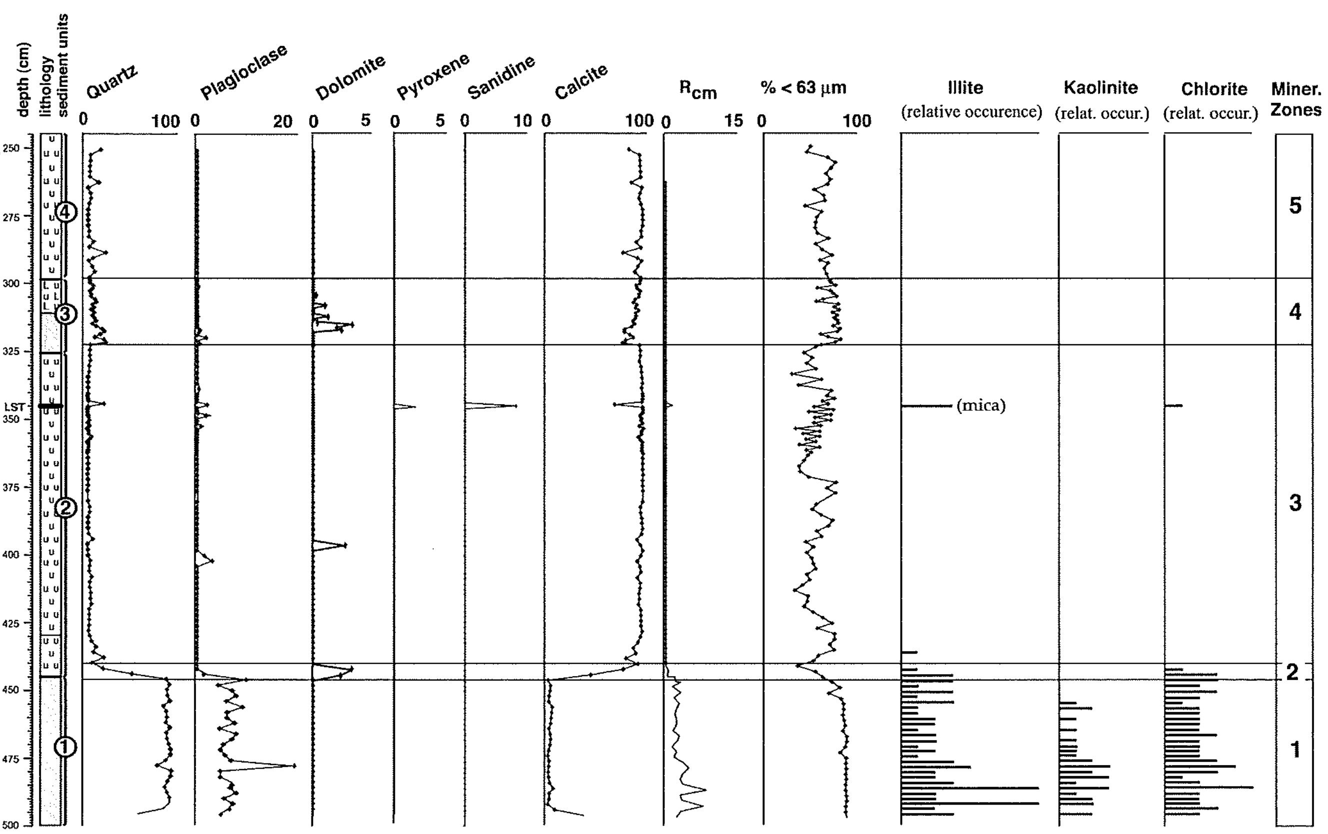

Fig. 7. Grain size (by sieving) and mineralogy record from Lautrey core 6 (analysis: A.V. Walter-Simonnet).

deposits correspond to detrital sedimentation as a result from erosion in the catchment area and long-distance transport. The importance of the wind is also illustrated by the presence of exogenic clay minerals, such as illite and chlorite. Above 475–470 cm depth, the decrease in Rcm as well as the weakening and subsequent disappearance of kaolinite reflect a weakening of mineral sources and/or wind strength.

MZ-2 (445–440 cm) is marked by a rapid decrease in quartz and plagioclase, a correlative increase in calcite, a quasi-disappearance of illite and chlorite, and a narrow peak in dolomite. It reflects warmer climatic conditions with the transition from accumulation of allochthonous detrital input to formation of biogenic carbonate deposits in the lake basin.

MZ-3 (440–322 cm) is characterised by high, relatively constant values of calcite. Regarding the grain size, the <63 µm fraction shows values generally lower and more variable than in MZ-1. Short-lived peaks of plagioclase (at level 402 cm) and dolomite (at level 396.5 cm) may be related to erosion of some specific, limited parts of the catchment area.

Analyses indicate that the three successive peaks in MS at levels 345, 348.5 (Laut 1) and 352.5 cm (Laut 2) correspond to samples containing volcanic glass shards and magmatic minerals as well as calcite, quartz and clay minerals. On the basis of petrographic and SEM observations, the mineral composition of these tephra layers has been extensively described in Vanniere et al. (2004). Sample 345 cm corresponds to the LST as classically observed in other European sites (van der Bogaard and Schmincke, 1985), whereas the mineral composition of the LAUT 1 and LAUT 2 horizons suggests a trachytic volcanism similar to the Chaîne des Puys volcanoes in the Massif Central (France), where two tephras from Le Puy de la Nugère have been dated by Juvigné et al. (1996) and Vernet and Raynal (2000) to 12,010 ± 150 and 11,360 ± 130 ^{14}C yr BP (Vanniere et al., 2004).

The beginning of MZ-4 (325–298 cm) is marked by a minor decrease in calcite and a rapid increase in the <63 µm fraction and in quartz, plagioclase and dolomite. This indicates a reactivation of the detrital input inherited from long-distance transport (quartz) and erosion processes in the catchment area (dolomite), as well as a weakening of autochthonous sedimentation of biogenic carbonate. All these point to a cool and windy period. The later part of MZ-4 shows a progressive recovery of the biogenic sedimentation correlative with a reduction of detrital input.

During MZ-5, the calcite quasi-exclusively dominates the sedimentation apart from some minor peaks of quartz.

8. Magnetic susceptibility measurements

MS measurements have proved to be a useful guide for the detection of environmental changes (Thouveny et al., 1994; Stockhausen and Zolitschka, 1999). Erosion, soil processes in the catchment area and lake productivity can result in different assemblages of magnetic minerals in lake sediment sequences. Previous work in carbonate lakes in England and France have shown that MS maxima may reflect intense detrital events in response to (1) climate cooling and changes in vegetation cover during the Lateglacial period (Nolan et al., 1999), or (2) forest clearings and land use history (Higgitt et al., 1991). Volume MS depends mainly on magnetite concentration in sediments. Nevertheless, in the case of low concentration of ferrimagnetic minerals, the MS values can be largely influenced by diamagnetic minerals, such as quartz and carbonate (Thompson and Oldfield, 1986).

8.1. Methods

The volume MS was measured using the MS2E1 surface scanning sensor (Nowaczyk, 2001). This sensor of high sensitivity and small spatial resolution is well suited for measuring MS of split cores at a high resolution. The measurements were systematically carried out at 0.5 cm intervals with a sensitivity of 0.1×10^{-8} SI.

8.2. The MS record

Five MS zones can be distinguished from the MS record of core 6 as follows (Fig. 8).

MSZ-1 corresponds to sediment unit 1 and is characterised by high MS values. Subzone MSZ-1a shows higher values than subzone MSZ-1b. Subzone MSZ-1c is a transitional zone with a rapid fall in the MS values. MSZ-2 displays a general trend towards low values interrupted by minor maximums at levels 440–424, 428–425 and 419–415 cm. In MSZ-3, MS values show a relatively constant and low level except for samples 355–342 cm, where higher values are associated with three tephra layers (see Section 7), and for samples 333–326 cm, where a slight increase is observed. MSZ-4 is marked by a rapid increase in MS values followed by a progressive decline affected by a short-lived minimum at level 310 cm. A rapid fall in MS values occurs between samples 301 and 298 cm. MSZ-5 (Preboreal pollen zone) indicates a recovery of values prevailing during MSZ-3, followed by a general trend towards weakening.

Generally speaking, a correspondence is apparent between higher MS values and sediment units 1 and 3 characterised by a large proportion of allochthonous minerogenic deposits, whereas sediment units 2 and 4 marked by biogenic carbonate formation in the lake coincide with lower MS values. Moreover, it is noteworthy that even during the deposition of minerogenic sediment unit 3, MS values never reach the maximal values characteristic for MSZ-1a and MSZ-1b. In addition to the mineralogy data, this suggests a mixture of allochthonous and autochthonous sediments.

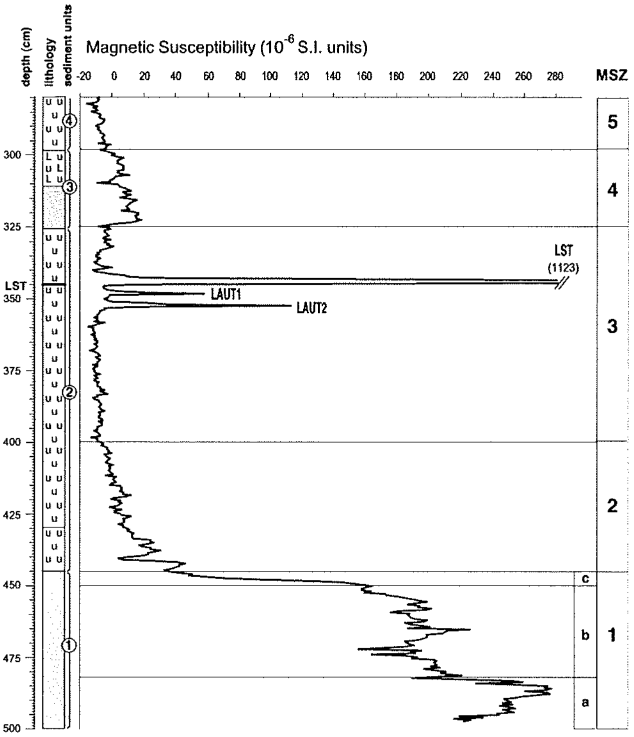

Fig. 8. Magnetic susceptibility record from Lautrey core 6 (analysis: G. Bossuet and B. Vannière).

9. Oxygen-isotope analysis

9.1. Method

The shifts in oxygen-isotope ratio measured in precipitated lake carbonates are generally assumed to reflect climate changes without any lag. It is hypothesised that the isotopic composition depends only on the ratios in the atmospheric water vapour and the temperature. However, as noted by Ammann et al. (2000), three weaknesses may affect this basic assumption as follows:

- Detrital or reworked carbonates may alter or distort the climatic signal.
- Variations in isotopic ratios caused by changes in moisture origin may be difficult to separate from changes due to temperature.
- Hydrological changes reflected by lake-level fluctuations may also be responsible for changes in isotopic ratios.

However, Lotter et al. (1992) have shown that not only major shifts in the oxygen-isotope profiles obtained from analysis of bulk carbonate in Swiss lakes, but also minor shifts can be compared with equivalent features recognised in the Greenland oxygen-isotope record. Moreover, similar oxygen-isotope records obtained from bulk carbonate samples have been established for the Last Glacial–Interglacial transition from several Jura lake sediment sequences (Eicher, 1987; Magny, 1995; Aalbersberg et al., 1999).

The development of an oxygen-isotope profile for Lautrey core 6 was considered important in order to generate a direct record of climate changes that is independent from biotic and abiotic proxies. It is then possible to evaluate the response of ecosystems to climatic variations. A second objective was to derive an indirect time-scale for the sequence by correlating the ^{18}O record with that of the GRIP ice core, as discussed below (see Section 12.1).

Bulk sediment samples for measurements of the $^{18}O/^{16}O$ ratio were analysed at 0.5 cm intervals for the section spanning the Younger Dryas pollen zone and at 1 cm intervals for the rest of the sediment core. Care was taken that the analysed samples consisted entirely of carbonate, with no shell fragments. Oxygen-isotope ratios were analysed on a Finnigan MAT 252 mass spectrometer equipped with an automated carbonate extraction line. Samples were digested in concentrated orthophosphoric acid at a temperature of 80 °C. All data are reported relative to the V-PDB standard.

9.2. The oxygen-isotope record

The large fluctuations in values below level 445 cm in the Oldest Dryas pollen zone clearly show that the climatic signal was strongly perturbed by effects of old carbonate lithoclasts originating from the Jurassic and Cretaceous rocks in the catchment area. The occurrence of clay minerals, quartz, dolomite and lithoclasts illustrated in Figs. 7 and 10 suggests possible perturbations of the climatic signal provided by the oxygen-isotope record during the Lateglacial Interstadial and the Younger Dryas pollen zone. Nevertheless, the isotopic profile reconstructed above 445 cm depth generally shows a rather coherent picture (Fig. 9).

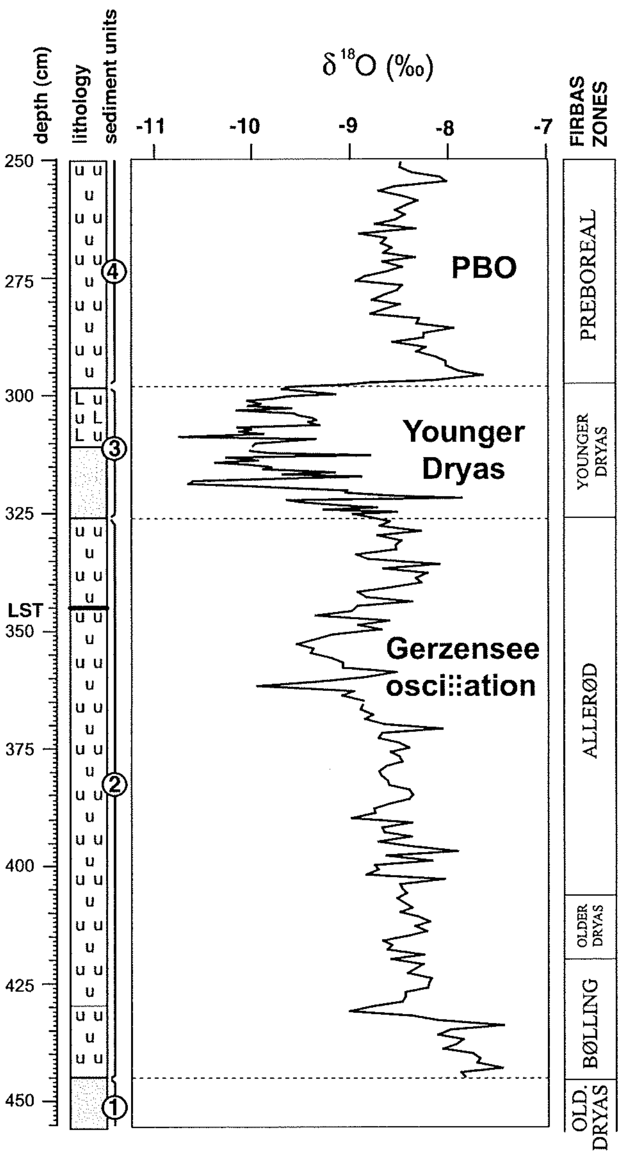

Fig. 9. Oxygen-isotope record from Lautrey core 6 (analysis: G. Aalbersberg).

The oxygen-isotope profile of core 6 presents two well-marked maxima. The first between 445 and 435 cm occurs at ca 12,590 ± 45 ^{14}C yr BP and coincides with the beginning of Bølling–Allerød pollen zone. The second, at 295 cm depth, is dated to 10,000 ^{14}C yr BP and corresponds to the beginning of the Holocene. These two maxima reach similar levels of isotopic values and reflect important warming phases.

Another prominent feature is the long-lasting minimum which culminates between 326 and 298 cm depth. It develops between 10,960 ± 45 and 10,000 ± 40 ^{14}C yr BP and corresponds to the Younger Dryas pollen zone. The end of this cold event shows an abrupt increase in $^{18}O/^{16}O$ ratio as is also observed in the Gerzensee and GRIP oxygen-isotope records (Johnsen et al., 1992). However, in contrast to the classical characteristics of the onset of the Younger Dryas pollen zone in these records, the isotopic profile of Lautrey core 6 does not present a rapid decrease in isotopic values at that time, even though the lithostratigraphy indicates a sharp transition at level 326 cm from carbonate lake-marl to clayey-silty deposits. The abrupt input of lithoclasts from the catchment area at the Younger Dryas onset (see Section 10, Fig. 10) was probably responsible for perturbations of the isotopic signal. Furthermore, the oxygen-isotope signal during the Younger Dryas biozone shows rapid and strong (>2‰) fluctuations,

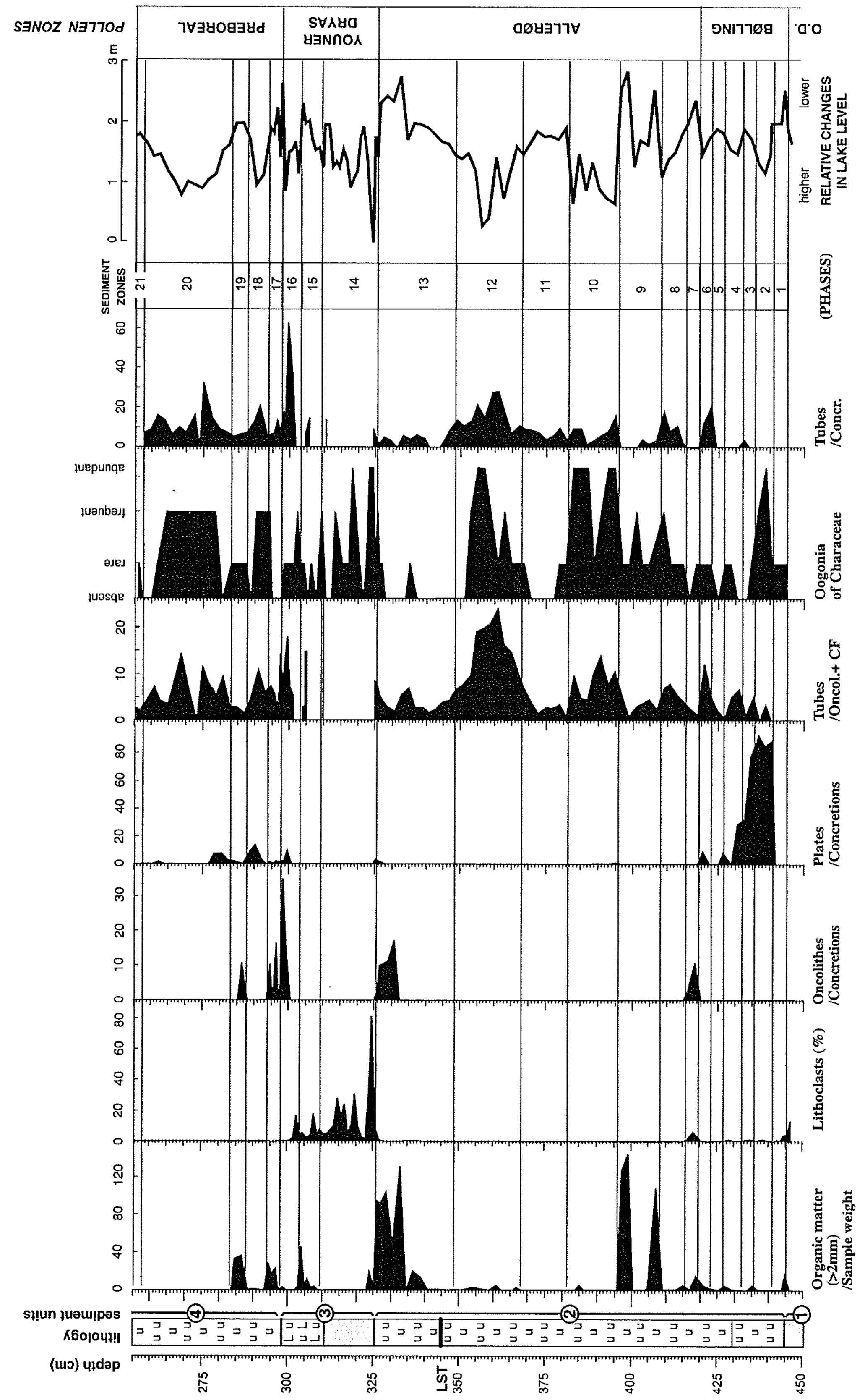

Fig. 10. Sediment diagram and lake-level record from Lautrey core 6 (analysis: M. Magny).

equally attributable to the presence of allochthonous material.

Shortly after the beginning of the Holocene, a less pronounced minimum develops between 284 and 266 cm depth, i.e. between 10,120±40 and 9975±45 ^{14}C yr BP and corresponds to the Preboreal oscillation (PBO) (Lotter et al., 1992; Björck et al., 1997). It was preceded by a short-lived minimum at level 289 cm.

Two other minima appear between levels 363 and 352 cm. They occur after 11,575±45 ^{14}C BP and immediately precede the deposition of LST. These events can be attributed to the Gerzensee oscillation (Lotter et al., 1992; Björck et al., 1998). As noted by Schwander et al. (2000), the magnitude of the isotope signal during the Gerzensee oscillation and PBO reaches about one-third to one-half of the magnitude of the big shifts at the Bølling and Holocene onsets.

Before the Gerzensee oscillation, no particularly prominent event can be recognised except from that culminating at level 430 cm, i.e. inside of the Bølling pollen zone. No major climate cooling in the isotope profile of Lautrey core 6 can be observed between 419 and 404 cm depth, i.e. at the time of the Older Dryas pollen zone (see Section 4). Detrital inputs from the catchment area can be suspected to have perturbed the isotope signal as suggested, e.g., by a peak of lithoclasts in the fraction $<63\,\mu$m between levels 420 and 415 cm (see Section 10, Fig. 10).

10. Lake-level reconstruction

Lake-level reconstructions for the Lateglacial period provide useful proxy palaeoclimatic data for continental areas (Gaillard and Moulin, 1989; Bohncke and Vandenberghe, 1991) and high-resolution studies have shown an in-phase behaviour between lake-level and isotope signals (Magny, 2001).

10.1. Methods

The reconstruction of past changes in lake level for the Lautrey core 6 is based on a particular sedimentological approach which uses a combination of several markers and comparisons with modern analogues observed in sediments in present-day lakes (Magny, 1992a, b, 1998) as follows:

- *Lithological criteria*: Littoral sediments are often characterised by a larger quantity of OM originating from shore vegetation than open water parts of the lake. Fine carbonate lake-marl is deposited in deeper water.
- *The macroscopic components of lake marl*: The coarser fractions (larger than 0.2 mm) of lake-marl accumulated in the Jura lakes are mainly composed of carbonate concretions of biochemical origin (Magny, 1992a, b, 1998). These concretions can be divided into several morphotypes. Modern analogues based on surface samples taken along transects perpendicular to the shore have revealed, that each morphotype shows a characteristic spatial distribution from the shore to the profundal zone reflecting both the hydrodynamics and aquatic vegetation belts. Oncolithes characterise near-shore areas; cauliflower-like forms dominate the littoral platform, plate-like and tube-like forms develop on the edge and slope of the littoral platform and are associated with *Nuphar-Potamogeton*- and Characeae belts, respectively.

10.2. The lake-level record

Table 2 provides a summarised description of the 21 successive local sediment zones (SZ) distinguished from the sedimentological analysis of Lautrey core 6 (Fig. 10). The quasi-absence of biogenic carbonate concretions below 445 cm depth did not permit the establishment of a lake-level record from sediment unit 1.

SZ1 corresponds to a rapid fall in lake level at the transition between the Oldest Dryas and Bølling pollen zones. Rather unstable lake-level conditions characterise SZ-2 to 9. Two more pronounced maxima appear centred at levels 438 and 410 cm, and two marked lowering phases at 406 and 398 cm depth, as shown by the large amount of coarse OM inherited from the near-shore areas.

SZ-10 and 12 represent two major lake-level maxima. Each was followed by a well-developed phase of lower water level (SZ-11 and 13). During the latter part of SZ-13, peaks of OM and oncolithes reflect a major lowering.

The beginning of the Younger Dryas pollen zone is marked by a rapid rise in lake-level culminating at 324 cm depth (SZ-14). A general trend towards lowering can be recognised over the stadial period.

The onset of the Holocene corresponds to a rapid fall in water level (SZ-17) followed by two successive phases of higher lake level, a first short-lived (SZ-18) and a second more prolonged (SZ-20).

Generally speaking, the pattern of hydrological changes reconstructed at Lautrey corresponds well with lake-level records reported in previous studies of sites in west-central Europe (Magny, 2001).

11. Quantitative reconstructions of climatic parameters

With the exception of isotope studies, most of the quantitative reconstructions of palaeoclimates from Europe and North America until now have been obtained from coleopteran, cladoceran, chironomid

Table 2
Lateglacial and early Holocene lake-level changes reconstructed from Lautrey core 6

Zones/phases	Lake level	Main sedimentological markers
21	Lower	Decrease in tube concretions and Characeae oogones
20	Higher	Peak of tube concretions and Characeae oogones
19	Lower	Peak of oncolithes
18	Higher	Peaks of plate and tube concretions, and oogone maximum
17	Lower	Peak of oncolithes, maximum of organic matter
16	Higher	Peaks of plate and tube concretions, and oogone maximum
15	Lower	Peak of organic matter, decrease in Characeae oogones
14	Higher	Peaks of lithoclasts and Characeae oogones
13	Lower	Peaks of organic matter and oncolithes, decrease in tube concretions and Characeae oogones
12	Higher	Peaks of tube concretions and Characeae oogones
11	Lower	Decrease in tube concretions and Characeae oogones
10	Higher	Peaks of tube concretions and Characeae oogones
9	Lower	Bipartited phase: peak of organic matter, decrease in tube concretions and Characeae oogones
8	Higher	Peaks of tube concretions and Characeae oogones
7	Lower	Peaks of organic matter and oncolithes
6	Higher	Peak of tube concretions
5	Lower	Small peak of organic matter, decrease in tube concretions
4	Higher	Peak of tube concretions
3	Lower	Small peak of organic matter, decrease in plate concretions and Characeae oogones
2	Higher	Peaks of plate concretions and Characeae oogones
1	Lower	Peak of organic matter, decrease in lithoclasts

and pollen-assemblage data. Coleoptera and chironomid-assemblage data primarily provide temperature reconstructions, whereas pollen data may provide information on both temperature and precipitation. Lake-level data offer an additional constraint to refine the modern analogue approach developed for pollen data (Guiot et al., 1993; Magny et al., 2001). Moreover, the quantitative reconstructions based on coleopteran, chironomid and pollen data provide only indirect palaeoclimatic inferences based on the response of plant and animal communities to climate changes. This response may also have been modulated by multiple non-climatic factors, such as the specific sensitivity of different organisms, edaphic conditions, colonisation and immigration processes and, more generally speaking, complex interactions between biota in ecosystems (van Geel, 1996; Hoek, 2001). The project initiated at Lake Lautrey offers the opportunity of a comparison of quantitative palaeoclimatic reconstructions based on biological climate indicators. The results are presented in Fig. 11 and discussed in Sections 12 and 13.

11.1. Pollen-based reconstruction

To provide more accurate and reliable palaeoclimatic estimates, two independent methods have been used as follows. In the "Best Analogue method" (BAM), the similarity between fossil and modern pollen assemblages is evaluated (Guiot, 1990). The modern spectra which have the smallest chord distance to given fossil assemblages are considered the best modern analogues, and used for the reconstruction of palaeoclimate. For each fossil pollen assemblage, the 10 best analogues are selected; consequently, their climatic parameters are averaged to provide the climate estimates. Furthermore, the best analogues selection is constrained by biomes and lake levels (Guiot et al., 1993; Magny et al., 2001).

The plant functional types (PFTs) method is a transfer function in which pollen percentages are first transformed into PFT scores (Peyron et al., 1998). PFTs are broad classes of plants defined by their structural and functional features (Prentice et al., 1996). The principle of the method is that PFT scores derived from the modern pollen samples are calibrated in terms of climatic parameters, using a non-linear regression method (artificial neural network). Then, the calibration is applied to the fossil PFT scores to provide the climate estimates.

The modern pollen data set used in the quantitative reconstructions includes 868 surface pollen samples from Eurasia including the Mediterranean basin, Pyrenees, Scandes Mountains, Kazakhstan and the Tibetan plateau (Peyron et al., 1998) to get samples more representative of some specific past vegetation types. Table 3 presents the correlation coefficients between observed and reconstructed values of climate parameters. The standard best modern analogue method and the PFT method, based on groups of pollen taxa, have been tested and compared to reconstructed mid-Holocene past climate. Although both methods indicate similar climatic patterns, the PFT method provides more consistent results (Peyron et al., 2000). On the basis of modern pollen data set coupled with known climatic conditions, the climatic parameters (i.e. the

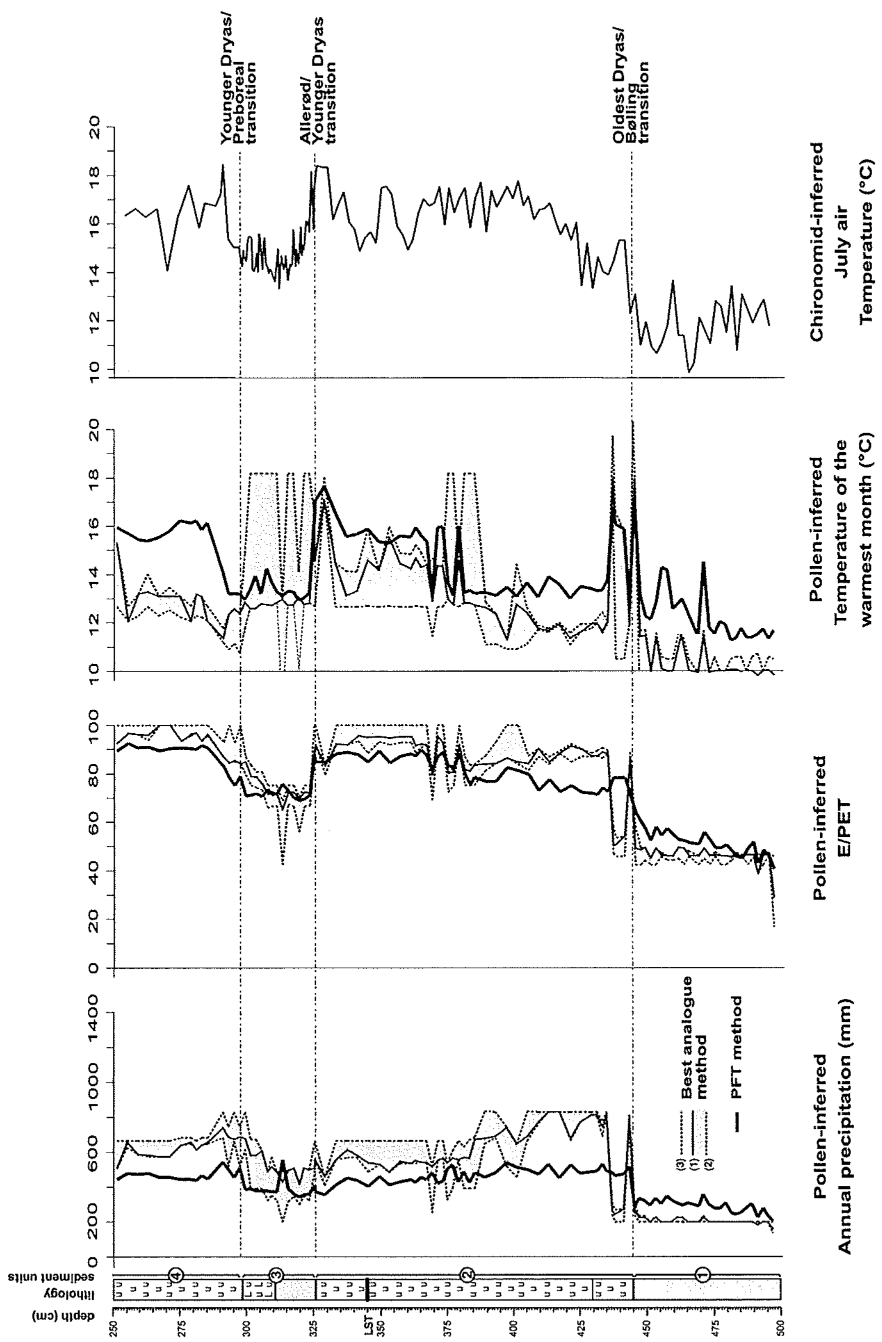

Fig. 11. Pollen- and chironomid-based quantitative reconstructions of climatic parameters from Lautrey core 6 (analysis: O. Peyron, O. Heiri and L. Millet). The curves reconstructed from the best analogue method show (1) the mean value calculated over the analogues, (2) the mean minimum and (3) the mean maximum values.

mean temperature of the warmest month, the annual precipitation and the ratio of real to potential evapotranspiration: E/PET) have been calculated using an artificial neural network calibration (Harrison et al., 1993; Peyron et al., 1998). The validation tests (Table 3) may suggest that the BAM reconstructions are more accurate than the PFT method. In theory, the artificial neural networks used in the calibration are able to learn and reproduce any pattern perfectly. However, if the network is fitted too closely to the input data, there is a risk that estimates of new data will be incorrect. Consequently, even if the correlation coefficients are lower with the PFT method than with the MAT, we consider the calibration procedure to be optimal because the relationships between the input and the output variables are learnt in a generalised fashion and can therefore be used for predictions of unknown outputs.

Table 3
Correlation coefficients between observed and reconstructed values of climate parameters obtained from application of both modern analogue technique (MAT) and plant functional types (PFT) approaches to the modern pollen samples

Climatic parameter	Best analogues method		Plant functional types method		
	Correlation coefficient (r^2)	RMSE	Correlation coefficient for the calibration	Correlation coefficient for the verification	RMSE
Temperature of the warmest month (°C)	0.94	2.0	0.88±0.016	0.87±0.020	3.1
Annual precipitation (mm)	0.90	162	0.81±0.014	0.80±0.030	212
Ratio of real to potential evapotranspiration (%)	0.94	9.8	0.91±0.007	0.90±0.012	13.3

Note: In the PFT method, the original data set has been divided into training and verification sets. The artificial neural network is calibrated on samples from the training set. Samples of the verification set are used to verify the prediction of the climatic parameters. Samples included in both sets correspond to data randomly extracted in the modern data set. This procedure has been repeated to reach 30 simulations using bootstrap technique. Coefficients of correlation and standard deviation after the calibration and the verification have been calculated. Root mean square error (RMSE) is also indicated.

11.2. Chironomid-based reconstructions

Recently, there is an increasing interest in subfossil chironomid assemblages to establish quantitative records of past changes in summer temperature. Several models have been developed (Lotter et al., 1997; Olander et al., 1999; Brooks and Birks, 2000) which measure the relationship between the present-day summer temperatures and chironomid assemblages in surficial lake sediments. The chironomid-based July air temperature record presented in Fig. 11 was reconstructed from a chironomid-temperature inference model based on a modern training set from the Jura mountains, Swiss Plateau and Swiss Alps (Heiri, 2001; Heiri et al., 2003a). The transfer function is based on weighted averaging-partial least-squares regression and has a leave-one-out-cross-validated coefficient of determination (r^2) of 0.80, and a root mean square error of prediction of 1.53 °C for July air temperature.

During two intervals of the Lake Lautrey record, chironomid assemblages are dominated by taxa not present in surface sediment assemblages used to calibrate the transfer function. This non-analogue situation was mainly due to the occurrence of *C. ambigua* and to *Pagastiella*. As a consequence, temperature inferences from samples with a high proportion of *C. ambigua* and *Pagastiella* (CAZ-2 and the oldest part of CAZ-6) are based on only a part of the chironomid fauna and on a comparatively lower number of chironomid specimens. As discussed by Heiri and Millet (2005), this implies that inferred temperatures at the end of the Oldest Dryas and at the beginning of the Younger Dryas pollen zones should be interpreted with caution, as they are based on samples with a high proportion of *C. ambigua* and *Pagastiella*. Moreover, the Lake Lautrey sediment sequence represents sublittoral/littoral deposits and Millet et al. (2003) have suggested that the chironomid record of Lake Lautrey may also reflect changes in trophic and oxygen conditions in addition to changes in substratum. Recent studies indicate that a bias in inferred temperatures is possible if chironomid-temperature inference models calibrated on deep-water sediments are applied to near-shore assemblages (Heiri et al., 2003b). In lakes of a similar water depth as the Lake Lautrey palaeolake, this bias has been estimated to be of ca 0.4–0.5 °C magnitude and is therefore relatively small in comparison with the Lateglacial temperature changes inferred for the Lake Lautrey record (Fig. 11).

12. Synthesis of environmental and climatic changes

Taken together, the records presented above offer a basis for a tentative synthesis of environmental and climatic changes at Lake Lautrey during the Last Glacial–Interglacial transition. However, in order to evaluate the rapidity of changes and possible lags and offsets in biotic and abiotic responses to climate variations, it is necessary to estimate the sampling resolution of these records by establishing an absolute calibrated time-scale.

12.1. Construction of an age-depth model

Fig. 12 presents the strategy used to construct an age-depth model for Lautrey core 6. It results from the combination of tephra, radiocarbon and isotope data described in the previous sections.

First, the LST horizon offers a useful time-marker dated to ca 12,850 cal yr BP (see Section 3).

Second, 12 AMS radiocarbon dates provide a time framework (Fig. 12B, Table 1 in Section 3) fully

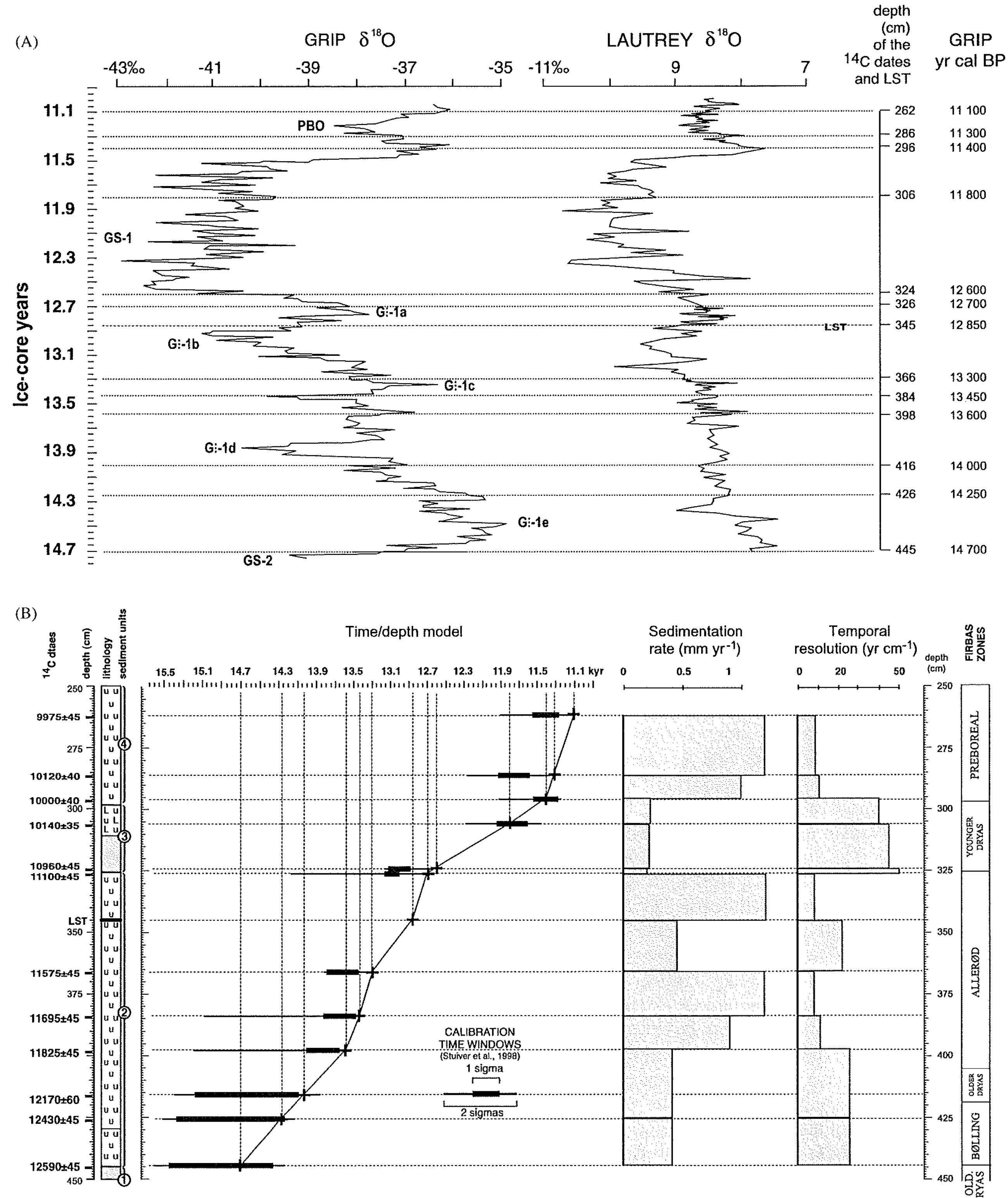

Fig. 12. Correlation between the ^{18}O record of Lautrey core 6 and that of GRIP ice core (A), within the constraints imposed by the age of LST and the limits of the time windows given by the calibration of the radiocarbon dates as shown in B. The points marked by + correspond to chosen time inside the time window given by the calibration according to a comparison of the Lautrey oxygen-isotope record with that of the GRIP record (Johnsen et al., 1992) rather than to the probability distributions. The inferred sedimentation rate and corresponding temporal resolution for, as an example, a 1 cm sampling interval, are indicated in B. Due to disturbances of the Lautrey oxygen-isotope record by detrital input at the Oldest Dryas–Bølling and the Allerød–Younger Dryas transitions, the abrupt changes in the lithology at levels 445 and 326 cm have been chosen to place the GS-2/GI-1e and GI-1a/GS-1 transitions. This is consistent with the pollen and chironomid stratigraphies.

consistent with the pollen and isotope stratigraphy available for the Jura mountains region (de Beaulieu et al., 1994; Magny, 1995; Bégeot, 2000) and more generally, for west-central Europe (Ammann and Lotter, 1989; Lotter et al., 1992; Brauer et al., 1999). However, when attempting to produce an absolute time-scale, difficulties appear due to the uncertainties associated with (1) the size of the time windows given by the calibration of the radiocarbon ages, and (2) periods of near-constant ^{14}C age at ca 12,700–12,600 and 10,000–9900 cal yr BP (Lowe et al., 1999). We have also to keep in mind that the calibration back to 12,600 $\partial^{14}C$ in IntCal 1998 is still not fully reliable.

By direct comparison with the GRIP ice-core isotope record, the oxygen-isotope record obtained from Lautrey core 6 provides the possibility to overcome the difficulties mentioned above. A similar strategy was used previously (Grafenstein et al., 1999; Ammann et al., 2000) with the basic assumption that the shifts in ^{18}O record reflects air mass changes and climatic variations without any lag. As illustrated by Fig. 1, Lake Lautrey is located close to the sites of Gerzensee (Swiss Plateau), Meerfelder Maar and Ammersee (Germany) where a quasi-synchronicity has been observed between climatic events recorded in the Greenland ice-sheet and those reconstructed in west-central Europe, based on (1) varved sediments (Brauer et al., 2000), (2) a comparison between oxygen-isotope records (Grafenstein et al., 1999; Ammann et al., 2000), or (3) a combination of oxygen-isotope and pollen stratigraphies (Lotter et al., 1992). Keeping the disturbance of the isotopic signal at Lautrey due to detrital inputs at the beginning of Younger Dryas biozone and during the Older Dryas oscillation in mind (see Figs. 6, 7 and 10), the correlations presented in Fig. 12 show a reasonable agreement between the Lautrey and GRIP isotopic records.

Thus, on the basis of a general similarity between the GRIP and Lautrey oxygen-isotope records (see Section 9) and taking into account the limits of the time windows given by the calibration (intercept method in IntCal 4.3, Stuiver et al., 1998), each of the 12 levels radiocarbon dated at Lautrey has been correlated with a level of the GRIP record (tuning by wiggle matching between GRIP and Lautrey oxygen-isotope records). The LST horizon provided an additional time linkage. In between the intervals defined by LST and the radiocarbon dated levels, no further tuning by wiggle matching has been done, but a mean sedimentation rate has been calculated for each interval as illustrated in Fig. 12. This sedimentation rate allows the estimation of the variations in the time resolution reached by the samples from the different segments of the Lautrey core 6. Due to disturbances of the Lautrey oxygen-isotope record by detrital input at the Oldest Dryas–Bølling and the Allerød–Younger Dryas transitions, the abrupt changes in lithology at levels 445 and 326 cm have been chosen to determine the positions of the GS-2/GI-1e and GI-1a/GS-1 transitions. This is consistent with the pollen stratigraphy.

12.2. Environmental evolution and climatic history

For the pollen and chironomid biostratigraphical data sets, detrented correspondence analysis (DCA) was used to measure the gradient length of the first principal components analysis (PCA) axis in Standard Deviation units (Ter Braak and Smilauer, 1998). This resulted in a gradient length lower than 4 for both the data sets, justifying the further use of the linear response model and hence of PCA. In PCA, percentage of pollen and chironomid data were log-transformed ($Y' = \log[Y \times 1 + 1]$) and centred on species. According to PCA, the first axis explains, respectively, 56% and 23% of the variation of pollen and chironomid data sets, respectively. All ordinations were implemented using the CANOCO program for Windows 4.0 (Ter Braak and Smilauer, 1998).

In order to make the comparison with other data more objective, the more complex pollen and chironomid data are presented in Figs. 13 (Oldest Dryas biozone) and 14 (Bølling–Allerød biozones and Holocene) using curves defined by the scores of PCA axis 1. As illustrated by Fig. 4, the pollen PCA axis 1 mainly reflects the AP/NAP curve, i.e. below 405 cm primarily the *Betula* and above this level primarily the *Pinus* percentages. Fig. 5 shows that the chironomid PCA axis 1 appears to mirror chiefly the percentages of *C. ambigua* and *Stictochironomus*.

12.2.1. Sediment unit 1 (Fig. 13)

Basal sediment unit 1 provides evidence for an open herbaceous landscape with a limited herbaceous vegetation cover and corresponds to GS-2a. Because OM suitable for radiocarbon dating is virtually absent, it is difficult to evaluate the duration of the period represented by sediment unit 1. Assuming a sedimentation rate similar to that prevailing during the deposition of sediment unit 3 (GS-1) which is also composed of clayey silts, level 500 cm may date to before 17,200 cal yr BP, though this is an approximative assessment only, because units 1 and 3 are comparable neither climatically, nor from a point of view of vegetation cover.

All the evidence points to a cool climate resulting in low pollen concentration and the absence of biogenic carbonate sedimentation. Wind-facetted quartz, clay mineral inputs and long-distance transported *Pinus* pollen grains point to strong winds. In the lake, the accumulation of allochthonous deposits dominates, as indicated by the mineralogy and high MS values. The chironomid assemblages indicate oligo-mesotrophic conditions and well-oxygenated water in the lake basin. Sediments from this period have a weak TOM due to a

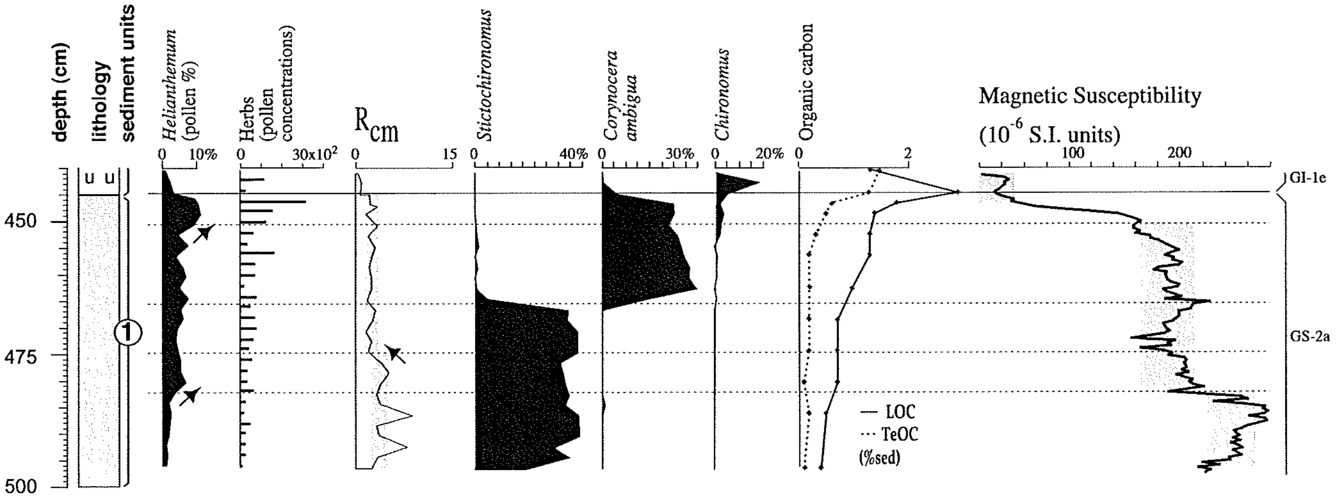

Fig. 13. Environmental synthesis for the Greenland Stadial 2a as documented by Lautrey core 6.

weak development of soils and vegetation in the catchment area. The quasi-constant values of quartz, calcite and the <63 μm grain-size fraction suggest a relatively stable landscape over the entire period.

However, there are some indications of changes in environmental conditions. At 482–480 cm depth, the MS values undergo a first abrupt fall, coinciding with a slight rise in *Helianthemum* percentages and, more generally, herbaceous pollen concentrations (PAZ-1b/1a transition). At level 485–480 cm, LOC also marks a first quite small increase in lake productivity followed by a second at level 465 cm when an important change in chironomid fauna suggests a higher organic accumulation as well as a slight reduction of oxygen concentration. Furthermore, the clear reduction of Rcm values at 475 cm depth suggests a decrease in the wind strength and/or in the production of source regions, where an increase in the vegetation cover and a greater stabilisation of soils may be responsible for a decline of allochthonous inputs. The progressive retreat of *C. ambigua* and the increase in *Chironomus* fit well with the increase in LOC values (higher lake productivity).

Finally, a major last step of environmental changes occurs in the later part of sediment unit 1 from level 450 cm upwards. It is marked by a disappearance of kaolinite input, an abrupt fall in MS and <63 μm fraction, a rise in TeOC, while herbaceous pollen concentrations double and *Helianthemum* forms a peak. Taken together, this suggests slightly warmer conditions favouring a higher lake productivity and the development of the vegetation cover and soils on the catchment slopes, whereas wind strength decreases.

The quantified climatic parameters indicate generally cool and dry conditions during the entire period, with summer temperature (mean July) fluctuating around 10.5–12 °C (PFT and BA methods) (Fig. 11). These values are close to those inferred from the chironomid fauna, which, however, suggest a greater climate variability over the period (Fig. 11).

12.2.2. Transition between sediment units 1 and 2

All evidence points to a major warming at around 445 cm depth as indicated by the abrupt development of the biogenic carbonate sedimentation in correlation with the disappearance of the detritic input, and by heaviest oxygen-isotope values. In agreement with the pollen data, this suggests a rapid stabilisation of the catchment slopes by an increasing vegetation cover. First among the AP taxa, *Juniperus* shows a rapid expansion between levels 445.5 and 444.5 cm from 1% to 7% in less than 40 yr. It was followed by *Betula* which reaches ca 35% from 444.5 to 442.5 cm depth. Both TeOC and LOC mark an abrupt rise suggesting strong soil development and lake productivity. The aquatic fauna reveals an abrupt change with the rapid decline of *C. ambigua* between levels 446.5 and 444.5 cm.

The quantitative reconstructions from pollen data point to a summer temperature (mean July) peaking at 17–18 °C as early as level 444.5 cm. This is confirmed by the chironomid-based reconstruction, which provides a slightly delayed and lower maximum of July air temperature (15.3 °C at level 442 cm). The warming is associated with an important increase in annual precipitation (PANN) as well as in the available moisture which is also of crucial importance for vegetation development.

12.2.3. Sediment unit 2

Regarding the history of the vegetation, the sediment unit 2 record suggests a picture typical for the Lateglacial reforestation phase in the region, with a succession of juniper scrub, birch woodland and, finally, pine forest reaching a first maximum at level 400.5 cm (i.e. ca 13,600 cal yr BP). During this period, the development of the vegetation cover progressively reduces erosional processes on the catchment slopes as inferred from the decline in MS values, which stabilise from level 400 cm upwards. This fits well with the general increase in TOM (relative to LOM) reflecting the increasing development and maturation of catchment soils between 445 and 400 cm depth.

However, superimposed on this general trend, there is evidence for the occurrence of distinct cooling events responsible for regressive phases in the vegetation development. Three successive episodes of decrease in *Betula* described in Section 4 from both percentages and pollen concentrations appear to have been registered by other biotic and abiotic markers as well (Fig. 14). The first decrease of *Betula* at level 440 cm is synchronous with a climate cooling as reflected by the oxygen-isotope profile and with a peak in MS, a rise in lake level, a decrease in TOM as well as in the *Chironomus* percentages. The second phase, at 430–428 cm depth (i.e. ca 14,350 cal yr BP), appears to be less pronounced in terms of decline in the percentages and pollen concentrations of *Betula*, but it is in phase with a rise in *Artemisia* and *Juniperus* percentages and concentrations, a negative isotope anomaly, and a higher lake level. The third phase consists of two successive birch minima at level 418–416 and 410–408 cm (ca 14,050 and 13,850 cal yr BP). It is paralleled by a well-marked second maximum of *Juniperus* percentages, a higher lake level, two decreases in TOM ratio, a slight rise in MS values at level 418 cm and less anoxic conditions as suggested by a decrease in *Polypedilum*. However, only a weak signal appears in the oxygen-isotope profile, possibly masked by detritic inputs. Taken together, these three successive phases of *Betula* decline mark distinct cooling episodes resulting in (1) less anoxic conditions in the lake basin, and (2) a clearing of the vegetation cover correlative with an increasing detrital input to the lake.

From 400 to 326 cm depth, the landscape is characterised by relatively dense pine forests (Allerød pollen zone) as reflected by quasi-constant low MS values, while maximum value of TOM/LOM ratio suggests a good maturation of catchment soils. However, like the preceding Bølling period, this warm Allerød phase was interrupted by a series of cooling episodes. Shortly after a first maximum at level 400.5 cm, both the percentages and pollen concentrations of *Pinus* show two successive declines at 394.5 and 386.5 cm depth (i.e. ca 13,550 and 13,450 cal yr BP). They are associated with two minor peaks of juniper percentages. The isotope profile indicates a cooling phase concomitant with a rise in lake level, a fall in TOC and TOM, while the chironomid fauna suggests a better-oxygenated water in the lake (see Section 5).

The next cooling episode appears less pronounced in the percentages or pollen concentrations of *Pinus* at

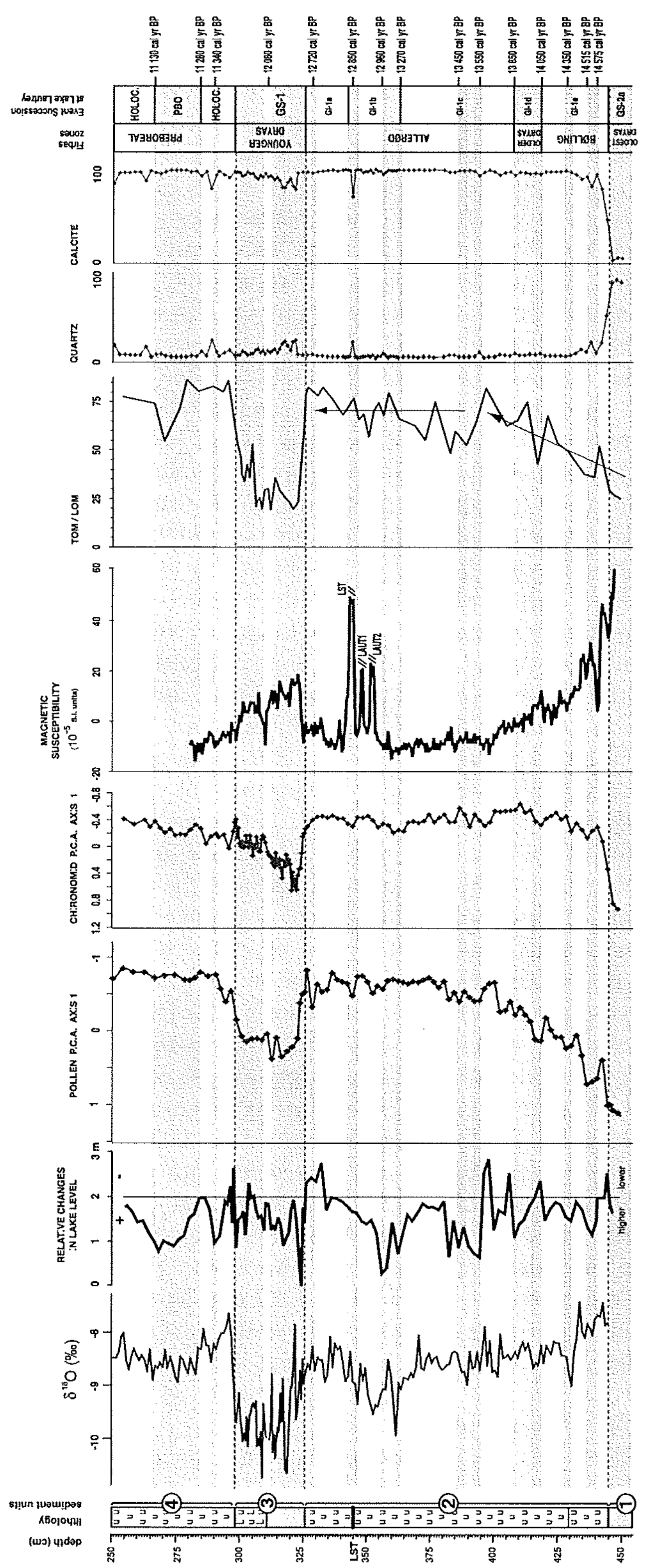

Fig. 14. Environmental synthesis for Greenland Interstadial 1, Greenland Stadial 1 and early Holocene as documented by Lautrey core 6. The pollen and chironomid data are presented using curves of scores of PCA axis 1. Grey bands correspond to cooling events documented by several biotic and/or non-biotic indicators. The right-hand column presents the event succession established from Lautrey core 6 for GI-1, GS-1 and early Holocene periods. The ages are inferred from the time-depth model presented in Fig. 12.

level 363 and 355 cm (i.e. ca 12,270–12,960 cal yr BP) than by negative isotope anomalies, higher lake level as well as, between 360 and 350 cm depth, less anoxic conditions in the lake basin as inferred from the chironomid assemblages. It was followed by another short cold spell, which began before the LST deposition and was responsible for lower percentages and pollen concentration of *Pinus* at levels 346.5 and 342.5 cm, lower oxygen-isotope values at 346 and 342 cm depth, and a brief increase in the detrital input to the lake basin marked by a peak of quartz at level 345 cm.

The chironomid-based temperature record suggests two short-term decreases in summer temperature centred on ca 360 and 343 cm depth (Fig. 11). The first of these is coeval with a decrease in the Lac Lautrey ^{18}O record (Fig. 9) and may be related to the beginning of GI-1b (see Fig. 14). However, the second begins just before and ends just after the deposition of the LST, during a period which is generally considered to have featured a comparatively warm climate. Possibly this is an artefact in the record due to the application of a chironomid-temperature transfer function calibrated on mid-lake samples to a littoral sediment core.

The last part of sediment unit 2 provides contrasting evidence for the history of environmental conditions. Maximal TOM values between 336.5 and 326.5 cm depth, as well as more anoxic conditions and a large development of the aquatic vegetation in the lake basin as inferred from the chironomid assemblages, suggest still rather favourable conditions. However, more severe climate conditions can be inferred from a general decrease in the pollen concentrations from level 330 cm concomitant with higher MS values. Moreover, a short-lived but well-marked cooling event can be observed at level 328.5 cm (i.e. ca 12,720 cal yr BP) from a conspicuous pollen concentration minimum, a fall in TOM values and a reduction of *Polypedilum* and *Glyptotendipes*, i.e. both chironomid taxa associated with more anoxic conditions and well-developed aquatic vegetation. Thus, the general trend initiated from 330 cm depth and the cool spell observed at 328.5 cm depth may be considered to be precursory signs of the next significant cooling event registered by sediment unit 3.

12.2.4. Sediment unit 3

All proxies, with the exception of the oxygen-isotope record which appears to be partly confused by detrital inputs, point to a marked cooling over the transition from sediment units 2 to 3. With respect to the lithology, the abrupt transition at level 326 cm from yellow-beige carbonate lake-marl to grey clayey silts provides a first indication of strong changes in climatic and environmental conditions. From levels 326 to 324 cm, i.e. within approximately 100 yr between 12,700 and 12,600 cal yr BP, a sudden increase in lithoclasts (Fig. 10) indicates a strong reactivation of surficial runoff. As early as level 325.75 cm, the AP percentages and concentrations show a first rapid decline followed, after a short-lived stop at 324.75 cm depth, by a second and more durable reduction from level 323.75 cm upwards. The rapid increase in MS values between 325 and 322.5 cm depth reflects increasing detrital inputs (reduction of the vegetation cover). The re-appearance of quartz at sample 322 cm and dolomite at sample 317 cm illustrates the reactivation of detrital input due to runoff and stronger wind.

In the lake basin, the chironomid fauna reacts at 325.75 cm depth and, in particular, shows a rapid re-expansion of *C. ambigua*, which had completely disappeared during GI-1. However, in contrast to the cool period documented by sediment unit 1, the calcite curve does not register a lowering at the GS-1 onset. This means that the summer temperature still allows the formation of biogenic carbonate, even if cooler temperature led to a strong reduction of the processes and consecutively of the sedimentation rate.

The chironomid-based quantitative reconstruction of climatic parameters reveals a decrease of the summer temperature from 18.4 to 15.5 °C as early as 325.5 cm depth. This is prior to the signal reconstructed from the pollen data, which indicate a cooling from 17 to 13.2–12.8 °C. In the same period, PANN and the available moisture dramatically fall. This could have led to death of local trees, lower vegetation cover and apparent increase in *Artemisia* percentage but not influx.

GS-1 as documented by sediment unit 3 shows a general trend towards a slight warming. Evidence of this general evolution can be observed in the isotopic curve, as well as in the progressive reduction of *C. ambigua*. Similarly, lake-level fluctuations, LOM percentage and MS values show a general downward trend. On the catchment slopes, the vegetation cover slightly restored as suggested by the increase in pollen concentrations from level 304.75 cm (i.e. 11,750 cal yr BP), and the progressive disappearance of detrital yield associated with wind input and erosional processes over the catchment area.

In the middle of GS-1, at 312–310 cm depth, there is ample evidence for a short-lived warming episode which is reflected by a lowering of the MS values, a fall in lake level, peaking values of TeOC and LOC, and a decrease in *C. ambigua* concomitant with a positive oxygen-isotope anomaly. The vegetation cover gives a similar signal with the start of a slight increase in the pollen concentrations at level 310.75–308.75 cm. The PFT reconstruction also indicates a greater moisture availability during this warmer episode.

12.2.5. Sediment unit 4

At the transition from the sediment units 3 to 4, the oxygen-isotope profile gives a clear signal of an abrupt climatic warming between levels 298 and 296 cm. This favoured biogenic carbonate precipitation and resulted in a fourfold rise in sedimentation rate. The AP percentages abruptly rise at level 294.5 cm. Similarly, in the lake basin, *Chironomus* shows a continuous re-expansion from 297.75 cm depth, while *C. ambigua* is reduced to very low values at level 299.75 cm before disappearing at level 297.25 cm. On the catchment slopes, a rapid restoration of soils accompanies the development of the vegetation cover. The pollen-based quantitative reconstructions of climatic parameters suggest that the climate warming was associated with a reactivation of the hydrological cycle as shown by an increase in PANN and available moisture, while the lake-level record displays a rapid fall. The temperature maximum reconstructed from pollen data appears to be delayed in comparison with the rapidity illustrated by the various proxy data presented above. This may reflect migrational lags as shown at Gerzensee in Switzerland by Lotter et al. (2000). Moreover, the chironomid-based reconstructions indicate a warming of rather limited magnitude.

During the early Holocene, the oxygen-isotope profile gives evidence for two successive cooling events, a short one centred at level 290 cm (i.e. ca 11,340 cal yr BP) followed by a more durable negative oscillation culminating at 284–266 cm depth (i.e. ca 11,280–11,130 cal yr BP). These episodes are associated with a higher lake level as well as a more or less marked decline of *Chironomus* and a reduction of the TOM. No clear signal can be observed from the vegetation cover during either event. The chironomid-based reconstructions suggest two successive declines of the summer temperature from 18.5 to 15.5 °C and from 17.5 to 14 °C, whereas the pollen-based quantifications reveal a summer temperature decrease from 16.2 to 15.2 °C for the second episode.

13. Discussion and conclusions

13.1. A high-resolution record of climatic changes

The Lautrey data set allows the construction of a detailed sequence of climatic and environmental changes in the central Jura mountains during the Last Glacial–Interglacial transition. As discussed in Section 9, the Lautrey isotope record established from bulk sediment shows perturbations of the climatic signal probably due to detrital input from the catchment area, in particular during events GS-2a and GI-1d, and at the beginning of GS-1. However, keeping in mind these limitations and using the information provided by other proxies, the Lautrey oxygen-isotope profile can broadly be compared with that from the GRIP ice core considered as a climatic type profile (Fig. 12A). The environmental synthesis presented in Section 12.2 reveals that, at the Lautrey site, the major forcing factor of environmental change was variation in climate such as registered by the isotope record or lake-level fluctuations. Figs. 13 and 14 summarise the succession of climatic events recognised from core 6. This sequence of events in general shows a good agreement with that established for the North Atlantic region and west-central Europe (Lotter et al., 1992; Björck et al., 1997, 1998; Grafenstein et al., 1999; Ammann et al., 2000; Brauer et al., 2000) and provides some additional indications discussed below.

During GS-2a, the Lautrey record provides insights into limited environmental changes from level 482 cm upwards, clearly strengthened above 450 cm depth, i.e. at, respectively, ca 16,500 and 15,000 cal yr BP (ages extrapolated from the sedimentation rate). The first change may find an equivalent in the start of a shrub-phase with *Betula nana*, *Salix* and *Juniperus* (i.e. Swiss pollen zone CHb-1c, Ammann et al., 1996) dated to 13,600 ± 200 ^{14}C yr BP (i.e. 16,672–15,997 cal yr BP) at Rotsee, 13,360 ± 280 ^{14}C yr BP (i.e. 16,448–15,662 cal yr BP) at Lobsigensee, and to 13,335 ± 120 ^{14}C yr BP (i.e. 16,276–15,755 cal yr BP) at Schleinsee (Ammann and Lotter, 1989). The second change at level 450 cm may be coeval with the substantial expansion of *Juniperus* before the radiocarbon plateau at 12,700–12,600 ^{14}C yr BP and observed in the upper part of the Swiss pollen zone CHb-1c at ca 13,000 ^{14}C yr BP (i.e. 15,800–15,300 cal yr BP) and in the French northern Alps at 13,040 ^{14}C yr BP (David, 2001). These data recall the discussion by Walker et al. (2003) about a possible rise in temperature in western Europe earlier than the 14,700 cal yr BP Greenland thermal maximum.

During GI-1, the Lautrey data set gives insights into the occurrence of two cooling events between the thermal maximum at 14,700 cal yr BP and the GI-1d event (Fig. 14). At Gerzensee, two cold episodes may be inferred from increases in NAP and oxygen-isotope anomalies within the pollen zones CHb-2 and 3a (Lotter et al., 1992). Such Intra-Bølling Cold Periods (IBCPs) have also been documented by various palaeoclimatic records from west-central Europe (Bégeot, 2000; Magny and Richoz, 2000; David, 2001), the Norwegian Sea (Karpuz and Jansen, 1992), the Cariaco Basin (Hughen et al., 1998) and the Greenland ice cores (Johnsen et al., 1992; Stuiver et al., 1995).

Furthermore, the section 394.5–386.5 cm (i.e. ca 13,550–13,450 cal yr BP) of the Lautrey record confirms the occurrence of an additional cold event (GS-1c2 as defined by Brauer et al. in 2000 from the Meerfelder Maar sequence in Germany). This event is well marked in both the GRIP and Ammersee isotope records, where it is dated to ca 13,450 cal yr BP (Johnsen et al., 1992; Grafenstein et al., 1999) and has also been observed in Coleopteran MCR data from Gransmoor in NE England (Walker et al., 2003) and in the pollen profile from Längsee in Austria (Schmidt et al., 2002). It may also have equivalents in an oxygen-isotope negative anomaly and/or an episode of *Pinus* decline within zone CHb-4a at Gerzensee in Switzerland (Lotter et al., 1992).

The very short-lived cooling observed in sample 328.5 cm (i.e. 12,720 cal yr BP) between the LST deposition and the GS-1 onset may find an equivalent at Soppensee, Switzerland, where core SO86-14 shows a short pronounced decline in *Pinus* dominance correlative with a marked peak of *Betula* and a slight increase in *Artemisia* between the LST and the GS-1 start (Lotter et al., 1992). More generally speaking, the last cold episode of the Gerzensee oscillation observed at 346.5–342.5 cm depth and the general cooling trend illustrated by a clear decrease in pollen concentrations from 355 cm depth (i.e. since the GI-1b event and before the GS-1 start), may be compared with the long-term decrease in temperature reconstructed as early as 13,100 cal yr BP at Llanilid in South Wales (Walker et al., 2003).

In the middle of GS-1, the conspicuous short-lived warm event recognised at 312–310 cm depth (ca 12,080 cal yr BP) is paralleled by an intriguing brief positive oxygen-isotope anomaly in both the GRIP and Ammersee records to ca 12,050 cal yr BP. The pollen record established at Lake Nimgun, south-western Alaska (Hu et al., 2002) and a sea-surface temperature record from the central Mediterranean sea (Sbaffi et al., 2004) reveal a similar short-lived warming episode dated to 12,100–12,000 cal yr BP. The general warming trend shown by most of the Lautrey data over the GS-1 is similar to that illustrated by the GRIP oxygen-isotope and Calcium records (Brauer et al., 2000), as well as by the Ammersee and Gerzensee ^{18}O records (Grafenstein et al., 1999; Ammann et al., 2000).

Finally, the two successive cooling events centred at ca 11,350 and 11,200 cal yr BP have equivalents in the GRIP record, the second corresponding to the PBO (Lotter et al., 1992; Björck et al., 1997) and the first to a precursor episode. Such multiple cold oscillations during the early Holocene have also been observed on the Swiss Plateau (Magny, 2001; Magny et al., 2003) and in Sweden (Björck and Wastergard, 1999). The possible correlations addressed above between brief cooling events observed at Lake Lautrey and other west European sites in addition to the more classic GI-1d, GI-1b and PBO oscillations, suggest interesting working hypotheses, but still need to be tested by further investigations in other sites on the basis of high-resolution analysis and chronology.

13.2. *Comparison of the quantitative reconstructions*

Regarding the quantitative reconstructions of climatic parameters, Table 4 presents a comparison of results obtained from the various methods used at Lautrey as well as (1) from pollen and cladocera-based transfer functions at Gerzensee in Switzerland (Lotter et al., 2000), (2) from coleopteran data in the Swiss Plateau (Gaillard and Lemdahl, 1994; Coope and Elias, 2000) and in the Paris Basin (Limondin-Lozouet et al., 2002), and (3) from geological–palaeoecological data and AGCM experiments in Europe (Isarin and Bohncke, 1999; Renssen and Isarin, 2001; Renssen and Bogaart, 2003). Additional data are provided by previous studies at Lake Le Locle in the Swiss Jura mountains (Magny et al., 2001). The following discussion focuses mainly on the major periods of climatic changes.

Although general agreement can be observed between the data to outline an identical succession of warming (GS-2a/GI-1e and GS-1/Preboreal transitions) and cooling (GS-2a and GS-1) phases between the various sites, there are also discrepancies depending on the periods and/or methods used. Generally speaking, the temperature levels reconstructed from the Lautrey and Le Locle data sets for cool and warm periods are closely similar to those inferred from coleopteran data, but higher than those reconstructed at Gerzensee or in west-central Europe using other approaches. The temperature values obtained at Lautrey and Le Locle for the beginning of the GI-1 and the Holocene are also closer to those prevailing today in the study area than the reconstructed temperature obtained from other sites. Furthermore, the relatively high summer temperature reconstructed for GS-1 at Lautrey in comparison with those obtained for GS-2a fits well with the continuity of the authigenic carbonate sedimentation during the Younger Dryas cold event at Lautrey and Le Locle.

Moreover, the magnitude of the temperature changes reconstructed at Lautrey, Le Locle, Gerzensee and more generally in west-central Europe, most often differs by a factor 2. For example, the magnitude of the reconstructed cooling during the PBO ranges from 0.5 to 3.5 °C. These divergences are related to differences in the techniques of reconstruction (BA and PFT methods, transfer functions) and in modern databases used, as well as in the sensitivity of the climatic indicators used (chironomids, cladocera, pollen, geological features). Furthermore, non-climatic factors may also have an impact on the biotic indicators used for climatic reconstructions (Ammann et al., 2000).

Regarding the annual precipitation and its seasonal distribution throughout the Last Glacial–Interglacial transition at Lautrey, the pollen-based reconstructions clearly show a reactivation of the hydrological cycle at the onset of GI-1 and Holocene marked by an increase in PANN and available moisture. This is paralleled by an abrupt increase in snow accumulation over the Greenland ice-sheet during the same period (Alley et al., 1993). Such a general reactivation of the hydrological cycle probably reflects the retreat of sea ice (Renssen and Isarin, 2001) and increased evaporation over the

Table 4
Comparison of quantitative palaeoclimate reconstructions in west-central Europe using various approaches

Sites of regions	References	Method	GS-2	GI-1e	GI-1b	GI-1/GS-1 transition	GS-1 latter part	GS-1/Proboreal transition	Proboreal oscillation
Lake Lautrey 788 m a.s.l.	This study	Chironomids	11–12 °C	15.5 °C (≈ +4 °C)	16.8–15 °C (≈ −2 °C)	18.4–15.5 °C (≈ −3 °C)	13.5–14 °C (≈ +0.5 °C)	13.9–15.5 °C (≈ +1.5 °C)	17.5–14 °C (≈ −3.5 °C
		Pollen data (PFT)	11–12 °C	16.5 °C (≈ +4.5X)	?	17–13.2 °C (≈ −4 °C)		Lag, 13–16 °C (≈ +3 °C)	16.2–15.2 °C (≈ −1 °C
		Pollen data (BAM)	11.5–12 °C	16.5 °C (≈ +5.5 °C)	?	17–12.8 °C (≈ −4 °C)	7		
		Pollen data (PFT)	10.5–11.5 °C	500 mm	7	400 mm	450 mm	500 mm	470 mm
		Relative lake level	300 mm	Lower	Higher	Higher	Lower	Lower	Higher
Lake Le Lock, 915 m a.s.l.	Magny et al. (2001)	Pollen and lake-level data					13.2–14.2 °C (≈ +1 °C)	14–16 °C (≈ +2 °C)	16–14 °C (≈ −2 °C)
Gerzensee, 603 m a.s.l.	Ammann et al. (2000) and Letter etal. (2000)	Pollen data (CF)			12–10.7 °C (≈ −1.3 °C)	11.5–8.7 °C (≈ −3 °C)	9–10 °C (≈ +1 °C)	10–12 °C (≈ +2 °C)	12–11.5 °C (≈ −0.5 °C)
		Cladocera (CF)			12–11.2 °C (≈ −0.8 °C)			9–11.5 °C (≈ +2.5 °C)	
Hauterive-Champreveyres, 428 m a.s.l. (Lake Neuchatel)	Coope and Elias (2000)	Coleoptera (MCR)	July: 9 °C; January: −25 °C	July: 16 °C; January: 0 °C					
Grand-Marais, 587 m a.s.l.	Gaillard and Lemdahl (1994)	Coleoptera (MCR)	July: 10 °C; January: −10 °C	July: 15 °C; January: 0 °C					
South-Western Switzerland	Wohlfarth et al. (1994)	Pollen and isotope data		12–14 °C		≈ −3 to −4 °C			
West-central Europe	Isarin and Bohncke (1999), Renssen and Isarin (2001) and Renssen and Bogaart (2003)	Geological - ecological data, and AGCM		≈ 10 °C	12 °C (≈ +3 °C)			10–11 to 10–12 °C (≈ +1 °C)	9–11–12–14 °C (≈ +3 °C)
Paris Basin	Limondin-Lozouet et al. (2002)	Coleoptera (MCR)		Conty: 15–19 °C; Houdancourt 17–18 °C					
		River channels	Braided	Incision (> meandering)		Braided, accumulation		Incision (> meandering)	

Note: The location of the sites is indicated in Fig. 1. The data for west-central Europe were originally published as estimations at sea-level elevation and they have been corrected for this study referring to the altitude of Lake Lautrey and assuming a lapse rate of 0.6 °C per 100 m.

ocean due to higher temperatures. The phases of rapid warming at 14,700 and 11,500 cal yr BP were also characterised by a major lake-level lowering in the Jura mountains and on the Swiss Plateau (Magny, 2001) and an important incision of valley floors in western Europe (Antoine, 1997; Vandenberghe, 2003). Keeping in mind that the carbonate concretions used to reconstruct lake levels (see Section 10) form during the warm season, an increase in PANN suggests a seasonality marked by dry summers and wet winters for the beginning of GI-1e and Preboreal. This implies that the lake-level lowering is related to summer dryness, while river incision may be a result of increasing precipitation and higher discharge during the winter, or the snow melting season in addition to a possible impact of changes in vegetation cover (Vandenberghe, 2003). Conversely, the rise in lake level and the return of rivers to braided channels at the beginning of GS-1 suggest an opposite pattern of seasonality marked by wetter summers and drier winters as a result of a southward shift of (1) the sea ice during the winter and (2) the storm track in the summer in agreement with AGCM experiments (Renssen and Isarin, 2001; Renssen and Bogaart, 2003).

13.3. The response of terrestrial and aquatic organisms to climatic changes

The various biotic and abiotic records presented in this paper provide a coherent picture of local environmental and climatic changes around Lake Lautrey during the Last Glacial–Interglacial transition. They give insights into the dynamics of the ecosystem and the response of terrestrial and aquatic organisms to climatic changes. The warmer periods such as GI-1 and the Preboreal are characterised by an increasing biodiversity and complexity of the ecosystems, which show a great sensitivity to multiple successive climatic oscillations. However, the relative stability of the MS signal (except for the peaks due to tephras) and TOM values above 400 cm depth (except for secondary oscillations) indicates that, after the completion of the reforestation, the vegetation cover is less sensitive to climate impact than during the first part of the Lateglacial Interstadial. Finally, the MS and TOM curves, and the pollen diagram indicate that the restoration of the forest after GS-1 was much more rapid than after GS-2a.

Furthermore, biotic and abiotic indicators may not show proportionate signals in response to an identical forcing factor. An illustration of this is given at 483–480 cm depth by the contrast between the slight increase in herbaceous pollen concentration and the considerably more abrupt fall in MS values. This probably reflects non-linear processes associated with critical thresholds, the crossing of which governs the geomorphological (or biological) response to climatic changes (Walker et al., 2003). Conversely at the GS-1 onset, because the signals given by MS, quartz and dolomite mainly depend on the reduction in forest density, these indicators appear to be late in comparison with the chironomids and the arboreal pollen concentration.

A focus on the diverse records around the three major phases of climate change at the GS-2a/GI-1e, GI-1a/GS-1 and GS-1/Preboreal transitions reveals that indicators show responses that are more or less simultaneous (Fig. 14). The most striking evidence for this can be observed at the beginning of the GI-1 and at the GS-1 start. At level 444.5 cm, i.e. less than ca 20 yr after the abrupt change from allochthonous to authigenic sedimentation at level 445 cm, aquatic and terrestrial organisms mark a first clear expansion with the rapid development of *Juniperus* (level 444.5 cm) and *Betula* (level 442.5 cm) on the catchment area, while (1) *Chironomus* marks an expansion as early as level 444.5 cm and a first peak at 442.5 cm depth (i.e. ca 65 yr after the onset of biogenic calcite deposition), and (2) *C. ambigua* strongly declines at level 444.5 cm and has almost disappeared at level 442.5 cm. The LOC and TeOC curves indicate a synchronous signal at level 444.5 cm.

At the beginning of GS-1, the first responses of the vegetation and chironomid fauna occur simultaneously at 325.75 cm depth. *C. ambigua* appears at level 324.75 cm and reaches maximal values as early as 322.75 cm. Thus, within ca 150 yr, the chironomid assemblages show a very different picture. The rapidity of the change is nearly similar for the vegetation cover.

At the beginning of the Holocene, the chironomid taxa react at 297.75 cm depth (re-appearance and continuous re-expansion of *Chironomus*), while *C. ambigua* has completely disappeared at level 297.25 cm (i.e. ca 30 yr after level 298 cm). The pollen percentages indicate a first restoration of the forest at 296.5 cm depth, i.e. ca 70 yr after the shift to warm chironomid assemblages. Pollen concentrations show a rapid increase at 294.5 cm depth. Thus, as observed by Ammann et al. (2000) at Gerzensee, the response of organisms appears less telescoped during less abrupt climatic changes like the GS-1/Preboreal transition. In that case, as suggested by Birks et al. (2000) from Lake Krakenes in Norway and by Yu (2000) from Twiss Marl Pond in Canada, the earliness of the chironomid response observed at Lautrey supports the view that, in addition to terrestrial beetles (Coope et al., 1998), aquatic organisms are probably the best recorders of Lateglacial climatic changes.

Acknowledgments

Financial support for this study was provided by the French CNRS (program ECLIPSE). Isotope measurements were carried out during a CLIVARNET project financed by the Dutch Science Foundation NWO. The authors express their sincere thanks to J.C Rougeot for his help with the figure drawings, and to John Olsen for his help with the English language. An earlier draft of this manuscript benefited greatly from comments by H.H. Birks and A.F. Lotter. Finally, we acknowledge J.J. Lowe and an anonymous reviewer for their helpful and constructive remarks to improve the manuscript.

References

Aalbersberg, G., Beets, C.J., Vandenberghe, J.F., Coevert, A.F., 1999. Natural climate variability in the Lateglacial: high resolution stable isotope analyses and geochemistry from Jura lakes (Eastern France). Terra Nostra 10, 15–18.

Alley, R.B., Meese, D.A., Shuman, C.A., Gow, A.J., Taylor, K.C., Grootes, P.M., White, J.W.C., Ram, M., Waddington, E.D., Mayewski, P.A., Zielinski, G.A., 1993. Abrupt increase in Greenland snow accumulation at the end of the Younger Dryas event. Nature 362, 527–529.

Ammann, B., Lotter, A., 1989. Late-Glacial radiocarbon and palynostratigraphy on the Swiss Plateau. Boreas 18, 109–126.

Ammann, B., Gaillard, M.-J., Lotter, A.F., 1996. Switzerland. In: Berglund, B.E., Birks, H.J.B., Ralska-Jasiewiczowa, M., Wright, H.E. (Eds.), Palaeoecological Events During the Last 15000 Years. Wiley, New York, pp. 155–170.

Ammann, B., Birks, H.J.B., Brooks, S.J., Eicher, U., von Grafenstein, U., Hofman, W., Lemdahl, G., Schwander, J., Tobolski, K., Wick, L., 2000. Quantification of biotic responses to rapid climatic changes around the Younger Dryas—a synthesis. Palaeogeography, Palaeoecology, Palaeoclimatology 159, 313–349.

Amorosi, A., Centineo, M.C., Dinelli, E., Luchini, F., Tateo, F., 2002. Geochemical and mineralogical variations as indicators of provenance changes in Late Quaternary deposits of SE Po Plain. Sedimentary Geology 151, 273–292.

Antoine, P., 1997. Modifications des systèmes fluviatiles à la transition Pléniglaciaire–Tardiglaciaire et à l'Holocène: l'exemple du bassin de la Somme (Nord de la France). Géographie Physique et Quaternaire 51, 93–106.

de Beaulieu, J.-L., Richard, H., Ruffaldi, P., Clerc, J., 1994. History of vegetation, climate and human action in the French Alps and the Jura over the last 15000 years. Dissertationes Botanicae 234, 253–276.

Bégeot, C., 2000. Histoire de la végétation et du climat au cours du Tardiglaciaire et du début de l'Holocène sur le Massif jurassien central à partir de l'analyse pollinique et des macrorestes végétaux. Ph.D., University of Franche Comté, Besançon.

Bertrand, P., Brocero, S., Lallier-Vergès, E., Tribovillard, N., Bonifay, E., 1992. Sédimentation organique lacustre et paléoclimats du Pleistocène aux moyennes latitudes: exemple du lac du Bouchet, Haute Loire, France. Bulletin de la Société Géologique de France 163, 427–433.

Birks, H.H., Wright, H.E., 2000. Introduction to the reconstruction of the late-glacial and early Holocene aquatic ecosystems at Krakenes Lake, Norway. Journal of Paleolimnology 23, 1–5.

Birks, H.H., Battarbee, R.W., Birks, H.J.B., 2000. The development of the aquatic ecosystem at Krakenes Lake, western Norway, during the late-glacial and early Holocene—a synthesis. Journal of Paleolimnology 23, 91–114.

Björck, J., Wastergard, S., 1999. Climate oscillations and tephrochronology in eastern middle Sweden during the last glacial–interglacial transition. Journal of Quaternary Science 14, 399–410.

Björck, S., Kromer, B., Johnsen, S., Bennike, O., Hammarlund, D., Lemdahl, G., Possnert, G., Rasmussen, T.L., Wohlfarth, B., Hammer, C.U., Spurk, M., 1996. Synchronized terrestrial-atmospheric deglacial records around the North-Atlantic. Science 274, 1155–1160.

Björck, S., Rundgren, M., Ingolfsson, O., Funder, S., 1997. The Preboreal oscillation around the Nordic seas: terrestrial and lacustrine responses. Journal of Quaternary Science 12, 455–465.

Björck, S., Walker, M.J.C., Cwynar, L.C., Johnsen, S., Knudsen, K.-L., Lowe, J.L., Wohlfarth, B., INTIMATE Members, 1998. An event stratigraphy for the last termination in the North Atlantic region based on the Greenland ice-core record: a proposal by the INTIMATE group. Journal of Quaternary Science 13, 283–292.

van der Bogaard, P., Schmincke, H.U., 1985. Laacher See Tephra: a widespread isochronous late Quaternary tephra layer in central and northern Europe. Geological Society of America Bulletin 96, 1554–1571.

Bohncke, S.J.P., Vandenberghe, J., 1991. Palaeohydrological developments in the Southern Netherlands during the last 15 000 years. In: Starkel, L., Gregory, K.J., Thornes, J.B. (Eds.), Temperate Palaeohydrology. Wiley, Chichester and New York, pp. 253–281.

Bossuet, G., Richard, H., Magny, M., Rossy, M., 1997. Nouvelle occurrence du Laacher See Tephra dans le Jura central. L'étang du Lautrey (France). Comptes Rendus Académie des Sciences, Paris 325, 43–48.

Bossuet, G., Camerlinck, C., Dabas, M., Martin, J., 2000. Contribution des méthodes géophysiques (électrique, électromagnétique et radar sol) à l'étude des dépressions lacustres. L'exemple du Lautrey (Jura, France). Ecolgae Geologicae Helvetiae 93, 147–156.

Bourdon, S., Laggoun-Defarge, F., Maman, O., Disnar, J.R., Guillet, B., Derenne, S., Largeau, C., 2000. Organic matter sources and early diagenetic degradation in a tropical peaty marsh (Tritivakely, Madagascar). Implications for environmental reconstrcution during the Sub-Atlantic. Organic Geochemistry 31, 421–438.

Brauer, A., Endres, C., Günter, C., Litt, T., Stebich, M., Negendank, J.F.W., 1999. High resolution sediment and vegetation responses to Younger Dryas climate change in varved lake sediments from Meerfelder Maar, Germany. Quaternary Science Reviews 18, 321–329.

Brauer, A., Günter, C., Johnsen, S.J., Negendank, J.F.W., 2000. Land-ice teleconnections of cold climatic periods during the last Glacial/Interglacial transition. Climate Dynamics 16, 229–239.

Brodersen, K.P., Lindegaard, C., 1999. Mass occurrence and sporadic distribution of *Corynocera ambigua* Zetterstedt (Diptera, Chironomidae) in Danish lakes. Neo- and palaeolimnological records. Journal of Paleolimnology 22, 41–52.

Brooks, S., Birks, H.J.B., 2000. Chironomid-inferred late-glacial and early Holocene mean July air temperatures for Kråkenes Lake, western Norway. Journal of Paleolimnolgy 23, 77–89.

Clark, P.U., Marshall, S.J., Clarke, G.K.C., Hostetler, S.W., Licciardi, J.M., Teller, J.T., 2001. Freshwater forcing of abrupt climate change during the last glaciation. Science 293, 283–287.

Coope, G.R., Elias, S.A., 2000. The environment of Upper Palaeolithic (Magdalenian and Azilian) hunters at Hauterive-Champréveyres, Neuchâtel, Switzerland, interpreted from coleopteran remains. Journal of Quaternary Science 15, 157–175.

Coope, G.R., Lemdahl, G., Lowe, J.J., 1998. Temperature gradients in northern Europe during the last glacial–interglacial transition (14–9 ^{14}C kyr BP) interpreted from coleopteran assemblages. Journal of Quaternary Science 13, 419–433.

Cour, P., 1974. Nouvelles techniques de détection des flux et des retombées polliniques: étude de la sédimentation des pollens et des spores à la surface du sol. Pollen et Spores 1, 103–141.

David, F., 2001. Le tardiglaciaire des Etelles. Comptes Rendus Académie des Sciences, Paris 324, 373–380.

Disnar, J.R., Guillet, B., Keravis, D., Di-Giovanni, C., Sebag, D., 2003. Soil organic matter (SOM) characterization by Rock-Eval pyrolysis: scope and limitations. Organic Geochemistry 34, 327–343.

Eicher, U., 1987. Die spätglazialen sowie frühpostglazialen Klimaverhältnisse im Bereich der Alpen: Sauerstoffisotopenkurven kalkhaltiger Sedimente. Geographica Helvetica 2, 637–642.

Espitalié, J., Deroo, G., Marquis, F., 1985. La pyrolyse Rock-Eval et ses applications. Revue Institut Français du Pétrole 40, 6 563–579 and 755–784.

Friedrich, M., Kromer, B., Spurk, M., Hofman, J., Kaiser, K.F., 1999. Paleo-environment and radiocarbon calibration as derived from Lateglacial/Early Holocene tree-ring chronologies. Quaternary International 61, 27–39.

Gaillard, M.J., Lemdahl, G., 1994. Lateglacial insect assemblages from Grand-Marais, south-western Switzerland—climatic implications and comparison with pollen and plant macrofossil data. Dissertationes Botanicae 234, 287–308.

Gaillard, M.J., Moulin, B., 1989. New results on the Late-glacial history and environment of the lake of Neuchâtel (Switzerland). Sedimentological and palynological investigations at the Paleolithic site of Hauterive-Champréveyres. Ecolgae Geologicae Helvetiae 82, 203–218.

Grafenstein, U., Erlenkeuser, H., Brauer, A., Jouzel, J., Johnsen, S.J., 1999. A mid-European decadal isotope-climate record from 15,500 to 5000 years BP. Science 284, 1654–1657.

Guiot, J., 1990. Methodology of palaeoclimatic reconstruction from pollen in France. Palaeogeography, Palaeoclimatology, Palaeoecology 80, 49–69.

Guiot, J., Harrison, S.P., Prentice, I.C., 1993. Reconstruction of Holocene precipitation patterns in Europe using pollen and lake-level data. Quaternary Research 40, 139–149.

Harrison, S.P., Prentice, I.C., Guiot, J., 1993. Climatic controls on Holocene lake-level changes in Europe. Climate Dynamics 8, 189–200.

Heiri, O., 2001. Holocene palaeolimnology of Swiss mountain lakes reconstructed using subfossil chironomid remains. Ph.D. Thesis, Inauguraldissertation der Philosophisch-naturwissenschaftlichen Fakultät der Universität Bern.

Heiri, O., Lotter, A.F., 2001. Effect of low count sums on quantitative environmental reconstructions: an example using subfossil chironomids. Journal of Paleolimnology 26, 343–350.

Heiri, O., Millet, L., 2005. Reconstruction of Late Glacial summer temperatures from chironomid assemblages in Lac Lautrey (Jura, France). Journal of Quaternary Science 20, 1–12.

Heiri, O., Birks, H.J.B., Brooks, S.J., Velle, G., Willassen, E., 2003a. Effects of within-lake variability of fossil assemblages on quantitative chironomid-inferred temperature reconstruction. Palaeogeography, Palaeoclimatology, Palaeoecology 199, 95–106.

Heiri, O., Lotter, A.F., Hausmann, S., Kienast, F., 2003b. A chironomid-based Holocene summer air temperature reconstruction from the Swiss Alps. The Holocene 13, 477–484.

Higgitt, S.R., Oldfield, F., Appleby, P.G., 1991. The record of land use change and soil erosion in the late Holocene sediments of the Petit Lac d'Annecy, eastern France. The Holocene 1, 14–28.

Hoek, W.Z., 2001. Vegetation response to the 14.7 and 11.5 ka cal. BP climate transitions: is vegetation lagging climate? Global and Planetary Change 30, 103–115.

Hofmann, W., 1971. Zur Taxonomie und Palökologie subfossiler Chironomiden (Dipt.) in Seesedimenten. Archiv für Hydrobiologie Beiheft Ergebnisse der Limnologie 6, 1–50.

Hofmann, W., 1986. Chironomid analysis. In: Berglund, B.E. (Ed.), Handbook on Holocene Palaeoecology and Palaeohydrology. Wiley, Chichester, pp. 715–727.

Holtzappfel, T., 1985. Les minéraux argileux. Préparation. Analyse diffractométrique et détermination. Société Géologique du Nord, 12.

Hu, F.S., Lee, B.Y., Kaufman, D.S., Yoneji, S., Nelson, D.M., Henne, P.D., 2002. Response of tundra ecosystem in southwestern Alaska to Younger-Dryas climatic oscillation. Global Change Biology 8, 1156–1163.

Hughen, K.A., Overpeck, J.T., Lehman, S.J., Kashgarian, M., Southon, J., Peterson, L.C., Alley, R., Sigman, D.M., 1998. Deglacial changes in ocean circulation from an extended radiocarbon calibration. Nature 391, 65–68.

Isarin, R.F.B., Bohncke, S.J.P., 1999. Mean July temperatures during the Younger Dryas in northwestern and central Europe as inferred from climate indicator plant species. Quaternary Research 51, 158–173.

Johnsen, S.J., Clausen, H.B., Dansgaard, W., Fuhrer, K., Gundestrup, N., Hammer, C.U., Iversen, P., Jouzel, J., Stauffer, B., Steffensen, J.P., 1992. Irregular glacial interstadials recorded in a new Greenland ice core. Nature 359, 311–313.

Juvigné, E., Bastin, B., Delibrias, G., Evin, J., Gewelt, M., Gilot, E., Streel, M., 1996. A comprehensive pollen- and tephra-based chronostratigraphic model for the Late Glacial and Holocene periods in the French Massif Central. Quaternary International 34-36, 113–120.

Karpuz, N.K., Jansen, E., 1992. A high-resolution diatom record of the last deglaciation from the SE Norwegian Sea: documentation of rapid climatic changes. Paleoceanography 7, 499–520.

Kubler, B., 1987. Dosage quantitative des minéraux des roches sédimentaires par diffraction X. Cahiers de l'Institut de Géologie de Neuchâtel, série ADX.

Larocque, I., 2001. How many chironomid head capsules is enough? A statistical approach to determine sample size for paleoclimatic reconstruction. Palaeogeography, Palaeoclimatology, Palaeoecology 172, 133–142.

Limondin-Lozouet, N., Bridault, A., Leroyer, C., Ponel, P., Antoine, P., Chaussé, C., Munaut, A.V., Pastre, J.F., 2002. Evolution des écosystèmes de fond de vallée en France septentrionale au cours du Tardiglaciaire: l'apport des indicateurs biologiques. In: Bravard, J.P., Magny, M. (Eds.), Variations paléohydrologiques en France depuis 15000 ans. Errance, Paris, pp. 31–48.

Lotter, A.F., Birks, H.J.B., Eicher, U., Siegenthaler, U., 1992. Late-glacial climatic oscillations as recorded in Swiss lake sediments. Journal of Quaternary Science 7, 187–204.

Lotter, A.F., Birks, H.J.B., Hofman, W., Marchetto, A., 1997. Modern diatom, Cladocera, chironomids and chrysophyte cyst assemblages as quantitative indicators for the reconstruction of past environmental conditions in the Alps. I. Climate. Journal of Paleolimnology 18, 395–420.

Lotter, A.F., Birks, H.J.B., Eicher, U., Hofman, W., Schwander, J., Wick, L., 2000. Younger Dryas and Allerod summer temperatures at Gerzensee (Switzerland) inferred from fossil pollen and cladoceran assemblages. Palaeogeography, Palaeoecology, Palaeoclimatology 159, 349–362.

Lowe J., Ed., 1994. Climate changes in areas adjacent to the North Atlantic during the last Glacial–Interglacial transition. Journal of Quaternary Science 9, 93–198.

Lowe, J.J., Birks, H.H., Brooks, S.J., Coope, G.R., Harkness, D.D., Mayle, F.E., Sheldrick, C., Turney, C.S.M., Walker, M.J.C., 1999. The chronology of palaeoenvironmental changes during the Last Glacial–Holocene transition: towards an event stratigraphy for the British Isles. Journal of Geological Society, London 156, 397–410.

Magny, M., 1992a. Sédimentation et dynamique de comblement dans les lacs du Jura au cours des 15 derniers millénaires. Revue d'Archéométrie 16, 27–49.

Magny, M., 1992b. Holocene lake-level fluctuations in Jura and the northern subalpine ranges, France: regional pattern and climatic implications. Boreas 21, 319–334.

Magny, M., 1995. Paleohydrological changes in Jura (France) and climatic oscillations around the North Atlantic from

Allerod to Preboreal. Geographie Physique et Quaternaire 49, 401–408.

Magny, M., 1998. Reconstruction of Holocene lake-level changes in the Jura (France): methods and results. In: Harrison, S.P., Frenzel, B., Huckried, U., Weiss, M., (Eds.), Palaeohydrology as Reflected in Lake-Level Changes as Climatic Evidence for Holocene Times. Paläoklimaforschung 25, 67–85.

Magny, M., 2001. Palaeohydrological changes as reflected by lake-level fluctuations in the Swiss Plateau, the Jura mountains and the northern French Pre-Alps during the Last Glacial–Holocene transition: a regional synthesis. Global and Planetary Change 30, 85–101.

Magny, M., Richoz, I., 2000. Lateglacial lake-level changes at Montilier-Strandweg, Lake Morat, Switzerland and their climatic significance. Quaternaire 11, 129–144.

Magny, M., Guiot, J., Schoellammer, P., 2001. Quantitative reconstruction of Younger Dryas to mid-Holocene paleoclimates at Le Locle, Swiss Jura, using pollen and lake-level data. Quaternary Research 56, 170–180.

Magny, M., Thew, N., Hadorn, P., 2003. Late-glacial and early Holocene changes in vegetation and lake-level at Hauterive/Rouges-Terres, Lake Neuchâtel (Switzerland). Journal of Quaternary Science 18, 31–40.

Meyers, P., Lallier-Vergès, E., 1999. Lacustrine sedimentary organic matter records of Late Quaternary paleoclimates. Journal of Paleolimnology 21, 345–372.

Millet, L., Verneaux, V., Magny, M., 2003. Lateglacial paleoenvironmental reconstruction using subfossil chironomid assemblages from Lake Lautrey (Jura, France). Archives für Hydrobiologie 156, 405–429.

Moore, D.M., Reynolds, R.C.J., 1997. X-ray Diffraction and the Identification and Analysis of Clay Minerals, second ed. Oxford University Press, New York.

Nolan, S.R., Bloemendal, J., Boyle, J.F., Jones, R.T., Oldfield, F., Whitney, M., 1999. Mineral magnetic and geochemical records of late Glacial climatic change from two northwest European carbonate lakes. Journal of Paleolimnology 22, 97–107.

Nowaczyk, N.R., 2001. Logging of magnetic susceptibility. In: Last, W.M., Smol, J.P. (Eds.), Tracking Environmental Change Using Lake Sediments, Vol. 1. Kluwer Academic Publisher, Dordrecht, The Netherlands, pp. 155–170.

Olander, H., Birks, H.J.B., Korhola, A., Blom, T., 1999. An expanded calibration model for inferring lakewater and air temperatures from fossil chironomid assemblages in northern Fennoscandia. The Holocene 9, 279–294.

Peyron, O., Guiot, J., Cheddadi, R., Tarasov, P., Reille, M., de Beaulieu, J.L., Bottema, S., Andrieu, V., 1998. Climatic reconstruction in Europe for 18 000 yr BP from pollen data. Quaternary Research 49, 183–196.

Peyron, O., Jolly, O., Bonnefille, R., Vincens, A., Guiot, J., 2000. Climate of East Africa 6000 14C yr B.P., as inferred from pollen data. Quaternary Research 54, 90–101.

Prentice, I.C., Guiot, J., Huntley, B., Jolly, D., Cheddadi, R., 1996. Reconstructing biomes from palaeoecological data: a general method and its application to European pollen data at 0 and 6 ka. Climate Dynamics 12, 185–194.

Quinlan, R., Smol, J.P., 2001. Chironomid-based inference models for estimating end-of-summer hypolimnetic oxygen from south-central Ontario shield lakes. Freshwater Biology 46, 1529–1551.

Renssen, H., Bogaart, P.W., 2003. Atmospheric variability over the 14.7 kyr BP stadial–interstadial transition in the North Atlantic region as simulated by an AGCM. Climate Dynamics 20, 301–313.

Renssen, H., Isarin, R.F.B., 2001. The two major warming phases of the last deglaciation at 14,7 and 11,5 ka cal BP in Europe: climate reconstructions and AGCM experiments. Global and Planetary Change 30, 117–153.

Saether, O.A., 1979. Chironomid communities as water quality indicators. Holarctic Ecology 2, 65–74.

Sbaffi, L., Wezel, F.C., Curzi, G., Zoppi, U., 2004. Millennial- to centennial-scale palaeoclimatic variations during Termination I and the Holocene in the central Mediterranean Sea. Global and Planetary Change 40, 201–217.

Schmidt, R., van den Bogaard, C., Merkt, J., Müller, 2002. A new Lateglacial chronostratigraphic tephra marker for the south-eastern Alps: the Napolitan Yellow Tuff (NYT) in Längsee (Austria) in the context of a regional biostratigraphy and palaeoclimate. Quaternary International 88, 45–56.

Schwander, J., Eicher, U., Ammann, B., 2000. Stable isotopes of lake marl at Gerzensee and Leysin (Switzerland), covering the Younger Dryas and two minor oscillations, and their correlation to the GRIP ice core. Palaeogeography, Palaeoecology, Palaeoclimatology 159, 215–230.

Sifeddine, A., Bertaux, J., Mourguiart, P., Martin, L., Disnar, J.R., Laggoun-Defarge, F., 1998. Etude de la sédimentation lacustre d'un site de forêt d'altitude des Andes centrales (Bolivie). Implications paléoclimatiques. Bulletin de la Société Géologique de France 169, 395–402.

Stockhausen, H., Zolitschka, B., 1999. Environmental changes since 13 000 cal. BP reflected in magnetic and sedimentological properties of sediments from Lake Holzmaar (Germany). Quaternary Science Reviews 18, 913–925.

Stuiver, M., Grootes, P.M., Braziunas, T.F., 1995. The GISP2 $D^{18}O$ climate record of the past 16,500 years and the role of the sun, ocean and volcanoes. Quaternary Research 44, 341–354.

Stuiver, M., Reimer, P.J., Bard, E., Beck, J.W., Burr, G.S., Hughen, K.A., Kromer, B., McCormac, G., van der Plicht, J., Spurk, M., 1998. Int cal 98 radiocarbon age calibration, 24 000–0 cal BP. Radiocarbon 40, 1041–1083.

Ter Braak, C.J.F., Smilauer, P., 1998. Canoco Reference Manual and User's Guide to Canoco of Windows. Centre for Biometry Wageningen.

Thompson, R., Oldfield, F., 1986. Environmental Magnetism. Allen & Unwin, London.

Thouveny, N., Beaulieu, J.L., Bonifay, E., Créer, K.M., Guiot, J., Icole, M., Johnsen, S., Jouzel, J., Reille, M., Williams, T., Williamson, D., 1994. Climate variations in Europe over the past 140 kyr deduced from rock magnetism. Nature 371, 503–506.

Vandenberghe, J., 2003. Climate forcing of fluvial system development: an evolution of ideas. Quaternary Science Reviews 22, 2053–2060.

Van Geel, B., 1996. Factors influencing changing AP/NAP ratios in NW-Europe during the Late-Glacial period. Il Quaternario 9, 599–604.

Vanniere, B., Bossuet, G., Walter-Simonnet, A.V., Ruffaldi, P., Adatte, T., Rossy, M., Magny, M., 2004. High-resolution record of environmental changes and tephrochronological markers of the Last Glacial–Holocene transition at Lake Lautrey (Jura, France). Journal of Quaternary Science 19, 797–808.

Vernet, G., Raynal, J.P., 2000. Un cadre tephrostratigraphique réactualisé pour la préhistoire tardiglaciaire et holocène de Limagne (Massif Central, France). Comptes Rendus Académie des Sciences, Paris 330, 399–405.

Walker, M.J.C., Coope, G.R., Sheldrick, C., Turney, C.S.M., Lowe, J.J., Blockley, S.P.E., Harkness, D.D., 2003. Devensian Lateglacial environmental changes in Britain: a multi-proxy environmental record from Llanilid, South Wales, UK. Quaternary Science Reviews 22, 475–520.

Wiederholm, T., 1983. Chironomidae of the Holarctic region. Keys and Diagnoses. Part 1. Larvae. Entomologica Scandinavica Supplement 19, 1–457.

Wohlfarth, B., Gaillard, M.-J., Haeberli, W., Kelts, K., 1994. Environment and climate in southwestern Switzerland during the last termination, 15-10 ka BP. Quaternary Science Reviews 123, 361–394.

Yu, Z., 2000. Ecosystem response to Lateglacial and early Holocene climate oscillations in the Great Lakes region of North America. Quaternary Science Reviews 19, 1723–1747.